DEVELOPMENT OF AMINO ACID DEPLETING ENZYME FOR THE TREATMENT OF CANCER

CHONG HIU CHI

Ph. D

The Hong Kong Polytechnic University

2015

The Hong Kong Polytechnic University

Department of Applied Biology and Chemical Technology

Development of Amino Acid Depleting Enzyme for the Treatment of Cancer

Chong Hiu Chi

A thesis submitted in partial fulfilment of the requirements for the degree of Doctor of Philosophy

September 2014

Certificate of Originality

I hereby declare that this thesis is my own work and that, to the best of my knowledge and belief, it reproduces no material previously published or written, nor material that has been accepted for the award of any other degree or diploma, except where due acknowledgement has been made in the text.

Chong Hiu Chi

September 2014

Abstract

Gastric and colorectal cancers are the top five most commonly diagnosed cancers around the world. These cancers are usually asymptomatic in the early stage and essentially, early detection can be achieved merely by screening program. Nevertheless, poor prognosis represents a major problem in advanced stage gastric cancer and metastatic colorectal cancer. It is therefore of paramount importance to develop new therapeutics for these cancers.

Metabolic reprogramming has been proposed as one of the hallmarks of cancer. Differential requirement of various nutrients such as amino acids has been observed in cancer cells. The best known example of amino acid depleting enzyme is the pegylated bacterial asparaginase (Oncaspar), which has been approved by the US FDA as the first-line treatment for acute lymphoblastic leukemia (ALL) in children. Elevated requirement of arginine has been observed in different types of cancer and thus, a novel arginine depleting enzyme, engineered *Bacillus caldovelox* arginase (BCA) was developed in this study. Plasmid vector carrying the BCA gene was transformed into *E. coli* cells for the overexpression, which is mediated by IPTG induction. The thermostable BCA protein with a 6xHis-tag fused to its C-terminus was purified through a simple two-step purification scheme, with heat treatment followed by metal affinity column chromatography. In our structure-based rational drug design, a unique cysteine residue was strategically placed on the surface of the BCA molecule to facilitate site-specific pegylation. Characterization of both the native and the pegylated BCA were performed. Briefly, the major proportion of native BCA exists in hexameric structure while monomeric structure of BCA presents in tiny amount as determined by gel filtration

column. The size of BCA increased from 33275.25 Da to about 55 kDa after pegylation. Pegylation do not significantly alter the secondary structure of BCA and comparable enzyme activity was observed for both native and pegylated BCA. The enzymatic activity of BCA was found specific to arginine when tested against 40 different amino acids. The stability of BCA was further improved by pegylation for which 90% activity could be retained for 32 months of storage.

The *in vitro* anti-cancer effects of BCA were tested on three gastric cancer (MKN45, BCG823 and AGS) and two colorectal cancer (HCT-15 and HCT116) cell lines. All the cell lines lacking the expression of OTC were found to be vulnerable to the BCA treatment and arrested in different phases (G2/M and S) of cell cycle while four out of the five cell lines tested were found to undergo apoptotic cell death. Pharmacological study revealed that the circulating half-life of BCA was extended by 12-fold after pegylation while an intraperitoneal injection of this pegylated BCA in mice reduced the serum arginine to an undetectable level for 5-6 days. Importantly, efficacy studies showed that the pegylated BCA effectively suppressed the growth of tumor xenograft in mice and its efficacy is comparable to that of 5-FU. Furthermore, synergistic effect was observed when the pegylated BCA was tested in combination with 5-FU. These promising results warrant the pegylated BCA for further study and cancer patients might benefit from this novel treatment strategy in the future.

Acknowledgements

I would like to express my sincere gratitude to my supervisor, Prof. Thomas Y. C. Leung, for his valuable support, guidance and in depth discussion of all critical scientific issues arising from my research work. Throughout the PhD. study, his training for me was not limited to develop independent, critical and logical thinking, but also providing me the excellent opportunity for internship to which I can broaden my horizon through joining different internationally renowned research institutes where I can appreciate the research atmosphere in both academic and industrial setting. I always feel grateful to Dr. Thomas W. H. Lo for his critical comments and suggestions to my study and more importantly the *in vivo* study would never be completed without the support from his research team.

It is also my honor to be a member of Lo Ka Chung Centre for natural anti-cancer drug development. The generous support and resource provided to my study are gratefully acknowledged.

I would like to thank Dr. H. K. Yap and Dr. T. L. Lam for teaching me all the skills about molecular cloning which were of paramount important for the rational design of different fusion proteins in my study. Precious comments and helpful discussion from Dr. Gabriel K. Y. Wong is highly appreciated during my preparation of this thesis. Much obliged from the administrative support from Ms. Sammi S. M. Tsui who greatly streamline the daily operation of the laboratory.

Special thank also goes to my friends and teammates, Dr. P. K. So, Dr. Ryan H. Y. Chow, Dr. K. Y. Kung, Dr. Fiona H. Y. Shiu, Dr. Kenneth K. C. Wong, Dr. John H. K. Lum, Dr. Fred W. F. Lee, Dr. Yoki K. C. Butt, Dr. Waitig W. T. Wong, Ms. Y. S. Siu, Ms X. L.

Wei, Ms. Shirley S. L. Chu, Mr. C. F. Kim and Mr. W. Y. Kan, for their general support and friendship.

Lastly, I would like to express my thanks to the technicians of the Department of Applied Biology and Chemical Technology, especially Mr. C. H. Cheng, Ms Sarah K. L. Yeung and Ms. Ivy Tao for their technical assistance.

Table of Contents

List of figures

Chapter 1:

Chapter 3:

Chapter 4:

Chpater 5:

List of tables

Chapter 1:

Chapter 3:

Chapter 4:

List of abbreviations

2-D PAGE	Two-dimensional polyacrylamide gel electrophoresis
5-FU	5-Fluorouracil
AAA	Amino acid analyzer
ABD	Albumin binding domain
ABD035	Femtomolar affinity ABD
ADC	Arginine decarboxylase
ADI	Arginine deiminase
ADI-SS $PEG_{20,000\ mw}$	Random pegylated ADI with 20 kDa PEG
AFM	Arginine-free medium
AIF	Apoptosis inducing factor
ANOVA	Analysis of variance
Ara-C	Cytarabine
ASL	Argininosuccinate lyase
ASS	Argininosuccinate synthase
AUC	Area under the curve
BCA	*Bacillus caldovelox* arginase
BCA-ABD	BCA fused with ABD
BRAF	B-Raf proto-oncogene, serine/threonine kinase
CD	Circular dichroism
CD4	cluster of differentiation 4
cdk	Cyclin-dependent kinases
cDNA	complementary DNA

CEA	Carcinoembryonic antigen
CQ	Chloroquine
CV	Column volumn
Da	Dalton
DISC	Death-inducing signaling complex
DNA	Deoxyribonucleic acid
EGFR	Epidermal growth factor receptor
eIF2α	eukaryotic initiation factor 2 alpha
ELISA	Enzyme-linked immunosorbent assay
EPR	Enhanced permeability and retention
ERBB2	Erb-B2 receptor tyrosine kinase 2
ESI	Electrospray ionization
Fc	Fration crystallizable
FcRn	Neonatal fragment crystalliable receptor
FDA	Food and Drug Administration
FITC	Fluorescein isothiocyanate
h	Hour/Hours
HCC	Hepatocellular carcinoma
HER2	Human epidermal growth factor receptor 2
HIF-1α	Hypoxia-inducible factor 1-alpha
HSA	Human serum albumin
i.p.	Intraperitoneal
IEF	Isoelectric focusing
IgG	Immunoglobulin G
IPTG	Isopropyl β-D-1-thiogalactopyranoside

k	Kilo
KRAS	Kirsten rat sarcoma viral oncogene homolog
LAL	Limulus amebocyte lysate
LC3	Light chain 3
LPS	Lipopolysaccharide
MALDI-ToF	Matrix-Assisted Laser Desorption/Ionization Time-of-Flight
min	Minute/Minutes
MOMP	Mitochondria outer membrane permeability
mRNA	messenger Ribonucleic acid
MS	Mass Spectrometry
MW	Molecular weight
NMR	Nuclear magnetic resonance
NMWC	Nominal molecular weight cut-off
NRMSD	Normalized root-mean-square deviation
OTC	Ornithine transcarbamylase
PBS	Phosphate buffered saline
PCR	Polymearse chain reaction
PDB	Protein data bank
PEG	Polyethylene glycol
PI	Popidium iodide
pI	Isoelectric point
PIK3CA	Phosphatidylinositol-4,5-bisphosphate 3-kinase, catalytic subunit alpha
PS	Phosphatidylserine
PTEN	Phosphatase and tensin omolog
RES	Reticuloendothelial system

rhArg	recombinant human arginase I
RNA	Ribonucleic acid
RT-PCR	Reverse transcription-polymerase chain reaction
scDb	Single-chain diabody
scDB-ABD	scDB fused with ABD
scFv	Single-chain variable fragment
SCID	Severe combined immunodeficiency
sCR1	Soluble complement receptor type 1
SD	Standard deviation
SDS-PAGE	Sodium dodecyl sulfate polyacrylamide gel electrophoresis
SEM	Standard error of mean
siRNA	Small interfering ribonucleic acid
SpG	Streptococcus protein G
SUNBRIGHT ME-200MA	20 kDa PEG activated maleimide
T-ALL	T cell acute lymphoblastic leukemia
TFF	Tegential flow filtration
TNF	Tumor necrosis factor
TRAIL	Tumor necrosis factor-related apoptosis-inducing ligand

1. Introduction

1.1. Overview of gastric and colorectal cancers

Cancer remains one of the leading causes of death worldwide. Gastric and colorectal cancers were ranked the top 5 most commonly diagnosed cancers worldwide and together, accounting for 17.5% (2.22 million) of the total new case and 18.1% (1.34 million) of total cancer related death in 2008 (Jemal et al., 2011). Reviewing the recent trend of gastric and colorectal cancers, a significant decrease of the incidence rate for gastric cancer has been recorded in the past few decades while an increasing trend has been observed for colorectal cancer in most of the country (Bertuccio et al., 2009; Center et al., 2009). The early stage of gastric and colorectal cancers is usually asymptomatic. Early detection usually achieved through screening program and primarily removed by surgical resection. Treatment for advance stage cancer involves surgery and adjuvant chemotherapy or chemoradiotherapy ("Global Cancer Facts & Figures 2nd Edition," 2011). However, the prognosis for the advanced stage gastric cancer and the metastatic colorectal cancer remains poor (Bang et al., 2010; Siegel et al., 2012). Despite the recent clinical trials for gastric cancer demonstrated that addition of Trastuzumab, monoclonal antibody against HER2, to chemotherapy improved overall survival in patients when compare to chemotherapy alone, only 7 - 34% of patients showing overexpression of HER2 in their tumors (Bang et al., 2010). Albeit overexpression of epidermal growth factor receptor (EGFR) occurs in 60 to 80 percent of patients with colorectal cancer, only a subset of patients (10 - 20%) are benefited from the therapy of centuximab and panitumumab, monoclonal antibody directed against EGFR (Bardelli & Siena, 2010; Cunningham et al., 2004). Patients with oncogenic alternation of the EGFR downstream signaling cascade, such as KRAS, BRAF and PIK3CA mutation and lost of PTEN

activity, are usually resistant to the targeted therapy. Even patients who are "quadruple negative" and respond very well at the beginning, prolonged anti-EGFR treatment rendering the cells to develop acquired resistance possibly mediated through EGFR mutation and overexpression of the ERBB2 receptor together with the increased level of EGFR ligand heregulin (Bardelli & Janne, 2012; Bardelli & Siena, 2010; De Roock et al., 2011). Based on these situations, new treatment strategy through addition of kinase inhibitors may reverse the resistance of the targeted therapy on one hand, while we should keep on exploring new treatment modality based on differential requirement sustaining the growth of cancer cells.

Metabolic reprogramming has been considered as a hall mark of cancer for which it may show a distinctive nutrient requirement, such as amino acid, to support the increased proliferation of tumors (Hanahan & Weinberg, 2011). Asparagine, arginine, methionine, glycine and leucine have been found to play critical roles in different types of cancers. Among these amino acids, the best illustrated example is the non-essential amino acid, asparagine, for which leukemia cells are unable to *de novo* synthesize and thus it must be obtained from the systemic circulation. Treatment modality aimed to deplete or lower the asparagine level, through injection of asparaginase, demonstrated a strong anti-proliferating effect and induced apoptosis in the leukemia cells. Nowadays, pegasparaginase has been approved by FDA for the first-line treatment of acute lymphoblastic leukemia (ALL) in children (Dinndorf et al., 2007). This successful story brings up an innovative approach to which amino acid depleting enzymes could be formulated as a potential anti-cancer therapeutics.

1.2. *De novo* synthesis of arginine

Arginine is a semi-essential or conditionally essential amino acid because *de novo* synthesis of arginine is inadequate to meet our body requirement under certain circumstances/conditions such as during different stages of development, injury or diseases. The intestinal-renal axis is the route of arginine synthesis in adult for which citrulline could be produced from glutamine in the enterocyte and released to the systemic circulation and then it will be converted to arginine in the proximal renal tubules, through a tightly coupled enzymatic activity of argininosuccinate synthase (ASS) and argininosuccinate lyase (ASL), and released into the circulation. Various levels of ASS and ASL expression have been detected in normal cells such as endothelial cells suggesting that citrulline can be used as a precursor for arginine synthesis. However, cancer cells showing down-regulated or even lacking the expression of ASS are prone to arginine depletion and thus auxotrophic for arginine.

1.3. Normal and malignant cells in response to arginine depletion

Since cancer cells are auxotrophic for arginine, restricting the supply of arginine has been explored to inhibit the proliferation of cancer cells. The role of arginine in cancer growth has been recognized since 1930. An experiment to evaluate the stimulatory effects of different amino acids in tumor growth found that arginine exhibits the strongest stimulation to the growth of M63 tumor xenograft (Gilroy, 1930). The *in vitro* growth of carcinoma 63 was directly proportional to the arginine added to the culture medium and 0.1% of arginine containing medium increased the mitotic activity by almost 200% when compared to the control while the mitosis of normal epithelial cells from embryo lung was unaffected by the addition of arginine (Bach & Lasnitzki, 1947). Rats bearing Jensen sarcoma were found to excrete substantially more urinary creatine parallel to the growth of tumor which may indicate the preferential utilization of arginine during tumor growth (Bach & Maw, 1953). The addition of purified arginase to fibroblast and Jensen sarcoma cultures resulted in reduction of mitosis and similar effects were also observed when the embryo extract of the medium was replaced with Tyrode solution (arginine free buffer solution) (Simon-Reuss, 1953). More recently, the study of the requirement of arginine in HeLa cells demonstrated the growth is strictly dependent on the exogenous supply of arginine in culture medium and 90% cells died in 3-4 days when cultured in medium containing 10^{-6} M arginine but almost all cells survived and recoverable after 4 days in culture containing 10^{-6} M leucine. Among the eleven essential amino acids tested in the culture of HeLa cells, the requirement of arginine far higher than all other essential amino acids such as leucine. The consumption of arginine is almost 3 times higher in HeLa cells than normal fibroblasts (D. N. Wheatley et al., 2000). Despite the arginine requirement may vary with different cancer cell lines/types, further study in a panel of 26 cell lines

demonstrated that the malignant cells usually died in 2-5 days but normal cells could survive for more than 3 weeks upon resumption of arginine supply in culture (Scott et al., 2000). Moreover, the differential response of normal and cancer cells were further elucidated with reference to the machinery controlling the progression of cell cycle. Upon arginine deprivation, normal fibroblasts with stringent cell cycle control will be arrested at the restriction point in the G0/G1 phase within 4-6 h. Since the Cyclin D/cdk 4 complex mediated the progression through G1 phase, downregulation of cdk 4 on arginine depletion explain the arrest of normal fibroblast at G0/G1 phase. However, malignant cells with aberrant cell cycle control possibly at restriction point may allow the cells to keep cycling into the S phase and protracted sojourn in S phase leading to cell death via apoptosis (Lamb & Wheatley, 2000). Interestingly, recent study revealed that both T cell acute lymphoblastic leukemia (T-ALL) and primary T cell response to the arginase treatment by arresting in the G0/G1 phase but apoptotic cell death could be detected only in the T-ALL cell lines. This suggested that other mechanisms may exist to regulate the cell cycle progression during arginine-deficient state and more importantly, the underlying principle leading to apoptosis in T-ALL cells but not primary T cell should be further investigated (Hernandez et al., 2010).

The differential requirement of arginine and preferential cell death in response to arginine depletion in malignant cells offers an eminently targeting approach for the development of arginine depleting enzymes for cancer treatment.

1.4. Arginine depleting enzymes

Arginine depleting enzymes such as, recombinant human arginase I (rhArg) and recombinant arginine deiminase (ADI) derived from *Mycoplasma hominis*, have been developed and intended to treat cancers such as melanoma and hepatocellular carcinoma (HCC) in clinical setting for which the incidence of ASS deficiency are highest among different cancer types (Dillon et al., 2004).

The use of arginine decarboxylase (ADC) has received less attention despite of ADC converts arginine to non-urea cycle product, agmatine; however, pegylation of ADC almost completely abolished the enzymatic activity and limited the *in vivo* use of this enzyme as cancer therapeutic (D. N. Wheatley & Campbell, 2002; D. N. Wheatley et al., 2000).

1.4.1. Expression of urea cycle enzymes and the resistance toward arginase and arginine deiminase (ADI)

Deprivation of arginine from culture using arginase has been successfully arrested the growth of cancer cells but this effect could be partially reversed by providing the medium with citrulline but not other urea cycle intermediates, such as ornithine or argininosuccinate. Interestingly, treatments with ADI do not consistently inhibit the growth of different cancer cell types (Cheng et al., 2007). These observations are related to the expression of urea cycle enzymes and the enzymatic end-product generated by different arginine depleting enzymes. For example, arginine will be converted to citrulline and ornithine by ADI and arginase, respectively. Both of citrulline and ornithine are the intermediates of urea cycle, successful conversion of these intermediates back to arginine would confer the cells resistance to the arginine depleting enzymes. Thus, a strong correlation between the expression of the urea cycle enzymes, namely OTC, ASS and ASL, and the end-product generated by the arginine depleting enzymes has been established (Lam et al., 2009).

Considering the breakdown of arginine to ornithine and urea by arginase in culture condition, the intracellular activity of ornithine transcarbamylase (OTC) converts ornithine and carbamoyl phosphate to citrulline. While ASS and ASL catalyzed the coupled reaction for which citrulline and aspartic acid will be converted to argininosuccinate and the regeneration of arginine and fumarate will be mediated through the enzymatic reaction of ASL which usually constitutively express inside the cell (Figure 1. 1)(Lam et al., 2009).

Cancer cells expressing OTC, ASS and ASL will be able to recycle ornithine to arginine and thus resistant to arginase treatment. Conversely, cancer cells lacking the expression of OTC, ASS or ASL will not be able to regenerate arginine and manifested as growth inhibition. Since most of the cancer cells do not express OTC in culture, transfection of the HCC cell line with OTC expression plasmid has been found to confer resistance to these cell lines upon arginase treatment providing that these cell lines express both ASS and ASL (Cheng et al., 2007; D. N. Wheatley & Campbell, 2003; D. N. Wheatley et al., 2005).

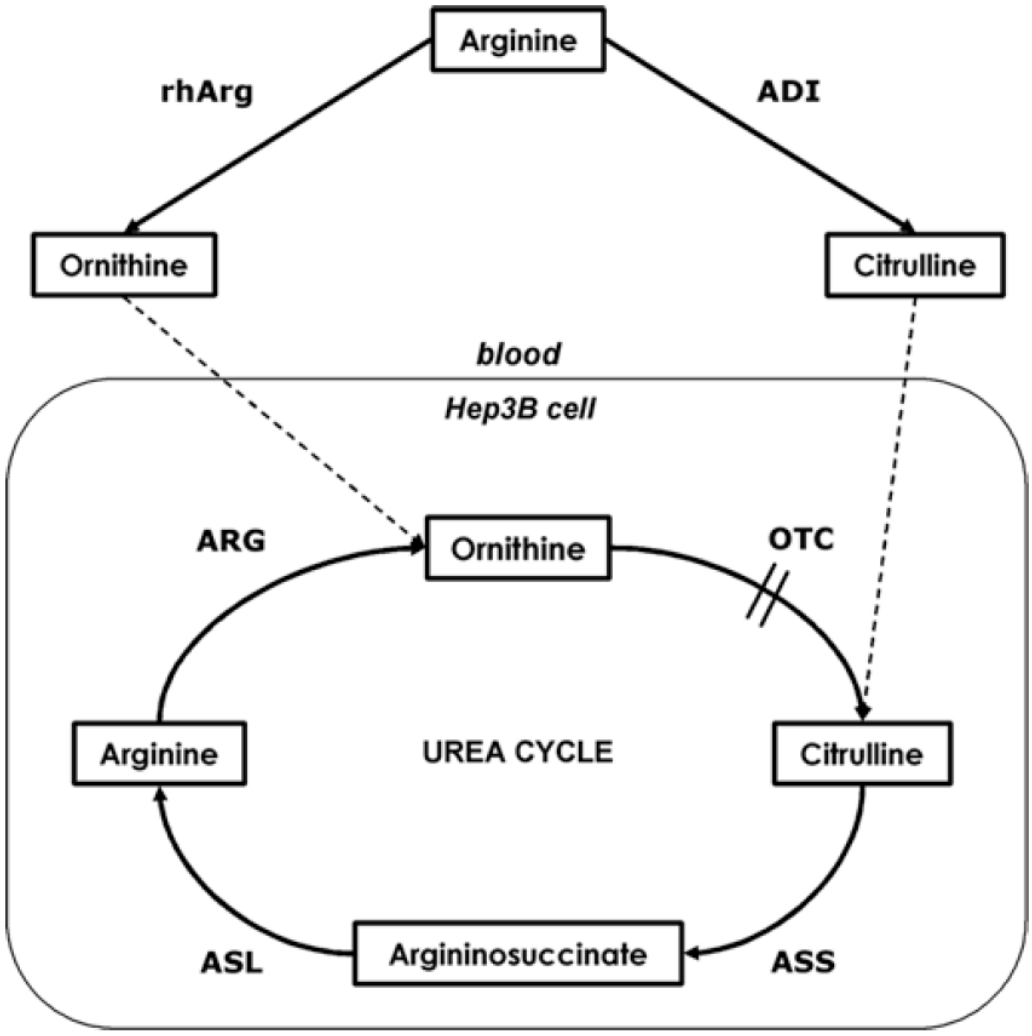

Figure 1. 1. Model relating the expression of urea cycle enzymes and resistance to arginase and ADI treatment (Lam et al., 2009).

For the treatment with ADI, cancer cells express both ASS and ASL will be able to regenerate arginine from citrulline and the growth will be unaffected (Shen et al., 2003). In contrast, cancer cells lacking the expression of either ASS or ASL will be unable to recycle citrulline, hence hampering the growth of cancer cells (Bowles et al., 2008). These results were further confirmed by transfection of ASS siRNA to a small cell lung cancer cell line, SW1222. The expression of ASS in SW1222 was successfully down regulated by the ASS siRNA and the cell become sensitive to ADI treatment (Kelly et al., 2011). In addition, ASS mRNA-deficient melanoma cells transfected with ASS expression plasmid confer resistance to the ADI treatment for both *in vitro* and *in vivo* study (Ensor et al., 2002).

In conclusion, a strong correlation between the expression of urea cycle enzymes and the resistance toward arginase and ADI treatment has been generalized in culture condition. In the hope of further confirm the correlation between ADI resistance and ASS expression in clinical settings, profiling the expression levels of ASS from biopsy sample using real-time PCR and immunohistochemistry staining has been adopted before and during ADI treatment in melanoma patients (L. G. Feun et al., 2012; Ott et al., 2012).

1.4.2. Arginine deiminase as cancer therapeutic agent

Arginine deiminase (ADI) is a microbial enzyme that catalyzes the conversion of arginine to citrulline and ammonia. Mycoplasma contamination has been reported as the cause of growth inhibition in mammalian cell culture (Robinson & Wichelhausen, 1956). ADI was identified as the active principle responsible for depleting the essential nutrient, arginine, in culture which leading to the morphological changes and altered growth rate (Gill & Pan, 1970; Sasaki et al., 1984). The anti-tumor property of ADI was reported since 1990. Mycoplasma extract was found to exert growth inhibitory effect to both human and murine transformed cells (Miyazaki et al., 1990). Further study to test the *in vitro* anti-tumor activity of purified ADI against 6 murine tumor cell lines confirmed that ADI can effectively inhibit the tumor growth for which the IC_{50} value range from 5 to 20 ng/ml. The 6 murine tumor cell lines were injected to mice intraperitoneally, daily injection of the native preparation of ADI significantly prolong the survival time in four out of six tumor lines during the *in vivo* study (Takaku et al., 1992).

More recently, cell culture studies using ADI originated from *Mycoplasma hominis* demonstrated a very potent anti-proliferative effect against melanoma and HCC cell lines possibly mediated through cell cycle arrest and/or apoptosis (Ensor et al., 2002; Gong et al., 1999). To further evaluate the *in vivo* anti-tumor properties of ADI, the circulation half-life was extended through random pegyation using 20 kDa PEG. Once a week injection of the pegylated ADI (ADI-SS $PEG_{20,000\ mw}$) effectively suppress the growth of melanoma transplanted to the tumor bearing mice when compared to the control or unmodified ADI. Moreover, ADI-SS $PEG_{20,000\ mw}$ could also prolong the survival time of HCC tumor bearing mice from less than 7 weeks, when treat by native ADI or saline, to

24 weeks. Interestingly, transfection of ASS to these cell lines making it more resistant to the ADI treatment during both *in vitro* and *in vivo* study (Ensor et al., 2002). Through these proof-of-concept studies, more extensive research has been done on profiling the expression of ASS and the efficacy of ADI to different cancer cell lines. Reports from the literature show that about 10 tumor types respond to the *in vitro* ADI treatment including, although vary in the depth of study, leukemia, mesothelioma, neuroblastoma, melanoma, hepatocellular carcinoma, renal cell carcinoma, stomach, pancreatic, lung and prostate cancer (Bowles et al., 2008; Ensor et al., 2002; Gong et al., 2000; Kelly et al., 2011; J. E. Kim et al., 2009; R. H. Kim et al., 2009; Syed et al., 2013; Szlosarek et al., 2006; Yoon et al., 2007). All these cell lines have a down-regulated or undetectable level of ASS expression. More recently, the tumor biopsy samples from patients diagnosed with renal cell carcinoma and pancreatic cancer also reveal the low incidence of ASS expression which may further expand the use of ADI in these cancers (Bowles et al., 2008; Yoon et al., 2007).

Beside targeting the cancer cells with negative ASS expression, ADI also exhibit a strong antiangiogenic effects for which the growth of new blood vessels would be inhibited in the tumor mass and in turn starving the tumor through nutrient restriction (Park et al., 2003). Based on these results, ADI is a seemingly magic bullet against different types of tumor with negative ASS expression. It has been suggested that profiling the urea cycle enzyme should be adopted especially to determine the ASS expression in the tumor biopsy and therefore a better clinical outcome could be predicted in the foreseeable future (L. G. Feun et al., 2012; Ott et al., 2012). Despite of the personalized approach to identify the tumor with down-regulated ASS expression, tumor expressing ASS would be

ostensibly resistant to this therapeutic due to the capability of the cells to recycle citrulline.

In contrast, arginase, an enzyme that catalyzes last step of urea cycle which converts arginine to ornithine and urea. Except primary culture of hepatocyte and a few minimal deviation hepatoma cell lines, cancer cells are lacking the OTC expression and thus unable to recycle ornithine (Philip et al., 2003). It is plausible that arginase could become effective to both ASS positive and negative cells as long as OTC is down-regulated and this may suggest arginase could be a potential candidate for further investigation.

1.4.3. Arginase as cancer therapeutic agent

The study of arginase as an anti-neoplastic agent could be dated back to 1950s. Early study either using liver extract or purified arginase consistently demonstrated the promising *in vitro* growth inhibitory effects in a number of mouse carcinomas. It has been suggested that the underlining growth inhibitory effects is mediated through the inhibition of mitosis and DNA synthesis.

Further investigation on the *in vivo* anti-tumor efficacy of arginase produced very controversial findings among different laboratories. Bach and Swaine performed a very impressive study having 360 rats transplanted with Walker 256 carcinomas demonstrated that 4 days of arginase treatment could elicit up to 77% of growth retardation (Bach & Swaine, 1965). Studies from Wiswell and Iron & Boyd demonstrated the anti-tumor effects of native arginase in accordance with the mice bearing mammary cancer for which 28% reduction of tumor size was observed. Mice receiving arginine injections or untreated control all died of tumor growth after the 10^{th} daily injection while all mice in the treatment group remain alive at the end of the 10^{th} injection. Similar study with Swiss mice that prone to develop spontaneous tumors were treated with 9 to 240 units of arginase and found that 30-70% reduction in tumor size could be achieved and none of the mice receiving the treatment died of their rumors (Irons & Boyd, 1952; Wiswell, 1951). However, when Greenberg and Sassenrath were trying to verify the study with similar experimental setup, they not only failed to reproduce the favorable results for mammary cancer, but the findings with lymphosarcoma and ascites tumor were also disappointing along with their study. Although the horse arginase could bring down the arginine to about one-seventh of the original serum levels transiently, it is speculated that

sustained low level of arginine is required to inhibit the tumor growth (Greeberg & Sassenrath, 1953). Similar reports has been observed in the studies with murine leukemia cells, L5178Y and L1210, for which complete destruction was observed in culture after 24 hours incubation with arginase, and again the *in vivo* efficacy is not in line with this study and the author ascribed these disappointing results to the high K_m value of the horse arginase (Storr & Burton, 1974). Pegylation has been used successfully to extend the circulation half-life of the bovine arginase where native and the pegylated enzyme could retain 10% and 52% of enzyme activity, respectively, after 12 h of injection (Savoca et al., 1979). Pegylated bovine arginase was effectively against the Taper liver tumor and prolonged the mean survival time of the tumor bearing mice. In contrast, treatment with L6178Y leukemia is dismal because the mean survival time is almost the same between the treatment group receiving either saline or pegylated arginase. The disparity between the *in vitro* and *in vivo* studies was attributed to the high Km value of both native and pegylated bovine arginase at physiological pH (Savoca et al., 1984). When compared to ADI, it is almost 1000 times more potent than bovine arginase (Miyazaki et al., 1990). These negative findings seem not to support the notion that arginase could be a potential therapeutic for cancer treatment.

However, recently, a very impressive study about the depletion of arginine from the systemic circulation in human subject was achieved through systemic release of hepatic arginase via transhepatic arterial embolization in patient diagnosed with advanced and metastatic liver cancer. Most of the patients showing various degrees of tumor regression except 2 non-responders with insignificant changes in the plasma arginine level (Cheng et al., 2005). This encouraging result revived the interest in arginase for cancer treatment.

Our laboratory found that the pegylated arginase could effectively suppress the growth of HCC and melanoma in both *in vitro* and *in vivo* studies and subsequently, *Hernandez et al* and *Hsueh et al* also reported the anti-tumor effect of pegylated arginase toward acute lymphoblastic T-cell leukemia and prostate cancer, respectively (Hernandez et al., 2010; Hsueh et al., 2012).

Recombinant human arginase attenuated the growth of tumor cells by inducing cell cycle arrest and apoptosis. Our laboratory demonstrated that liver cancer cell lines, such as HepG2, Hep3B, Huh7 and PLC/PRF/5, with low level of OTC transcript and undetectable level of OTC activity were inhibited by the arginase treatment possibly because of these cancer cells are incapable of recycling ornithine to arginine while the WiDr and A549 cell lines expressing OTC retained normal growth even in the presence of arginase. On the contrary, transfection of OTC expression plasmid to HepG2, PLC/PRF/5 and Huh7 confers the resistance to arginase treatment. These results support the notion that expression of OTC together with the coupled expression of ASS and ASL, enabling the recycling of the arginine precursor, ornithine (Cheng et al., 2007). More in depth study about these HCC cell lines revealed that the growth inhibitory effect of arginase was due to cell cycle arrest. Wheatley et al suggested that cancer cells with defective restriction checkpoint at G1 phase will keep cycling into the cell cycle while normal cells arrest at G1 phase (Lamb & Wheatley, 2000). Through cell cycle distribution analysis, Hep3B was arrested at G2/M phase and the expression of cell cycle related genes, cyclin B1 and cdc2, critical for the G2/M transition were downregulated. On the contrary, upregulation of Cyclin A1 in both HepG2 and PLC/PRF/5 explains the

observed S phase arrest but the expression of its cdk partner, cdk2, remained unaltered in response to arginase treatment (Lam et al., 2009).

Melanoma cell lines lacking the expression of ASS were sensitive to the ADI treatment because the cancer cells were unable to recycle the arginine precursor, citrulline. Investigation using human arginase to treat melanoma cell lines showed that arginase could also induce growth inhibition for both *in vitro* and *in vivo* study. The growth retardation on melanoma cell lines was related to cell cycle arrest and apoptosis induced by arginase. The study confirmed that cell lines from both human and murine origin that are sensitive to ADI treatment could also be inhibited by arginase. Arginase exerts growth inhibitory effects on the A375 cell line by arresting the cells at both S and G2/M phase. When the A375 cells were exposed to low dose of arginase, the cells arrested mainly in S phase while G2/M phase arrest become more prominent during high dose of arginase incubation. These were supported by upregulation of Cyclin D, E and A and the respective partners, cdk 6 and cdk 2 throughout different dose of arginase treatment while the downregulation of cdc2, together with downregulated Cyclin B expression, at high dose of arginase may responsible for the more significant G2/M phase arrest because the transition from G2 to M phase is mediated by the Cyclin B/cdc2 complex. In contrast, ADI only induces G2/M phase growth arrest in A375 cell line with an overall change on the cell cycle effectors similar to the arginase treatment. Except cdc2, downregulation was seen in all doses of ADI. Besides, Lam *et al* also speculated that the differential response of A375 to arginase and ADI may be due to the enzymatic end-product generated by these enzymes. Ornithine produced by arginase may be converted to polyamines and exhibiting stimulatory effects on cancer cells and pushing the cells

cycling from G1 into S phase as manifested by the relatively lower G0/G1 population observed during arginase treatment (Lam et al., 2010).

Despite HCC and melanoma cell lines undergo cell cycle arrest largely in the S and G2/M phase arrest during arginase treatment, leukemia cell lines exhibit G0/G1 phase arrest likely because of a cell type dependent response (Lam et al., 2009; Lam et al., 2010). The G0/G1 arrest was confirmed with downregulated expression of Cyclin D3 at protein level where the transcript levels remain steadily throughout the incubation. Study with the polysomes and the levels of phosphorylated eukaryotic initiation factor 2 alpha (eIF2α) suggested the global suppression of the translation machinery induced by arginase treatment. Depletion of arginine in T cell acute lymphoblastic leukemia (T-ALL) not only induced cell cycle arrest but also caspase-dependent apoptosis in a time dependent manner via intrinsic pathway. However, when normal primary T cells were incubated with arginase, the cells also being arrested in the G0/G1 phase but not undergo apoptosis. These differential responses between normal and malignant T cells in response to arginase treatment remain to be elucidated (Hernandez et al., 2010).

The promising anti-tumor effects of arginase on HCC, melanoma and leukemia also translated into animal study and even better results could be obtained when combined with different chemotherapeutics. When pegylated arginase was used singly to treat the Hep3B, HepG2 and PLC/PRF/5 tumor bearing mice, a considerable growth inhibition as manifested by the reduced tumor size could be observed in a dose dependent manner (Lam et al., 2009). Interestingly, treatment with low dose of 5-FU did not retard the tumor growth but combination with arginase produced synergistic effects probably because arginine depletion sensitizing the cells to sub-clinical dose of 5-FU therapy

(Cheng et al., 2007; Lam et al., 2009). Similarly, when pegylated arginase was combined with Cytarabine (Ara-C) for the treatment of T-ALL bearing mice, combined therapy significantly prolonged the survival when compared with either pegylated arginase or Ara-C alone (Hernandez et al., 2010).

These promising data obtained from both *in vitro* and *in vivo* study warrants arginase for further evaluation. Especially, through the understanding of the signaling pathways in response to arginine depletion, such as activation of apoptosis, autophagy and cell cycle progression, a more effective treatment strategy through combination of therapeutic agents targeting different pathways could hopefully be developed in the future.

1.4.4. Advance from previous study of recombinant human arginase

Previous study demonstrated that systemic arginine depletion could be achieved by random and multi-pegylated recombinant human arginase. Since regulatory authorities is imposing stringent requirement for the detailed characterization of the drug product whenever possible, presence of a mixture of isomers different in number of PEG attachment and position of PEG conjugated to the lysine residues make the characterization of these isomers nearly impossible. In view of this situation, a site-specific pegylation approach was used in the current investigation that a cysteine residue was rationally engineered to the surface of BCA for which conjugation with a 20 kDa PEG could be easily characterized.

To prepare the recombinant human arginase from the expression from E. coli cells, a series of column chromatography was used for downstream purification. We explored the possibility of using a heat stable arginase, BCA, so as to simplify the purification for which a 2-step purification scheme was developed in this study.

In addition, previous study of pegylated recombinant human arginase only focused on the treatment of hepatocellular carcinoma. We evaluate the strategy of arginine depletion by BCA by expanding the spectrum of cancer types to colorectal and gastric cancer. The underlying mechanisms leading to the growth arrest and cell death was further elucidated.

1.5. Needs for half-life extension technology:

Protein and peptide biopharmaceuticals, such as cytokines, enzymes, antibodies and hormones, have been developed since the advance of recombinant DNA technology (Frokjaer & Otzen, 2005). These promising therapeutics have been widely used in different pathophysiological conditions including hormonal, metabolic, immunological and haematological disorder and cancer. The first generation biopharmaceuticals were designed base on the unmodified, native form of proteins (Hubbell, 2010). These proteins either serve to mimic the functions of the human protein like replacement therapy, such as insulin and monoclonal antibodies (Szymkowski, 2005). Treatment using the first generation biopharmaceuticals received number of drawbacks including physiochemical instability, short circulating half-life, proteolytic instability and immunogenicity. Patients under this kind of therapeutics need frequent administration to maintain the drug efficacy. Besides, even the therapeutics were considered to be immune tolerant, for example, chronic treatment with recombinant human interferon still lead to the formation of neutralizing antibodies and reduced the drug efficacy afterward (C. Ross et al., 2000; Sorensen et al., 2003). In view of these problems, different strategies have been evolved to overcome the limitations including pegylation and FcRn mediated recycling of fusion protein.

1.5.1. Pegylation

Since 1970s, Abuchowski *et al* first demonstrated that attachment of PEG could extend the circulation half-life of BSA and bovine liver catalase with retained activity in the circulation and reduced immunogenicity. Numerous of polymers have been invented to serve this purpose since then which could be further categorized into biodegradable and non-biodegradable polymers. The former one include poly(glutamic acid) (PGA), colominic (polysialic) acid and hydroxyethyl starch while the latter make up of polyethylene glycol (PEG), poly(glycerol) (PG), poly(2-oxazoline), poly(acrylamide), poly(vinylpyrrolidone) and poly(N(2-hydroxypropyl)methacryamide) (PHPMA). Among these polymers, PEG has been widely used for protein conjugation because PEG is chemically inert, non-toxic, non-immunogenic as well as "Generally Regard As Safe" by Food and Drug Administration (FDA) which makes pegylation as a gold standard to improve the physiochemical properties of therapeutic proteins (Hubbell, 2010; Jevsevar et al., 2010). In 1990, the first FDA-approved pegylated protein therapeutic, Adagen, was made available in the market for treating severe combined immunodeficiency (SCID) disease. Nowadays, numerous pegylated protein therapeutics entered different phases of clinical trials and there are nine FDA-approved pegylated protein therapeutics available in the market (Table 1. 1).The rationale of pegylation is basically through attachment of PEG to the therapeutic protein and achieving favorable physiochemical properties such as increasing size of the overall therapeutic, introducing steric hindrance to abrogated intermolecular interactions and enhancement of tumor accumulation through passive targeting (Figure 1. 2) (F. M. Veronese & Pasut, 2005).

Table 1. 1. Different formats of PEG backbone. (A) Forked (B) branced, (C) multi-armed and (D) combed shaped PEG.

Drug	Protein name	PEG size	Site(s) of attachment	Indication	Native half-life (hr.)	Conjugate half-life (hr.)	Year of approval	Company
Adagen® Pegadamase	Adenosine deaminase	5 kDa (11-17 units)	Nonspecific, lysine, serine, tyrosine, histidine	Severe combined immunodeficiency	-	-	1990	Enzon
Oncarspar® Pegaspargase	Asparaginase	5 kDa Multiple	Nonspecific, lysine, serine, tyrosine, histidine	Acute lymphoblastic leukemia	20	357	1994	Enzon
Krystexxa® Pegloticase	Mammalian urate oxidase	10 kDa (10-11 units)	Non-specific lysine	Gout	4	154-331	2010	Savient pharmaceuticals
PEGASYS® Peginterferon-α2b	Interferon alfa-2a	40 kDa	Lysines 31, 121, 131 or 134	Hepatitis C	3-8	65	2002	Hoffmann-La Roche
PEG-INTRON® Peginterferon-α2a	Interferon alfa-2b	12 kDa	Histidine 34 (major)	Hepatitis C	7-9	48-72	2001	Schering-plough / Enzon
Cimzia® PEG-Certolizumab pegol	Anti-TNFα Fab'	40 kDa	Cysteine	Rheumatoid arthritis Crohn's disease	-	-	2008	UCB
Neulasta® Pegfilgrastim	G-SCF	20 kDa	N-terminal methionine	Febrile neutropenia	3.5-3.8	42	2002	Amgen / Nektar
Somavert® Pegvisomant	hGH antagonist B2036	5 kDa (4-6 units)	Nonspecific, lysine, N-terminal phenylalanine	Acromegaly	0.5	>100	2003	Pfizer / Nektar
Mircea® Epoetin beta-methoxy polyethylene glycol	Epoetin-β	30 kDa	Lysine 46 or 52	Anemia accociate with kidney disease	7-20	134-139	2007	Hoffman-La Roche

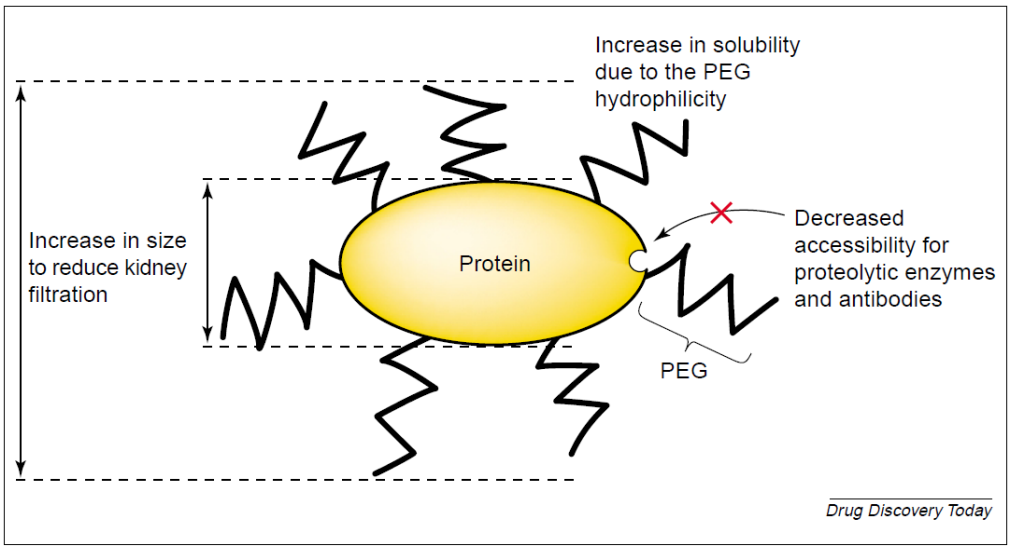

Figure 1. 2. The overall physiochemical changes after pegylation (F. M. Veronese & Pasut, 2005).

Since PEG polymer is nonionic and hydrophilic in nature, and it is highly hydrated by water molecules. Different studies showed that the oxygen atom in each PEG subunit could bind up to 3 water molecules. Therefore, when a protein conjugated with a 20 kDa PEG, it makes the hydrodynamic volume by approximately 5 to10-fold greater than could be predicted from protein with the same molecular weight, which is significantly higher than the threshold value of glomerular filtration and thus the elimination through renal clearance could be minimized (Fishburn, 2008; Roberts et al., 2002). Besides, PEG moiety can adopt dynamic conformation in solution and create a shell-like structure in which PEG polymer could wrap around the protein surface (Morar et al., 2006). By using this model, it could clearly explain the reason why the conjugates are more resistance to proteolytic degradation, as the access to the susceptible residues are impaired. Similarly, the antigenic determinants are being shield from exposure and thereby reduce the formation of neutralizing antibodies and uptake by RES cells. Furthermore, *in vitro* protein stability could also be improved by pegylation because hydrophobic region that involved in protein interaction and subsequent aggregation could be also minimized. Aggregated protein therapeutic could lead to immunological response when administrated to patients and rendering the drug ineffective. Moreover, active angiogenesis in solid tumor usually resulted in increased tumor vasculation and blood flow. Additionally, tumors can also produce some mediators and enzymes, such as nitric oxide and metalloproteinases, which further enhance the permeability of the tumor vasculature with respect to the normal tissue. This unorganized and leaky vasculature allows the conjugates to enter the neoplastic tissues and the extravasted conjugates remains as a result of reduced or undeveloped lymphatic drainage. This allows the passive

accumulation of the biopharmaceuticals inside the tumor mass and such phenomenon was termed “enhanced permeability and retention” (EPR) (Figure 1. 4) (Maeda et al., 2000).

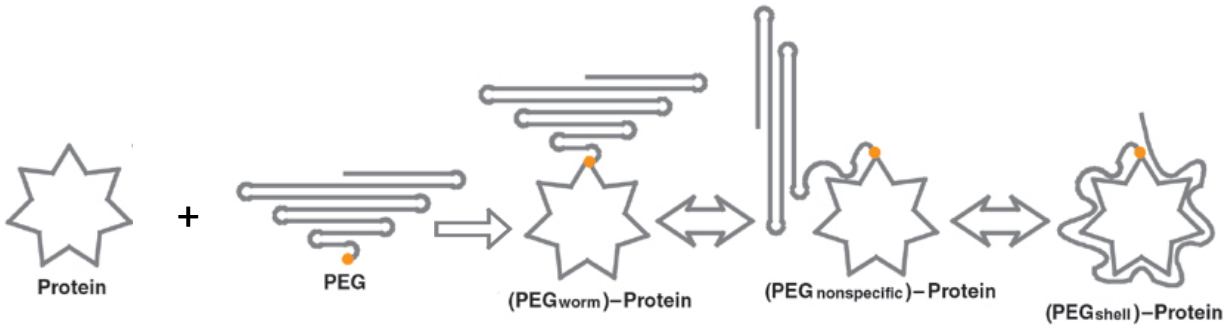

Figure 1. 3 . Dynamic structures of PEG moiety in the solution (Morar et al., 2006).

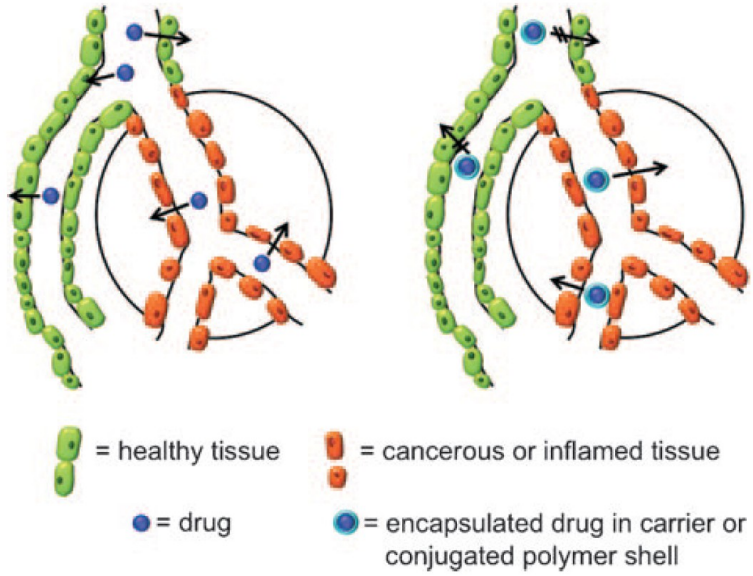

Figure 1. 4. Schematic representation of the enhanced permeability and retention (EPR) effect (Knop et al., 2010).

A successful pegylation is governed by throughout understanding on both of the structure-function relationship of the target proteins as well as the physiochemical properties of the PEG molecules. For protein, reactive amino acids, such as lysine, cysteine, histidine, arginine, aspartic acid, glutamic acid, serine, threonine, tyrosine, N-terminal amino acid, C-terminal amino acid as well as the vininal hydryxyl group of glycoprotein are potential candidates for conjugation (Pisal et al., 2010).

In general, the N-terminal amino acid, lysine and cysteine are most commonly exploited for PEG conjugation in which the distribution and the prevalence of these reactive amino acids will determine the site and the number of PEG attachment, respectively. For example, lysine is one of the most abundant amino acids in the protein and it may contribute up to 10% of the total amino acids. Pegylation through this amino acid usually resulted in a mixture of conjugates, these isomers vary from the number of PEG attached to the site of attachment (Roberts et al., 2002). It could be expected that isomer having more conjugations would exhibit longer circulation half-life but the different in the degree of conjugation would imply the less conjugated protein are more exposed in the circulation and therefore more immunogenic and susceptible to clearance. Moreover, isomers exist even the protein have the same degree of modification, these isomers may vary in the pharmacological properties possibly through modification of residue that would severely affect the receptor binding affinity in certain forms of isomer. Separation of isomers from the heterogeneous mixture could be very challenging which makes the characterization of therapeutics more complicated. Usually, more stringent requirement has been imposed by FDA towards the pegylated biopharmaceutical which required the

evidence of reproducibility and thereby minimizing the batch to batch variation (Harris & Chess, 2003; F. M. Veronese & Pasut, 2005).

During the early development of pegylation, PEG molecules activated with different functional groups have been invented, mainly, to target lysine residues (Constantinou et al., 2010; Roberts et al., 2002). These molecules were produced in different chain length and proteins conjugated with longer chain are generally exhibiting slower clearance (Molineux, 2004). PEG molecule apart from linear format, such as branched chain, folk shape, multi-arm and comb shape have been created by different chemistries (Figure 1. 5). The branch chain PEG has been evaluated and demonstrated that it could offer a greater extension on circulation half-life. The difference are attributed to better shielding from proteolytic degradation and reducing immunogenicity rather than increase the hydrodynamic volume of the branch chain conjugates. In fact, conjugation to branched chain PEG do not resulted in significant different in hydrodynamic volume and some studies showed that the branched chain conjugates appear even smaller than the linear counterpart (Caserman et al., 2009; Francesco M. Veronese et al., 1997).

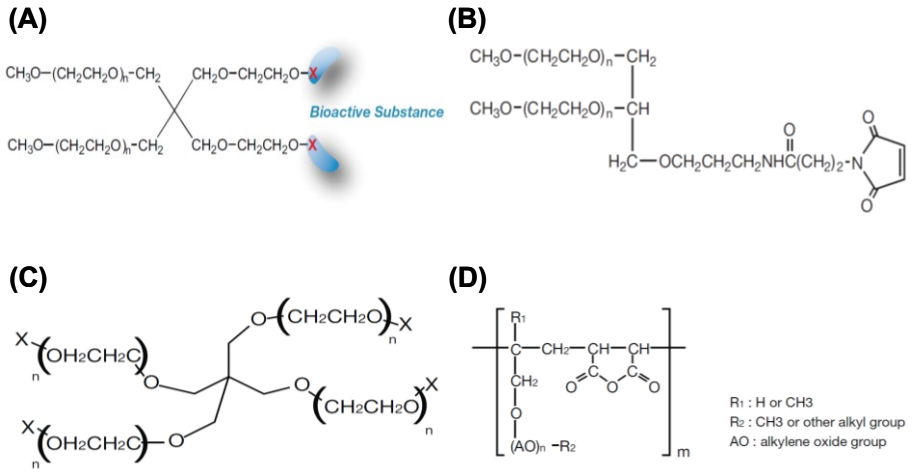

Figure 1. 5. Different formats of PEG backbone. (A) Forked (B) branced, (C) multi-armed and (D) combed shaped PEG (Info extracted from NOF catalogue ver.13).

Despite pegylation has been widely used by to extend the circulation half-life and improve physiochemical properties of many therapeutics. However, some drawbacks have been noted and it is also worthwhile to understand the limitations such as hampered interaction and activity resulted from steric hindrance, potential reactivity towards the immune system and accumulation of PEG in the body under certain circumstances. In general, pegylated proteins usually exhibit different physiochemical properties from the parent drug. The highly hydrated and flexible PEG moiety creates steric hindrance which impedes the enzyme-substrate or receptor-ligand binding and resulted in diminished *in vitro* biological activity. However, this can be compensated by prolonged plasma circulating time and thus increasing the overall systemic exposure. The resulting changes in the pharmacological profile creates an overall improvement on therapeutic efficacy and therefore (Table 1. 1), the *in vivo* biological activity is usually enhanced (Fishburn, 2008). Besides, PEG molecules are generally regarded as non-immunogenic, but a few reports in the literature suggest that chronic exposure and repeated administration of pegylated liposome and proteins could induce anti-PEG immune response resulted in formation of neutralizing antibodies again the PEG moiety (Ganson et al., 2006). Lastly, high dose of pegylated proteins could also induce the renal tubular vacuolization in some toxicology studies, yet this phenomenon disappears on cessation of treatment and no toxic consequences have been observed (Bendele et al., 1998). As a consequence, the use of PEG derivatives still regarded as immunologically safe and non-toxic under most circumstances.

Lastly, it is also worth to mention that Opaxio and FCE28068 using polymer PGA and PHPMA, respectively, are now in phase III clinical trial which may also facilitate the

development of alternative polymers (Knop et al., 2010). Since application of PEG molecules, especially for site-specific pegylation and branched chain PEG reagents, usually protected by numerous patents and strained marketing strategies, development of alternative polymers would definitely speed up the progress on drug development in the future (Jevsevar et al., 2010).

1.5.2. Albumin binding domain (ABD)

Recent discovery revealing the extended circulation half-life of Albumin and immunoglobulin G (IgG) was based on the neonatal fragment crystalliable receptor (FcRn) recycling process (Andersen & Sandlie, 2009). Since then genetic engineering of fusion proteins by tethering albumin, Fc region (fraction crystallizable) of IgG or the binding domains to the target therapeutics have been used to extend the circulating half-life (Kontermann, 2011).

The Fc receptor mediated recycling of fusion proteins make use of the nature of albumin and IgG when these proteins were constantly internalized through endocytosis, it will bind to the Fc receptor. Inside the endosome, the acidic environment, around pH 6, further enhance the binding of albumin and IgG moiety to the Fc receptor while the unbound ligands will be destined to the lysosomal compartment for degradation. The receptor-ligands complex will be returned to the cell membrane where physiological pH trigger the release of ligands and thus recycling back to the circulation and extended the half-life of fusion proteins (Figure 1. 6) (Andersen et al., 2011).

Instead of fusion to albumin or Fc region, non-covalent interaction with the albumin through fusion to streptococcus protein G (SpG) albumin binding domain has been recently developed to extend the circulation half-life of protein therapeutics, such as CD4, human soluble complement receptor type 1 (sCR1), affibody and single-chain diabody (scDb) (Makrides et al., 1996; P.A.; Nygren et al., 1991; R. Stork et al., 2007; Tolmachev et al., 2007).

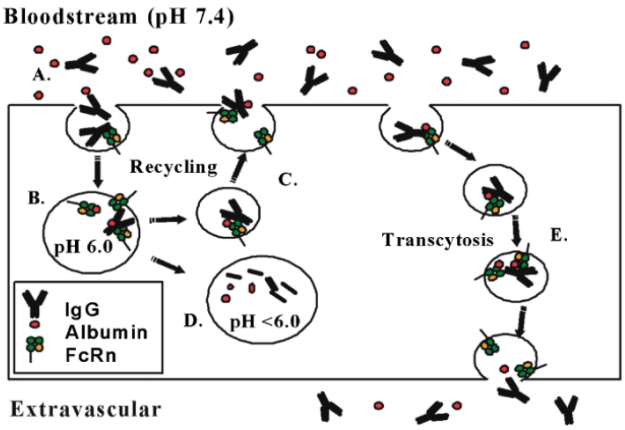

Figure 1. 6. Schematic illustration of the FcRn mediated recycling pathway (Andersen & Sandlie, 2009).

Many gram positive bacteria express surface receptor to serum proteins, like albumin, IgG, fibronectin and plasmin, which is regarded as the mechanism to escape from the host immune system and thus important for pathogenesis (Forsgren & Sjöquist, 1966; Kronvall et al., 1979; Kuusela, 1978; Lottenberg et al., 1987). Streptococcus protein G is one of the most studied bacteria surface receptors and it consists of 3 albumin binding domains and 3 IgG binding domains (Olsson et al., 1987). Since the discovery of ABD from SpG, various lengths of these moieties have been widely used as a tool for affinity purification of albumin and depletion of albumin from sample, such as serum for 2-D PAGE analysis (Dardé et al., 2007; P. A. Nygren et al., 1988). Besides, the use of ABD as affinity tag to facilitate the purification of target proteins has been proposed (P. A. Nygren et al., 1988). The break through development of ABD arises from the *in vivo* study aiming to extend the circulation half-life of CD4 through fusion to ABD. The circulation half-life of this CD4 fusion protein was extended from 15-24 h to 48 h when compared to the parent CD4 molecule. The even more promising result has been demonstrated in macaques for which the half-life of the native CD4 was found to increase from 6 h to 16 days after fusion to ABD (Makrides et al., 1996; P.A.; Nygren et al., 1991). More importantly, the same research group also confirm in the later study that fusion of ABD to sCR1 not only extend the circulation half-life by 1.6-2.9 folds but the fusion protein also retained the complement inhibitory activity and binding affinity to albumin (Makrides et al., 1996).

While the use of ABD in various lengths has been successfully demonstrated in different applications, the discussion below will be focused on the 46 amino acids which has been defined minimal albumin-binding motif and further evaluated from the structural and

functional perspectives (Sjolander et al., 1997). The structure analysis by NMR showed that ABD is a left-handed antiparallel triple-helix motif which is thermally and chemically stable but containing no disulphide bonds, metal ions, cross links and bound ligands (Johansson et al., 2002; Kraulis et al., 1996). The melting temperature of ABD was found to be about 70°C and was able to refold after thermal denaturation while up to 6 M guanidium hydrochloride denaturant could not completely unfold the ABD domain (Gülich et al., 2000; Rozak et al., 2005). The binding activity of ABD to albumin was determined by alanine scanning through which the surface exposed amino acid residues pointing to different directions were selected from each of the three helical structures. Further mutations around the participated amino acid confirmed the binding region on ABD is mainly located at helix 2 and some of the residues in vicinity located in helix 3 (Linhult et al., 2002). Through resolving the co-crystallized complex of ABD and HSA using X-ray crystallography, the domain II of albumin was found to interact with the helix 2 and 3 of ABD while the FcRn binding site was mapped on the domain III of HSA (Andersen et al., 2012; Lejon et al., 2004). The non-overlaping of ABD and FcRn binding domain on HSA molecule was manifested by a competitive ELISA study. The plate coated with HSA was incubated with FcRn and titrated against increasing concentration of ABD, HSA and IgG where high concentration of ABD do not interfere the binding of HSA and IgG toward FcRn. The same pH-dependent binding kinetic of HSA to FcRn could be reproduced even when ABD is fused to affibody molecule $(Z_{HER2-342})_2$. With the carefully consideration to the orientation of binding region for both ABD and affibody, the fusion protein could retain similar affinity toward the soluble recombinant domain of HER2 when compared to the parent molecule (Andersen et al., 2011). Besides, the

persistence of the binding activity between ABD fusion protein (ABD-scDb) and HSA at acidic condition (pH 6) also play an important role in the FcRn mediated recycling process. Conversely, if the ABD fusion protein exhibiting lower binding affinity at acidic pH such as inside the endosome, it may dissociate from albumin and diverted to lysosomal compartment for degradation. Thus, the extension of circulation half-life through FcRn mediated recycling will be hampered (R. Stork et al., 2009; R. Stork et al., 2007). These biochemical studies are also in coherence with the animal study trying to confirm the role of FcRn heavy chain in the knock-out mice model with a scDB molecule. The tri-functional scDB targeting both carcinoembryonic antigen (CEA) and CD3 was either tethered to ABD or conjugated to a 40 kDa PEG molecule. Basically, the circulation half-life of scDb (5.6 h) was significantly improved for both of these molecules, scDb-ABD and scDb-A'-PEG40, exhibit similar circulation half-life in normal mice model (47.9-53.0 h). However, a 2-fold reduction of the circulation half-life of scDb-ABD (24.8 h) has been observed when pharmacokinetic study was performed in FcRn heavy chain knock-out mice but comparable elimination half-life was recorded for the scDb-A'-PEG40 molecule (51.4 h) . These data provided support for the involvement of FcRn in recycling the fusion protein and hence prolong the half-life in the circulation. Interestingly, even both of these molecules exhibit similar circulation half-life, a 2-fold higher of tumor accumulation for scDb-ABD in the CEA+ tumor bearing mice has been reported in the biodistribution study (R. Stork et al., 2009). These observations was plausibly explained by the relatively small hydrodynamic radius of albumin bound scDb-ABD complex (4.8 nm), in contrasted to scDb-A'-PEG (7.9 nm), which facilitates the

extravasation and tumor penetration and thus increased accumulation (Roland Stork et al., 2008).

In view of the direct relationship between the affinity of the ABD molecule and the circulation half-life, ABD was engineered with different binding affinity by phage display system. The wild-type ABD possesses binding affinity to albumin from different species and nanomolar affinity toward HSA been used as a template. Out of the 46 amino acids from the ABD, 15 surface exposed amino acids located at helix 2 and 3 were chosen for various degree of randomization. Picomolar affinity was reported for the first generation variants where sequence features obtained from the individual variants were combined to produce the second generation variants. A set of 7 variants were generated and 6 of them were prone to aggregate in solution at room temperature. Except a variant, denote ABD035, which was exhibiting wild-type like secondary structure, relatively high melting point, 58 °C and able to refold after thermal denaturation. The biosensor study showed that ABD035 possess 50-500 fM affinity to HSA which is about 2400-fold increased when compared to the wild-type ABD (Jonsson et al., 2008).

The ABD035 variant was further evaluated to see if higher affinity or valency could translate into extended circulation half-life. The scDb-ABD fusions were engineered either by tethering wild-type ABD to both termini of scDb (scDb-ABD_2) or ABD with low, high (ABD035) and wild-type affinity to C-terminus of scDb. Surprisingly, the circulation half-life of scDB-ABD2 is similar to scDB-ABD, 37.9 and 36.4 h, respectively. This indicated that the increase of hydrodynamic radius through binding 2 albumins to scDB would not further extend the circulation half-life of scDb. While fusion of wild-type ABD to scDb extended the circulation to 36.4 h, a low and high affinity

version of ABD could also extend the circulation half-life of ABD to 28.4 h and 47.5 h, respectively. This results indicated that low affinity ABD could also exert a pronounce effect to extend the circulation half-life of fusion protein but increasing the affinity of ABD from nanomolar to fentomolar could still marginally improve the circulation half-life (Hopp et al., 2010). In addition, improvement in binding affinity could not only further extend the circulation half-life but also contribute to the biodistribution of the fusion molecule. Study with affibody molecule in 2 separate studies showed that fusion of ABD035 to $Z_{HER2:2891}$ extend the circulation half-life to 41 h while a previous study reported the circulation half-life about 35.8 h when $Z_{(HER2:342)2}$ was fused to the wild-type ABD (Orlova et al., 2013; Tolmachev et al., 2007). However, fusion to ABD035 further improved the biodistribution of $Z_{HER2:2891}$ by further reducing the hepatic and renal uptake by 1.8 and 2.8-fold, respectively, when compare to the wild-type ABD fusion (Orlova et al., 2013).

In conclusion, fusion to ABD offers an attractive approach to prolong the circulation half-life of different therapeutic molecules. The production of ABD may be cost efficient because it can be easily expressed in bacterial cell with high yield. The ABD is a relatively small domain of 5 kDa and fusion to this domain may produce only minimal interference to the target protein. Besides, ABD could be engineered to different affinity and in turn modulating the circulation half-life based on the purpose of different applications. Moreover, the preclinical study of ABD fusion protein in different model animal such as mice, rat, rabbit and monkey may be easily carried out because of the wide specificity of ABD toward the albumin from different species (Andersen et al., 2011). Lastly, the through deimmunization of ABD using *in silico* T-cell epitope

prediction programs, it should favor the clinical development of ABD in the future (Frejd, 2012).

2. Methodology

2.1. Construct of *Bacillus caldovelox* arginase (BCA) expression vector

The gene encoding wild type BCA (Pubmed accession no.: U48226) was order from GenScript and the pUC57 vector containing the BCA insert was transformed into TOP10 *E. coli* competent cells. To obtain single colonies, the transformed cells were streak on agar plate containing 100 µg/ml ampicillin and incubated at 37°C overnight. Single colonies were picked from the agar plate and inoculated into 5 ml LB medium containing 100 µg/ml ampicilin for overnight culture at 37°C. Glycerol stocks were prepared by aseptically adding 0.3 ml of 50% glycerol to 0.7 ml overnight culture. The glycerol stocks were kept at -80°C. For the preparation of mutant BCA (S161C), the cells from 1.5 ml overnight culture were collected by centrifugation at 10,000 x g. The plasmids were extracted from the *E. coli* cells using illustra plasmidPrep Mini Spin Kit (GE healthcare) and following manufacture's instructions. A pair of mutagenic oligonucleotide prime (5'-gacgcaaatcggcggatactgccccaaaatcaag-3' and 5'-cttgattttggggcagtatccgccgatttgcgtc-3') was designed and the mutation was engineered to the BCA using QuickChange Site-Directed Mutagenesis kit. Briefly, 50 ng of plasmid was used as template and 125 ng of each primer was included in a 50 µl reaction. Before the amplification, the reaction mixture was incubated at 95°C for 30 s. For the PCR reaction, 12 cycles of heat denaturation at 95°C for 30 s, annealing at 55°C for 1 min and extension at 68°C for 5.5 min were performed using DNA thermal MyCycler (Bio-Rad). The PCR reaction mixture was allowed to cool down to room temperature and 1 µl of Dpn *I* (10 U/µl) restriction enzyme was added to digest the methylated parental DNA template by incubating the reaction at 37°C for 1 h. After Dpn I digestion, the mutated plasmids were transform to the TOP10 competent cells and single colonies were obtained as described above. Glycerol stocks

were prepared and the mutation was confirmed by DNA sequencing. To sub-clone the engineered BCA gene into the pET-3a expression vector, a pair of primer flanking the engineered BCA gene was designed to incorporate a NdeI restriction site through the forward primer (5'- ggaattcc*CATATG*AAGCCAATTTCAATTATCG-3') while a BamHI restriction site together with the six-Histidine tag were added through the reverse primer (5'-cg*GGATCC*TTA*GTGATGGTGATGGTGATG*CATGAGTTTTTCACCAAACAACG-3'). For a 50 µl PCR reaction, 50 ng of plasmid DNA was used as template and amplified by 1 units of iProof High-Fidelity DNA Polymerase (Bio-Rad). The template was subjected to an initial denaturation step at 98°C for 30s while 30 cycles of amplification including heat denaturation at 98°C for 10 s, annealing at 55°C for 30s and extension at 72°C for 30 s. The forward and reverse primer at the final concentration of 1 µM was used for PCR and the reaction products were subjected to 1% agarose gel electrophoresis. The band gave the size corresponding to the BCA was excised from the gel and purified using illustra GFX PCR DNA and Gel Band Purification Kit (GE healthcare). Both purified PCR product and the pET-3a plasmid was double digested in the presence of 1 Unit of NdeI and BamHI endonuclease (NEB) in 50 µl reaction. The double digestion reaction was incubated at 37°C for 1 h. The digested plasmids and inserts were subjected to 1% agarose gel electrophoresis and the corresponding bands were purified. The digested and purified inserts and plasmid in a 3 to 1 ratio was ligated together with the help of T4 DNA Ligase (Life technologies) at room temperature for at least 1 h. The ligation product was transformed to TOP10 competent cells and the sub-cloning of engineered BCA to pET-3a vector was confirmed by endonuclease double digestion using NdeI and BamHI while the sequence of engineered BCA with the addition of six-

Histidine tag was confirmed by DNA sequencing. The pET-3a vector containing an engineered BCA with 6xHis-tag at C-terminus was named pET-3a-BCA(S161C) and transferred to BL21(DE3) for expression.

2.2. Expression and purification of BCA

An overnight seed culture of the *E. coli* strain BL21 (DE3)pLysS transformed with plasmid pET-3a-BCA(S161C) was prepared in 5 ml LB medium containing 100 μg/ml ampicilin and it was allowed to growth in the shake flask at 37℃ for 16 h with 280 rpm shaking. For 250 ml LB medium containing 100 μg/ml ampicilin, 2.5 ml overnight culture was added and cultured at 37 ℃ with shaking at 280 rpm until the optical density reach 0.8-0.9 at 600 nm. Isopropyl β-D-thio-galactopyranoside (IPTG) was added to final concentration of 0.2 mM. After 4 h induction, the cell was harvested by centrifugation at 12000 x g for 20 min at 4℃. The cell pellet could either be disrupted by sonication and proceed to purification, or kept at -20℃ until required. The cell pellet was suspended in 20 ml solubilization buffer [50mM Tris-HCl, 100mM NaCl, pH 7.4] containing 10 mM $MnCl_2$. The cell was first disrupted by sonication on ice for 10 min with pulse for ever 30 sec at 40% amplitude. The cell debris was removed by centrifugation at 12000 x g for 20 min at 4℃. The supernatant was incubated at 70℃ for 15 min and precipitates formed during the heat treatment step were removed by centrifugation. Soluble fraction was passed filtered through 0.22 μm filter before loading to the 5ml HisTrap Chelating HP column.

The flow through fraction was collected during sample loading and the unbound proteins were washed out by 5 CV of starting buffer or until the baseline level off. The target proteins bound on the column was eluted out by competitive gradient elution using imidazole [0.5M imidazole in start buffer]. The target fractions was identified and pooled together which will be buffer exchanged in 20 mM sodium phosphate at pH 7.4 using

Amicon Ultra-15 Centrifugal Filter Unit with 10 kDa MW cutoff following manufacture's instruction. The sample was filtered under sterile condition by 0.22 μm filter and stored at 4 ℃ until required.

2.3. Determination of BCA activity

The activity of BCA was assayed by direct colorimetric method using Diacetyl monoxime (DAMO) which determines the amount of product being formed, urea, in the enzymatic reaction. Briefly, a serial dilution of 0.3 ml BCA solutions together with 0.15 ml water and 720 mM arginine substrate at pH 7.4 was pre-incubated separately at 37 ℃ for 10 min. The enzymatic reaction was carried out by adding 0.3 ml arginine substrate to the pre-incubated enzyme solutions. The reaction mixture was incubated at 37℃ for exactly 5 minutes and quenching reagent [50% Trichloroacetic acid (TCA)] was added to stop the reaction. The sample blanks were prepared in the similar way but the same volume of enzyme solutions was added after TCA solution.

The urea formed from the above reaction was quantified using the DAMO direct colormetric method described by World Health Organization (WHO). This protocol has been adopted by WHO as the Standard Operating Procedures (SOP) for measuring the blood urea concentration. Several reagents were prepared regarding the SOP, **mixed acid reagent** was prepared by slowly adding 100 ml concentrated sulphuric acid to 400 ml distilled water followed by 0.3 ml stock acid reagent [0.5 g ferric chloride hexahydrate in 15 ml of distilled water and make up to 25 ml by concentrated phosphoric acid]. **Mixed color reagent** was prepared by mixing 35 ml stock colour reagent A [1 g diacetyl monoxime in 50 ml distilled water] and 35 ml stock colour reagent B [0.25 g thiosemicarbazide in 50 ml distilled water] and make up to 500 ml with distilled water. **Working urea standard** was prepared by adding 5 ml of stock urea standard [0.5 g urea in 50ml benzoic acid] to 45 ml benzoic acid [1 g/dl]. The DAMO assay was carried out by adding 100 µl of 20-fold diluted reaction mixture to a glass boiling tube and followed

by 3 ml of colour development reagent which is freshly prepared by mixing distilled water, mixed colour reagent and mixed acid reagent in 1:1:1 ratio. The tubes were incubated in boiling water bath for 15 min and allowed to cool to room temperature for 5 min. The absorbance at 540 nm was measured. One unit arginase was defined as the amount of enzyme that converts a micormole of arginine to ornithine and urea per minute at 37 ℃, pH 7.4. The enzyme activity was calculated using the following equations, the absorbance value of the sample was subtracted from its blank:

$$\Delta A_{540nm} \text{ Sample} = A_{540nm} \text{ Sample} - A_{540nm} \text{ Sample Blank}$$

The amount of urea produced was calculated from the standard curve:

$$\text{Units/ml enzyme} = \frac{(\text{umole of urea liberated})(df)}{(5)(0.3)}$$

df = Dilution factor of enzyme

0.3 = volume (in milliliters) of enzyme used

5 = time (in minutes) of the assay per the unit definition

2.4. Site-specification pegylation

Prior to pegylation, 2 mg/ml BCA was reduced in the presence of 10 equivalents of tris(2-caroxyethyl)phosphine (TCEP). The optimum amount of PEG for the pegylation of BCA was determined by adding different equivalents of PEG to BCA at pH 7.4 at 4°C. After optimized the amount of PEG for pegylation, the duration, pH and temperature was further evaluated. Sample collected at different time points were quenched with 100 mM cysteine and stored at -80°C until SDS-PAGE analysis.

2.5. Construction of BCA-ABD expression vector

A pair of prime encoding the albumin binding domain were constructed and amplified by overlap PCR. Briefly, 200 ng of primers was used as template and amplified by 1 units of iProof High-Fidelity DNA Polymerase (Bio-Rad). The primers were incubated at 98°C for 30s while 15 cycles of amplification including heat denaturation at 98°C for 10 s, annealing at 60°C for 30s and extension at 72°C for 15 s.

5'-Sense-ABD

GCGCAGCATGATGAAGCCGTGGATGCGAACAGCTTAGCTGAAGCTAAAGTCT
TAGCTAACAGAGAACTTGACAAATATGGAGTAAGTGACTATTACAAGAACC

5'-Anti-sense-ABD

TTAAGGTAATGCAGCTAAAATTTCATCTATCAGTGCTTTTACACCTTCAACAG
TTTTGGCATTGTTGATTAGGTTCTTGTAATAGTCACTTACTCCAT

The ABD domain constructed by this pair of prime was amplified by 2 different set of primes so as to construct BCA-6xHis-ABD (BHA) and BCA-ABD-6xHis (BAH). For the construction of BHA, the ABD was firstly amplified by following pair of primer for which the forward primer was designed for the overlap PCR with the BCA via the six-Histidine tag while BamHI restriction site and stop codon will be introduced for the ligation to pET-3a vector using the reverse primer:

Forward primer for cloning ABD:

5'- GCATCACCATCACCATCACGCGCAGCATGATGAAG-3'

Reverse primer for cloning ABD:

5'- cg*GGATCC*TTAAGGTAATGCAGCTAAAATTTCATCTAT-3'

The PCR product from the amplification of ABD was subject to 1.5% agarose gel electrophoresis and the PCR products were purified. While the engineered BCA with an extra mutation (V20P) was cloned using the following pair of primer for which the stop codon was deleted:

Forward primer for cloning BCA:

5'-ggaattcc*CATATG*AAGCCAATTTCAATTATCG-3'

Reverse primer for cloning BCA:

5'- GTGATGGTGATGGTGATGCA-3'

The BCA amplified by the above primer was subject to 1% agarose gel electrophoresis and the PCR products were purified. The above PCR product of BCA and ABD was tethered by overlap PCR. Similarly, 200 ng of BCA and ABD was used as template and amplified by 1 units of iProof High-Fidelity DNA Polymerase (Bio-Rad). The BCA and ABD were incubated at 98°C for 30s while 15 cycles of amplification including heat denaturation at 98°C for 10 s, annealing at 60°C for 30s and extension at 72°C for 30 s. The product from overlap PCR was used as template for further amplification using the following pair of primer:

Forward primer for cloning BHA:

5'-ggaattcc*CATATG*AAGCCAATTTCAATTATCG-3'

Reverse primer for cloning BHA:

5'-cg*GGATCC*TTAAGGTAATGCAGCTAAAATTTCATCTAT-3'

The PCR product was subjected to 1% agarose gel electrophoresis and the band corresponding to BHA was excised from the gel for purification.

For the construction of BAH, the ABD was firstly amplified by following pair of primer for which the forward primer was designed for the overlap PCR directly with the BCA while BamHI restriction site, six-Histidine tag and stop codon will be introduced for the via the reverse primer:

Forward primer for cloning ABD:

5'-CGTTGTTTGGTGAAAAACTCATGGCGCAGCATGATGAAG -3'

Reverse primer for cloning ABD:

5'-cg*GGATCC*TTAGTGATGGTGATGGTGATGAGGTAATGCAGCTAAAATTTCATCTAT-3'

The PCR product from the amplification of ABD was subject to 1.5% agarose gel electrophoresis and the PCR products were purified. While the engineered BCA with an extra mutation (V20P) was cloned using the following pair of primer for which the stop codon and six-Histidine tag were deleted:

Forward primer for cloning BCA:

5'-ggaattcc*CATAT*GAAGCCAATTTCAATTATCG-3'

Reverse primer for cloning BCA:

5'- GTGATGGTGATGGTGATGCA-3'

The BCA amplified by the above primer was subject to 1% agarose gel electrophoresis and the PCR products were purified. The above PCR product of BCA and ABD was tethered by overlap PCR. Similarly, 200 ng of BCA and ABD was used as template and amplified by 1 units of iProof High-Fidelity DNA Polymerase (Bio-Rad). The BCA and ABD were incubated at 98°C for 30s while 15 cycles of amplification including heat denaturation at 98°C for 10 s, annealing at 60°C for 30s and extension at 72°C for 30 s. The product from overlap PCR was used as template for further amplification using the following pair of primer:

Forward primer for cloning BAH:

5'-ggaattcc*CATAT*GAAGCCAATTTCAATTATCG-3'

Reverse primer for cloning BAH:

5'-cg*GGATCC*TTAGTGATGGTGATGGTGATGAGGTAATGCAGCTAAAATTTCATCTAT-3'

The PCR product was subjected to 1% agarose gel electrophoresis and the band corresponding to BHA was excised from the gel for purification. The PCR product encoding BHA and BAH and the pET-3a vector were double digested with NdeI and BamHI. The BHA and BAH were ligated to the pET-3a vector and transformed to TOP10 competent cells. The nucleotide sequence of BHA and BHA was confirmed by DNA sequencing. The pET-3a vector containing the BHA and BAH insert was transformed to the BL21(DE3) vector for protein expression.

2.6. Gel filtraiton

To determine the size and oligomeric structure of protein in native state, proteins were separated on the Superdex 200 HR Prep Grad XK26/60 gel filtration column. The column was equilibrated using 0.05M sodium phosphate pH 7.4 with 0.15 M NaCl. The gel filtration column was calibrated by a set of protein MW marker prepared at 1 mg/ml, ribonuclease A (15.6 kDa), BSA (66.0 kDa), Alcohol dehydrogenase (150.0 kDa), β-Amylase (200 kDa), Apoferritin (443.0 kDa), Thyroglobulin (669.0 kDa) (Sigma-Aldrich) while the column void volume was determined by blue dextran (2000 kDa). To determine the MW of our sample, 1-2 ml of sample was injected at the concentration 1-3 mg/ml).

2.7. Determination of molecular weight (MW) for pegylated BCA by MALDI-ToF MS

The MW of pegylated BCA was determined by MALDI-TOF MS. Mass spectra were acquired using a Waters Micromass MALDI micro MX Mass Spectrometer. Equal volume of pegylated BCA was mixed with 10 mg/ml spinapinic acid (SA) for which it was freshly prepared in 50% of 0.1% trifluoroacetic acid and 50% acetonitrile. An amount of 1 µl of sample-matrix mixture was spotted on the stainless steel sample plate until air dry for which the sample plate was placed into the mass spectrometer. Ionization of pegylated BCA was assisted by SA when irradiated by a nitrogen laser operating at a wavelength of 337 nm. Data were acquired in the positive linear mode of operation. The accelerating voltage in the ion source was 18 kV and the extraction delay 500 ns.

2.8. Amino acid analysis

To determine the amino acid content from the protein sample, equal volume of sample was mixed with 10% SSA (5-sulphosalicyclic acid) solution for 1 h at 4 °C so as to precipitate the protein from the sample. The protein precipitated was removed by centrifugation at maximum for 10 min. The supernatant was recovered and filter through 0.2 μm filter. Equal volume of lithium citrate loading buffer was mixed with the sample prior to amino acid analysis. Amino acid standards (A6282 and A 6407; Sigma-Aldrich) were prepared to give a final concentration of 10 nmole/20 μl. Furthermore, A Long Program could be used if the complete profile of amino acid composition in the sample is required or a Short Program could be used if a particular amino acid in the sample is interested.

2.9. Circular dichroism (CD) spectrometry

The circular dichroism (CD) of BCA before and after pegylation was determined by Jasco J-810 spectropolarimeter through monitoring the far-UV region (190 – 250 nm). Samples were buffer exchanged to 10 mM potassium phosphate at pH 7.4 and the protein concentration was adjusted to 0.3-0.5 mg/ml. Samples were loaded to a cuvette of 1 mm path length and the temperature was maintained at 25 °C throughout the analysis. Each spectrum was obtained from the average of 3 scans and the fractional content of secondary structures was analyzed by CDPro software.

To determine the thermal stability of different samples, the ellipticity at 222 nm was monitored at a function of temperature. Briefly, the ellipticity at 222 nm was monitored when the temperature was increase from 20 to 95 °C at a rate of 1 °C per min. The thermal denaturation curve of different sample could be monitored and the melting temperature (Tm) could be calculated by taking first derivative.

2.10. Determination of protein concentration

The protein concentration was determined by Bradford's assay. The Protein Assay Dye Reagent Concentrate (Bio-rad) was diluted 5 times before use. 20 ul of sample was mixed with 1 ml diluted dye reagent and incubated at room temperature for 10 min. To determine the protein concentration, the mixture was measure at 595 nm with Quick Start Bovine Serum Albumin Standard Set (Bio-rad) as standard in the range of 0-1 mg/ml.

2.11. Mammalian cell culture and proliferation assay

The cell lines MKN45, AGS, BGC823, HCT-15 and HCT-116 were maintained in RPMI Medium with 10 % FBS and 100 units/ml penicillin/streptomycin. The cells were cultured in an incubator set to 37°C, with the supply of humidified atmosphere of 95% air and 5% CO_2. When the cells were grown to 80-90% confluence, the culture medium was discarded and washed with PBS at pH 7.4. The cells were lifted by the treatment of 0.25% trypsin-EDTA at 37°C for 3 minutes. Complete medium was added to the culture container to inactivate the trypsin solution and the cell suspension was transfer to a 50 ml falcon tube. The cell pellet was obtained by centrifugation at 100 x g for 3 min. at room temperature. The supernatant was removed and the cell pellet was resuspended by complete medium through repeated pipetting. About 1/10 of the cells were passed into a new container of similar size.

To prepare a cell stock for long term storage, 1 x 10^6-10^7/ml of cells were prepared in complete medium containing 50% FBS and 5% DMSO and stored in cryogenic vials. The cryogenic vials were put into an isopropanol chamber and keep at -80°C freezer for 24 h. The vials were transferred to liquid nitrogen tank for long term storage. To thaw cells, the frozen stock was retrieved from liquid nitrogen and incubated at 37°C water bath for 1-2 min. The cell suspension was transferred to pre-warmed complete medium for culture. The cell lines used for the current study were checked and free from mycoplasma contamination.

2.12. Cell proliferation assay

Cells (5 x 10^3) in a volume of 100 µl of growth medium were seeded to each well of a 96-well plate and incubated for 24 h. The culture medium was replenished by arginine free medium (AFM) supplemented with different concentrations of arginine, fresh medium containing various concentrations of different arginine depleting enzymes as well as using these enzymes in combination with citrulline. The plate was incubated for an additional 1-3 days at 37 °C in an incubator containing a humidified atmosphere of 95 % air and 5 % CO2.

Quantitative cell proliferation assays were performed using MTT (3-[4,5-dimethylthiazol-2-yl]-2,5-diphenyl tetrazolium bromide) assays as widely described elsewhere which measure the dehydrogenase activity in metabolically active cells. Briefly, 10 µl of MTT (5 mg/ml) was added to each well and incubated for an additional 4 h to allow the reduction of tetrazolium salt by dehydrogenase in metabolically active cells. The reaction was quenched by adding 100 µl 0.1 N HCl in 10% SDS and the plate was allowed to stand overnight in the incubator to dissolve the formazan crystal. The resulting colored solution is quantified by using microplate reader (Biorad) at wavelength 570 nm with reference to 655 nm. The dada were analysed by Prism 4.0 (Graphpad Software) using non-linear regression model for sigmoidal curve fitting. The amount of arginine depleting enzyme required to kill 50% of the cells in a culture was defined as IC_{50}.

2.13. Semi-quantity reverse transcription-polymerase chain reaction (RT-PCR)

Cells were harvested in routine culture and the total RNA was extracted using the Qiagen RNeasy kit following manufacture's instruction. After RNA extraction, total RNA was reverse-transcribed into cDNA using iScript cDNA synthesis kit (Bio-Rad, CA) for which 1 μg of RNA was used to set up a 20 μl reverse transcription reaction at 42°C for 30 min using DNA thermal MyCycler (Bio-Rad). After the RT reaction, the reverse transcriptase was inactivated by incubation at 85°C for 5 min. For a 50 μl PCR reaction, 2 μl of cDNA from different cell line as well as the positive control of human liver cDNA library (Clontech) was used as template and amplified by 1 units of iTaq DNA polymerase (Bio-Rad). The iTaq DNA polymerase was activated at 95°C for 3 min while 30 cycles of amplification including heat denaturation at 95°C for 30 s, annealing at 55°C for 30s and extension at 72°C for 1.5 min. The forward and reverse primers for ASS, ASL, OTC, ARGI and GAPDH at the final concentration 1 μM were used for PCR and the reaction products were subjected to 1% agarose gel electrophoresis. The primer sequence and the corresponding size of PCR products were listed below:

Human ASS (448 bp product):

S: 5'-GGGGTCCCTGTGAAGGTGACC-3';

AS: 5'-CGTTCATGCTCACCAGCTC-3'

Human ASL (219 bp product):

S: 5'-CTCCTGATGACCCTCAAGGGA-3';

AS: 5'-CATCCCTTTGCGGACCAGGTA-3'

Human OTC (221 bp product):

S: 5'-GATTTGGACACCCTGGCTAA-3';

AS: 5'-GGAGTAGCTGCCTGAAGGTG-3'

Human ARGI (969 bp product):

S: 5'- ATGAGCTCCAAGCCAAAGTC-3';

AS: 5'- TCACTTAGGTGGTTTAAGGT-3'

Human GAPDH (307 bp product):

S: 5'-TGAACGGGAAGCTCACTGG -3';

AS: 5'-TCCACCACCCTGTTGCTGTA-3'

2.14. Immunoblotting

To determine the levels of different protein targets by immunoblotting, 50-100 µg protein samples were resolved on the protein gel and then transferred to the Immobilon-PSQ membrane (EMD Milipore) using Tetra blotting module (Bio-Rad) in the presence of transfer buffer (0.025 M Tris, 20% methanol, 0.192 M glycine and 0.03% SDS) at 100 V for 1.5 h with mixing inside the cool room. After the transfer, the membrane was blocked with blocking buffer (5% non-fat dry milk (Bio-Rad) in TBST buffer (0.02M Tris, 0.15 M NaCl, 0.05% Tween 20)) for 1 h at room temperature with mixing on a platform shaker. The membrane was washed with TBST for 3 times at room temperature, 5 min. each on the platform shaker. According to the manufacture's suggestion, the primary antibody was prepared in the range of 1:1000 to 1:10000 dilutions using 5% BSA (Roche) in TBST buffer and incubated overnight at 4°C with gentle agitation. The membrane was washed 3 times with TBST buffer at room temperature, 5 min each on the platform shaker. Secondary antibody was diluted to 1:10000 using blocking buffer and incubated with the membrane at room temperature for 1 h with agitation. The membrane was washed 3 times with TBST buffer, 5 min each. Discard the TBST buffer, Immobilon Western Chemiluminescent HRP Substrate (EMD Millipore) was added to the membrane and incubated at room temperature for 5 min. The chemiluminescent image was documented by ChemiDoc XRS system (Bio-Rad).

2.15. Cell cycle analysis by flow cytometry

For cell cycle analysis, 3×10^5 cells/well were seeded in 6-well plates 1 day prior to the treatment. After exposed to different concentration of BCA, the cells were collected after 24 h, 48 h and 72 h of treatment. The cells were lifted by adding 0.25% trypsin-EDTA (Invitrogen) and incubated at 37°C for 3 min. The cell pellets were obtained by centrifugation at 100 x g and washed twice with PBS at pH 7.4. The cells were fixed with 70 % ice-cold ethanol for at least 30 min and stored at -20 °C if not proceed further. Before cell cycle analysis, ethanol was removed from the fixed cells and washed with PBS at pH 7.4. The cells were then stained with propidium iodide (PI) staining solution (PI, 2 mg/ml; RNase A, 10 mg/ml in PBS) for 30 min at 37 ^{o}C in dark. Stained cells were analyzed using fluorescence-activated cell sorting (FACS; Beckton Dickinson Co). The percentages of cells in sub-G_1, G_0/G_1, S and G_2/M phases were analyzed using ModFit LT 3.0 (Verity Software House).

2.16. Evaluation of apoptosis by annexin V-FITC and PI double staining

To evaluate the induction of apoptosis by BCA, 3 x 10^5 cells were seeded in 6-well plate one day prior to different treatment conditions. The medium was withdrawn and replenished with complete medium supplemented with different concentration of BCA. After exposed to BCA for 24h, 48h and 72 h, both floating cells and adherent cells were collected. Briefly, the floating cells in culture medium were collected by centrifugation at 100 x g for 3 min at room temperature while the adherent cells were washed with PBS and lifted by incubating with 0.25% trypsin solution for 3 min at 37°C. After addition of complete medium, the cells were collected by centrifugation. The cells were washed with PBS and resuspended in 0.1 ml binding buffer (0.01 M HEPES, pH 7.4; 0.14 M NaCl; 2.5 mM $CaCl_2$) containing PI and annexin V-FITC. The cells were stained in dark at room temperature for 15 min and 0.4 ml of binding buffer was added to each tube prior to flow cytometry analysis using FACSAria (BD biosciences). The cytometer was set to acquire the data from 10000 cells for each sample and the data were analyzed by the FACSAria software.

2.17. Evaluation of apoptosis by the activation of caspase-3

After exposing 3 x 10^5 cells to different concentrations of BCA, the cells were harvested at different time points similar to the previous evaluation of apoptosis by PI and annexin-V double staining. Both floating and adherent cells were collected for active caspase-3 analysis using CaspGLOW fluorescein active caspase-3 staining kit (BioVision). Briefly, after washing with PBS, the cells were resuspended in 300 µl complete medium and 1 µl of FITC-DEVD-FMK was added to the cell suspension. The cells were stained for 45 min in culture condition inside the incubator and then washed twice with 0.5 ml Wash Buffer. The stained cells were resuspended in 0.3 ml of Wash Buffer and subjected to flow cytometry analysis using FACSAria (BD biosciences). The cytometer was set to acquire the data from 10000 cells for each sample and the data were analyzed by the FACSAria software.

2.18. Evaluation of mitochondria outer membrane permeabilization by JC-1 Dye

After exposing 3 x 10^5 MKN45 and HCT-15 cells to 15 U/ml BCA for 72 h, the cells were stained by JC-1 dye to evaluate the possibility of initiation of apoptosis through mitochondrial membrane permeabilization (MOMP). Briefly, both floating and adherent cells were collected at the end of the treatment for which the the cells were resuspended in 500 µl complete medium and 1 µl JC-1 dye was added to the cell suspension. The cells were stained for 10 min in culture condition inside the incubator and then washed twice with 0.5 ml PBS. The stained cells were resuspended in 0.5 ml PBS and subjected to flow cytometry analysis using FACSAria (BD biosciences). The cytometer was set to acquire the data from 10000 cells for each sample and the data were analyzed by the FACSAria software. The JC-1 dye accumulates in high concentration inside the mitochondria will give red fluorescent colour (590 nm) while the presence of J-monomer in cytosol gives green fluorescent signals (527 nm).

2.19. Animal Studies

2.19.1. Pharmacokinetic study of BCA

The pharmacokinetic properties of BCA before and after pegylation were investigated through single dose injection of 250 U/ml native and pegylated BCA to BALB/C mice via i.p. route. Mice of 4 to 8 weeks old were randomly assigned into two groups and each group consisted of 5-6 mice. Around 80-100 µl blood samples were collected from saphenous vein of the thigh before injection (time 0), and 4, 8, 24, and 48 h after injection of native BCA, while the blood samples from the group receiving pegylated BCA were collected at 0, 6, 24, 48, 72, 96, 120 and 144 h. Sera were prepared from the blood samples through centrifugation at 1500 x g for 10 min in a refrigerated centrifuge set to 4 °C. Prior to the determination of arginase activity, the urea present in the serum samples were removed by buffer exchange. The enzymatic activity of BCA was assayed for all collected samples using QuantiChrom Urea Assay Kit (Bioassay system).The mean serum activity-time curves were constructed and the elimination half-life of native and pegylated BCA were analysed by noncompartmental model while the AUC measuring the overall exposure was calculated by trapezoidal rule.

2.19.2. Pharmacodynamic studies of BCA

The serum samples collected for pharmacokinetic study were immediately used for the pharmacodynamic studies. To determine the arginine levels in the serum samples, 8 µl serum samples were mixed with 32 µl PBS. The protein content was cleared by precipitation using 40 µl of 10% 5'-sulfosalicylic acid (SSA; Sigma-Aldrich) solution and kept at 4 °C for 1 h. The supernatant was collected by centrifugation at maximum speed for 10 min in a refrigerated centrifuge set to 4°C. Equal volume of lithium citrate loading buffer was mixed with 70 µl of supernatant and filtered with 0.2 µm filter before subjected to amino acid analysis (Biochrom).

2.19.3. *In vivo* efficacy of different BCA treatment on nude mice bearing tumor xenograft

For the preparation of MKN45 tumor xenograft, 1 x 10^6 MKN45 cells were subcutaneously injected to the flank of BALB/c nude mice. When the tumors reached 1.5-2.0 cm in diameter, they were excised, cut into tumor fragments and implanted into the flank of nude mice. The tumor growth was closely monitored by measuring the tumor volume. Once the stable growth of tumors was maintained, the mice were randomly divided into 4 groups. Each group consisted of 10 mice with average tumor volume of about 400 mm^3. Pegylated BCA (250 U/ml) were administrated twice per week to nude mice bearing tumor xenograft through i.p. injection while weekly administration of 10 mg/kg 5-FU was either injected singly or in combination with 250 U/ml pegylated BCA. The control group were injected with PBS as vehicle control. Tumor dimensions were measured *in situ* twice per week throughout the treatment period using digital caliper and the tumor volume was estimated using the formula, 0.5 x length x $(width)^2$. For the body weight of the tumor bearing mice, it was monitored on a weekly basis throughout the course of treatment. At the end of the study, the mice were sacrificed and the tumors were excised for actual tumor weight measurement.

2.20. Statistical analyses

Statistical analyses were performed using Prism 4.0.

3. Preparation and characterization of BCA

3.1. Precis:

The successful development of recombinant human arginase as a potential anti-cancer therapeutic was largely attributed to the cutting-edge pegylation technology. The *in vitro* efficacy could be extended to the *in vivo* study only if the therapeutic enzymes could remain in the body and maintain a low level of arginine in the systemic circulation over a period of time. Formulation of recombinant human arginase with mPEG-SPA_{5000} resulted in a random conjugation of PEG to the lysine residues and the degree of pegylation/modification varied from 1 to 6 PEG molecules per arginase in the resultant isomeric mixture (Tsui et al., 2009). These isomers differ not only by the number of PEG modifications but also the site of attachment and thus variation in the pharmacological properties would be expected. Therefore, the US FDA is imposing stringent requirements on the reproducibility of pegylation and detailed characterization of pegylated products such as, identification of each isomer whenever possible (F. M. Veronese & Pasut, 2005). Recent advancement in pegylation technology allows the synthesis of functional moieties on the PEG molecules that specifically react with cysteine residues. Generally, the abundance of surface accessible free cysteine is comparatively lower than the lysine residue. Rational approach could thus be exploited to introduce cysteine residue(s) to the protein surface by genetic engineering and allowing precise control of the site(s) of pegylation (Harris & Chess, 2003). Site-specific pegylation provides advantages such as relatively homogeneous product and avoidance of any unfavorable conjugation that would hamper the ligand-receptor binding or enzymatic activity of the therapeutic proteins (Ensor et al., 2002; Foser et al., 2003; Grace et al., 2001).

Study to generate the revolutionary arginase therapeutic using rational genetic engineering approach would be the focus of this chapter. Arginase originated from the extreme thermophile *Bacillus caldovelox* was considered owing to the thermostability that may facilitate the design, purification and characterization of the enzyme. Based on the X-ray crystal structure which has been resolved, a cysteine residue and a six-histidine tag were rationally introduced to the surface and C-terminus of the protein, respectively, by genetic engineering. The *Bacillus caldovelox* arginase (BCA) was cloned into the pET3a vector and transformed into the *E.coli* strain BL21(DE3). In the presence of isopropyl β-D-1-thiogalactopyranoside (IPTG), expression of target gene was driven by the strong T7 promoter. Shake flask culture was used as a pilot to test the expression of BCA and a simple 2-step purification scheme was set up to purify the BCA to almost homogeneity, as examined by SDS-PAGE.

Modification of BCA with 20 kDa PEG, ME-200MA, linked via engineered cysteine residue was optimized on the bases of pH, temperature, duration and the molar excess of PEG required for the pegylation process. Characterization of both native and pegylated BCA revealed physical properties that may provide insight to help establish the large scale purification process. In order to produce a sufficient amount of BCA for *in vivo* efficacy and pharmacological studies, a robust and large scale purification scheme was established to handle the cell mass produced by fed-batch fermentation.

Moreover, considering the half-life extension strategy other than chemical modification, a fusion protein, BCA-ABD, has been constructed through tethering the albumin binding domain (ABD) to the C-terminus of BCA. The preliminary findings shown that the fusion

protein not only retained the affinity to human serum albumin (HSA) but also the catalytic activity of BCA.

3.2. Construction of BCA expression vector

The gene encoding BCA (Pubmed accession no.: U48226) was ordered from GenScript where it was synthesized by *de novo* and inserted into pUC57 cloning vector. The single cysteine residue was introduced by site-directed mutagenesis while the six-histidine tag was added to the C-terminus to facilitate the protein purification process. The engineered BCA gene was subcloned into the pET-3a vector and transformed into BL21(DE3) competent cells for BCA expression.

3.2.1. Rational approach for site-specific pegylation

In contrast to targeting lysine residues for random pegylation, a site-specific approach was used through exploiting the structure-function relationship of BCA. When considering the site to introduce the cysteine residue, amino acid residues at the interface of hexameric structure, making up the domain of active site, coordinating the manganese co-factor or interacting with the above functional domains would not be considered. Moreover, the site of PEG conjugation was introduced further away from the active site so as to minimize the effect of steric hindrance that may be introduced by the PEG moiety. Using the crystal structure of BCA (PDB: 2CEV) available in the protein data bank (PDB) (Bewley et al., 1999), a surface-exposed serine residue at position 161 was mutated to cysteine (Ser161→Cys) through site-directed mutagenesis (Figure 3. 1). The mutation was confirmed by DNA sequencing where the point mutation of A to T at position 481 corresponds to the mutation of serine to cysteine residue at position 161 (Figure 3. 2 and Figure 3. 3).

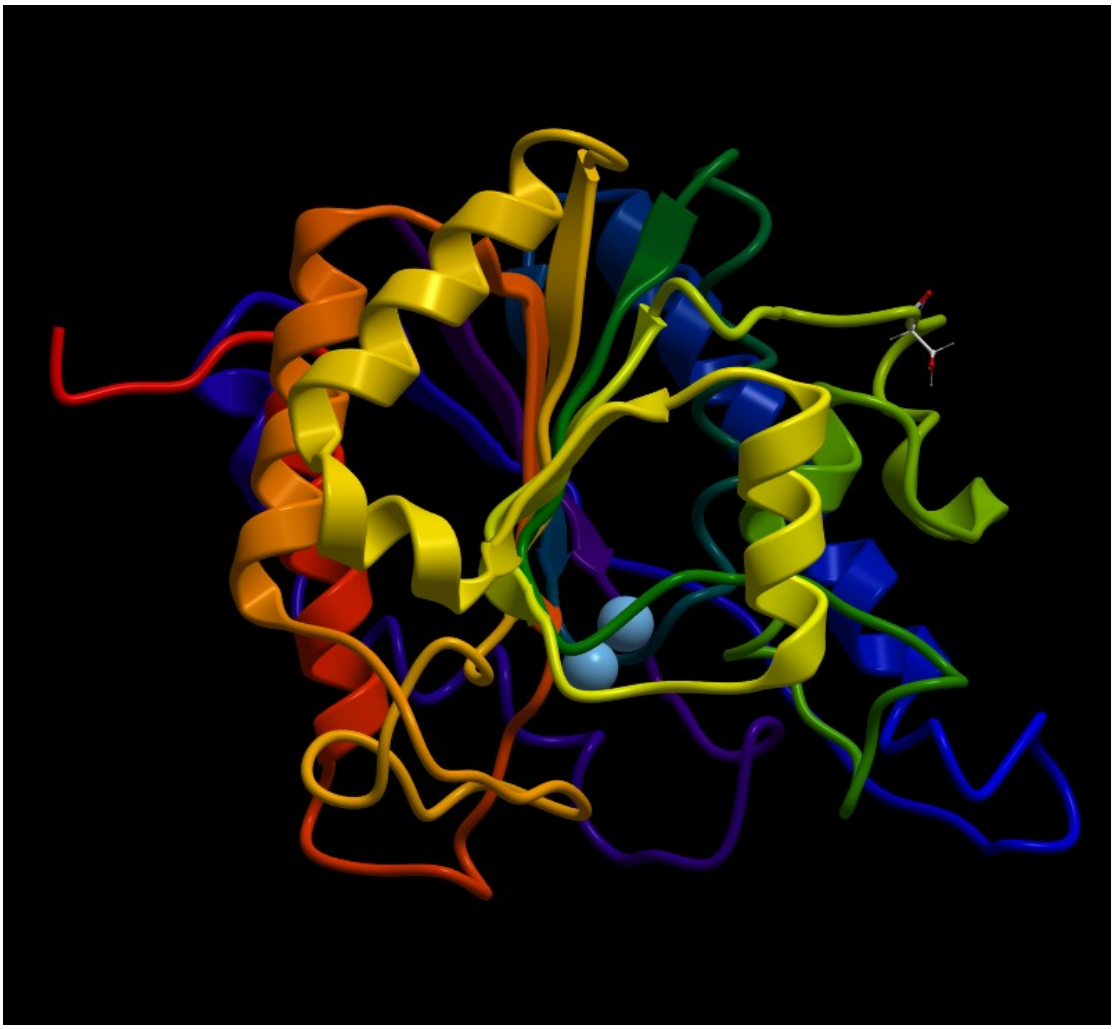

Figure 3. 1. Crystal structure of BCA (PDB: 2CEV) retrieved from the protein data bank. The ribbon diagram shows the structure of BCA containing the two catalytic manganese ions co-factors (Blue spheres) and the surface exposed serine residue at position 161 is showen by the ball and stick representation (Right). The surface-exposed and extended C-terminal regions (Red) are located opposite to the serine residue (Left).

```
Query  1    ATGAAGCCAATTTCAATTATCGGGGTTCCGATGGATTTAGGGCAGACACGCCGCGGCGTT  60
            ||||||||||||||||||||||||||||||||||||||||||||||||||||||||||||
Sbjct  1    ATGAAGCCAATTTCAATTATCGGGGTTCCGATGGATTTAGGGCAGACACGCCGCGGCGTT  60

Query  61   GATATGGGGCCGAGCGCAATGCGTTATGCAGGCGTCATCGAACGTCTGGAACGTCTTCAT  120
            ||||||||||||||||||||||||||||||||||||||||||||||||||||||||||||
Sbjct  61   GATATGGGGCCGAGCGCAATGCGTTATGCAGGCGTCATCGAACGTCTGGAACGTCTTCAT  120

Query  121  TACGATATTGAAGATTTGGGAGATATTCCGATTGGAAAAGCAGAGCGGTTGCACGAGCAA  180
            ||||||||||||||||||||||||||||||||||||||||||||||||||||||||||||
Sbjct  121  TACGATATTGAAGATTTGGGAGATATTCCGATTGGAAAAGCAGAGCGGTTGCACGAGCAA  180

Query  181  GGAGATTCACGGTTGCGCAATTTGAAAGCGGTTGCGGAAGCGAACGAGAAACTTGCGGCG  240
            ||||||||||||||||||||||||||||||||||||||||||||||||||||||||||||
Sbjct  181  GGAGATTCACGGTTGCGCAATTTGAAAGCGGTTGCGGAAGCGAACGAGAAACTTGCGGCG  240

Query  241  GCGGTTGACCAAGTCGTTCAGCGGGGGCGATTTCCGCTTGTGTTGGGCGGCGACCATAGC  300
            ||||||||||||||||||||||||||||||||||||||||||||||||||||||||||||
Sbjct  241  GCGGTTGACCAAGTCGTTCAGCGGGGGCGATTTCCGCTTGTGTTGGGCGGCGACCATAGC  300

Query  301  ATCGCCATTGGCACGCTCGCCGGGGTGGCGAAACATTATGAGCGGCTTGGAGTGATCTGG  360
            ||||||||||||||||||||||||||||||||||||||||||||||||||||||||||||
Sbjct  301  ATCGCCATTGGCACGCTCGCCGGGGTGGCGAAACATTATGAGCGGCTTGGAGTGATCTGG  360

Query  361  TATGACGCGCATGGCGACGTCAACACCGCGGAAACGTCGCCGTCTGGAAACATTCATGGC  420
            ||||||||||||||||||||||||||||||||||||||||||||||||||||||||||||
Sbjct  361  TATGACGCGCATGGCGACGTCAACACCGCGGAAACGTCGCCGTCTGGAAACATTCATGGC  420

Query  421  ATGCCGCTGGCGGCGAGCCTCGGGTTTGGCCATCCGGCGCTGACGCAAATCGGCGGATAC  480
            ||||||||||||||||||||||||||||||||||||||||||||||||||||||||||||
Sbjct  421  ATGCCGCTGGCGGCGAGCCTCGGGTTTGGCCATCCGGCGCTGACGCAAATCGGCGGATAC  480

Query  481  AGCCCCAAAATCAAGCCGGAACATGTCGTGTTGATCGGCGTCCGTTCCCTTGATGAAGGG  540
             ||||||||||||||||||||||||||||||||||||||||||||||||||||||||||||
Sbjct  481  TGCCCCAAAATCAAGCCGGAACATGTCGTGTTGATCGGCGTCCGTTCCCTTGATGAAGGG  540

Query  541  GAGAAGAAGTTTATTCGCGAAAAAGGAATCAAAATTTACACGATGCATGAGGTTGATCGG  600
            ||||||||||||||||||||||||||||||||||||||||||||||||||||||||||||
Sbjct  541  GAGAAGAAGTTTATTCGCGAAAAAGGAATCAAAATTTACACGATGCATGAGGTTGATCGG  600

Query  601  CTCGGAATGACAAGGGTGATGGAAGAAACGATCGCCTATTTAAAAGAACGAACGGATGGC  660
            ||||||||||||||||||||||||||||||||||||||||||||||||||||||||||||
Sbjct  601  CTCGGAATGACAAGGGTGATGGAAGAAACGATCGCCTATTTAAAAGAACGAACGGATGGC  660

Query  661  GTTCATTTGTCGCTTGACTTGGATGGCCTTGACCCAAGCGACGCACCGGGAGTCGGAACG  720
            ||||||||||||||||||||||||||||||||||||||||||||||||||||||||||||
Sbjct  661  GTTCATTTGTCGCTTGACTTGGATGGCCTTGACCCAAGCGACGCACCGGGAGTCGGAACG  720

Query  721  CCTGTCATTGGAGGATTGACATACCGCGAAAGCCATTTGGCGATGGAGATGCTGGCCGAG  780
            ||||||||||||||||||||||||||||||||||||||||||||||||||||||||||||
Sbjct  721  CCTGTCATTGGAGGATTGACATACCGCGAAAGCCATTTGGCGATGGAGATGCTGGCCGAG  780

Query  781  GCACAAATCATCACTTCAGCGGAATTTGTCGAAGTGAACCCGATCTTGGATGAGCGGAAC  840
            ||||||||||||||||||||||||||||||||||||||||||||||||||||||||||||
Sbjct  781  GCACAAATCATCACTTCAGCGGAATTTGTCGAAGTGAACCCGATCTTGGATGAGCGGAAC  840

Query  841  AAAACAGCATCAGTGGCTGTAGCGCTGATGGGGTCGTTGTTTGGTGAAAAACTCATGTAA  900
            ||||||||||||||||||||||||||||||||||||||||||||||||||||||||||||
Sbjct  841  AAAACAGCATCAGTGGCTGTAGCGCTGATGGGGTCGTTGTTTGGTGAAAAACTCATGCAT  900

Query  901
            ||||||||||||||||||
Sbjct  901  CACCATCACCATCACTAA  918
```

(6xHis-tag) coding sequence

Figure 3. 2. DNA sequence aligment between the wild-type gene and engineered BCA gene. Query and Sbjct represent the wild-type gene and the engineered BCA gene, respectively. An A to T mutation was introduced by SDM at position 481 (red in color) which would generate a Cys residue of position 161 in the protein. The six-histidine tag coding sequence was added to the 3'-end of the DNA (underlined) during the cloning of the BCA gene from the pUC57 vector.

MKPISIIGVPMDLGQTRRGVDMGPSAMRYAGVIERLERLHYDIEDLGDIPIGKAERLHEQ
GDSRLRNLKAVAEANEKLAAAVDQVVQRGRFPLVLGGDHSIAIGTLAGVAKHYERLGVIW
YDAHGDVNTAETSPSGNIHGMPLAASLGFGHPALTQIGGYCPKIKPEHVVLIGVRSLDEG
EKKFIREKGIKIYTMHEVDRLGMTRVMEETIAYLKERTDGVHLSLDLDGLDPSDAPGVGT
PVIGGLTYRESHLAMEMLAEAQIITSAEFVEVNPILDERNKTASVAVALMGSLFGEKLMH
HHHHH

Figure 3. 3. The protein sequence of the engineered BCA. The cysteine residue at position 161 and 6xHis-tag are highlighted in yellow and blue, respectively.

3.2.2. Engineering of polyhistidine tag to BCA

Downstream purification of BCA was facilitated by introducing a 6-histidine tag (6xHis-tag) to the C-terminus of BCA. A pair of primers flanking the coding region of BCA has been designed not only for subcloning the BCA(S161C) to the pET3a vector but also to introduce the 6xHis-tag at the C-terminus. The PCR product was analyzed on 1% agarose gel where the band in between 900-1000 bp corresponded to the target DNA (Figure 3. 4). The target DNA was extracted from the agarose gel. The engineered BCA gene and pET3a vector were double-digested with NdeI and BamHI restriction endonucleases. The products after restriction digestion were cleaned up and ligated together using T4 DNA ligase. The ligation product was transformed into the Top10 competent cells and the colonies formed on the agar plate containing ampicillin represent the transformation of pET-3a plasmid. Colonies were inoculated into 5 ml LB broth containing ampicillin for overnight culture at 37°C. To confirm the successful subcloning of the engineered BCA gene, plasmids were purified by miniprep and double digested with NdeI and BamHI. The products after restriction digestion were analyzed by electrophoresis in 1% agarose gel. The band at about 4.6 Kb and 0.95 Kb referred to the pET-3a vector and the gene encoding the engineered BCA, respectively. (Figure 3. 5). The gene sequence was further verified by nucleotide sequencing as shown in Figure 3. 2. The pET-3a vector containing an engineered BCA with 6xHis-tag at C-terminus was named pET-3a-BCA(S161C) (Figure 3. 6).

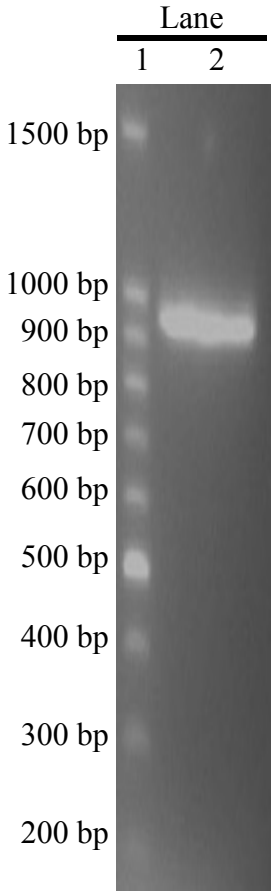

Figure 3. 4. Cloning of the BCA gene from the pUC57 vector. Lane 1 shows the 100 bp DNA ladder. The PCR product was analyzed on 1% agarose gel as shown in Lane 2. The band in between 900-1000 bp represents the gene coding the engineered BCA.

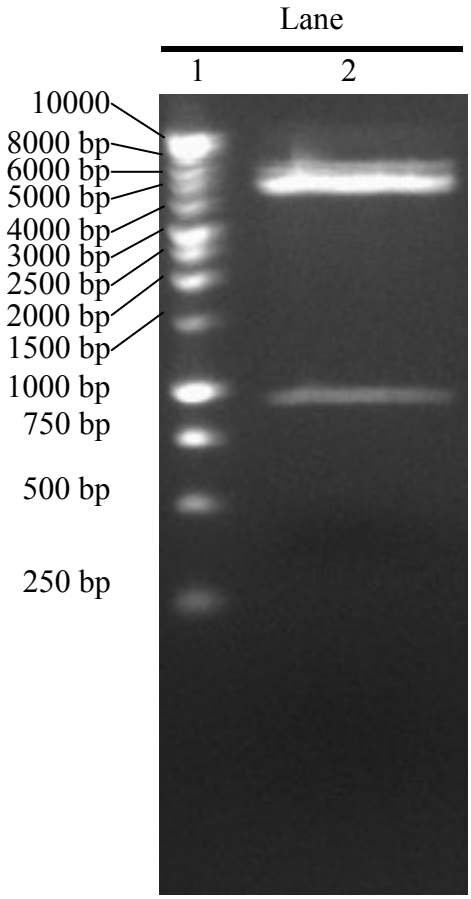

Figure 3. 5. Endonuclease digestion confirmed the sub-cloning of the engineered BCA gene to the pET-3a vector. Lane 1 is the 1 kb ladder. Lane 2 shows the product of restriction digestion analyzed on 1% agarose gel. The band in between 4-5 kb represents the fragment of the pET-3a vector while the band at around 1000 bp is the insert containing engineered BCA gene.

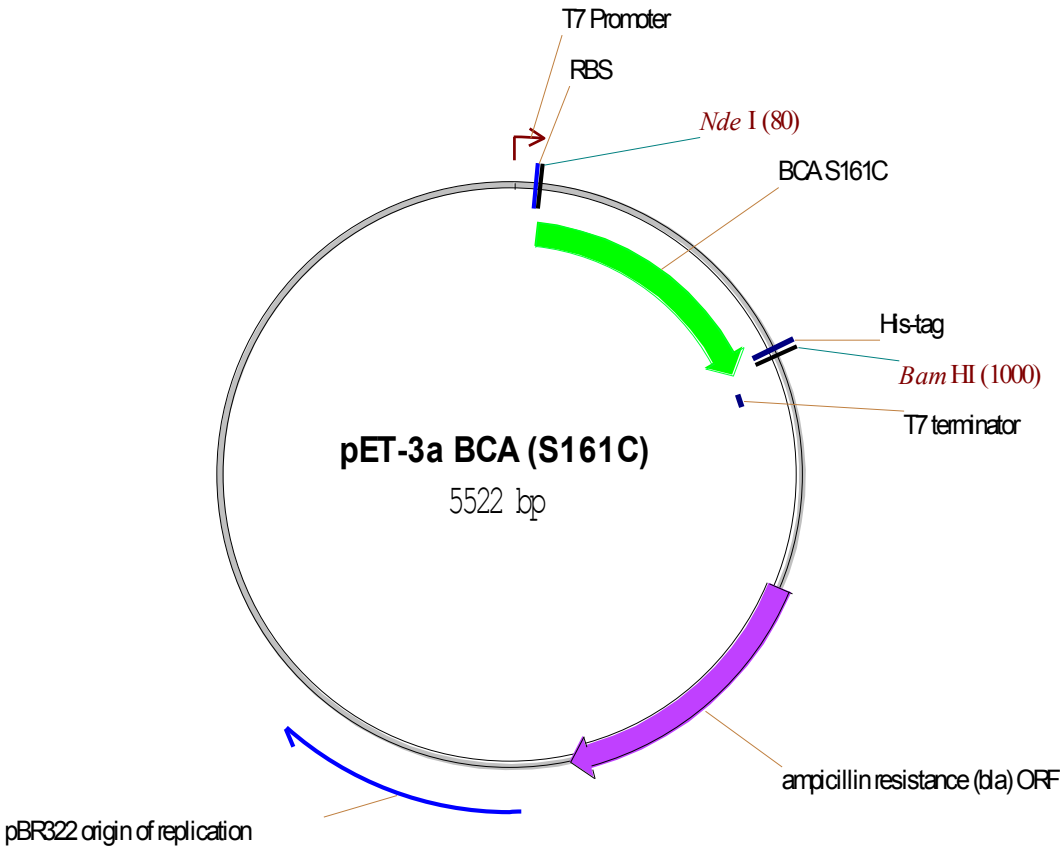

Figure 3. 6. Plasmid map showing the construct of engineered BCA expression vector, pET-3a BCA(S161C). The engineered BCA gene (Green arrow) was sub-cloned into the pET-3a vector through the NdeI and BamHI restriction sites and it is 5522 bp in size. In addition to the engineered BCA gene, the plasmid contains the β-lactamase gene for ampicillin resistance as well as an origin of replication.

3.3. Small scale purification of BCA from shake flask culture

To overexpress the engineered BCA, the plasmid, pET-3a-BCA(S161C), was transformed into *E. coli* BL21(DE3). Overexpression of BCA was mediated by IPTG induction for which the T7 RNA polymerase was expressed and it drives the expression of the BCA gene under the control of the T7 promoter. The downstream purification process was established based on the thermostable property of BCA and the 6xHis affinity tag. A two-step purification scheme combining heat treatment and metal chelating column effectively improved the purity of BCA for further characterization and *in vitro* efficacy study.

3.3.1. Heat treatment

BCA was overexpressed in *E. coli* cells by shake flask culture as described in the methodology. The cell pellet was collected by centrifugation after 4 hrs of IPTG induction. The cells overexpressing BCA were disrupted by sonication and the soluble fraction was separated from the total cell lysate by centrifugation. The soluble protein was incubated at 70 °C for 15 min and heat labile proteins precipitated during heat treatment were removed by centrifugation. The soluble protein showing improved purity after heat treatment is shown in Figure 3. 8.

3.3.2. Affinity purification by nickel affinity column chromatography

The partially purified BCA was loaded onto the nickel affinity column and unbound proteins were washed out. The target protein was eluted by increasing concentration of imidazole. The first step was a gradient of increasing concentration of elution buffer (containing 0.5 M imidazole) from 0 to 30% in 4 column volumes (CV) with which the non-specific bound proteins were eluted out from the column. In the second step, the elution buffer was maintained at 30% for 3 CV: this step was intended to separate the target protein from the non-specifically bound proteins. The third step increased the imidazole concentration from 30% to 70% in 6 CV and the target protein was eluted. For the last step, the imidazole concentration was increased from 70% to 100% in 3 CV for complete elution. The four-segment-elution profile of BCA from the nickel affinity column was shown in Figure 3. 7.

Selected fractions which displayed absorbance at 280 nm were analyzed on the 12% SDS-PAGE (Figure 3. 8). The fractions, A10 to B11, containing the target protein (about 33 kDa) were pooled and imidazole was removed by buffer exchange using Amicon Ultra centrifugal cassette with nominal molecular weight cut-off (NMWC) of 10 kDa. The purified BCA was maintained in phosphate buffer, sterilely filtered and stored at 4°C.

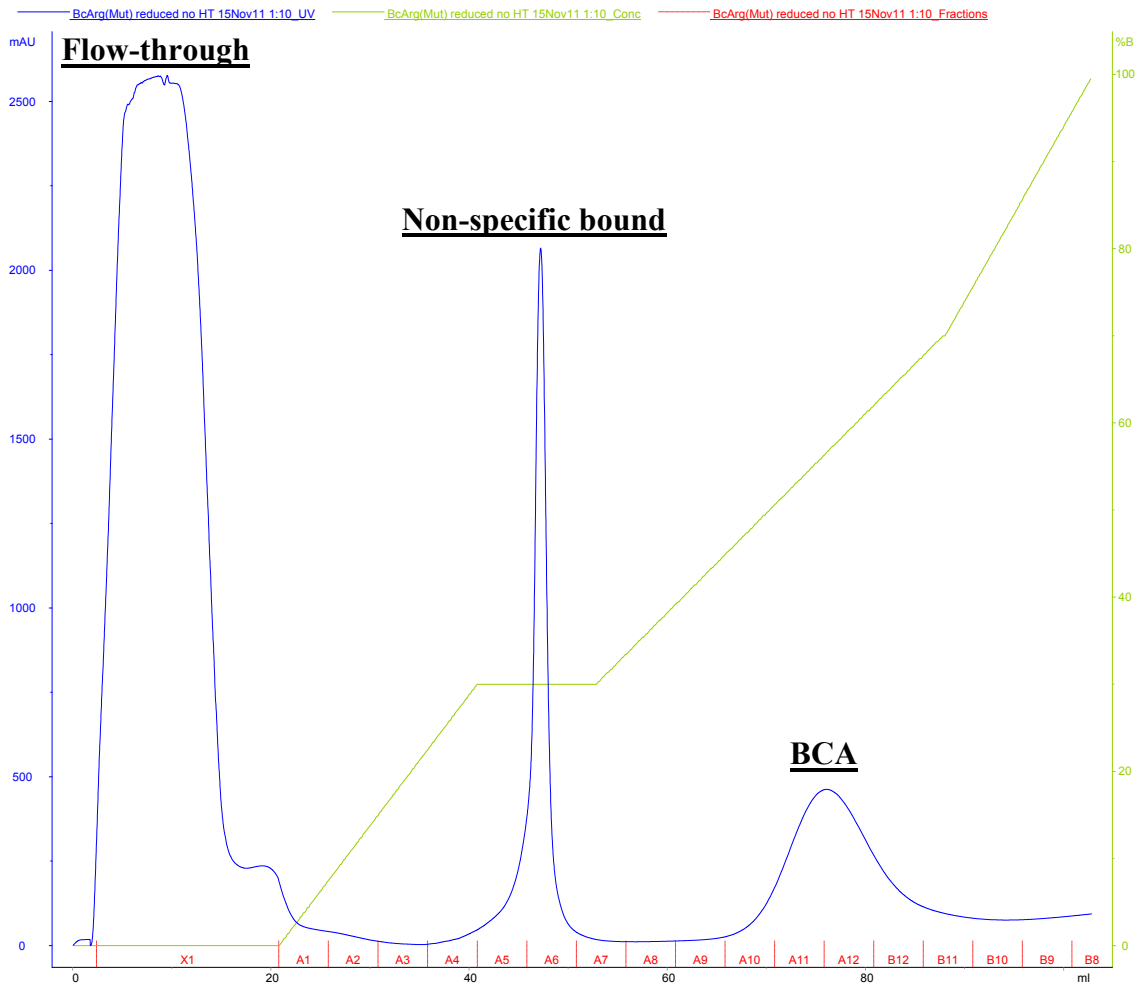

Figure 3. 7. Chromatogram showing small scale purification of the engineered BCA using the 5 ml HisTrap nickel affinity column. After sample loading, column was washed with starting buffer until the absorbance at 280 nm became steady. The first step of linear gradient elution started from 0 to 30 of elution buffer [containing 0.5 M imidazole] in 4 CV and the second step held at 30% elution buffer for 3 CV. In the third step, elution buffer increased from 30 to 70% in 6 CV and followed by 70 to 100% elution buffer in 2 CV for the last step. The elution profile was monitored by absorbance at 280 nm in mAU (milli absorption units).

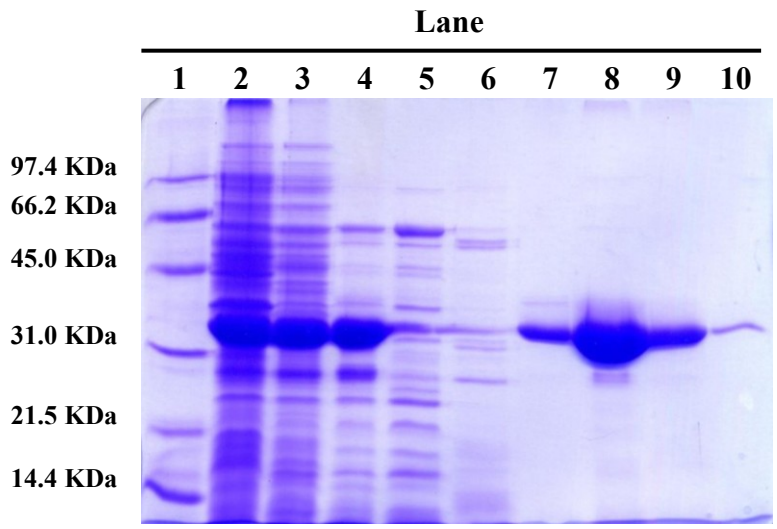

Figure 3. 8. Selected fractions collected from the small scale purification of BCA were analyzed by SDS-PAGE. Lane 1 is the low range molecular weight marker. Lane 2 represents total protein obtained from cell lysate. Lanes 3 and 4 show the soluble protein before and after heat treatment, respectively. Lane 5 is the unbound protein collected in fraction X1 during column washing. Lane 6 represents the non-specifically bound proteins in fraction A5. Lanes 7 to 10 represent fractions A10, A12, B12 and B11, respectively.

3.3.3. Overview of small-scale purification

The purification of BCA from shake-flask culture is summarized in Table 3. 1. From 250 ml shake-flask culture, about 28.7 mg of BCA was purified and the specific activity was found to be 317.9 U/mg. The purity of BCA was increased by about 3-fold and about 75% of BCA was recovered after the 2-step purification scheme.

Table 3. 1. Purification table showing the overview of small scale purification of the engineered BCA.

Sample	Total Volume (ml)	Enzyme Conc. (units/ml)	Protein Conc. (mg/ml)	Total Enzyme (*units)	Total Protein (mg)	Specific Activity (units/mg)	Fold of Purification	Yield (%)
Total Protein	10	1210	10.1	12100	101.2	119.6	1.0	100
After Heat Treatment	9.5	1098	5.6	10431	53.1	196.4	1.6	86.2
Final Product	3	3039	9.6	9117	28.7	317.9	2.7	75.3

*1 unit of BCA was defined as the amount of enzyme that converts 1 micromole arginine to ornithine and urea per minute at 37 °C, pH 7.4.

Fold of Purification: Divide the specific activity of each step by the first step
Percentage of Yield: The total activity from each step was compared to the first step.

3.4. Strategy to extend the circulation half-life of BCA

Therapeutic proteins such as cytokines, enzymes and hormones have been developed for treating different pathophysiological conditions such as cancer. These therapeutics usually possess a low molecule weight (usually <50 kDa) and thus are quickly eliminated by renal clearance, resulting in a circulation half-life of several minutes to a few hours. In order to maintain an effective therapeutic concentration in the systemic circulation, a frequent dosing schedule may be required and thus raising issues of patient compliance. In view of this problem, different strategies have been evolved to improve the pharmacokinetic properties of these therapeutic proteins. Conjugation of PEG to different therapeutic proteins, i.e. pegylation, has been shown to increase their hydrodynamic radius and hence slow down their elimination by renal clearance. Fusion protein strategy based on the recycling mechanisms of the Fc neonatal receptor (FcRn) has been established, in which fusion of fragment crystallizable (Fc) region of immunoglobulin, albumin or albumin binding peptide to proteins has been shown to increase their circulation half-life.

The abovementioned strategies will be applied to the formulation of BCA and more extensive studies through pegylation would be reported. Some preliminary findings about the fusion of BCA to albumin binding domain (ABD) would also be included.

3.4.1. Site-specific pegylation of BCA

Through introducing a cysteine residue to the surface of BCA by genetic engineering, PEG molecules activated with maleimide could react specifically with the cysteine residue and result in site-specific pegylation. In this study, PEG, ME-200MA, of molecular weight 20,000 Da and activated with maleimide would be used to modify BCA (Figure 3. 9). The pegylation conditions such as the molar ratio of PEG to BCA, duration, pH and temperature would be optimized.

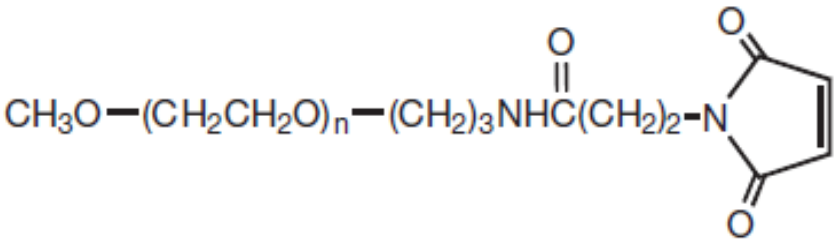

Figure 3. 9. Chemical structure of SUNBRIGHT ME-200MA. The PEG of 20,000 Da was activated with maleimide for the conjugation of cysteine residue on the surface of BCA.

3.4.1.1. Optimization of the PEG to BCA ratio for pegylation

The purified BCA was reduced in the presence of tris(2-caroxyethyl)phosphine (TCEP) to make sure that the single cysteine residue was not involved in disulfide bond formation and was therefore available for pegylation. The optimum amount of PEG was determined by adding 1, 5, 10 and 20 equivalent of PEG to the purified BCA and maintaining the reaction overnight in PBS buffer at pH 7.4 at 4 °C. During the course of pegylation, samples were collected at 0, 1, 2, 4, 9 and 18 and quenched with 100 mM cysteine, and stored at -80°C until SDS-PAGE analysis.

As shown in Figure 3. 10, when BCA was mixed with 1 equivalent of PEG, only a small fraction of the enzyme was modified, appearing as the band with lower mobility at about 100 kDa on SDS-PAGE. By increasing the PEG to 5 and 10 equivalents for pegylation, a dramatic increase of pegylated BCA was observed with concomitant decrease of native BCA on the SDS-PAGE. Increasing the PEG to 20 equivalents, however, produces only a very slight improvement in reducing the residual BCA. Regardless of the PEG to BCA ratio, the reaction seems to be completed within 1 h, and further extension of the duration does not seem to improve the pegylation efficiency.

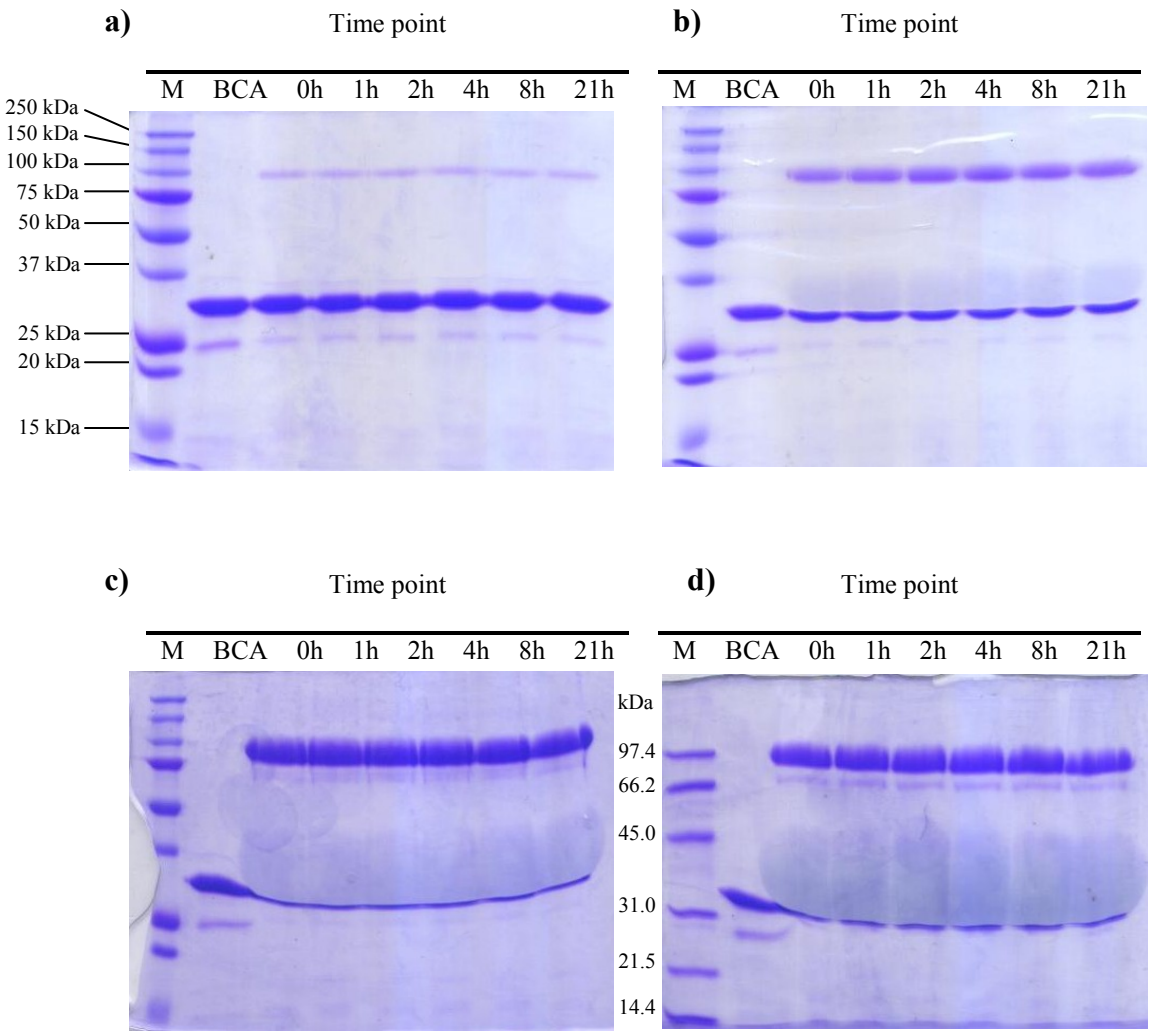

Figure 3. 10. The effects of PEG equivalents on the extent of BCA pegylation. BCA was incubated with a) 1, b) 5, c) 10 and d) 20 equivalents of PEG. Sample collected at different time points were quenched by 100 mM cysteine and analyzed on 12% SDS-PAGE.

3.4.1.2. Effects of pH and temperature

The effects of pH and temperature were investigated in the hope of improving the completeness of BCA pegylation. Considering the cost of PEG, the following optimization would be performed using 10 equivalents of PEG. As previous study showed that increases the PEG to 20 equivalents would only marginally improve the pegylation process. Purified BCA would be adjusted to different pH conditions through buffer exchange to sodium citrate pH 5.5 or sodium carbonate pH 9.5. The BCA samples adjusted to different pH values were pre-incubated at 4, 37 or 50°C for at least 30 min before pegylation. During the course of reaction, samples were collected at 0, 1, 2 and 19 hours and quenched with 100 mM cysteine and stored at -80 °C until being analyzed on SDS-PAGE.

The pegylation of BCA at various temperatures and pH values were analyzed on SDS-PAGE and (Figure 3. 11 – 13). When the pegylation reactions were incubated at pH 5.5 or 9.5, they progressed in a time-dependent manner but the reaction seemed to be much faster at pH 7.4 and it almost completed within an hour of incubation. However, combining the effects of temperature, pH and duration of pegylation did not further improve the completeness of BCA pegylation, as reflected by the amount of unpegylated BCA seen on the SDS-PAGE.

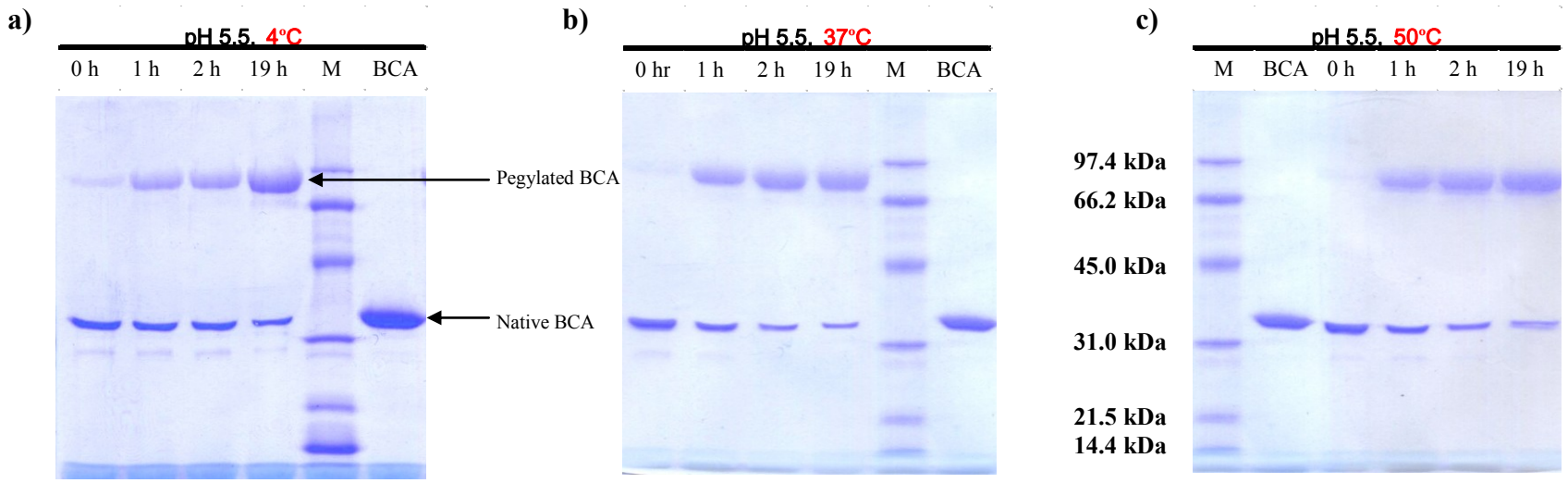

Figure 3. 11. The effect of temperature on BCA pegylation at pH 5.5. The pegylation of BCA was carried out at a) 4 °C, b) 37 °C and c) 50 °C. Samples collected at different time points were analyzed on 12% SDS-PAGE.

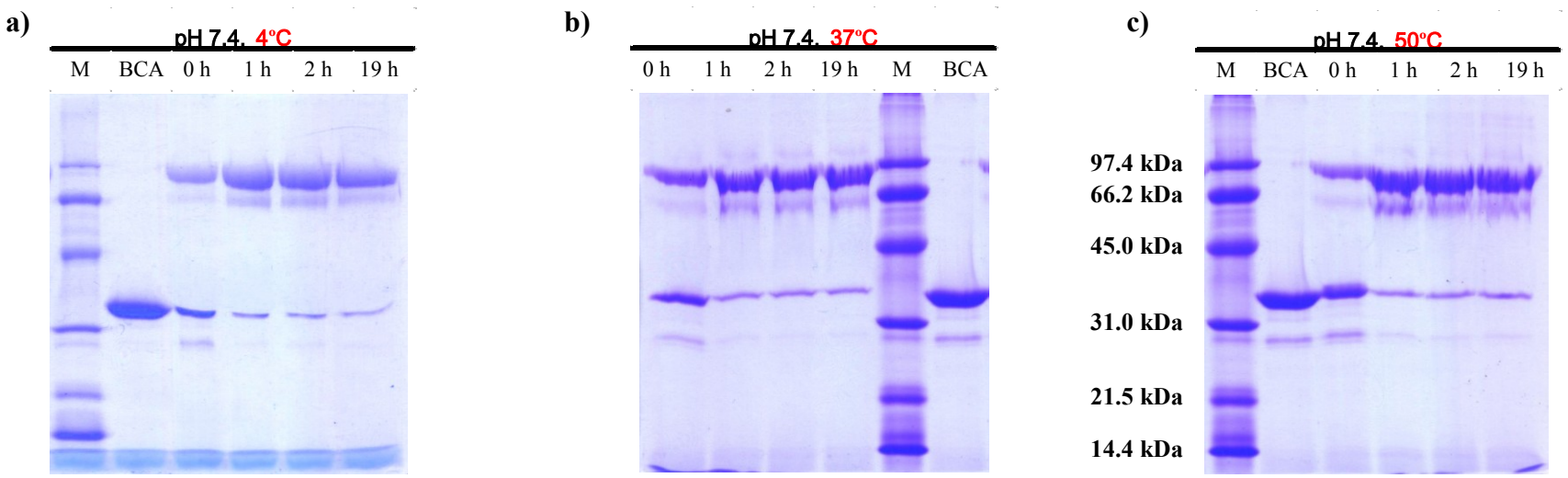

Figure 3. 12. The effect of temperature on BCA pegylation at pH 7.4. The pegylation of BCA was carried out at a) 4 °C, b) 37 °C and c) 50 °C. Samples collected at different time points were analyzed on 12% SDS-PAGE.

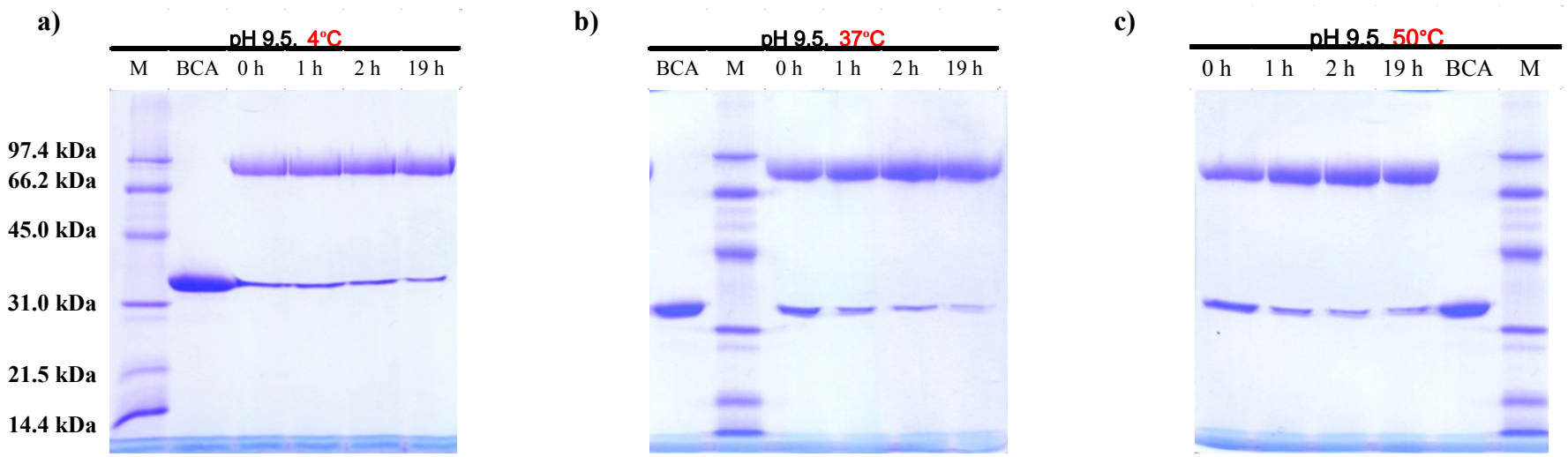

Figure 3. 13. The effect of temperature on BCA pegylation at pH 9.5. The pegylation of BCA was carried out at a) 4 °C, b) 37 °C and c) 50 °C. Samples collected at different time points were analyzed on 12% SDS-PAGE.

3.4.2. Fusion of albumin binding domain (ABD) to BCA

Fusion with long-lived proteins found in blood circulation, such as albumin or the Fc domain of IgG, has been shown to extend the circulation half-life of different protein therapeutics through Fc neonatal receptor (FcRn) recycling. Albumin binding domain (ABD) (Jonsson et al., 2008) derived from streptococcal protein G has been shown to have nanomolar affinity toward albumin where the binding of ABD to albumin does not interfere with FcRn binding thus does not affect the recycling process (Andersen et al., 2011; Jonsson et al., 2008). Fusion of ABD to single chain diabody (scDb) has been shown to extend the circulation life while retaining binding to the target receptor (R. Stork et al., 2009; R. Stork et al., 2007; Tolmachev et al., 2007).

Thus far, fusion of ABD to therapeutic enzyme like BCA to extend circulatory half-life is unprecedented. Preliminary biochemical studies revealing the functional aspect of the BCA-ABD fusion protein would be reported.

3.4.2.1. Binding of BCA-ABD to HSA revealed by non-denaturing PAGE analysis

When ABD is fused to BCA, it is important for the fusion protein to retain both the albumin binding capacity and the enzymatic activity. To demonstrate the binding capacity of ABD in the fusion protein, a fixed amount of human serum albumin (HSA) was incubated with BCA-ABD in different molar rations. The reaction mixtures were analyzed in their native condition on non-denaturing PAGE where the proteins were separated by size and conformation.

The mobilities of HSA and BCA-ABD alone are shown in Lane 6 and 7 of the non-denaturing PAGE, respectively (Figure 3. 14). A fixed amount of HSA (60 pmole) was titrated against BCA-ABD at various molar ratios and the results are illustrated in Lanes 1 – 5. By increasing the amount of BCA-ABD in the binding reaction, the amount of free HSA was reduced in a proportional manner and thus indicating the specific binding of BCA-ABD to HSA.

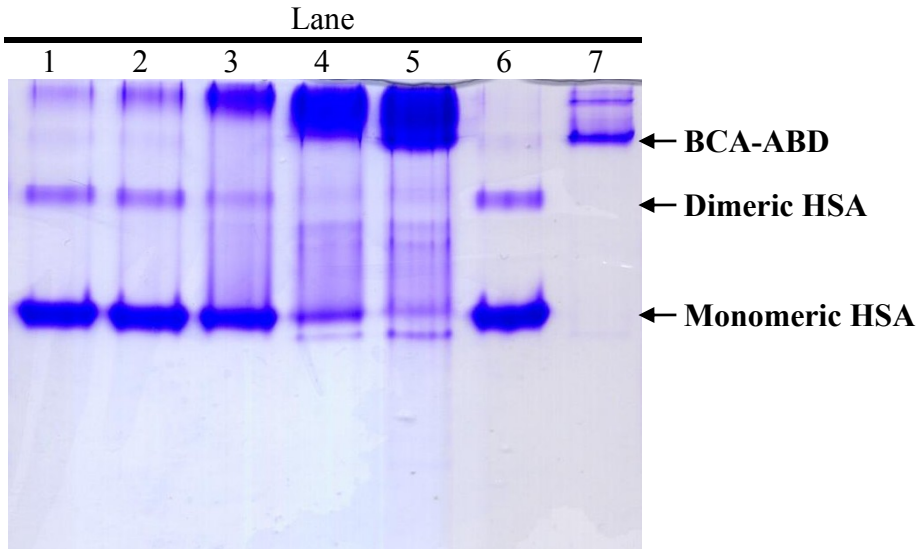

Figure 3. 14. Revealing the binding between BCA-ABD and HSA on non-denaturing PAGE. Fixed amount of HSA 60 pmole was mixed with 6, 12, 60, 300 and 600 pmole of BCA-ABD as shown in Lanes 1-5, respectively. The mobilities of 60 pmole of HSA and BCA-ABD on the non-denaturing PAGE are shown in Lanes 6 and 7, respectively.

3.4.2.2. Binding of BCA-ABD to HSA revealed by gel filtration chromatography

To further confirm the results of binding between BCA-ABD and HSA, the binding study was repeated but analyzed on a gel filtration column, Superdex 200 HR Prep Grad, XK26/60. The binding between BCA-ABD and HSA was expected to produce a dramatic shift in molecular weight. Protein complexes were separated in the native state on the gel filtration column.

The chromatogram of BCA-ABD is shown in Figure 3. 15a where the major peak with the elution volume of 149.8 ml refers to the hexamer of BCA-ABD while the peak eluted out at 210.6 refers to the monomeric BCA-ABD. The peaks eluted before the hexamer of BCA-ABD referred to the aggregates. The major and minor peak on the chromatogram of HSA should be due to the monomeric and dimeric structures of HSA, respectively (Figure 3. 15b). When HSA was mixed with BCA-ABD in a 1 to 1 ratio (Figure 3. 15c), the peak corresponding to the monomer of HSA decreased concomitantly in the presence of BCA-ABD and a major peak with retention volume of 125.81 ml was identified which did not exist in either the chromatogram of BCA-ABD or HSA alone. Based on elution volume, the molecular size was calculated to be about 584 kDa using the calibration curve on Figure 3. 19, which may refer to the hexameric structure of BCA-ABD in complex with HSA.

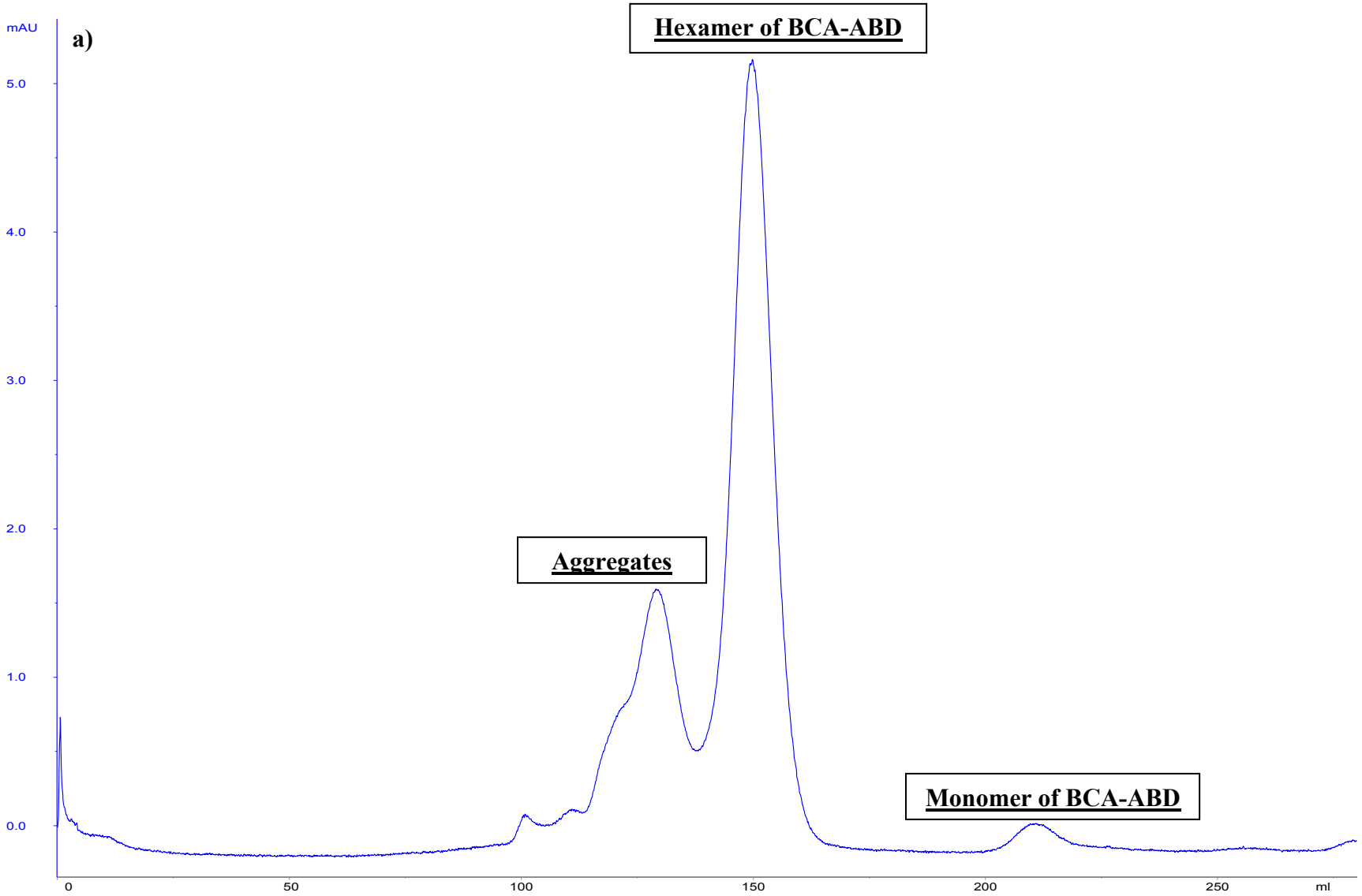
a)
Hexamer of BCA-ABD
Aggregates
Monomer of BCA-ABD
mAU
5.0
4.0
3.0
2.0
1.0
0.0
0
50
100
150
200
250
ml

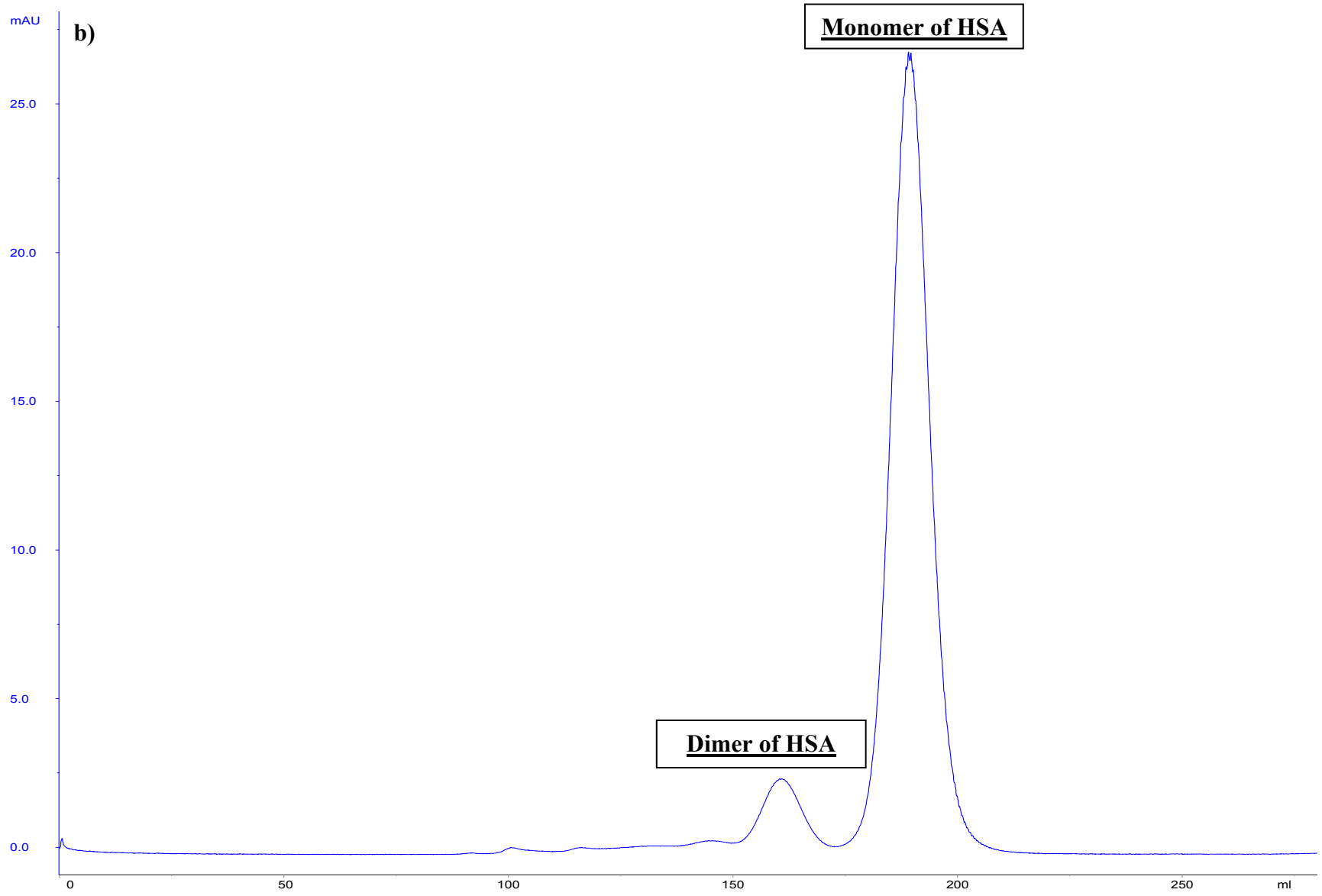
b)
Monomer of HSA
Dimer of HSA
mAU
25.0
20.0
15.0
10.0
5.0
0.0
0
50
100
150
200
250
ml

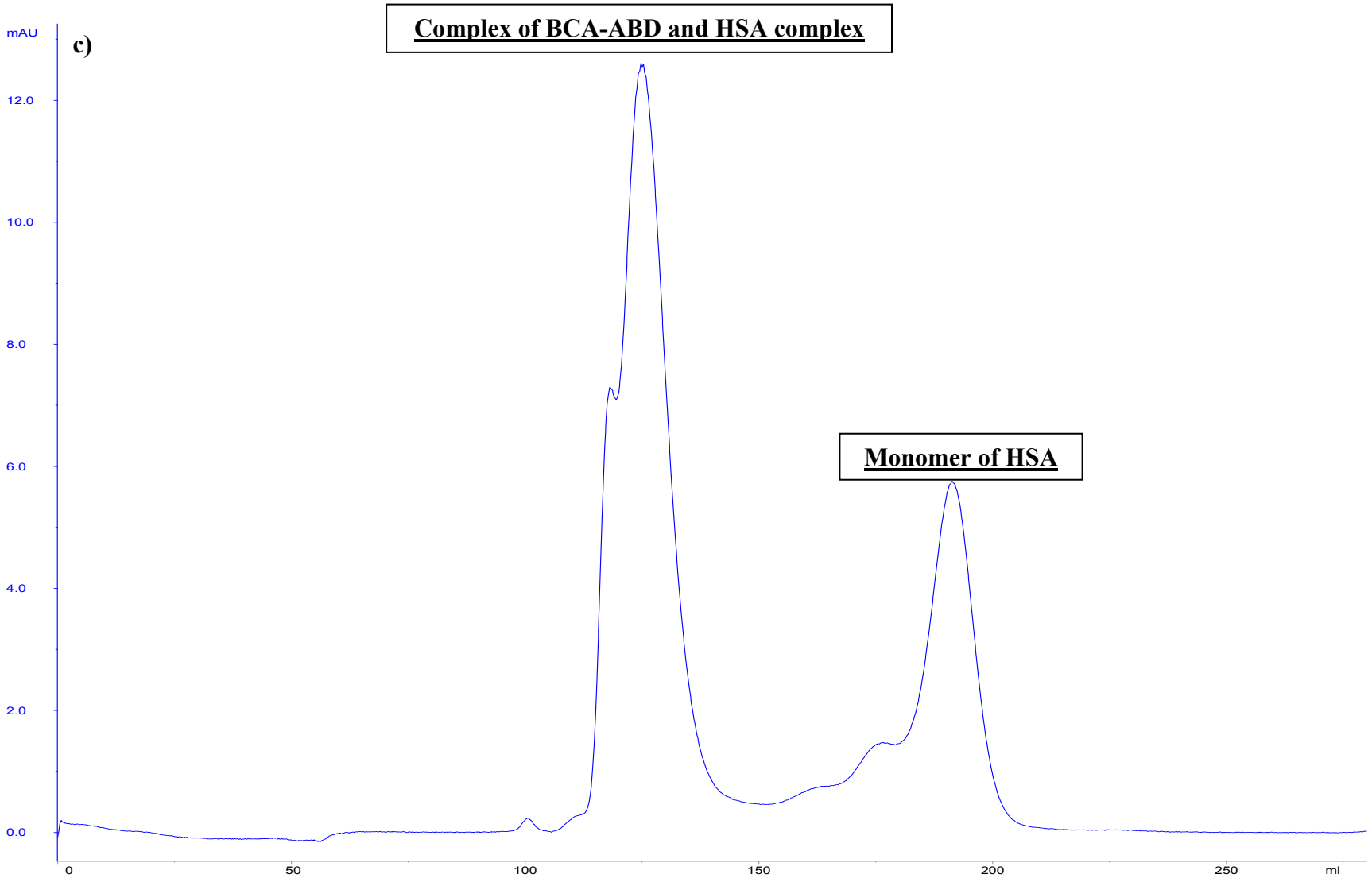
c)
Complex of BCA-ABD and HSA complex
Monomer of HSA
mAU
12.0
10.0
8.0
6.0
4.0
2.0
0.0
0
50
100
150
200
250
ml

Figure 3. 15. Chromatogram showing the elution profiles of BCA-ABD, HSA and the pre-incubated mixture of HSA and BCA-ABD (1 : 1 ratio) from Superdex 200HR Prep Grad XK26/60 gel filtration column. The elution profile of BCA-ABD (a) showing the peaks eluted at 149.8 ml and 210.6 ml, which referred to hexamer and monomer, respectively. The small peak having the elution volume of 129 ml and eluted before the hexamer of BCA-ABD was likely the aggregates. The elution profile of HSA (b) showing the peaks eluted at 162.9 ml and 191.6 ml which refer to dimer and monomer, respectively. The elution profiles of the pre-incubated BCA-ABD and HSA mixture (c). The peak at 191 ml refers to the monomer of HSA while the major peak having the elution volume of 125 ml likely due to the complex of BCA-ABD and HSA.

3.4.2.3. Enzymatic activity of the BCA-ABD fusion protein

The arginine catabolic activity of BCA-ABD was assayed in order to find out if the fusion protein retains the activity of BCA alone as well as whether the enzymatic activity would be affected in the presence of HSA.

Preliminary data showed that the activity of BCA-ABD was reduced by about 30% when compared to the engineered BCA. Interestingly, the activity of BCA-ABD was not affected by the various amounts of HSA added to the activity assay (Figure 3. 16).

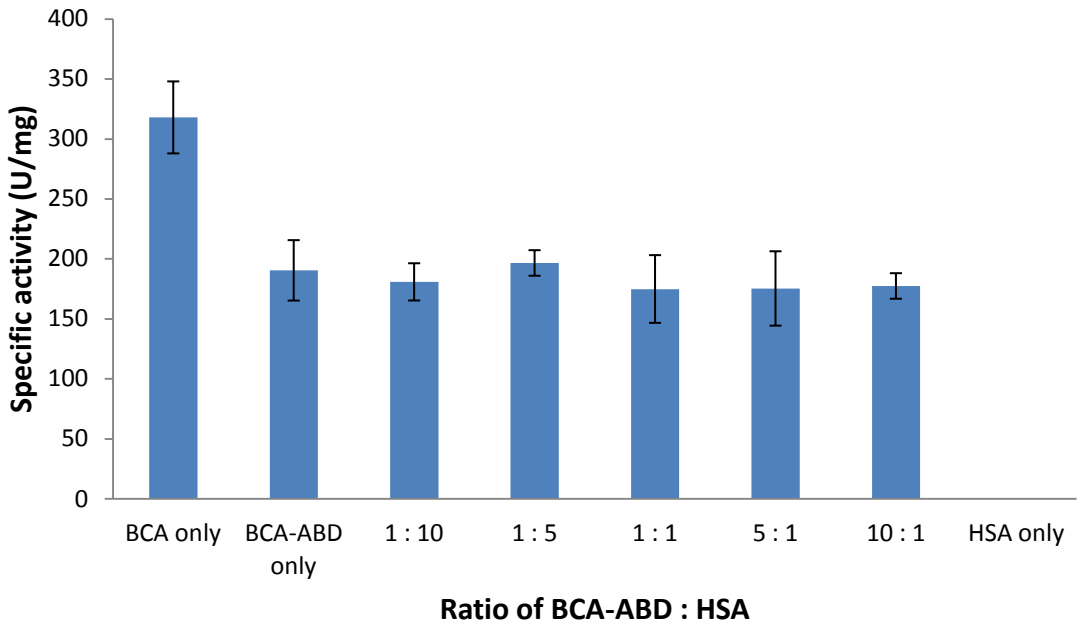

Figure 3. 16. The enzymatic activity of the BCA-ABD fusion protein. The specific activity of BCA-ABD was found to be one-third lower than BCA but not affected by the presence of various amounts of HSA.

3.4.2.4. Cytotoxicity of BCA-ABD on gastric cancer cells

The in *vitro* efficacy of BCA-ABD was tested by incubating the MKN45 cell line with various concentrations of BCA-ABD for 72 h and determining the viability of MKN45 by MTT assay. As shown in Figure 3. 17, the growth of MKN45 was inhibited by BCA-ABD in a dose-dependent manner. This further confirmed the cytotoxicity of the fusion protein in culture condition where the medium was supplemented with fetal bovine serum (FBS) and, including albumin as well as huge amounts of different proteins. The encouraging data from the biochemical studies should be further evaluated by *in vivo* efficacy and pharmacological studies.

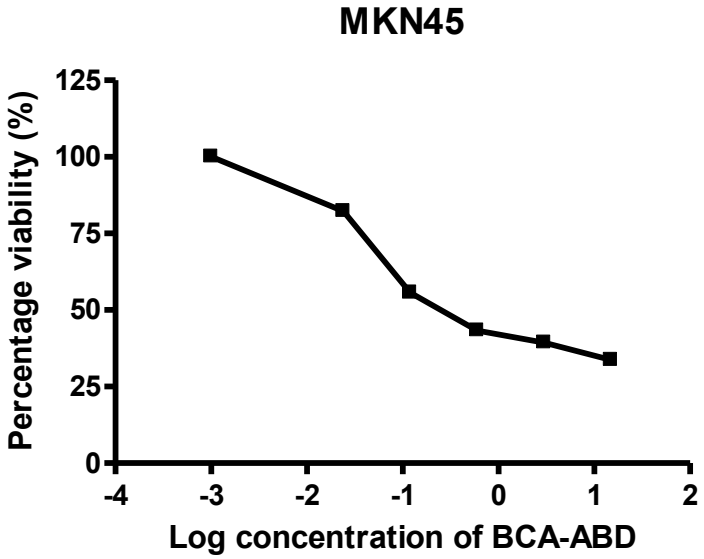

Figure 3. 17. Anti-cancer effect of BCA-ABD on MKN45 gastric cancer cell line. The growth of MKN45 was inhibited in a dose-dependent manner. The viability was determined by MTT endpoint colorimetric assay. Data shown are means ± SD (n=3).

3.5. Characterization of BCA

The physical properties of BCA were studied by means of different analytical techniques. The molecular size and multimeric structure of BCA were determined by combining the information from SDS-PAGE, gel filtration and mass spectrometry. The isoelectric point (pI) of BCA was resolved by isoelectric focusing. The thermostability was revealed by monitoring the secondary structure of BCA using circular dichroism (CD). These studies provided important information to develop the purification scheme, and through them additional features added by genetic engineering on the enzyme properties could be also evaluated. The study of enzyme activity over time would provide information for the storage conditions of BCA. In addition to arginine, the specificity of BCA towards other amino acids would be evaluated.

3.5.1. Size

3.5.1.1. SDS-PAGE

The molecular weight of BCA before and after pegylation was analyzed on 12% SDS-PAGE. The pegylated BCA was mixed with 20-fold molar excess of PEG and the reaction mixture without removing the residual PEG was resolved by SDS-PAGE. The gel was stained with Coomassie blue stain as shown in Figure 3. 18a. The band at about 33 kDa as shown in Lanes 2 and 3 represent the monomeric molecular weight of BCA. The molecular weight of pegylated BCA (Lane 4) was shifted to about 100 kDa which was about double the predicted molecular weight, i.e. 53 kDa. In addition, trace amount of unmodified BCA was found in the pegylated sample indicating the incomplete pegylation of BCA.

Using iodine stain, PEG was visualized on the SDS-PAGE gel for which the band at about 100 kDa was consistent with the Coomassie blue stained band, thus representing the pegylated BCA. The smear in between 30-50 kDa on the SDS-PAGE is due to the residual PEG.

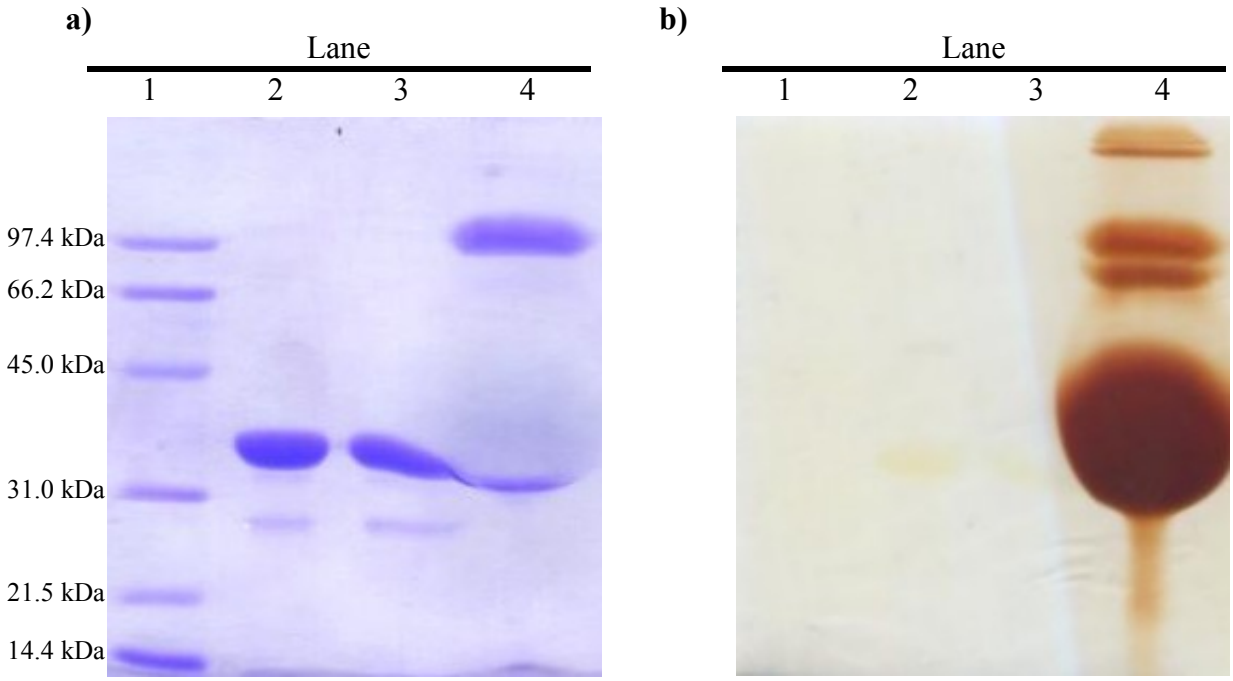

Figure 3. 18. Analysis of the molecular weight of native and pegylated BCA using SDS-PAGE. Equal amounts (10 µg) of native and pegylated BCA were resolved on 12% SDS-PAGE and stained with a) Coomassie blue stain and b) iodine stain. (a) The native BCA was found to have MW at about 33 kDa (Lanes 2 and 3) while pegylation increased the size of BCA to about 100 kDa (Lane 4). (b) Result from iodine stain revealed the size of pegylated BCA (Land 4) at about 100 kDa while the smear represents the free PEG. Native proteins (protein marker and BCA) without PEG conjugation was not visualized by iodine stain.

3.5.1.2. Gel filtration column

Gel filtration estimates the molecular weight of BCA based on the elution volume of a set of reference proteins. Protein in the native state was resolved by the Superdex 200 HR Prep Grad XK 26/60 and the elution volume (V_e) of different proteins were separated by their size and conformation. A set of proteins with different molecular weights were used for calibration and the standard curve is shown in Figure 3. 19. The column void volume (V_o) was determined by blue dextran which has the molecular weight of 2000 kDa.

The elution profile of engineered BCA is shown in Figure 3. 20a and 3 major peaks could be identified and the MW was calculated. The small peak having the Ve of 226.79 ml was estimated as the monomer and having the size of about 26.1 kDa. The peak, having the highest UV absorbance, being eluted out at 169.56 ml was found to have the molecular weight of about 152.0 kDa and predicted as the hexamer of engineered BCA. The presence of aggregate was suggested by the peak having the elution volume in between 120 to 150 ml which are corresponding to about 300 – 500 kDa.

When the wild-type BCA was analyzed by gel filtration chromatography, a similar elution profile was obtained (Figure 3. 20b). The presence of aggregates in the sample of BCA without cysteine mutation suggests that the presence of cysteine residue was not likely the cause of aggregation.

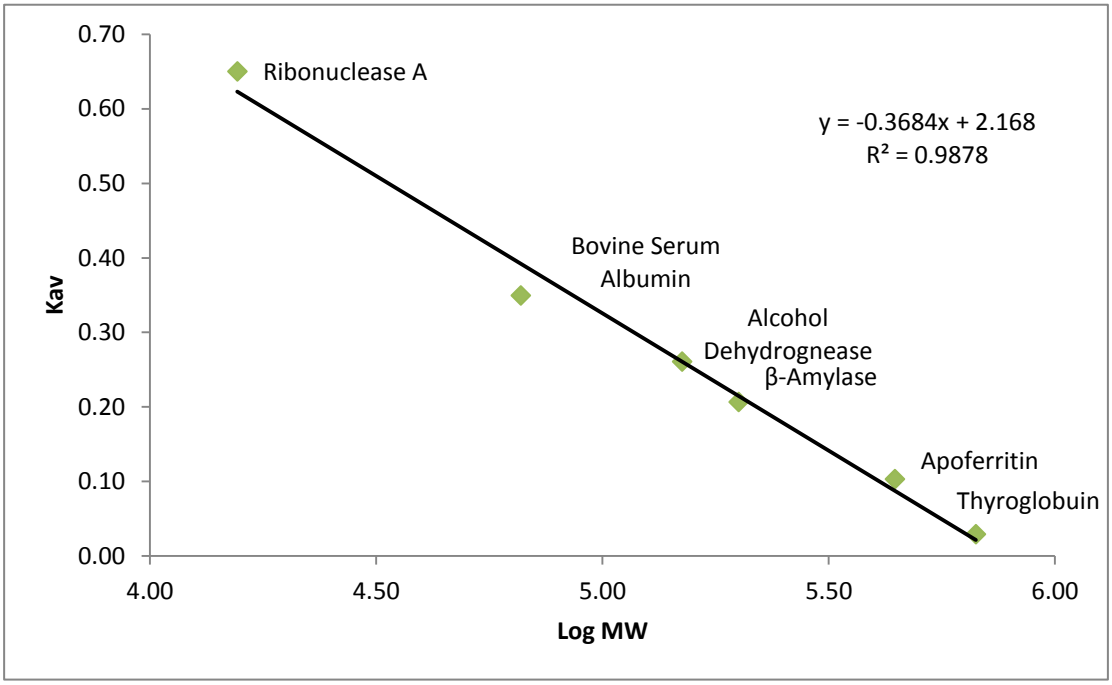

Figure 3. 19. Calibration curve for the Superdex 200 HR Prep Grad XK26/60 gel filtration column. The elution volume of each MW marker ribonuclease A (15.6 kDa), BSA (66.0 kDa), Alcohol dehydrogenase (150.0 kDa), β-Amylase (200 kDa), Apoferritin (443.0 kDa), Thyroglobulin (669.0 kDa) was determined on the gel filtration column while blue dextran (2000 kDa) was used to estimate the column void volume (V_o). The K_{av} value was determined by the equation below and plotted against Log MW.

$$K_{av} = \frac{V_e - V_0}{V_t - V_0}$$

Where

V_e = Sample elution volume

V_o = Void volume

V_t = Total bed volume

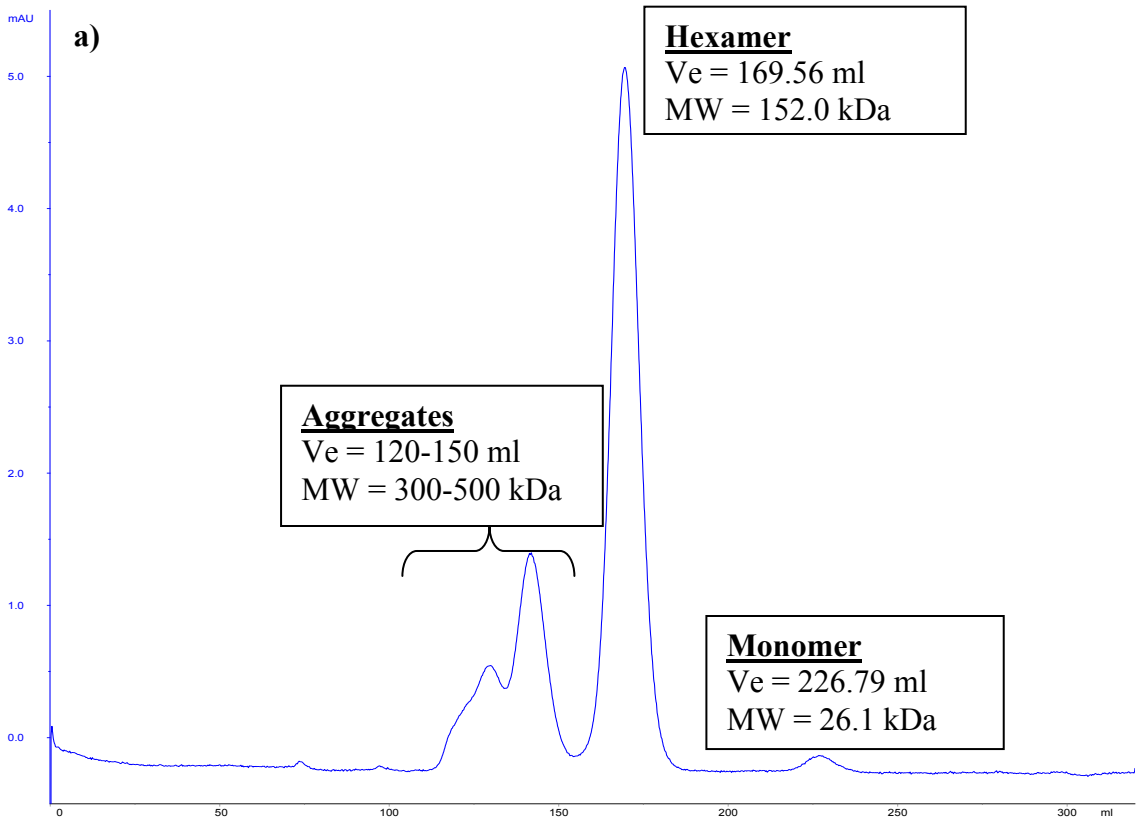
a)
Hexamer
Ve = 169.56 ml
MW = 152.0 kDa
Aggregates
Ve = 120-150 ml
MW = 300-500 kDa
Monomer
Ve = 226.79 ml
MW = 26.1 kDa
mAU
5.0
4.0
3.0
2.0
1.0
0.0
0
50
100
150
200
250
300
ml

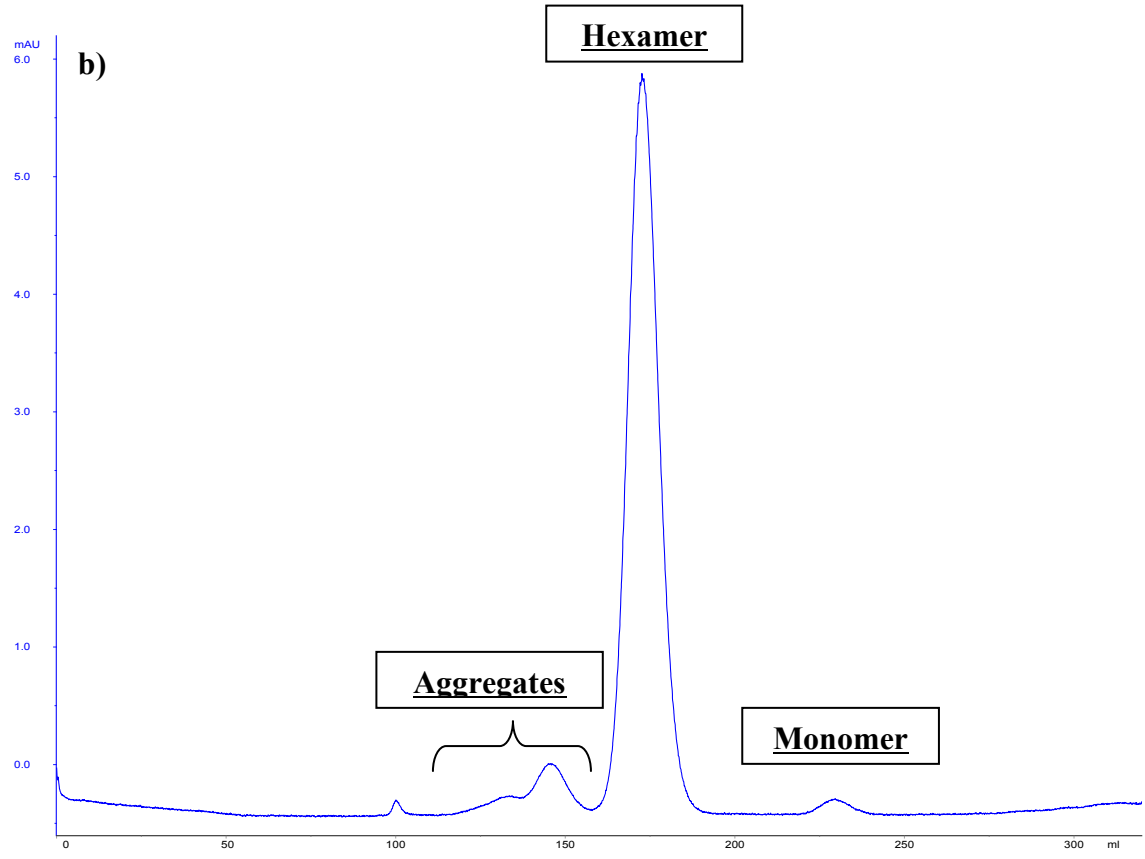
b)
Hexamer
Aggregates
Monomer
mAU
6.0
5.0
4.0
3.0
2.0
1.0
0.0
0
50
100
150
200
250
300
ml

Figure 3. 20. Chromatogram showing the elution profile of the wild-type and engineered BCA from gel filtration column. (a) The peaks having the elution volume of 169.6 ml and 226.8 ml are predicted as the hexamer and monomer of the engineered BCA, respectively. The peak eluted in preceding the hexamer suggests the presence of aggregates. Similar result as shown in (b) was obtained for the wild-type BCA.

3.5.1.3. Mass spectrometry

The mass of the engineered BCA was determined by electrospray ionization (ESI) mass spectrometry (MS). The ion source which generates multiply charged BCA was coupled with time-of-flight (ToF) mass spectrometer. Raw mass spectra of native BCA display a wide distribution of multiply charged peak (n = 22 - 47), where n is the charge state of a particular mass peak (Figure 3. 21a). The average mass of BCA was determined through transformation of the multiply charged spectra. The average mass of 33272.25 Da obtained from experiment was in good agreement with the calculated average mass (33272.24 Da) based on the protein sequence of BCA (Figure 3. 21b).

Pegylated BCA was analyzed by matrix-assisted laser desorption/ionization time-of-flight (MALDI-ToF) mass spectrometry. The protein sample was mixed with sinapinic acid (SA) and the mixture was allowed to air dry to form the analyte-matrix crystal. When the crystals were irradiated by nitrogen laser at 337 nm, the ionization of pegylated BCA was assisted in the presence of SA. Singly charged ions were generated and analyzed by the ToF analyzer in a positive [$M+H^+$], linear mode where the proteins were separated based on the mass (m) to charge (z) ratio (m/z). The mass spectrum of pegylated BCA is shown in Figure 3. 21c, in which two peaks are identified. The peak at 55 kDa was found in good agreement with the sum of molecular weight of BCA and ME-200MA and thus referred to the mono-pegylated BCA, while the peak at 33.4 kDa was the unmodified BCA. This data partly agreed with the results from the SDS-PAGE that a residual amount of unmodified BCA was present in the pegylated sample. In addition, it is noteworthy that the peak intensity did not represent the relative quantity of the pegylated and residual BCA because of different of ionization efficiency.

z = 40
m/z = 832.79

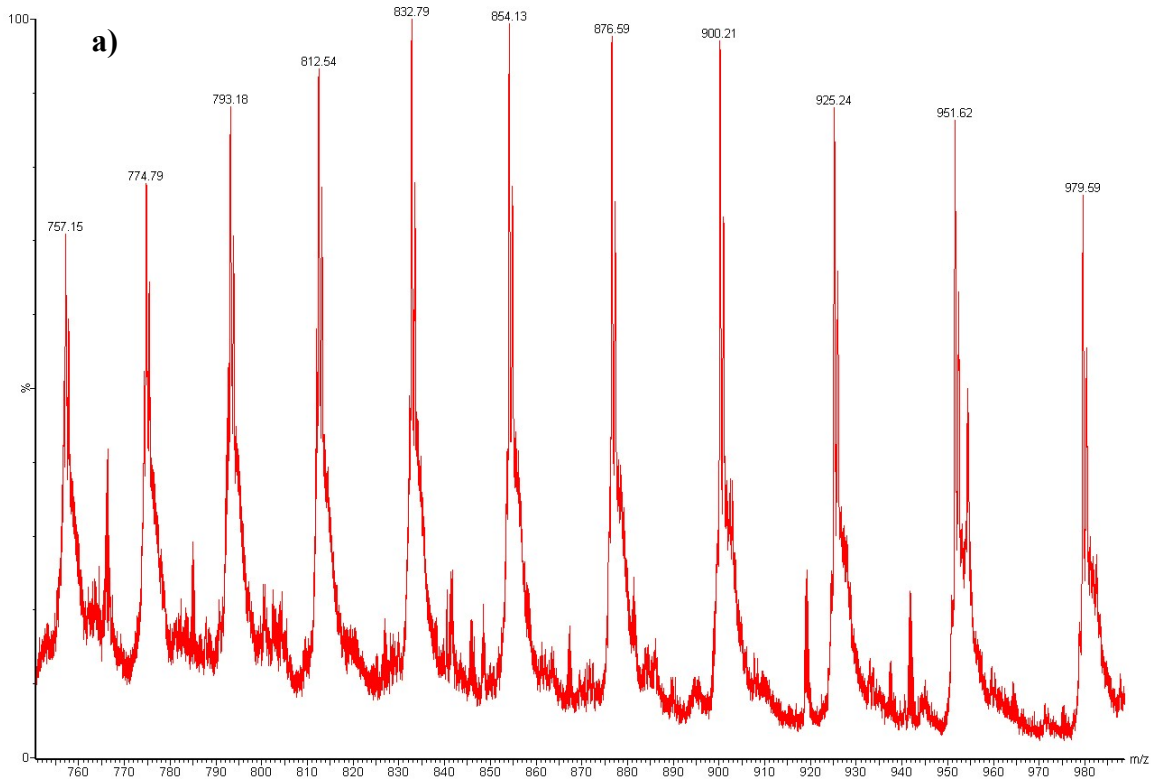
a)
100
%
0
757.15
774.79
793.18
812.54
832.79
854.13
876.59
900.21
925.24
951.62
979.59
760 770 780 790 800 810 820 830 840 850 860 870 880 890 900 910 920 930 940 950 960 970 980
m/z

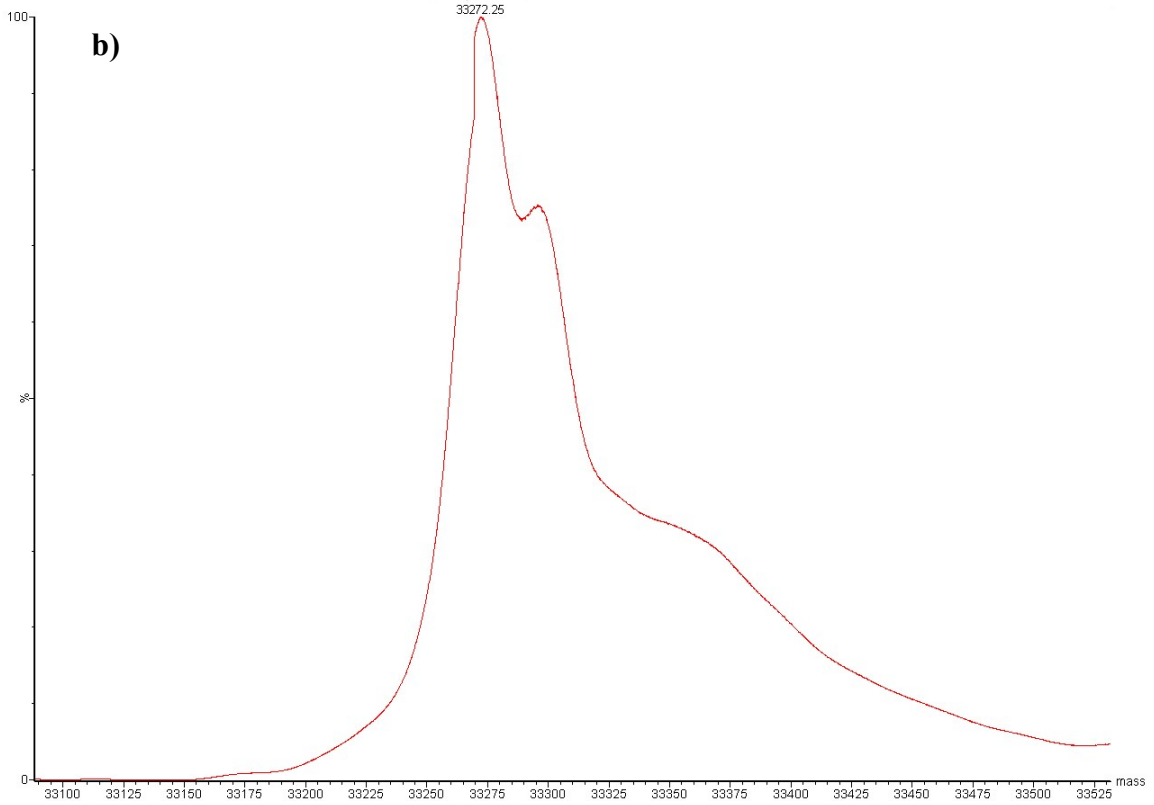
b)
100
%
0
33272.25
33100 33125 33150 33175 33200 33225 33250 33275 33300 33325 33350 33375 33400 33425 33450 33475 33500 33525
mass

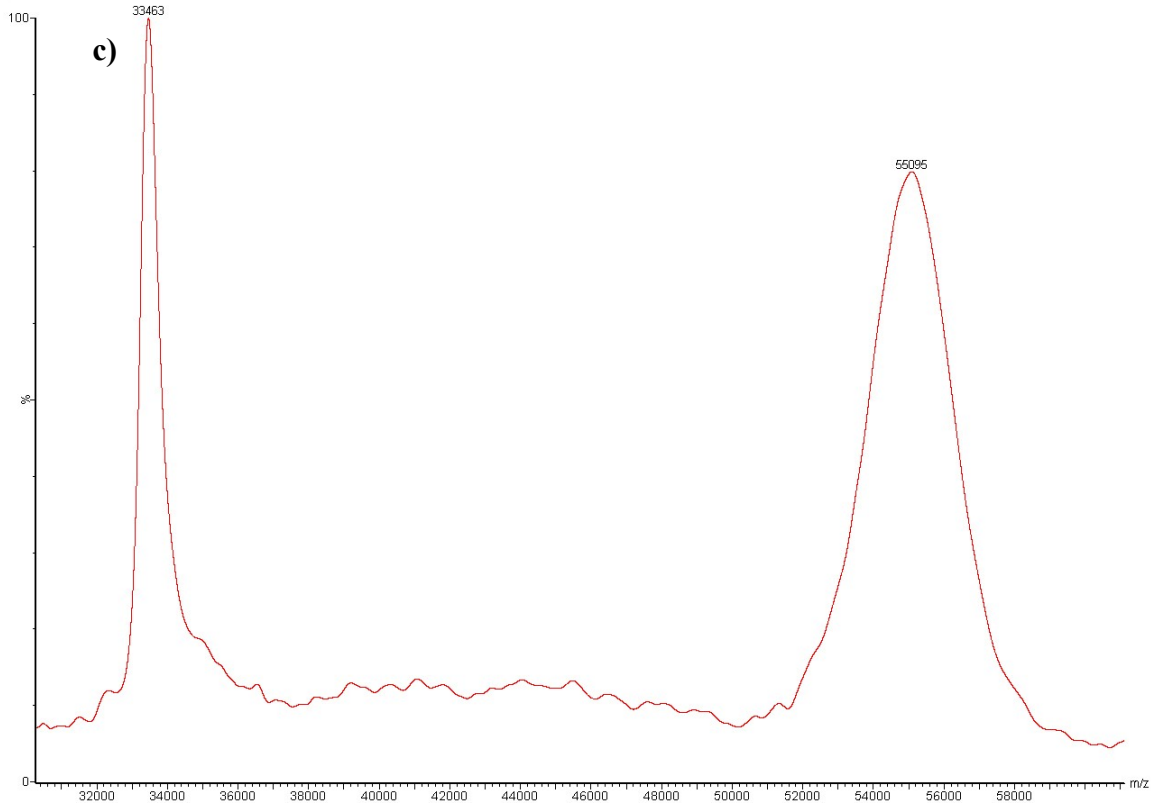

Figure 3. 21. Mass spectrum of native and pegylated BCA. (a) The spectrum of multiply charged BCA was obtained from ESI-MS. (b) The transformed mass spectrum of native BCA, indicating an average molecular weight of 33272.25 Da. (c) Mass spectrum of pegylated BCA. The peaks having the m/z ratio of 33,463 Da and 55,695 Da are referred to the native and pegylated BCA, respectively.

3.5.2. Isoelectric focusing

The isoelectric point (pI) of a protein is defined by its 3-dimensional conformation and surface electrostatic properties. Through determining the pI point of engineered BCA, important information could be gained to aid the formulation and purification scheme design. The dried polyacrylamide gel was rehydrated in the presence of ampholytes that make up the linear gradient of pH 3 – 10 for isoelectric focusing (IEF). After rehydration, the pH gradient was established through the pre-focusing step. The pI point of engineered BCA was determined with reference to a set of proteins with known pIs (Figure 3. 22). The result of IEF is shown in Figure 3. 23 and the relative mobility of the engineered BCA from the cathode was measured, yielding a pI value of 5.95.

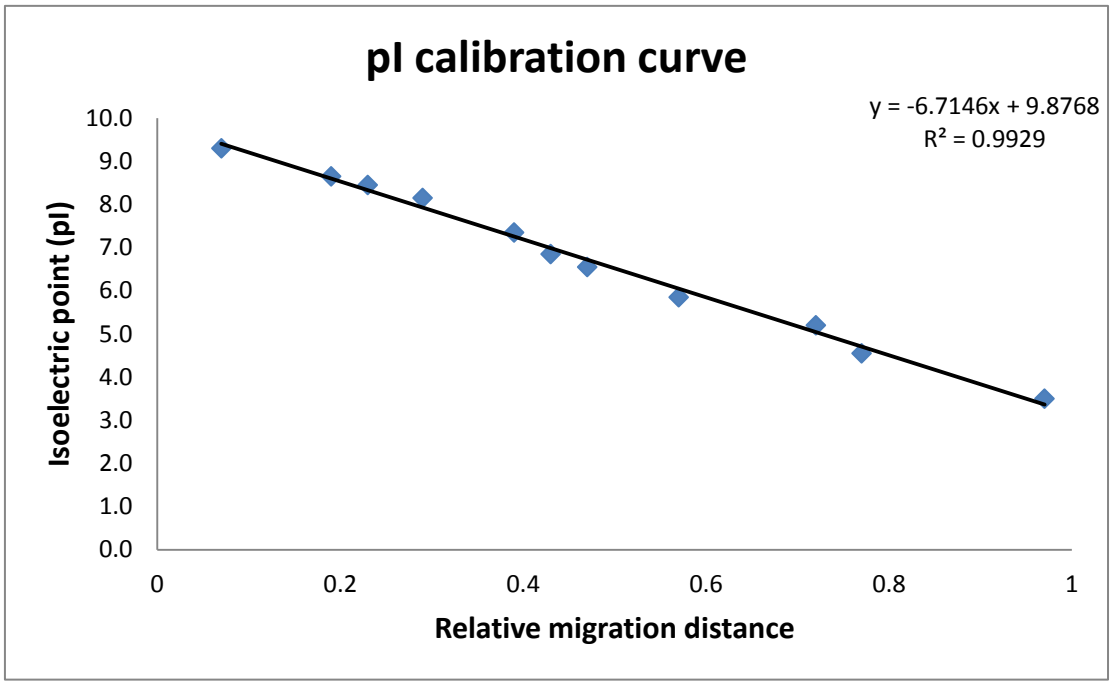

Figure 3. 22. Calibration curve for isoelectric focusing. The broad range pI markers were resolved on the polyacrylamide gel with a linear gradient between pH 3 to 10. The isoelectric point (pI) of the protein markers were plotted against the relative migration distance (distance travel from cathode divided by the distance between cathode and anode).

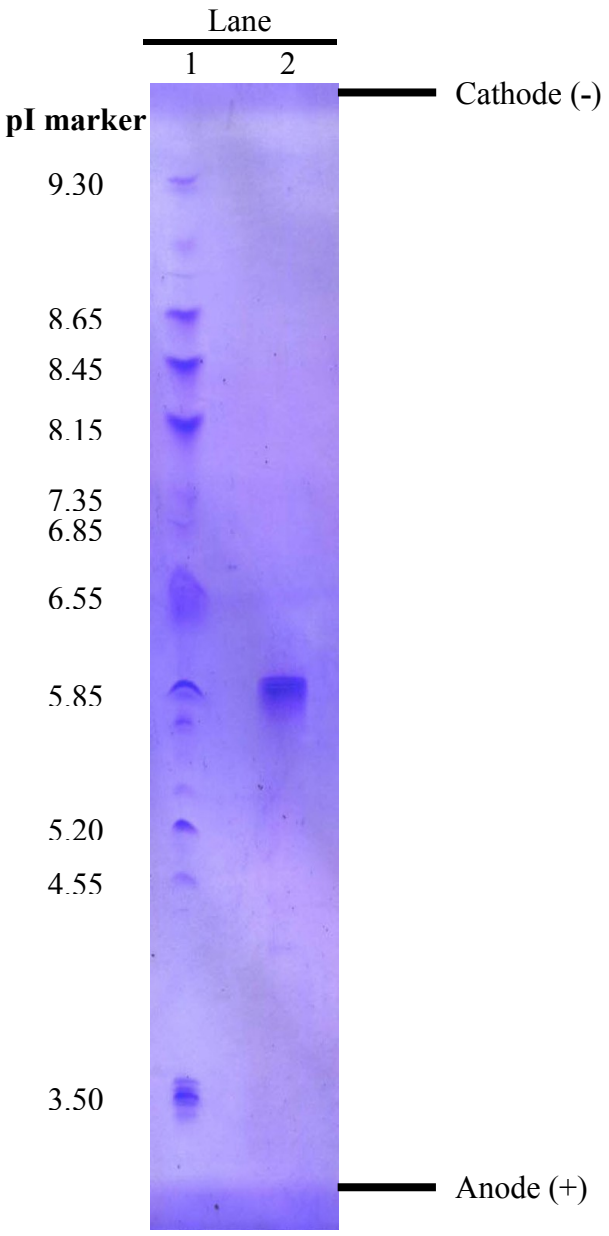

Figure 3. 23. Determination of the isoelectric point of engineered BCA. Lane 1 is the broad range marker (pH 3 – 10). Lane 2 is the engineered BCA and the relative migration distance was found to be 0.58.

3.5.3. Circular dichroism

The effect of PEG conjugation on the secondary structure of BCA was studied using circular dichroism (CD) spectroscopy and the far UV CD spectrum, in the range of 190-250 nm, was measured (Figure 3. 24). The fractional content of secondary structures was analyzed using CDSSTR in CDPro software and the analysis was performed with reference to a database consist of 48 soluble proteins, SPD48. The percentage of secondary structure and normalized root-mean-square deviation (NRMSD) for both native and pegylated BCA are summarized in Table 3. 2. The native BCA consists of 34.2% α-helices, 18.4% β-sheet, 20% turns and 26.4% unordered structure while similar results were obtained for pegylated BCA (35.4% α-helices, 18.8% β-sheet, 20.5% turns and 25.7% unordered structure) indicating that pegylation did not introduce significant changes to the secondary structure. The NRMSD values of 0.033 and 0.067 for the native and pegylated BCA, respectively, indicate a good agreement between the theoretical CD spectra calculated from the derived secondary structure and the experimental spectra.

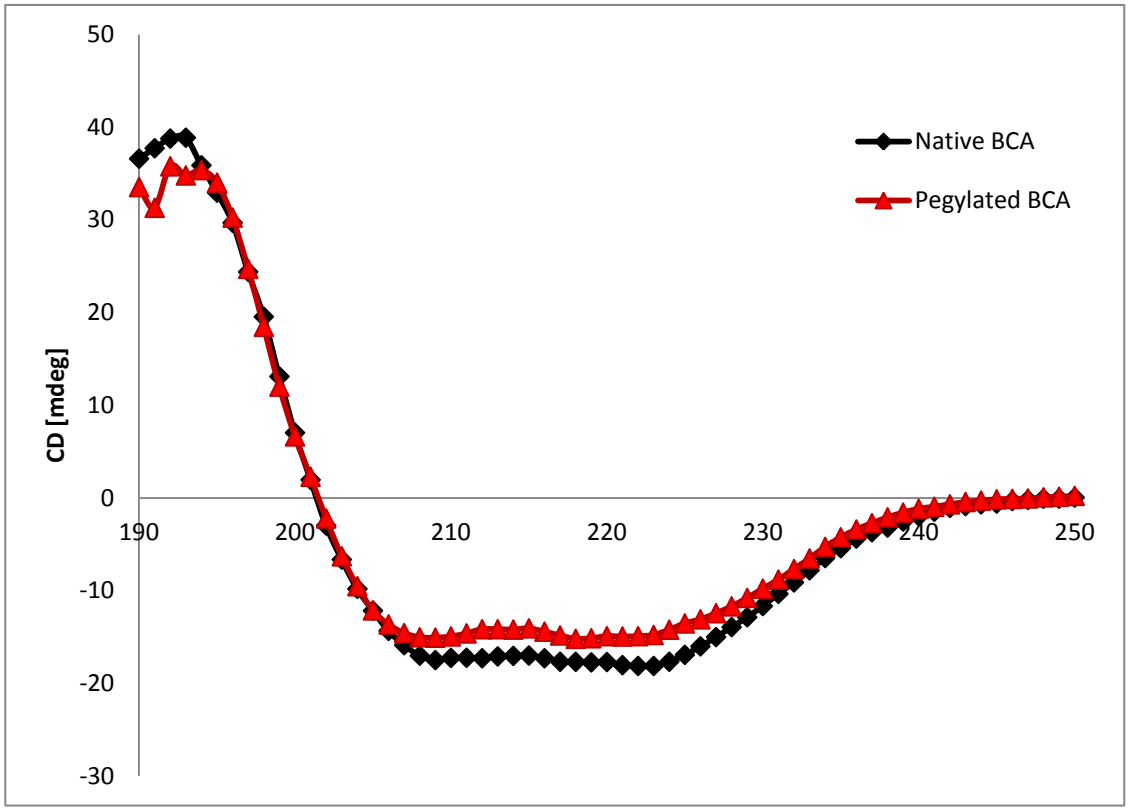

Figure 3. 24. Circular dichroism spectrum of native and pegylated BCA. The graph represents ellipticity values in millidegree (mdeg) against the far UV wavelengths (190 – 250 nm).

Table 3. 2. Fractional secondary structure of native and pegylated BCA analyzed by the CDSSTR program in CDPro software.

	α-helices (%)	β-sheet (%)	Turns (%)	Unordered structure (%)	NRMSD
Native BCA	34.2	18.4	20.0	26.4	0.033
Pegylated BCA	35.4	18.8	20.5	25.7	0.067

3.5.4. Enzyme specificity

Although asparaginase has been an effective therapeutic for acute lymphoblastic leukemia (ALL), it not only breaks down asparaginine, but also glutamine, which may result in some deleterious side effects (Durden & Distasio, 1980). Thus, substrate specificity is an important feature when developing enzyme therapeutics. We therefore assayed the specificity of engineered BCA in a mixture of 40 different amino acids. The mixture of amino acids was incubated with 10 U native and pegylated BCA, at 37°C for 12 hour. The change of amino acid content was monitored by amino acid analyzer (AAA) (Figure 3. 25). In the presence of BCA, arginine was reduced to an undetectable level and concomitantly the enzymatic products, urea and ornithine increased. Some fluctuations in the levels of amino acid were measured but since the variation was within 10%, it could be accounted for by the machine reproducibility. Based on the 40 amino acids tested, the specificity of both native and pegylated BCA has been confirmed and no sign of amino acid degradation other than arginine could be observed.

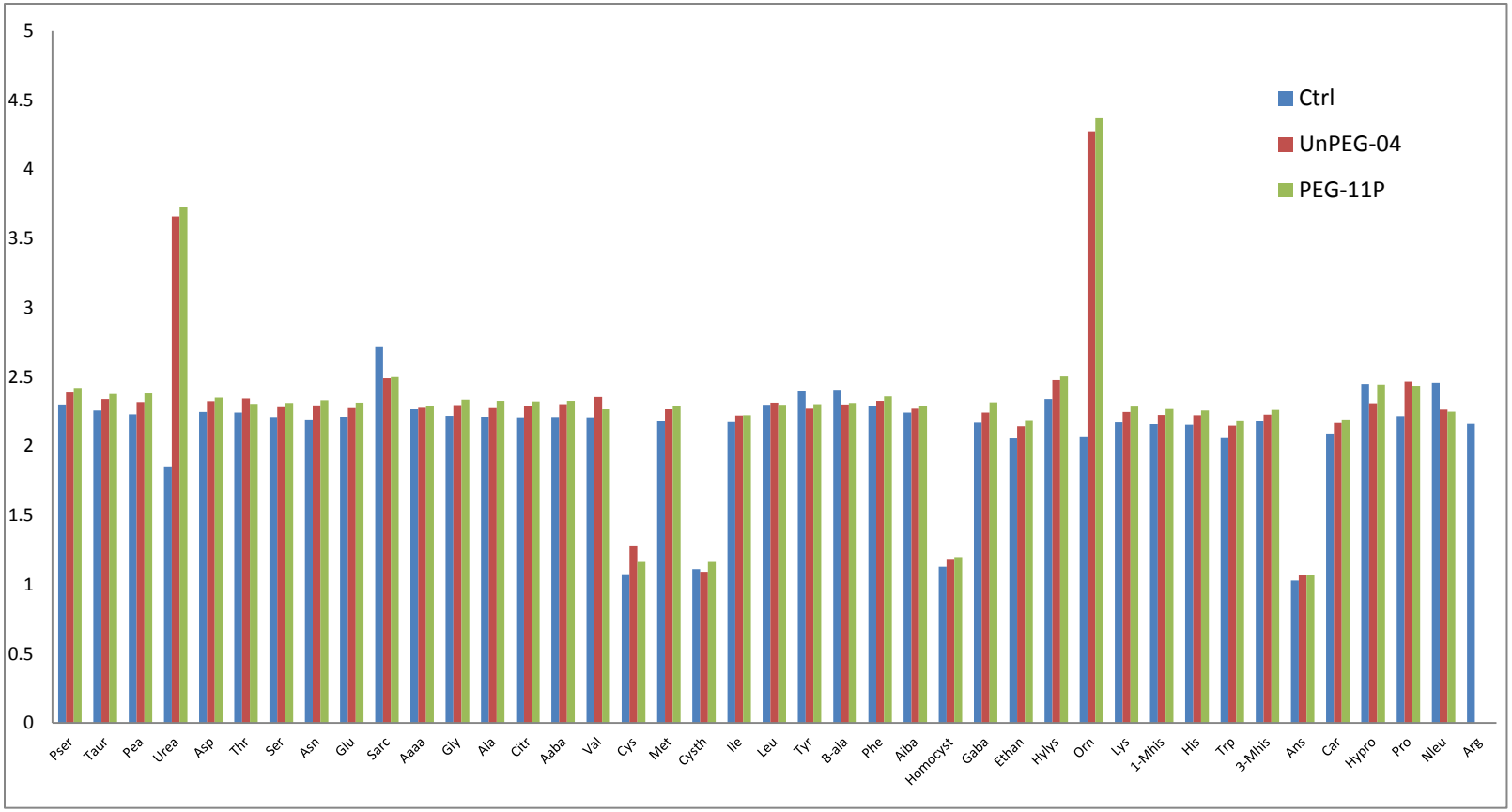

Figure 3. 25. Activity of BCA toward 40 different amino acids. When 10 U of native and pegylated BCA was incubated with amino acid mixture, arginine drops to an undetectable level with concomitant increase of urea and ornithine. The levels for the rest of the amino acids yielded less than 10% variation, which are considered as the acceptable variation between each run and thus no substantial differences could be seen between the control (without enzyme), native and pegylated BCA.

3.5.5. Thermal stability

The thermal stability of engineered BCA was studied using the technique of CD spectroscopy, which revealed the kinetics of protein unfolding with increasing temperature. The thermal stability was measured by following the ellipticity at 222 nm as a function of temperature, which increased from 20 to 95 °C at a rate of 1°C per min. The melt curves of engineered BCA and HuArg are shown in Figure 3. 26. The ellipticity in between 20-50 °C and 70-95 °C represent the native and unfolded state of HuArg, respectively. In contrast, the native and unfolded states for engineered BCA were found in between 20-75 °C and 90-95 °C, respectively. The melting temperature (Tm) is defined as the midpoint of transition from native to denatured state through thermal denaturation. The Tm was estimated through the first derivative of the ellipticity at 222 nm and the peaks at 60 °C and 82 °C represent the Tm values of HuArg and engineered BCA, respectively. The Tm of engineered BCA was 22 °C higher than the HuArg, suggesting the superior thermal stability when compared to the mesophilic protein.

a)

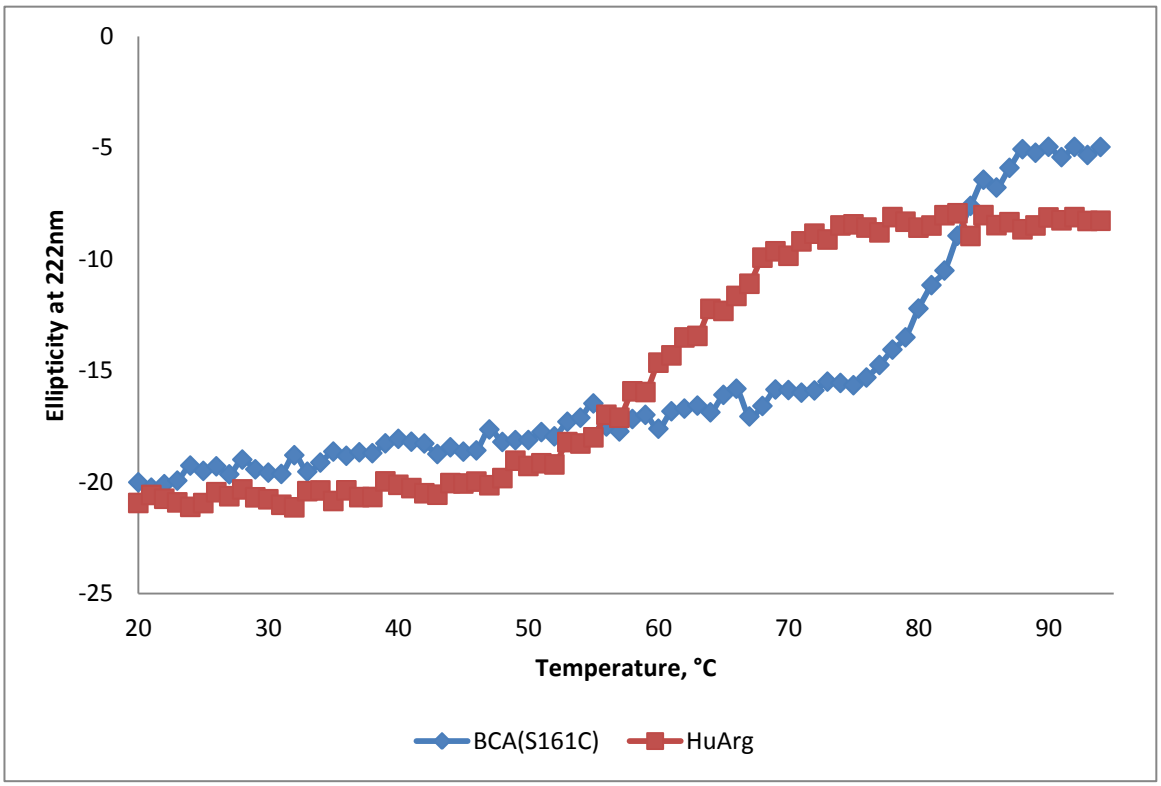
0
-5
-10
-15
-20
-25
Ellipticity at 222nm
20
30
40
50
60
70
80
90
Temperature, °C
BCA(S161C)
HuArg

b)

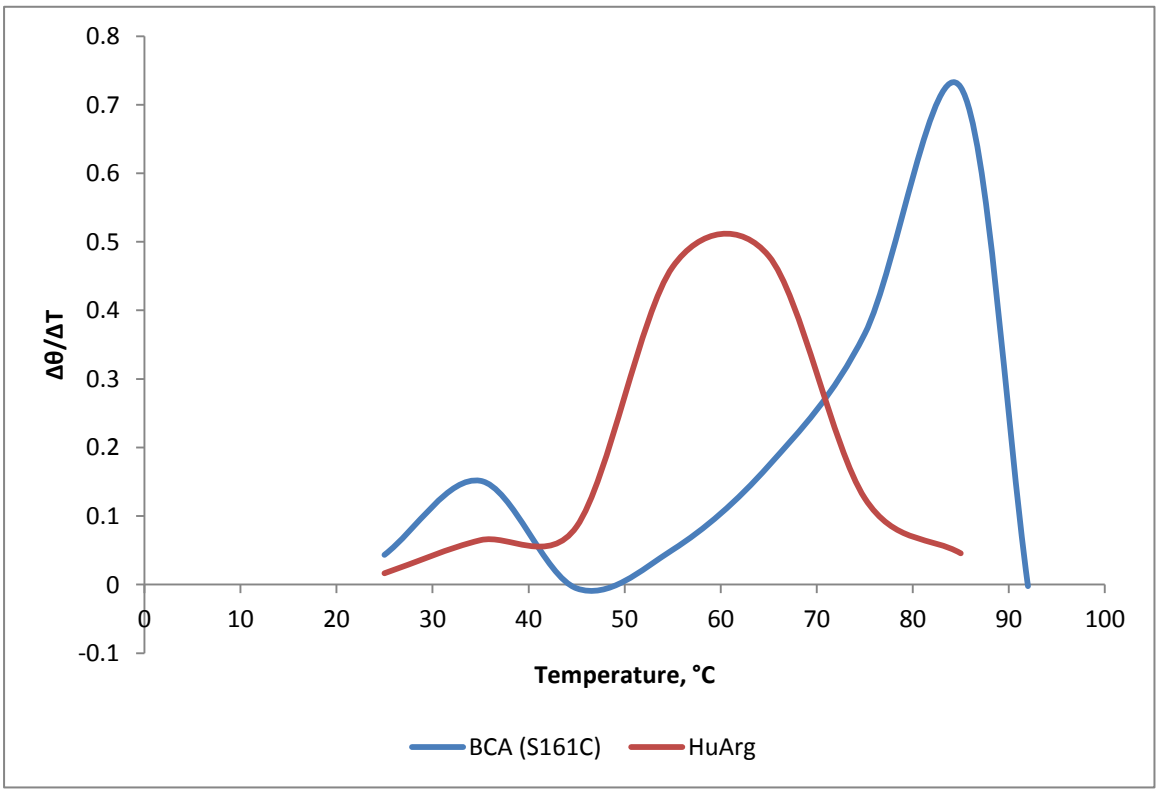
0.8
0.7
0.6
0.5
0.4
0.3
0.2
0.1
0
-0.1
ΔΘ/ΔT
0
10
20
30
40
50
60
70
80
90
100
Temperature, °C
BCA (S161C)
HuArg

Figure 3. 26. Thermal unfolding of native and engineered BCA and human arginase. (a) Protein melting curves of engineered BCA and HuArg were constructed by monitoring the CD ellipticity at 222 nm as a function of temperature. (b) By taking the first derivative of (a), the maxima correspond to the Tm values of protein melt curve. The Tm values of engineered BCA and HuArg were found to be 60 °C and 82 °C, respectively.

3.5.6. Enzyme stability

Enzyme stability over the period of storage was monitored by measuring the specific activity over a period of time which hopefully would provide insight to the shelf life of BCA. To facilitate the use of BCA for *in vitro* and *in vivo* studies, the purified enzyme was kept in 20 mM phosphate buffer and maintained in a sterile condition at 4 °C. The native BCA preserved its specific activity over 20 months of storage, but the activity dropped to about one-third 12 months later (Figure 3. 27). Pegylated BCA, on the other hand, demonstrated a very stable activity over the course of our 32-month study. Thus, the stability of BCA was significantly improved through pegylation.

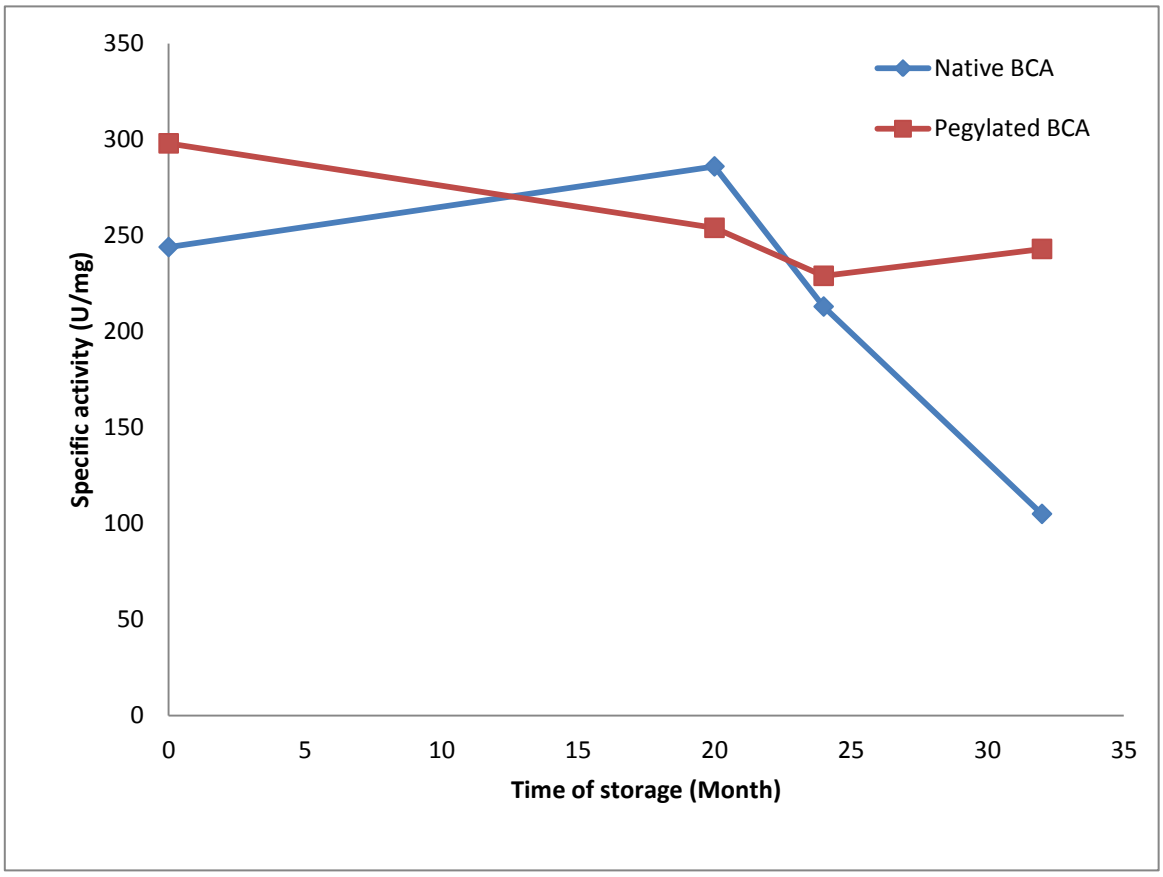

Figure 3. 27. Stability of BCA monitored over a period of storage. The specific activity of BCA was measured as a function of time. The activity of native BCA was preserved over 20 months of storage and dropped to about one-third by 32 months while pegylated BCA retained about 90 % of specific activity after 32 months of storage.

3.6. Large scale purification and pegylation of BCA

In order to prepare sufficient amount of native and pegylated BCA for *in vitro* and *in vivo* studies, the *E. coli* cells expressing BCA were produced in large quantity by fed-batch fermentation. To purify the BCA from the cells obtained from fed-batch fermentation, a large scale purification strategy was established based on the trial of purification from shake flask culture and also the information from the characterization of BCA. In general, the purification process is similar to the two-step purification (Section 3.3.2) and the results would be briefly described while the following report will focus on the purification of pegylated BCA.

The pegylated BCA is the key substance for efficacy and pharmacological studies and thus its quality was further improved with the help of different chromatographic techniques. For instance, the residual PEG after pegylation was successfully lowered. The undetectable level of residual PEG was confirmed by the iodine staining of SDS-PAGE. The endotoxin introduced by the gram-negative *E.coli* cells was significantly lowered, as revealed by the Limulus Amebocyte Lysate (LAL) assay. The purified enzyme with improved quality was filtered under sterile conditions and its specific activity was determined by bioassay.

3.6.1. Purification of native BCA from fed-batch fermentation

The fermentation of BCA-expressing *E. coli* cells in a 5 L bioreactor produced 248.86 g wet cell weight. The cell pellet was re-suspended in solubilization buffer containing DNAse and RNase which broke down the huge amount of DNA and RNA released by homogenization, thus reducing the viscosity of the cell lysate. The cell lysate, after passeing through the homogenizer for three times, was incubated at 37 °C for 15 minutes to further reduce the viscosity, followed by centrifugation to obtain the soluble fraction. The first step of purification removes the non-target impurities by heat treatment at 70 °C for 15 min which precipitated the heat labile protein, and the heat stable BCA was recovered by centrifugation.

Soluble fraction containing the target protein was further purified by Ni-affinity column with 196 ml bed volume packed in XK50. Briefly, a 4-segment elution program was used to elute the BCA from the Ni-affinity column. The first elution gradient from 0 to 30% elution buffer was intended to remove the protein that bound non-specifically on the column. The second segment was maintained at 30% which allowed complete elution of non-specific bound proteins. The target protein was eluted out in the third segment by increasing concentration of elution buffer from 30 to 70%. The fourth segment of 70 to 100% elution buffer eluted any remaining protein that was still bound on the column. The fractions that gave absorbance at UV wavelength 280 nm was analyzed by SDS-PAGE while the 24 fractions from E1 to A'5 (50 ml each), containing the target protein, were pooled together (Figure 3. 28 and Figure 3. 29). The pooled fractions containing high concentration of imidazole were desalted by tangential flow filtration (TFF) system, based on our understanding of the hexameric structure of BCA, membranes with 30 kDa

NMWC were installed. The purified BCA was maintained in PBS, filtered with 0.2 μm filter under sterile condition and stored at 4 °C until pegylation. Through the 2-step pilot scale purification, about 1096 mg of BCA protein was obtained and the specific activity was determined to be 264 U/mg.

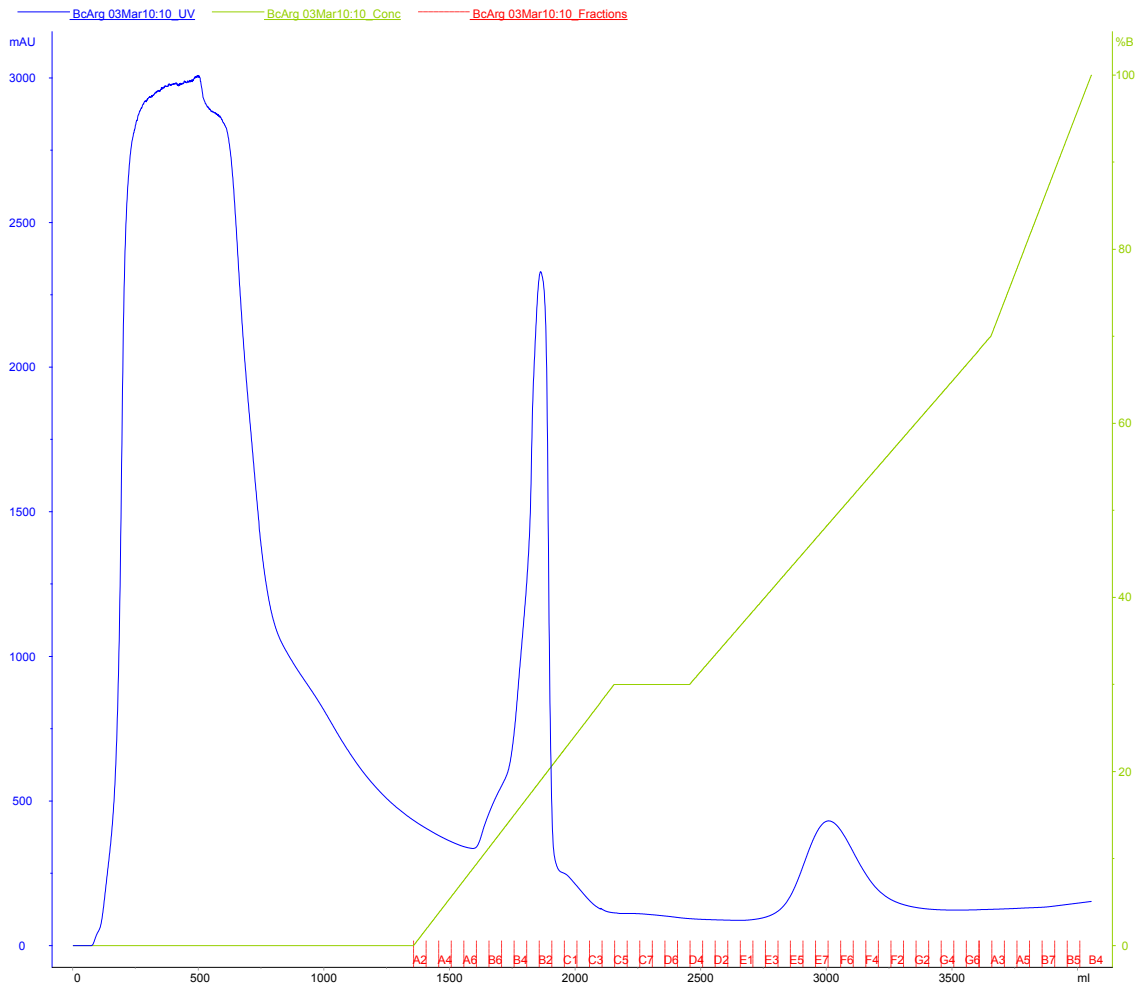

Figure 3. 28. Chromatogram showing the large scale purification of engineered BCA using XK50 nickel affinity column with 196 ml bed volume. Similar to the small scale purification, a four-segment elution gradient was adopted and the elution profile was monitored by absorbance at 280 nm.

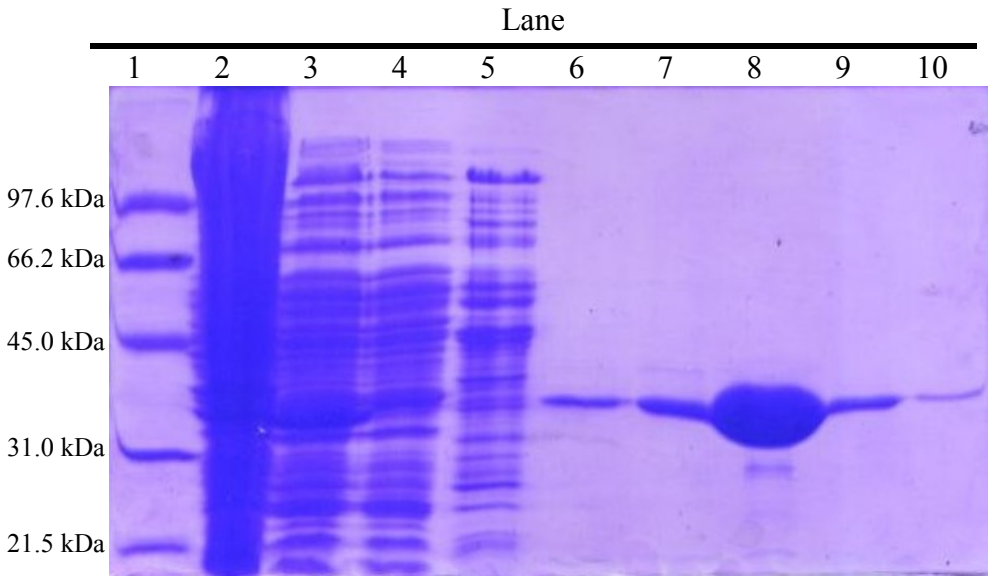

Figure 3. 29. Selected fractions from the large scale purification of engineered BCA were analyzed by SDS-PAGE. Lane 1 is the low-range marker. Lane 2 is the total protein from cell lysate. Lane 3 represents the soluble proteins collected after heat treatment. Lane 4 shows the protein flow through from the XK50 nickel affinity column. Lane 5 is the non-specific bound proteins (Pooled fractions from A6-C3). Lanes 6 to 10 represent fraction E2, E3, F7, G3 and A'5, respectively.

3.6.2. Pegylation of BCA and removal of residual PEG

Having optimized the pegylation conditions for BCA in Section 3.4.1.1-2, we dedicated to use 20 molar equivalents of PEG for the pegylation process as the amount of unpegylated protein shown in the SDS-PAGE was slightly lower when compared to 10 equivalents of PEG. Prior to pegylation, the protein was reduced by TCEP at room temperature for 4 h. To pegylate the BCA, about 800 mg of protein was diluted to 2 mg/ml and equally divided into 2 bottles. Equal volume of solution containing 20 equivalents of PEG was added to the protein solutions. The reaction was kept at 4 °C for overnight pegylation and a sample was collected after pegylation for SDS-PAGE analysis. The shift of the molecular mass of BCA from 33 kDa to 100 kDa confirmed the PEG conjugation (Figure 3. 30a). The band smear in between 31 kDa and 66 kDa as revealed by iodine staining of SDS-PAGE, was suggested to be the residual PEG (Figure 3. 30b). Two bottles of reaction mixture were processed separately and one of them will be fully described below as an example. The residual PEG was partially removed by TFF system equipped with 50 kDa NMWC membranes. The retentate and filtrate after TFF were examined using SDS-PAGE followed by iodine staining. Lane 4 was the sample collected after TFF, showing that the pegylated BCA was almost completely retained but amount of free PEG was lower when compared to Lane 2, which was equally loaded (10µg) sample collected before removal of free PEG. The slight difference in the band thickness and intensity may be due to the interference of Bradford's test by the presence of excessive amount of free PEG. Lane 3 shows the filtrate obtained during TFF which contained a substantial amount of PEG as manifested by iodine stain. Thus, a significant amount of free PEG was removed by TFF but the target protein was recovered from the retentate. The specific activity of pegylated BCA was found to be 215 U/mg which is

lower than the native BCA before pegylation and possibly interfered by the presence of free PEG.

To further remove the free PEG from the retentate, pegylated BCA was loaded onto nickel affinity column. With the help of His-tag at its C-terminus, pegylated BCA would bind to the Ni-column while free PEG would be collected in the flow through. The elution profile of pegylated BCA was monitored by UV absorbance at 280 nm and shown in Figure 3. 31. The target protein was eluted with a gradient elution from 0 to 70% of elution buffer and fractions having absorbance at 280 nm were analyzed by SDS-PAGE (Figure 3. 32). Lane 3 is the flow-through collected during sample loading, showing that a portion of pegylated BCA did not bind to the Ni-column, possibly due to the presence of free PEG that interfered with the binding of pegylated BCA. Lanes 4 to 10 show the fractions collected from gradient elution. Fractions A6-C2 (10 fractions), 500 ml total volume, containing the target protein, were pooled and analyzed by SDS-PAGE to confirm the removal of free PEG (Figure 3. 33). Lane 4 shows the pooled fractions from Ni-column and the free PEG was lowered to undetectable level by iodine staining on SDS-PAGE. The pooled fractions were desalted by TFF to remove imidazole. The pegylated BCA was kept in PBS, sterilely filtered and stored at 4 °C until endotoxin removal. The specific activity of pegylated BCA was found to be 257 U/mg which is comparable to the native enzyme before pegylation and about 72% of enzyme activity was recovered after pegylation. The overview of the purification process was summarized in Table 3. 4. Similar results were obtained from the removal of free PEG for the other batch of pegylation.

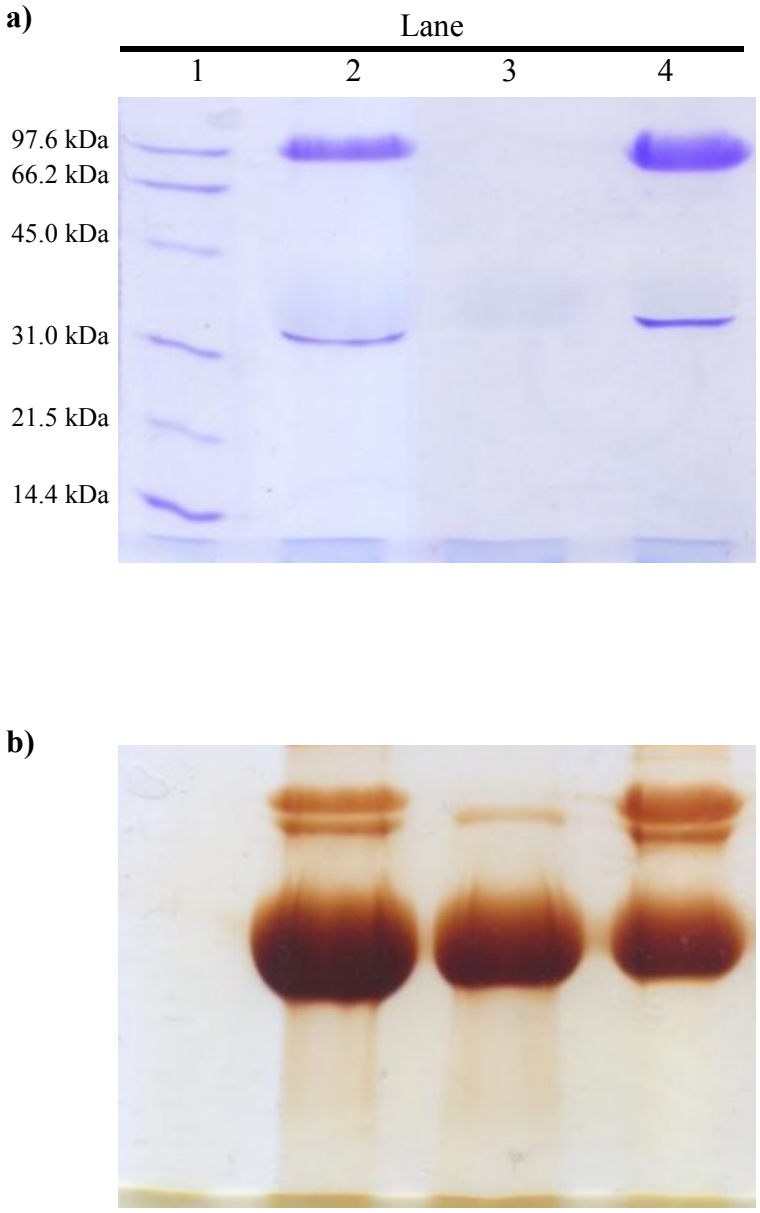

Figure 3. 30. Removal of free PEG through TFF. Sample collected during the TFF process was analyzed on the SDS-PAGE and visualized by a) Coomassie blue and b) iodine stain. The samples were loaded to the SDS-PAGE in the same configuration. Lane 1 is the low range protein marker. Lane 2 shows sample collected immediately after the pegylation reaction. Lanes 3 and 4 represent the filtrate and retentate collected from TFF, respectively. The band at about 100 kDa and 33 kDa as shown in (a) correspond to

pegylated and native BCA, respectively. Iodine stain (b) revealed the size of pegylated BCA at about 100 kDa on SDS-PAGE while the smear in between 31 and 66 kDa is the free PEG.

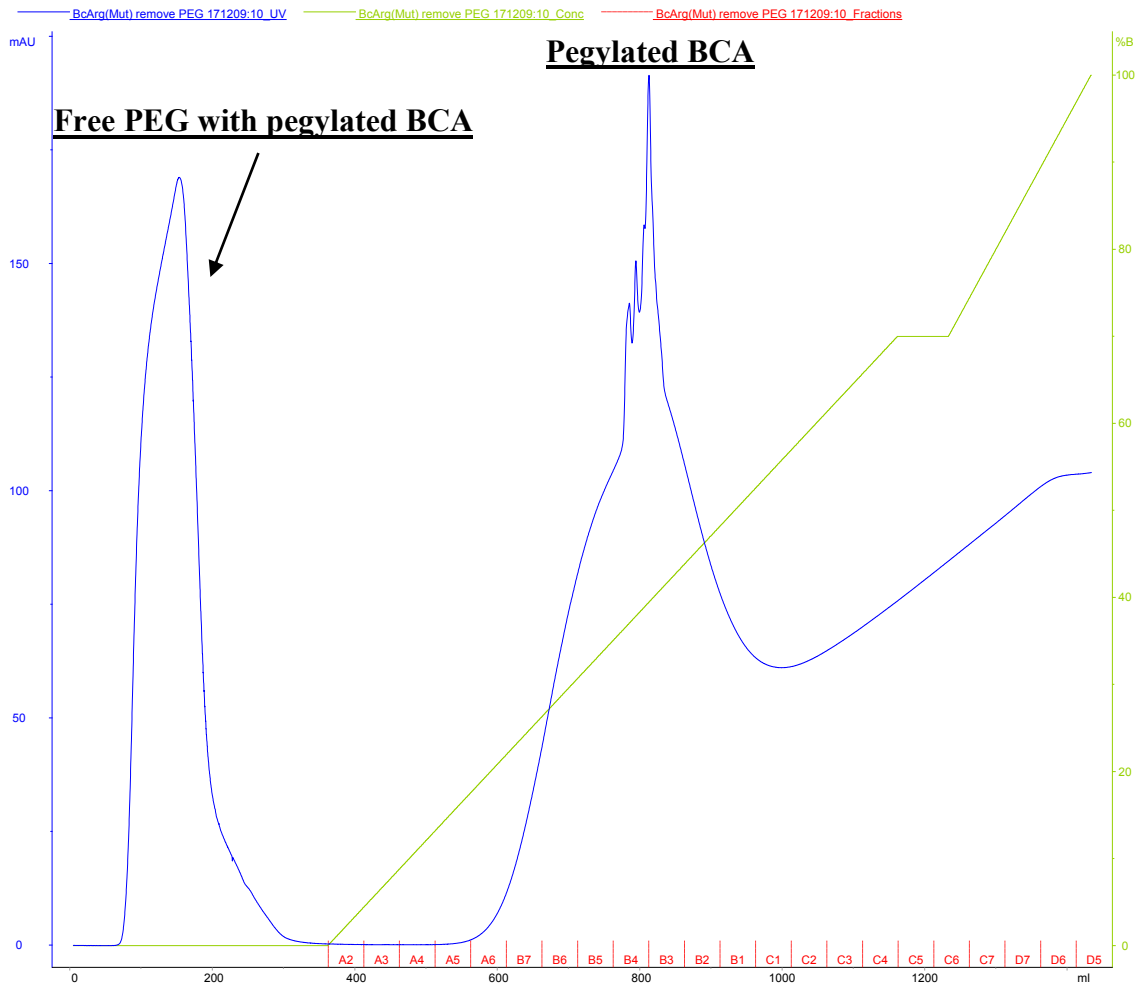

Figure 3. 31. Chromatogram showing the elution profile of pegylated BCA from the XK50 nickel affinity column. The pegylated BCA containing free PEG was loaded onto the column and washed until the absorbance at 280 nm returned to the baseline level. The target protein was eluted by linear gradient elution from 0 to 70% elution buffer and selected fractions having absorbance at 280 nm was analyzed on the SDS-PAGE.

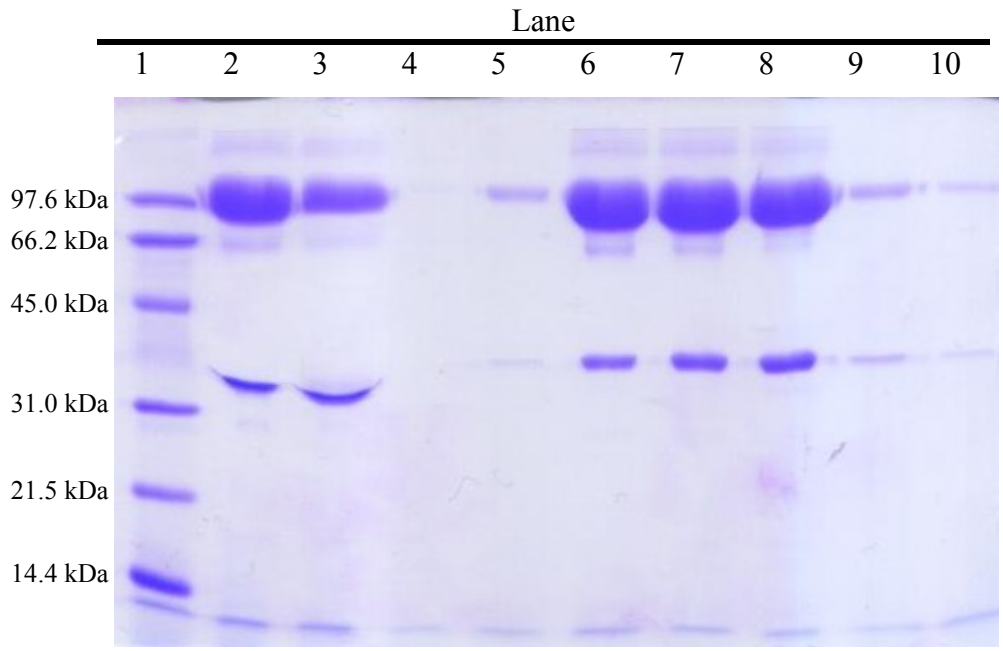

Figure 3. 32. Selected fractions from the purification of pegylated BCA were analyzed by SDS-PAGE. Lane 1 is the low-range marker. Lane 2 is the sample collected before XK50 nickel affinity column. Lane 3 shows the flow-through while Lanes 4 to 10 represent the fractions A5, A6, B5, B4, B3, C1 and C2 collected from the XK50 nickel affinity column, respectively.

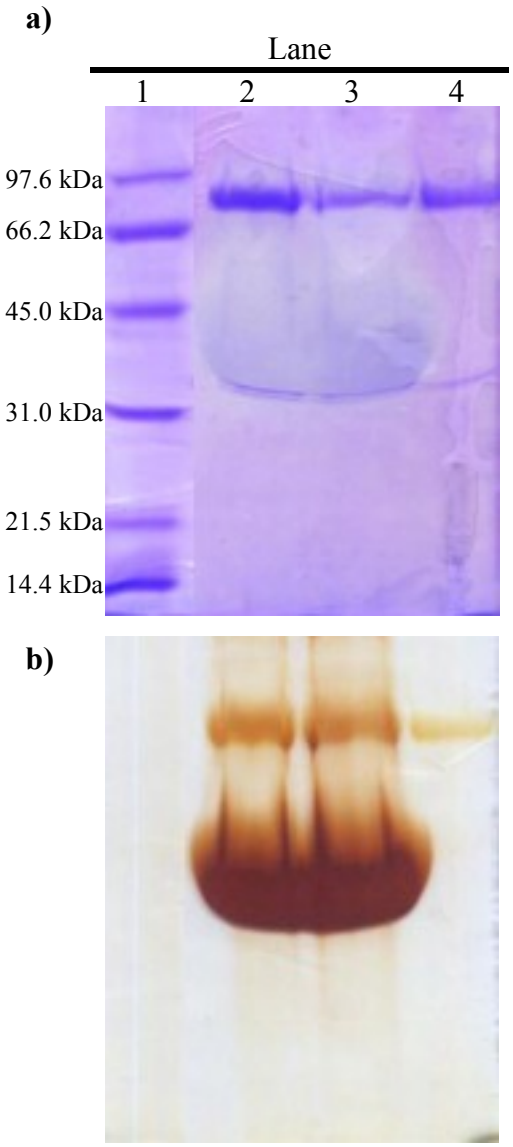

Figure 3. 33. Result from SDS-PAGE showing the pegylated BCA before and after removal of free PEG. The SDS-PAGE was stained by a) Coomassie blue and b) iodine stain. The samples were loaded in the same configuration. Lane 1 is the low-range marker. Lane 2 represents the sample collected before removal of free PEG by affinity chromatography. Lane 3 shows the flow-through from the XK50 nickel affinity column, which contains free PEG and pegylated BCA as shown in (b). Lane 4 is the pooled fractions eluted from the nickel affinity column, containing pegylated BCA but no detectable free PEG.

Table 3. 3. Summary for the purification of pegylated BCA.

Sample	Total Volume (ml)	Protein conc. (mg/ml)	Total Enzyme (units)	Total Protein (mg)	Specific Activity (units/mg)	Yield (%)
Native BCA for pegylation	200	2	105600	400.0	264.0	100
Pegylated BCA after TFF	95	5.95	121529	565.3	215.0	115.1
Pegylated BCA after Ni-column	68.5	4.32	76051	295.9	257.0	72.0

3.6.3. Removal of endotoxin

The use of *E. coli* expression system to produce protein therapeutics usually resulted in the contamination by lipopolysaccharide (LPS), known as endotoxin, which is a component of the *E. coli* outer cell membrane. A trace amount of endotoxin present in the therapeutics may induce a wide range of pathophysiological conditions and result in detrimental side effects such as endotoxin shock, tissue damage and even death (Magalhaes et al., 2007; Petsch & Anspach, 2000). Thus, the amount of endotoxin present in the therapeutics has been strictly regulated by FDA and the tolerance limit is dependent on the route of administration. For example, five endotoxin units (EU) per kg of body weight per hour were set as the limit for intravenous injection by all pharmacopoeias. It is of paramount importance to lower the endotoxin in our BCA preparation to an acceptable level, and therefore, separation techniques were adopted based on the differential properties of endotoxin and protein therapeutic.

The endotoxin present in the native BCA was removed by affinity chromatography using the Detoxi-Gel™ medium, which has immobilized polymixin B on the resins that binds to the lipid A portion of LPS. The XK26 column was packed with 20 ml Detoxi-Gel™ medium. Sample was loaded at a retarded flow rate (4 ml/min) and a pause of 10 min was introduced for every 20 ml of sample loaded to allow sufficient time for the binding of endotoxin.

For pegylated BCA, the endotoxin level was lowered by using Sartobind Q filter anion exchange filter, to which the negatively charged LPS (pI ~ 2) binds at neutral pH. The pegylated BCA was not adsorbed to the filter membrane possibly because the PEG was

shielding the surface charge of BCA; hence pegylated BCA was collected as flow through.

The endotoxin levels of the native and pegylated BCA were determined by Limulus amebocyte lysate (LAL) assay. The principle of this gel-clot assay is based on the activation of an enzyme cascade by LPS. The last step of the enzymatic reaction involves the clotting enzyme which cleaves the protein coagulogen to produce an insoluble product, coagulin, and form a gel matrix.

The BCA samples were prepared in a number of dilutions and added to the testing vials containing the LAL, which were incubated at 37 °C for 1 hour (Table 3. 4). The presence of gel-clot in the vials indicated that the sample contained an amount of endotoxin above the sensitivity limit of the LAL assay, which is 0.5 EU/ml. The endotoxin level was estimated through multiplying the sensitivity limit of the assay by the dilution folds of the sample. The endotoxin level of native BCA was in between 100 and 400 EU/ml while the pegylated sample was found below 20 EU/ml.

Table 3. 4. Determining the endotoxin level for native and pegylated BCA. The positive control contains 300 EU/ml endotoxin while the negative control refers to the LAL reagent water containing less than 0.25 EU/ml endotoxin. (✓ : Yes; X: No)

Sample	Dilution folds	Endotoxin Level (EU/ml)	Gel formation
Positive Control	---	---	✓
Negative Control	---	---	X
Pegylated BCA	40x	20	X
	200x	100	X
	800x	400	X
Native BCA	40x	20	✓
	200x	100	✓
	800x	400	X

3.7. Summary

Engineered BCA with a serine to cysteine mutation at position 161 introduced on the surface and a 6-histidine tag added to the C-terminus has been successfully cloned and expressed using the pET expression system. Purification of engineered BCA was achieved through a 2-step purification scheme combining heat treatment and nickel affinity column chromatography. This purification yields 28.7 mg of BCA from 250 ml shake-flask culture which corresponds to about 75 % recovery. The purity of BCA was increased by 3-fold and the specific activity was determined to be 319.9 U/mg.

Pegylation using SUNBRIGHT ME-200MA was optimized on the basis of mole ratio for which 10 to 20 equivalent of PEG resulted in the best pegylation efficiency. Optimization on pH and temperature did not show further improvement and thus the pegylation process was maintained at pH 7 and 4°C with overnight incubation.

The preliminary study on the fusion of ABD to the C-terminus of BCA has shown that the fusion protein binds HSA on both native PAGE and gel filtration column chromatography. Meanwhile, the specific activity of BCA-ABD was about one-third lower when compared to the engineered BCA alone. However, the activity was not affected by the presence of different amounts of HSA, and its anti-tumor activity was confirmed by its dose-dependent inhibition of MKN45 in culture condition.

The analysis from SDS-PAGE revealed the molecular size of native and pegylated BCA about 33 kDa and 100 kDa, respectively. Similar results for the native BCA were obtained from the ESI-MS study, for which the experimental value of 33275.25 Da was in good agreement with the calculated average molecular weight. On the contrary, the

size of pegylated BCA was found to be about 55 kDa which did not agree with the result from the SDS-PAGE and will be commented in the discussion. Results from the gel filtration column chromatography suggested the BCA exists in both hexameric and monomeric structures. Aggregates were found in both wild type and engineered BCA, implying the rational engineering done on BCA is not like the cause of aggregation. Further characterization using isoelectric focusing determines the pI of BCA to be 5.8. Formulation of BCA with PEG molecule does not significantly alter the secondary structure of pegylated BCA, as monitored by CD spectroscopy. Through monitoring the CD ellipticity at 222 nm, T_m values of engineered BCA and HuArg were found to be 82 °C and 60 °C, respectively.

The specificity of BCA to arginine was confirmed when tested against 40 different amino acids: only arginine was metabolized by the enzyme. The activity of native BCA dropped to about one-third after 32 months of storage whereas pegylated BCA retained 90% activity under the same storage condition.

Purification of native BCA from fed-batch fermentation was developed based on the small scale purification scheme established. Pegylated BCA was further purified through TFF and nickel affinity column chromatography to reduce the residue PEG to undetectable level as shown by SDS-PAGE analysis. The pegylated BCA remained active at the end of purification and showed specific activity of about 257 U/mg which is comparable to the native BCA, at 264 U/mg. The yield of purification for pegylated BCA was found to be 72%.

The amount of endotoxin present in the native and pegylated BCA was lowered through Detoxi-Gel™ and Sartobind Q filter, respectively. The endotoxin level was determined by LAL assay for which native BCA was found to contain 100-400 EU/ml entodoxin while pegylated BCA contains less than 20 EU/ml.

4. *In vitro* efficacy and mechanistic studies

4.1. Precis:

Studies highlighting the anti-cancer properties of arginase predate the 1950s. Depletion of arginine in the culture medium either using purified bovine arginase or liver extract, induced growth arrest in mouse carcinoma cell lines possibly by inhibiting DNA synthesis (Holley, 1967; Sasada & Terayama, 1969; Simon-Reuss, 1953). More strikingly, complete devastation of leukemia cell lines has been reported within 24 h of incubation but the cell death mechanisms were not fully described (Storr & Burton, 1974). However, the results of *in vivo* studies were controversial and incoherent with the promising effects observed in culture (Greeberg & Sassenrath, 1953; Irons & Boyd, 1952; Wiswell, 1951). In the past decade, the interest in arginase was rekindled by the encouraging observation that treatment by systemic release of hepatic arginase induced various degrees of remission in HCC patients (Cheng et al., 2005). Since then several reports in the literature demonstrated that human arginase could effectively retard the growth of several tumor types including HCC, melanoma, leukemia and prostate cancer (Hernandez et al., 2010; Hsueh et al., 2012; Lam et al., 2009; Lam et al., 2010). These promising results warranted arginase for further testing on different cancer cell types.

In this chapter, *in vitro* anti-cancer effects of the thermostable *Bacillus caldovelox* arginase (BCA) would be examined on a spectrum of gastric (MKN45, AGS and BGC823) and colorectal (HCT15 and HCT116) cancer cell lines. The study of arginine depletion on this panel of cancer cell lines, using arginine depleting enzymes or otherwise, is unprecedented. Through this study, the vulnerability of these cell lines toward different arginine depleting enzymes would be studied and the underlying mechanism with

reference to the expression of the urea cycle enzymes in both transcript and protein levels would be assayed using semi-quantitative RT-PCR and Western blot analysis, respectively. Through understanding the ability of the cancer cells to utilize citrulline, the precursor for arginine synthesis, may provide a more decisive explanation to the resistance against the use of arginine-depleting enzymes in some cell lines. Moreover, the effects of arginine depletion on cell cycle distribution would be revealed by propidium iodide (PI) staining, while apoptosis would be monitored by double staining using PI and fluorescent-labeled annexin-V. The observation of apoptosis would be further confirmed by monitoring the activation of caspase-3 through Western blot analysis and staining with fluorescent-labeled caspase-3 specific inhibitor over the period of arginine depletion. The effect of arginine depletion on the mitochondrial membrane potential would also be studied in the hope of understanding the pathway leading to apoptosis.

4.2. Arginine requirement for gastric and colorectal cancer cell lines in culture

To evaluate the arginine requirement for the panel of gastric and colorectal cancer cell lines, various amounts of arginine were added to arginine-deficient medium supplemented with 10 % dialyzed serum. After 72 h of incubation, the viability of the cancer cell lines was measured by MTT colorimetric assay. In all cell lines tested, cell viability was found to be proportional to the concentration of arginine in the culture medium (Figure 4. 1). An arginine concentration of 1.5 mM (or less) in the culture medium was sufficient to restore the growth of cancer cells comparable to the commercially available RPMI culture medium which contains 1.15 mM arginine. These results suggest that the extent of cell proliferation / growth inhibition strongly correlates with the amount of arginine in the culture. Similar results have been reported in the literature (Scott et al., 2000) and further supports the notion that cancer cells in general are auxotrophic for arginine and rely on the exogenous supply of the amino acid from the culture medium. Thus, arginine depleting enzyme such as arginine deiminase (ADI) and arginase that break down arginine to different products would be further evaluated.

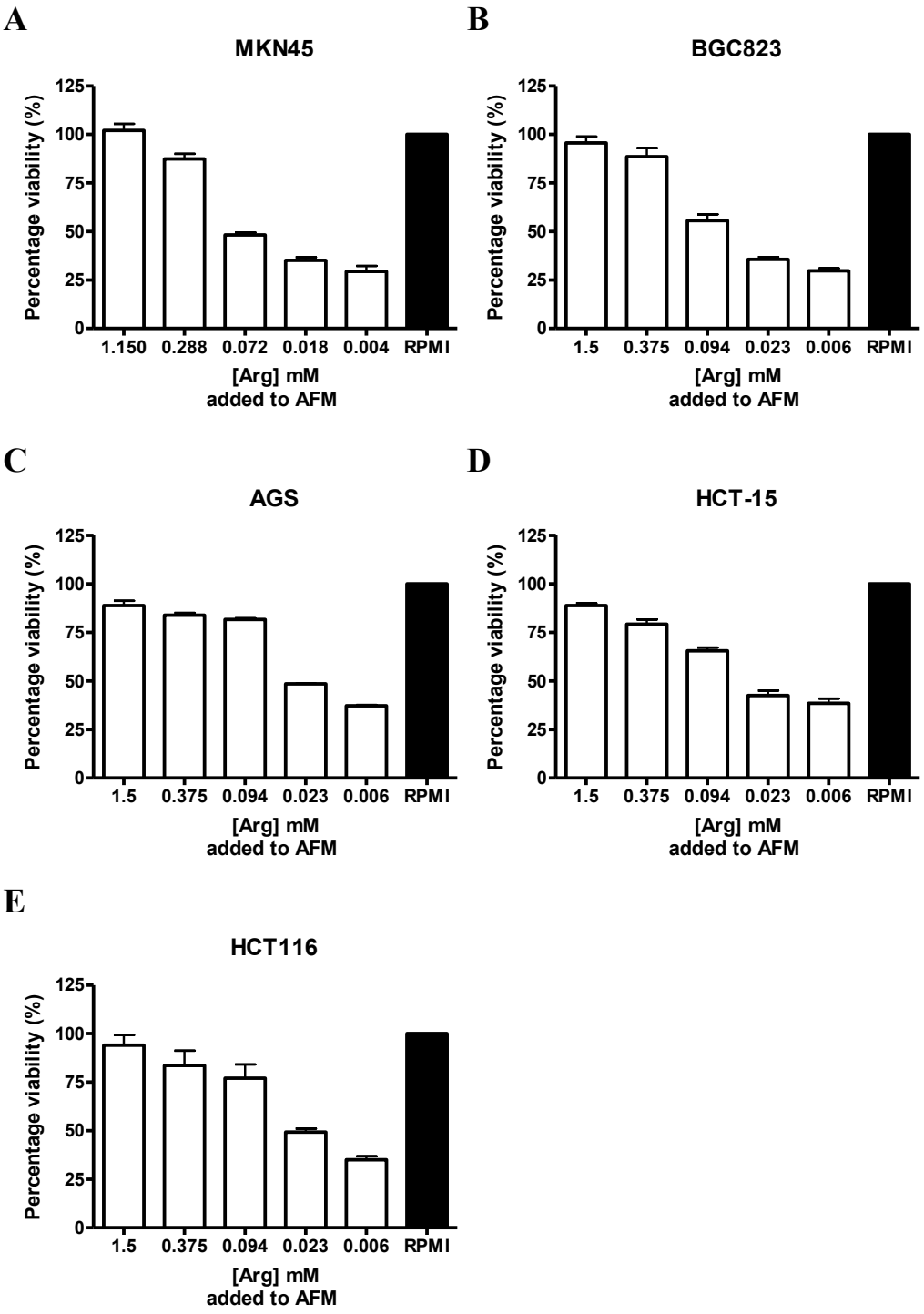
A
MKN45
Percentage viability (%)
125
100
75
50
25
0
1.150
0.288
0.072
0.018
0.004
RPMI
[Arg] mM
added to AFM
B
BGC823
Percentage viability (%)
125
100
75
50
25
0
1.5
0.375
0.094
0.023
0.006
RPMI
[Arg] mM
added to AFM
C
AGS
Percentage viability (%)
125
100
75
50
25
0
1.5
0.375
0.094
0.023
0.006
RPMI
[Arg] mM
added to AFM
D
HCT-15
Percentage viability (%)
125
100
75
50
25
0
1.5
0.375
0.094
0.023
0.006
RPMI
[Arg] mM
added to AFM
E
HCT116
Percentage viability (%)
125
100
75
50
25
0
1.5
0.375
0.094
0.023
0.006
RPMI
[Arg] mM
added to AFM

Figure 4. 1. Viability of gastric and colorectal cancer cell lines cultured in various concentrations of arginine for 72 h. The viability of gastric (A, B & C) and colorectal (D & E) cancer cell lines were compared to the control, commercially available RPMI medium, on the right hand side of each graph. Viability was determined by MTT endpoint colorimetric assay, where the formation of colorimetric product was based on mitochondrial dehydrogenase activity. Data shown are means ± SD (n = 3).

4.3. The effectiveness of BCA and ADI on gastric and colorectal cancer cell lines

Systemic depletion of arginine has been proposed as a potential treatment strategy for cancers. Out of the methods available in the literature, the current study focuses on the development of enzyme therapeutics that can break down arginine, such as arginase and ADI. Development of different arginine depleting enzymes has been reported, but cancer cells respond differently to these enzymes. When BCA is added to the culture medium, it breaks down arginine to ornithine and urea. Growth retardation was observed in both gastric and colorectal cancer cell lines and the effect was proportional to the amount of BCA present in the culture (Figure 4. 2). The IC_{50} value is defined as the amount of enzyme required to achieve 50% growth inhibition in the culture in 72 h. The viability was determined by MTT assay and summarized in Table 4. 1. Gastric cancer cell lines, MKN45, BGC823 and AGS gave similar IC_{50} values in between, 1.78 to 2.52 U/ml (10.92 to 15.33 μg/ml), for which BGC823 was most sensitive to the arginine depletion induced by BCA while MKN45 was the least. In contrast, the amount of BCA required to produce similar inhibition varies greatly between the colorectal cancer cell lines: HCT116 was more sensitive to arginine depletion and having an IC_{50} value of 0.46 U/ml (1.3 μg/ml), while 22.37 U/ml (131.2 μg/ml) BCA was required to produce 50% growth inhibition in the HCT-15 cell line.

When gastric and colorectal cancer cell lines were exposed to ADI, an arginine-depleting enzyme currently in clinical trial, only HCT116 showed suppressed growth with an IC_{50} value of 0.009 U/ml (0.33 μg/ml) while the rest of the cell lines were highly resistant to the treatment (Figure 4. 3). Even at the highest concentration of ADI (0.5 U/ml) , no significant inhibition could be observed when compared to the control. HCT116 was the

only cell line that was sensitive to both BCA and ADI. When the IC_{50} values were compared, it was found that ADI is about 4 times more potent than BCA in terms of the amount of protein added to the culture. These interesting observations in response to different arginine depleting enzymes are likely attributed to the enzymatic products generated, and the underlying mechanisms governing the resistance might be correlated to the expression of urea cycle enzymes. This will be further explored in the next section.

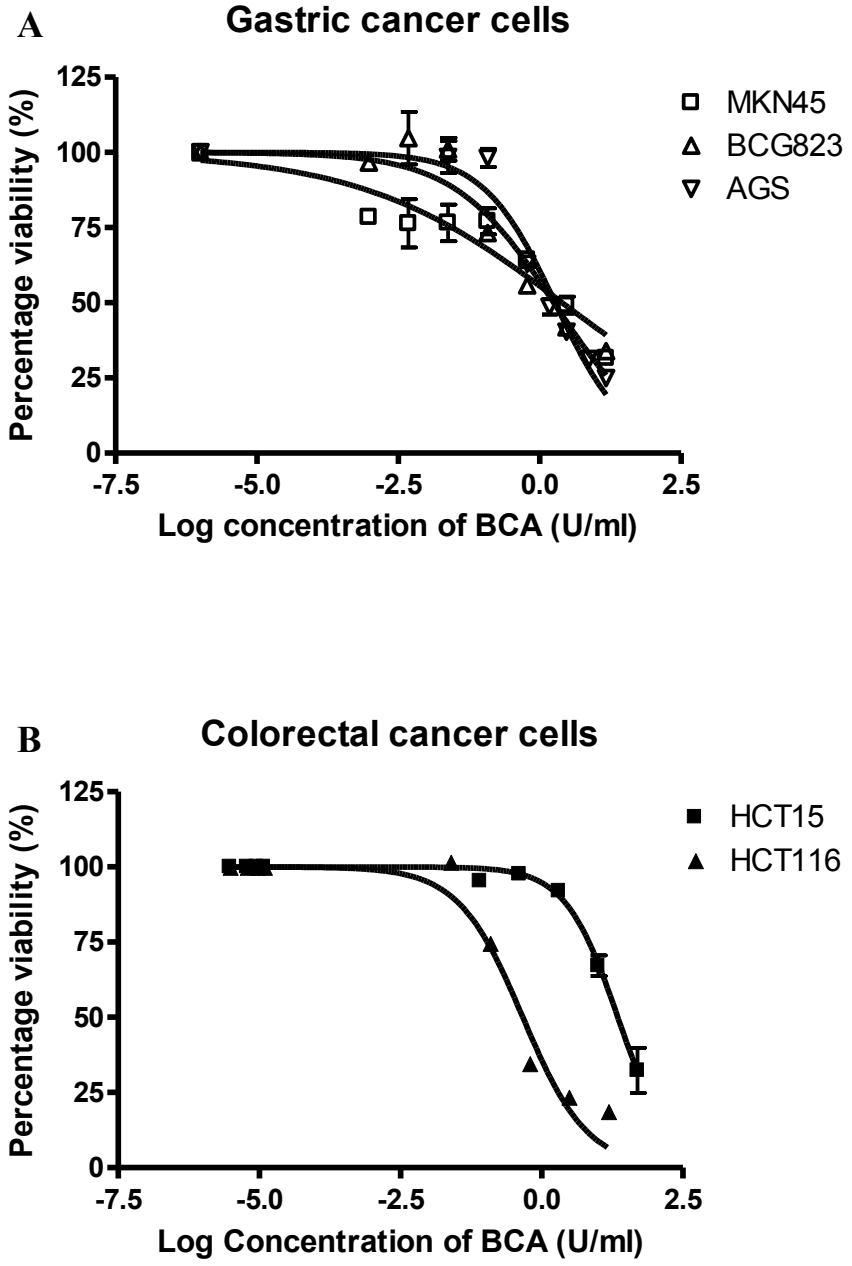

Figure 4. 2. Dose-response curves showing the growth inhibition of the gastric and colorectal cancer cell lines by BCA. Gastric (A) and colorectal (B) cancer cells show dose-dependent growth retardation in response to the arginine depletion induced by BCA. Data represented as means ± SD (n=3).

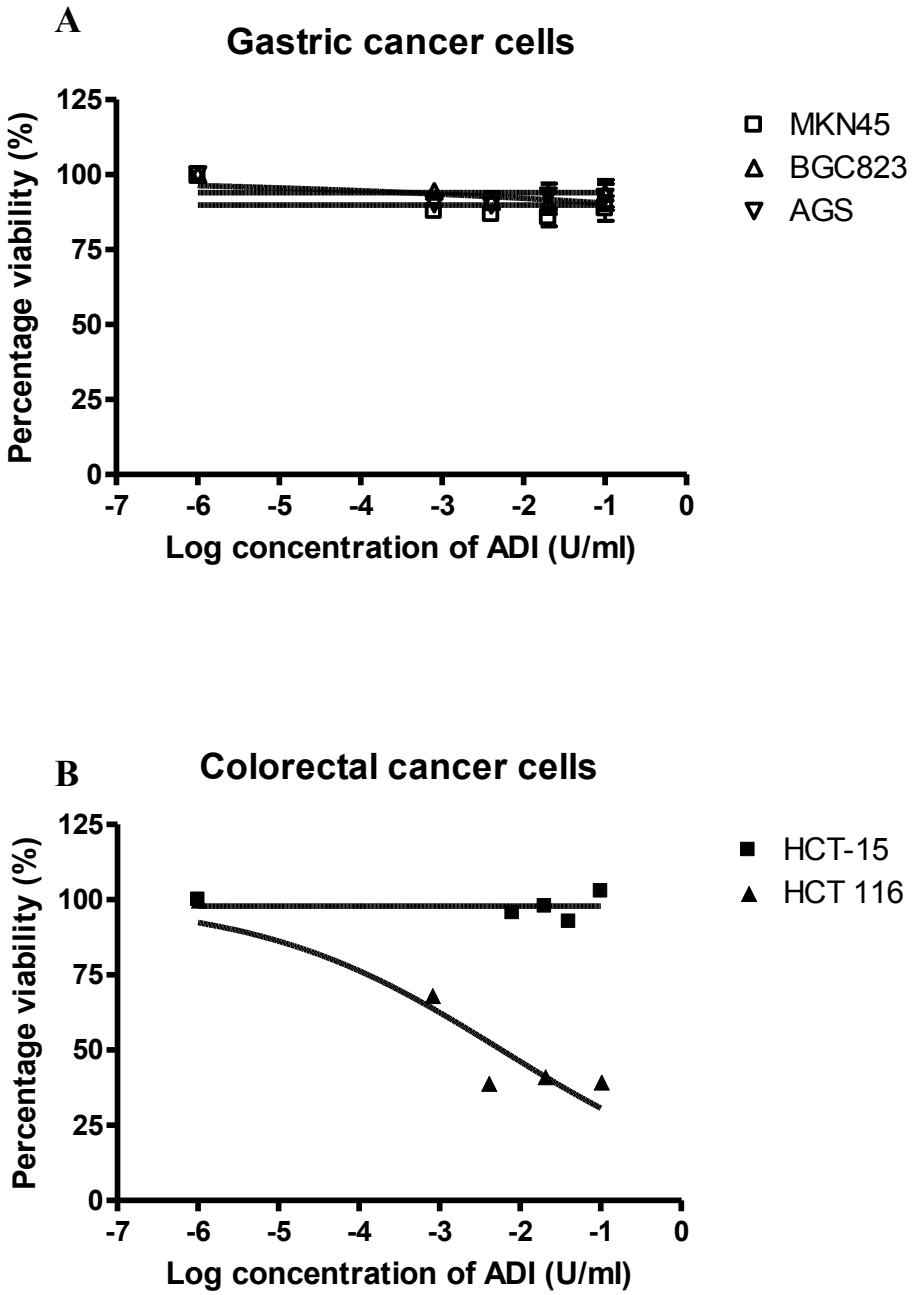

Figure 4. 3. Dose-response curves showing the growth inhibitory effect of ADI on gastric and colorectal cancer cell lines. None of the gastric cancer cell lines shown in (A) were being inhibited by ADI. For colorectal cancer (B), the growth of HCT116 is inhibited by ADI in a dose-dependent manner while HCT-15 could sustain growth at all tested doses of ADI. Data represented as means ± SD.

Table 4. 1. Summary of the IC_{50} values on the gastric and colorectal cancer cell lines after 72 h treatment with arginine depleting enzymes

	IC50 (BCA)		IC50 (ADI)	
	(U/ml)	(μg/ml)	(U/ml)	(μg/ml)
MKN45	2.52	15.33	NA	
BGC823	1.78	10.92	NA	
AGS	1.89	11.51	NA	
HCT-15	22.37	131.2	NA	
HCT116	0.46	1.3	0.009	0.330

*NA: Undetermined IC_{50} value within the dosage tested

4.4. Expression of urea cycle enzymes in gastric and colorectal cancer cell lines

Despite the fact that arginine could be catabolized by different arginine-depleting enzymes, the ability of these enzymes to induce growth arrest has been observed to be dramatically different. One notable difference between ADI and BCA is that the former produces citrulline and the latter produces ornithine, both of which are intermediates in the urea cycle and potential precursors of arginine. Therefore, the ability of the cancer cells to utilize and recycle these amino acids has been proposed as the mechanism of resistance toward the arginine depletion induced by these enzymes(Cheng et al., 2007; Ensor et al., 2002).

Conversion of citrulline to arginine requires the tightly coupled enzymatic reactions catalyzed by ASS and ASL while recycling of ornithine not only requires these 2 enzymes but also the expression of OTC which catalyzes the conversion of ornithine and carbamoyl phosphate to citrulline (Figure 1. 1). Understanding the cellular expression of ASS, ASL and OTC might help explain the effectiveness of the arginine-depleting enzymes on each specific cell line.

4.5. Expression profiling of the urea cycle enzymes at the transcription level

Expression of the urea cycle enzymes was monitored at the transcription level through semi-quantitative RT-PCR. The cells were harvested from routine cultures. mRNA was extracted and used as templates for cDNA syntheses. The level of mRNA expression can be assessed by PCR using gene-specific primers followed by agarose gel electrophoresis. Human fetal liver cDNA was included as a positive control. From the results of RT-PCR, ASS and ASL were found to be expressed in each of the cell lines (Figure 4. 4). Notably, OTC expression was absent in all 5 cell lines tested. In line with the predictions of our model (Figure 1. 1), these cell lines were all sensitive to BCA, whereas most of the ASS- and ASL- expressing cell lines were resistant to ADI action. One notable exception is HCT116, which was sensitive to ADI but expressed the ASS mRNA: such deviation deserves further investigation.

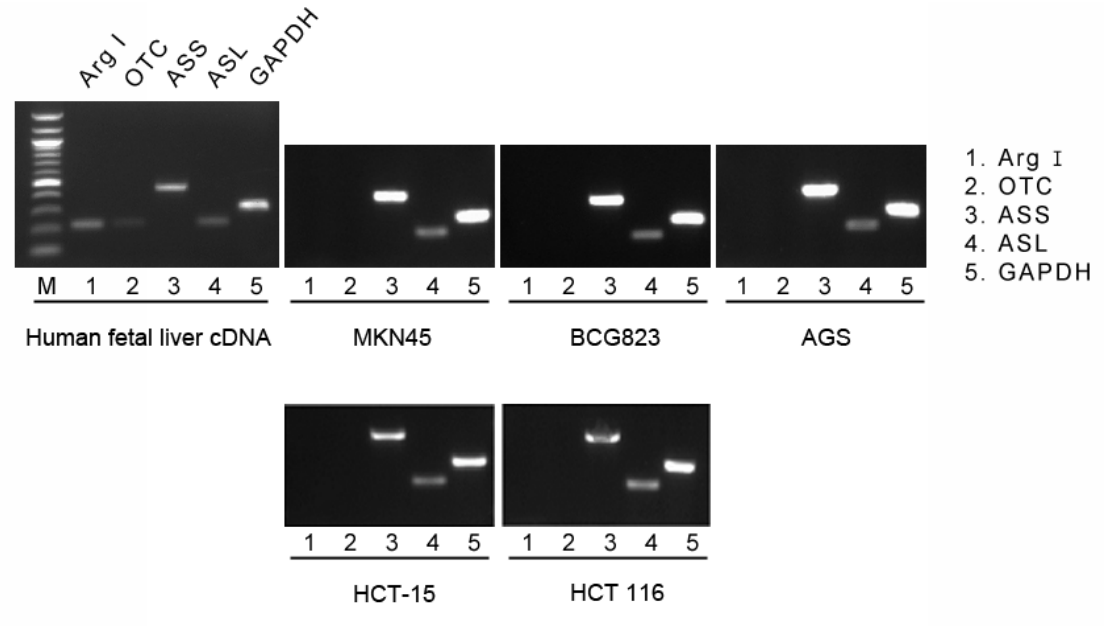

Figure 4. 4. Semi-quantitative RT-PCR analysis reveals the expression levels of urea cycle enzymes in the gastric and colorectal cancer cell lines. Positive control of the human fetal liver cDNA and GAPDH was included for normalization. Expression of ASS and ASL was consistently observed across all cell lines. Representative results are shown from 3 independent experiments.

4.5.1. Expression profiling the urea cycle enzymes at the protein level

One way to explain the unexpected result in Chapter 4.4.1 is that post transcriptional / translational control might result in low protein expression despite high transcript levels. To test if the expression of the urea cycle enzymes at protein level is consistent with the results from the transcript profiling, cells were harvested during routine cultures and the cell lysate was subjected to SDS-PAGE followed by Western blotting. The antibodies used in this experiment were known to cross-react between human and rat proteins, so the cell lysate from rat liver was included as a positive control (Figure 4. 5). Among the cell lines tested, expression of OTC protein was not detected. In contrast, all cell lines in the panel expressed ASS. In the gastric cancer cell lines, BGC823 and AGS showed similar levels of ASS expression but MKN45 expressed a relatively low amount. For the colorectal cancer cell lines, the ASS expression level in HCT116 was lower when compared to HCT-15. The ASS and OTC expression data agree with the transcript profiling of urea cycle enzymes. Low ASS protein in HCT116 could explain sensitivity to ADI. However, low ASS protein did not sensitize MKN45 to ADI treatment. Thus, the down regulation of ASS might have a more profound effect on citrulline utilization in HCT116 than MKN45.

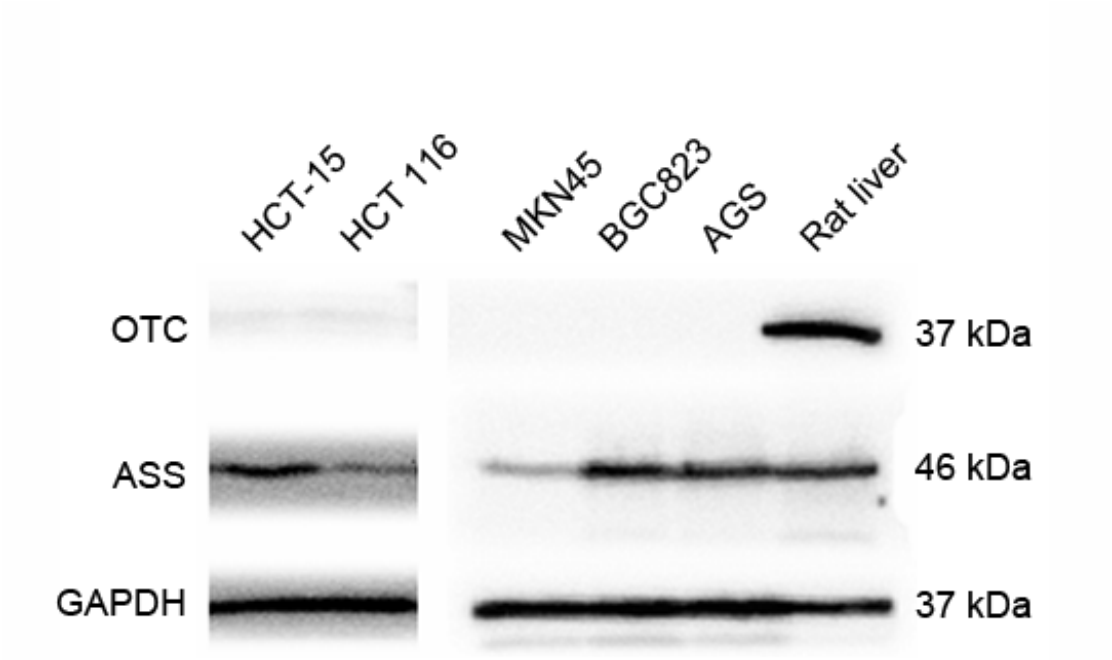

Figure 4. 5. Expression profiling of the urea cycle enzymes by Western blot. The cell lysates were obtained from routine cultures and the positive control was prepared from rat liver. Expression of OTC was not detected in the above panel but various levels of ASS were expressed in different cell lines. Similar results were obtained from 3 independent experiments.

4.5.2. Citrulline rescues the cancer cells in different extent in culture

In theory, the expression level of ASS could be deemed as a reliable marker to explain the reason why some cancer cells were responsive to BCA but resistant to ADI (Figure 1. 1). However, an exception has been observed in this study (Chapter 4.4.1 and 4.4.2), leading us to further investigate the ability of cancer cells to utilize citrulline and sustain proliferation during arginine depletion. It would be particularly important to test this assumption by supplementing citrulline to the culture medium during the treatment with BCA. With reference to the urea cycle, the cells lacking OTC may not recycle ornithine even in the presence of ASS but supplementing citrulline to the culture medium should be able to rescue the cells.

Media containing 0.0625, 0.25 or 1 mM citrulline were prepared in the presence of various concentrations of BCA while BCA with no citrulline supplement is considered as the positive control to induce growth inhibition. For MKN45 and HCT-15, growth inhibition by BCA could be reversed by the addition of citrulline. Approximately 0.25 mM citrulline could almost completely restore the growth of MKN45, but 1 mM citrulline was required to obtain a similar result in HCT-15 (Figure 4.6 A and B). For HCT 116, 1 mM citrulline could only rescue the cells slightly during arginine depletion (Figure 4. 6 C). This might suggest that citrulline was inefficiently recycled to produce arginine and explain why these cells are susceptible to ADI treatment despite detectable ASS expression. Further evidence from the literature shows that the A375 melanoma cell line is known for its lack of ASS expression (L. Feun et al., 2008) and thus high sensitivity to ADI treatment. Upon treatment with BCA, A375 cell viability was indistinguishable between BCA alone and in the presence of 2 mM citrulline (Figure 4. 6

D). These results suggest that the abilities of cancer cells to utilize citrulline precursor were manifested as the capability to reverse the growth inhibition induced by BCA which in turn are in good correlation with the mRNA and protein expression of OTC and ASS.

A

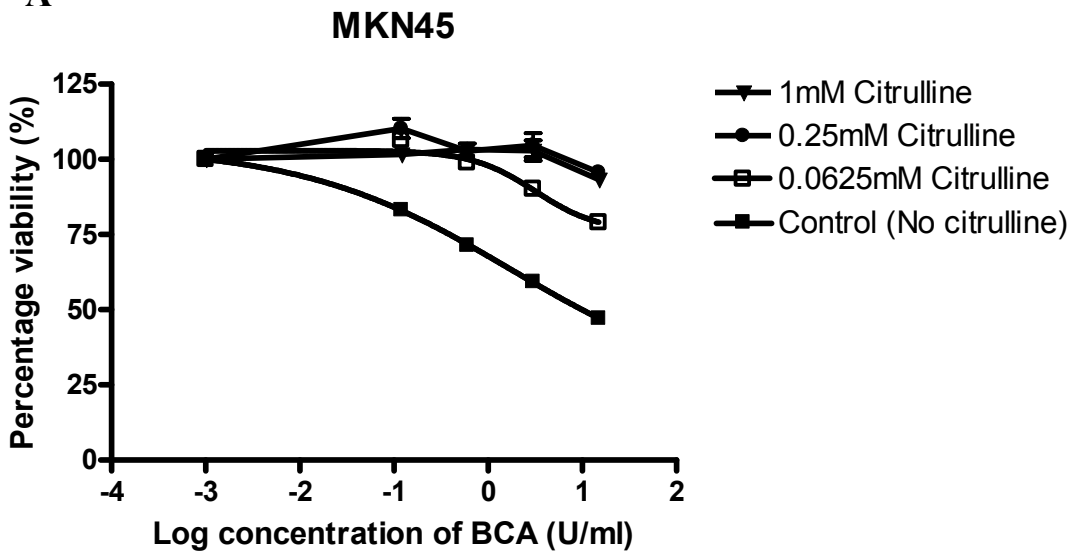
MKN45
Percentage viability (%)
125
100
75
50
25
0
-4
-3
-2
-1
0
1
2
Log concentration of BCA (U/ml)
1mM Citrulline
0.25mM Citrulline
0.0625mM Citrulline
Control (No citrulline)

B

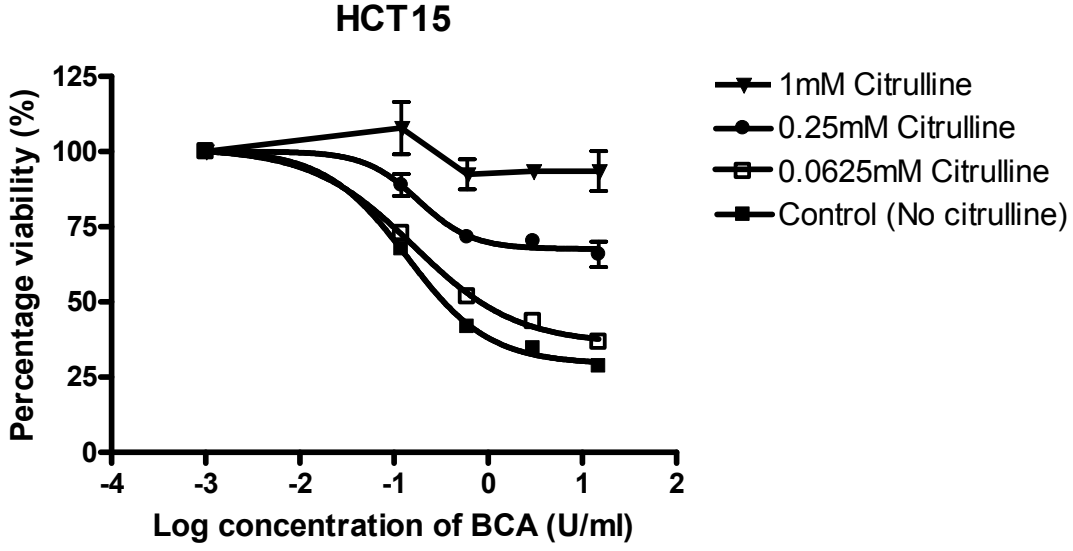
HCT15
Percentage viability (%)
125
100
75
50
25
0
-4
-3
-2
-1
0
1
2
Log concentration of BCA (U/ml)
1mM Citrulline
0.25mM Citrulline
0.0625mM Citrulline
Control (No citrulline)

C

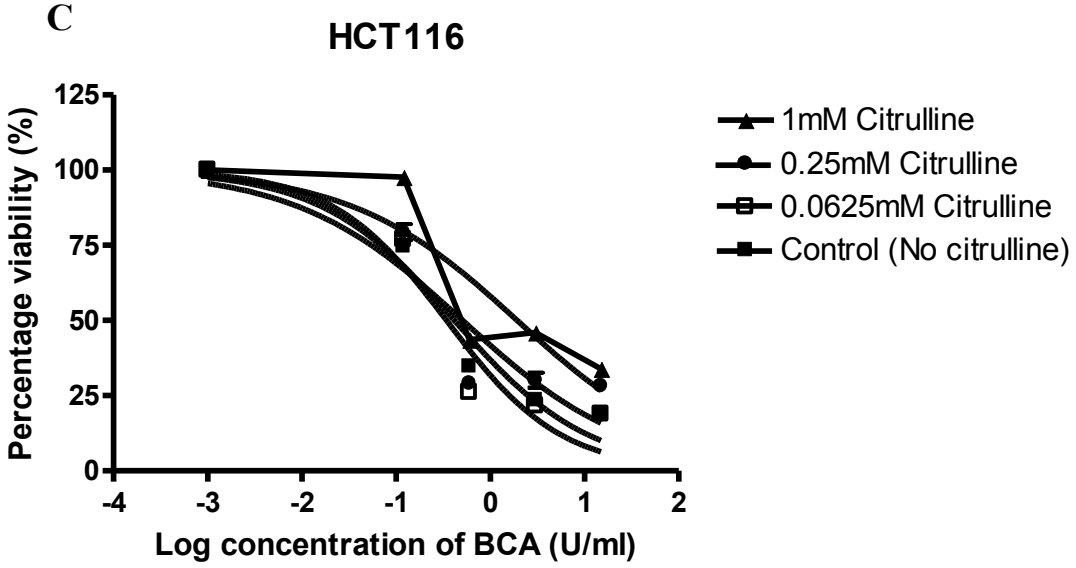
HCT116
Percentage viability (%)
125
100
75
50
25
0
-4
-3
-2
-1
0
1
2
Log concentration of BCA (U/ml)
1mM Citrulline
0.25mM Citrulline
0.0625mM Citrulline
Control (No citrulline)

D

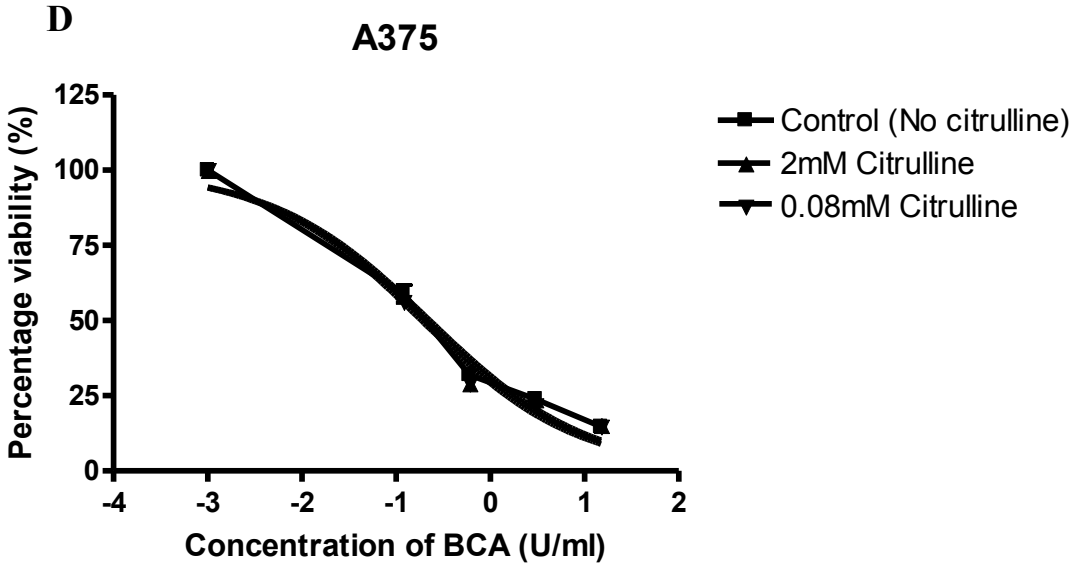
A375
Percentage viability (%)
125
100
75
50
25
0
-4
-3
-2
-1
0
1
2
Concentration of BCA (U/ml)
Control (No citrulline)
2mM Citrulline
0.08mM Citrulline

Figure 4. 6. Reversal of *in vitro* growth inhibition induced by BCA through citrulline supplementation. (A) The growth of MKN45 could be almost completely restored by 0.25 mM citrulline even at the highest dose of BCA while (B) only the highest dose of citrulline could resume HCT-15 proliferation. However, supplementing 0.25 to 1 mM citrulline to HCT 116 (C) only slightly improved the viability during the BCA treatment. (D) Melanoma cell line (A375) lacking ASS expression was not rescued by citrulline during BCA treatment.

4.5.3. BCA induces cell cycle arrest in gastric and colorectal cancer cell lines

On treatment with BCA, substantial growth inhibition has been observed in the panel of cancer cell lines. The underlying mechanism leading to the growth arrest could be related to the cell cycle machinery: normal cycling of DNA replication, chromosome segregation and separation of daughter cells with the same genetic information might be affected. Treatment with the chemical agents such as mimosine, supplementing excess amount of thymidine and withdrawing the serum from the culture medium could lead to cell cycle arrest in different phases (Jackman & O'Connor, 2001). To investigate the effects of BCA on cell cycle distribution, cells were exposed to various concentrations of BCA in the culture medium for 72 h and their cell cycle distribution was revealed by propidium iodide (PI) staining which allows the cellular DNA content to be measured by flow cytometric analysis. Cells in the G1 and G2/M phases would have a uniform distribution of DNA content where the amount of cellular DNA in the G2/M phase is approximately double that in the G1 phase as shown in the histogram (Figure 4. 7 A). S-phase distribution refers to the cell that is undergoing DNA synthesis and thus has a DNA content in between that found in G1 and G2/M phase.

MKN45 and HCT-15, having the highest IC_{50} values in response to BCA treatment, would be used as the representative for each tumor type on which more extensive studies would be performed. For MKN45, the cell line was exposed to various concentrations of BCA starting from 15 U/ml and 2-fold serial dilutions down to 0.94 U/ml were prepared. When exposing MKN45 to 15 U/ml BCA, the S-phase proportion of cells increased significantly from 41.94 to 68.36% while the distribution of G2/M phase was similar to the untreated control. Lower BCA doses (down to 0.94 U/ml) applied to the MKN45

yields similar S and G2/M phase distributions (Figure 4. 8 A). Incubating the rest of the gastric cancer cell lines with 15 U/ml BCA resulted in a significant increase of S-phase population in AGS (Figure 4. 8 C) and BGC823 (Figure 4. 8 D), from 33.60 to 47.75% and 46.78 to 58.26% , respectively.

Further investigation of colorectal cancer cells revealed that the cell cycle arrest induced by BCA was likely tumor type-specific. When HCT-15 was incubated with BCA, the G2/M population increased with the dosage, and a significant increase was observed with either 25 or 50 U/ml BCA for 72 h (Figure 4. 8 B). The G2/M phase subpopulation increased significantly from 10.45 to 27.08% when exposed to 25 U/ml BCA and rose to 32.07% in the presence of 50 U/ml BCA. On the other hand, S-phase population was not affected by the dosages applied. For HCT 116, adding 15 U/ml BCA to the culture not only increased the G2/M distribution from 9.77 to 29.19% but also led to a dual-phase arrest where the S-phase population also increased from 18.23 to 53.01% (Figure 4. 8 E).

During the flow cytometric analysis, a substantial increment with sub-G1 population has been noted in some of the cell lines such as MKN45 (Figure 4. 7). The Sub-G1 fraction is often used as an indirect indicator of apoptotic death, although the percentage of sub-G1 fraction was not reported together with data of the cell cycle distribution. This is mainly because of the cellular debris and apoptotic bodies might breakdown into multiple fragments and wrongly taken as the percentage of dead cells undergoing apoptosis in a particular treatment condition (Martin & Lenardo, 2001). Therefore, the sub-G1 fraction could be considered as a sign of apoptosis but quantitative measurement would be performed with a more sophisticated assay described in the next chapter.

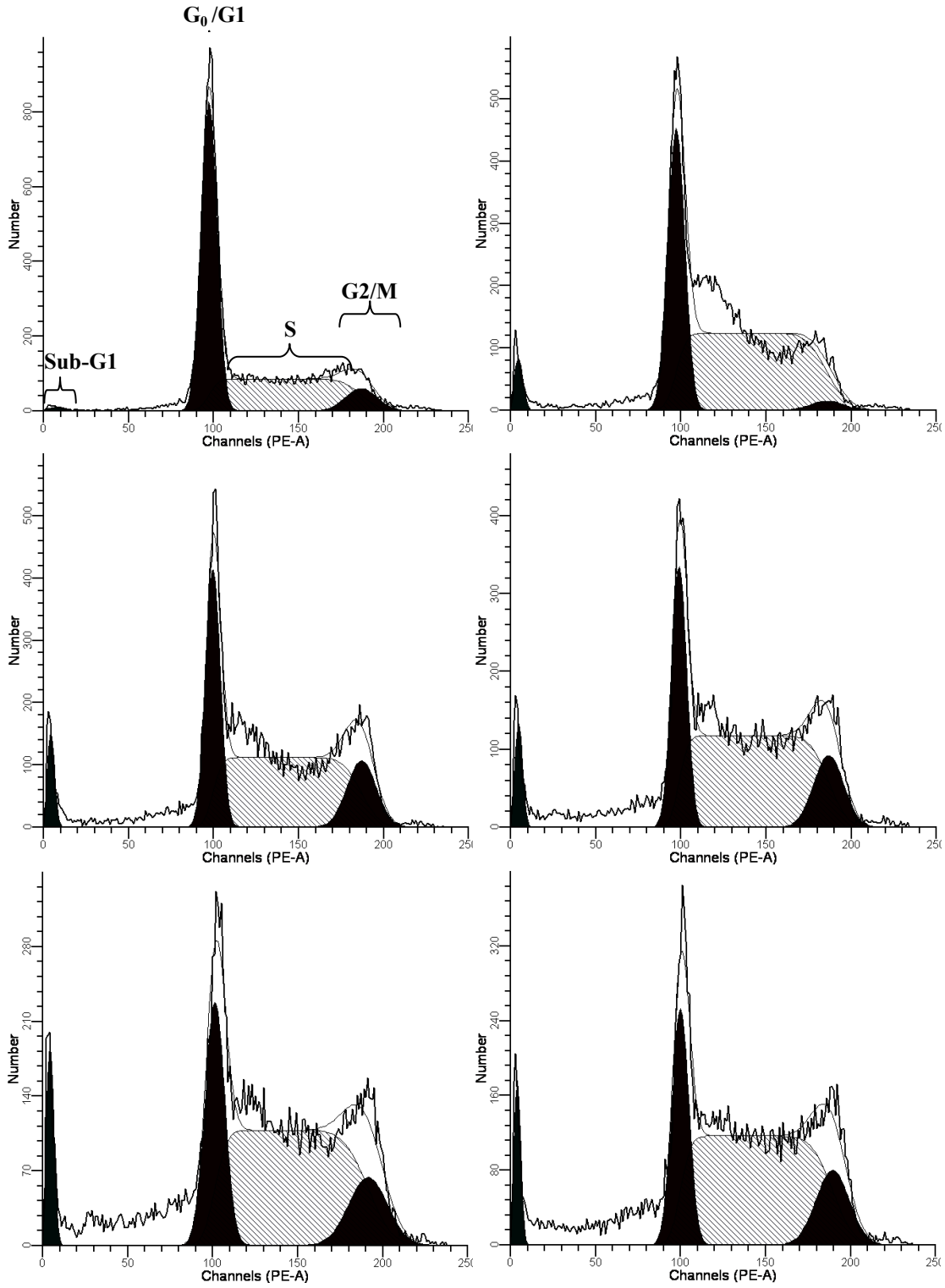
G0/G1
Sub-G1
S
G2/M
Number
Channels (PE-A)

Figure 4. 7. Histogram illustrating the cell cycle distribution of MKN45 with treatment of (A) untreated control, (B) 0.94 U/ml, (C) 1.88 U/ml, (D) 3.75 U/ml, (E) 7.5 U/ml and (F) 15 U/ml BCA for 72 h. DNA content in the fixed cells was revealed by PI stain. In addition to the S-phase arrest, sub-G1 population also increased in proportion to the BCA dosages.

A

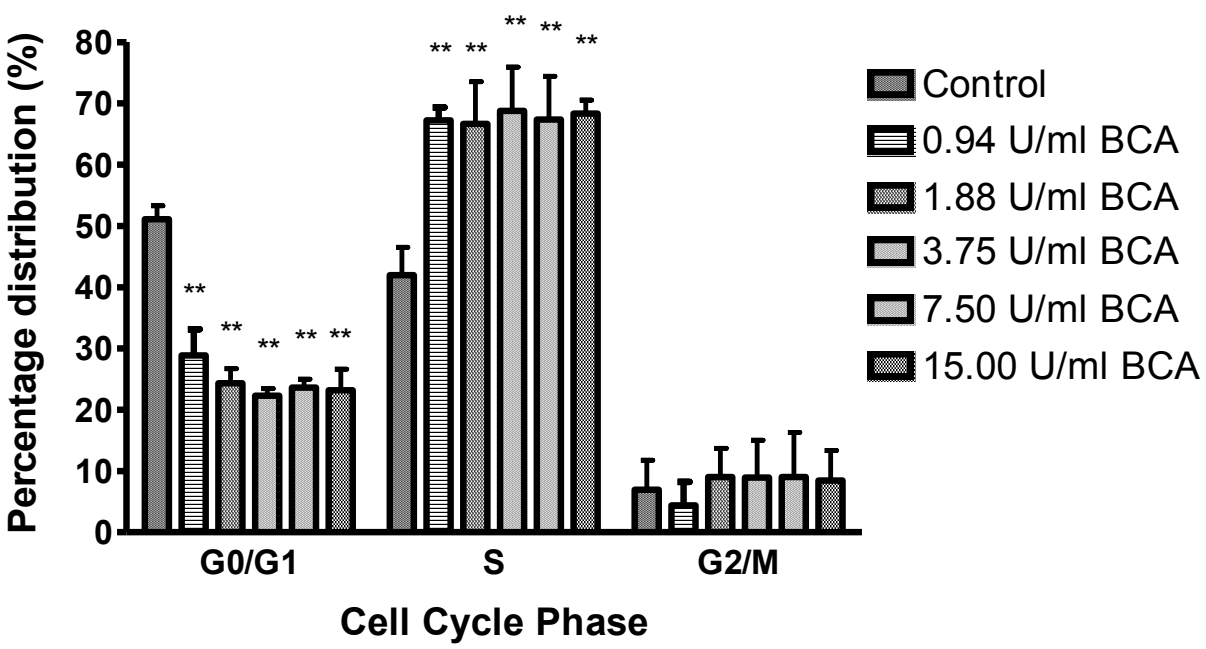
MKN45
Percentage distribution (%)
80
70
60
50
40
30
20
10
0
**
G0/G1
S
G2/M
Cell Cycle Phase
Control
0.94 U/ml BCA
1.88 U/ml BCA
3.75 U/ml BCA
7.50 U/ml BCA
15.00 U/ml BCA

B

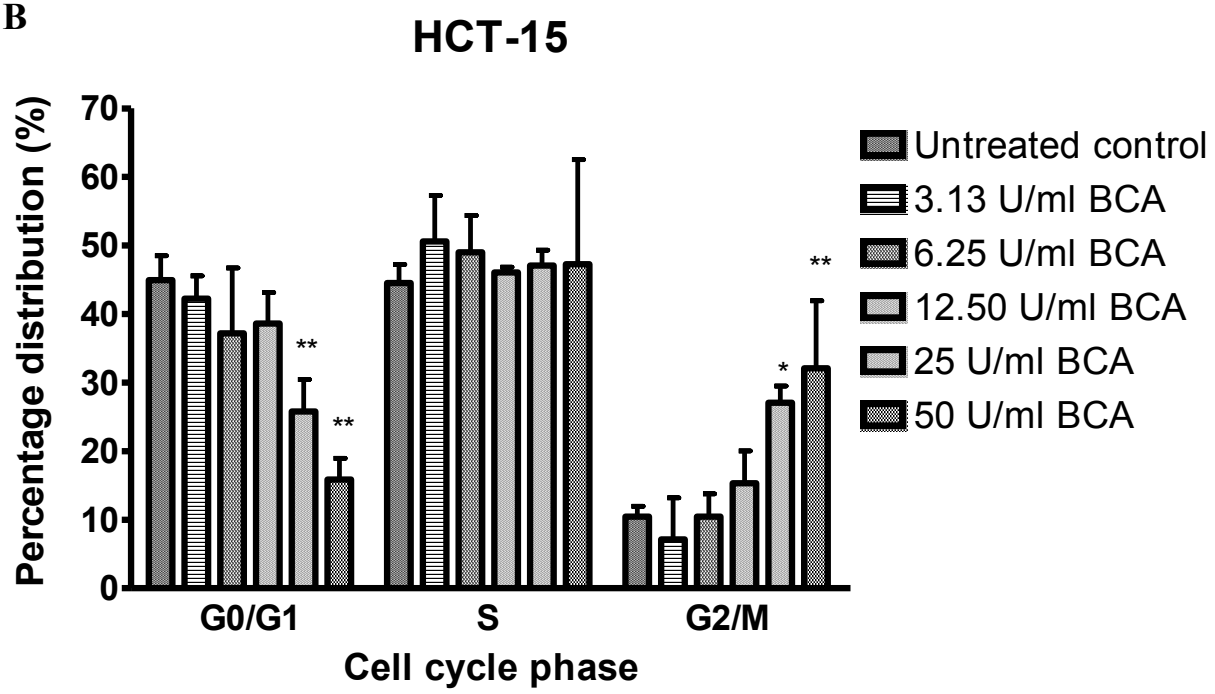
HCT-15
Percentage distribution (%)
70
60
50
40
30
20
10
0
**
*
G0/G1
S
G2/M
Cell cycle phase
Untreated control
3.13 U/ml BCA
6.25 U/ml BCA
12.50 U/ml BCA
25 U/ml BCA
50 U/ml BCA

C

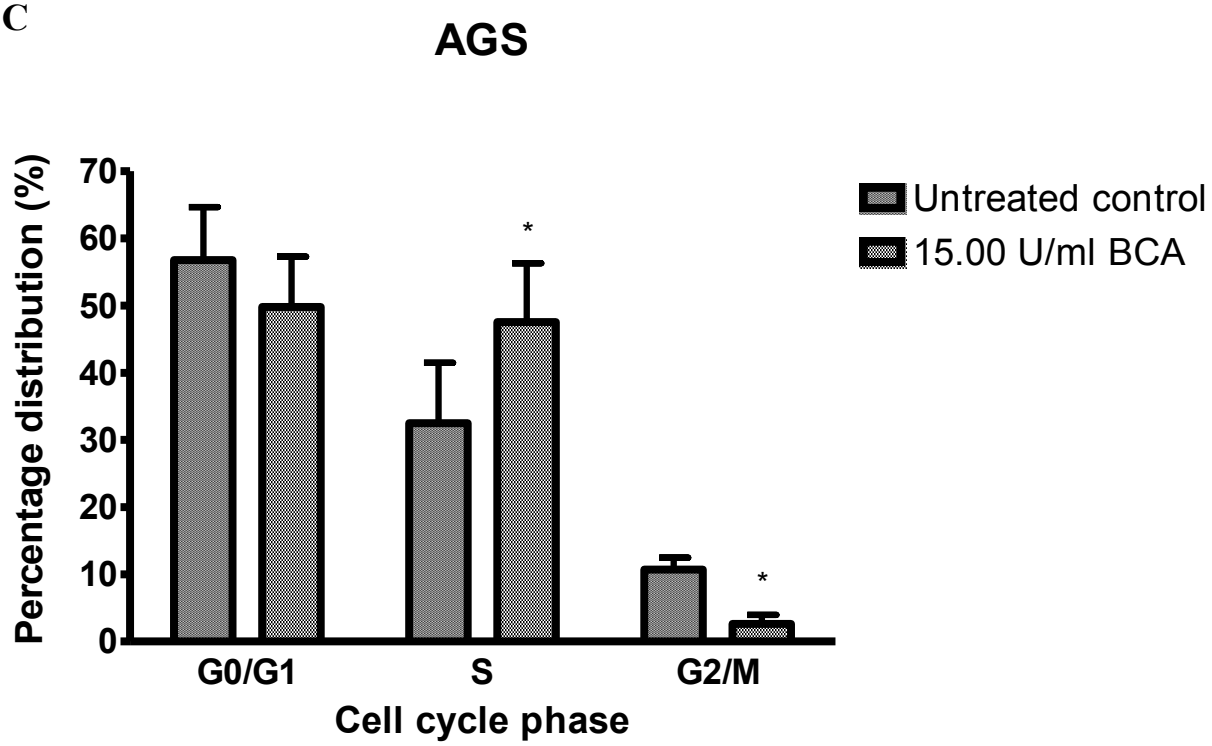
AGS
Percentage distribution (%)
70
60
50
40
30
20
10
0
*
*
G0/G1
S
G2/M
Cell cycle phase
Untreated control
15.00 U/ml BCA

D

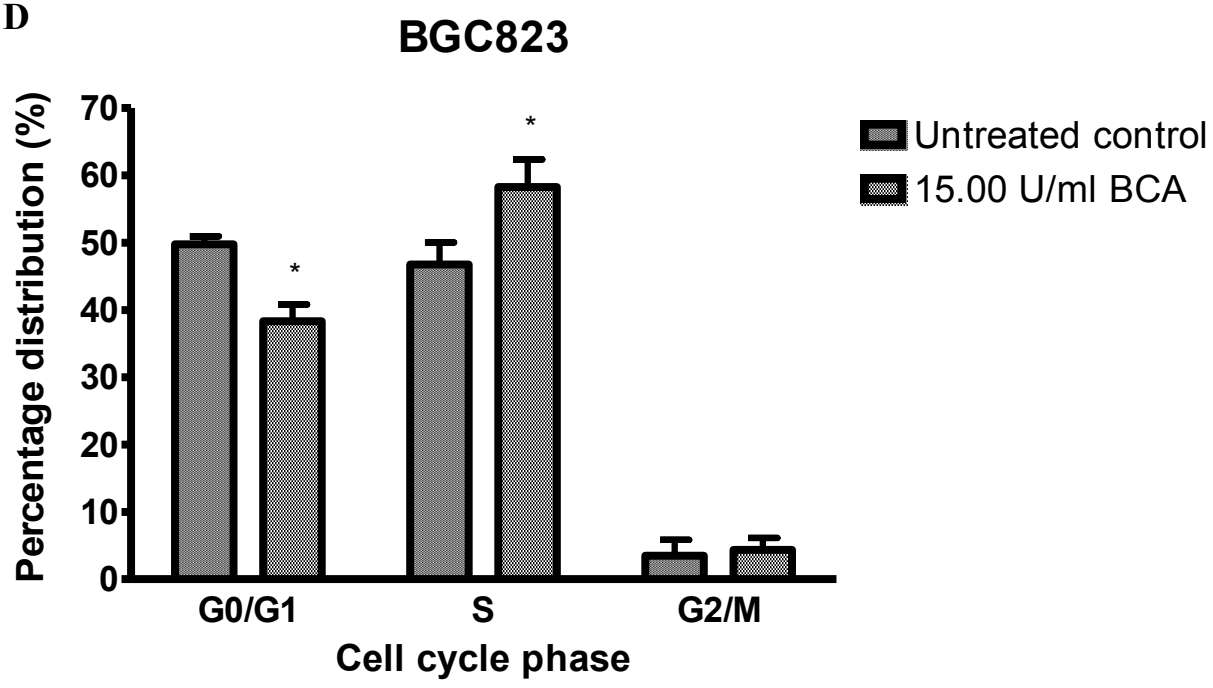
BGC823
Percentage distribution (%)
70
60
50
40
30
20
10
0
*
*
G0/G1
S
G2/M
Cell cycle phase
Untreated control
15.00 U/ml BCA

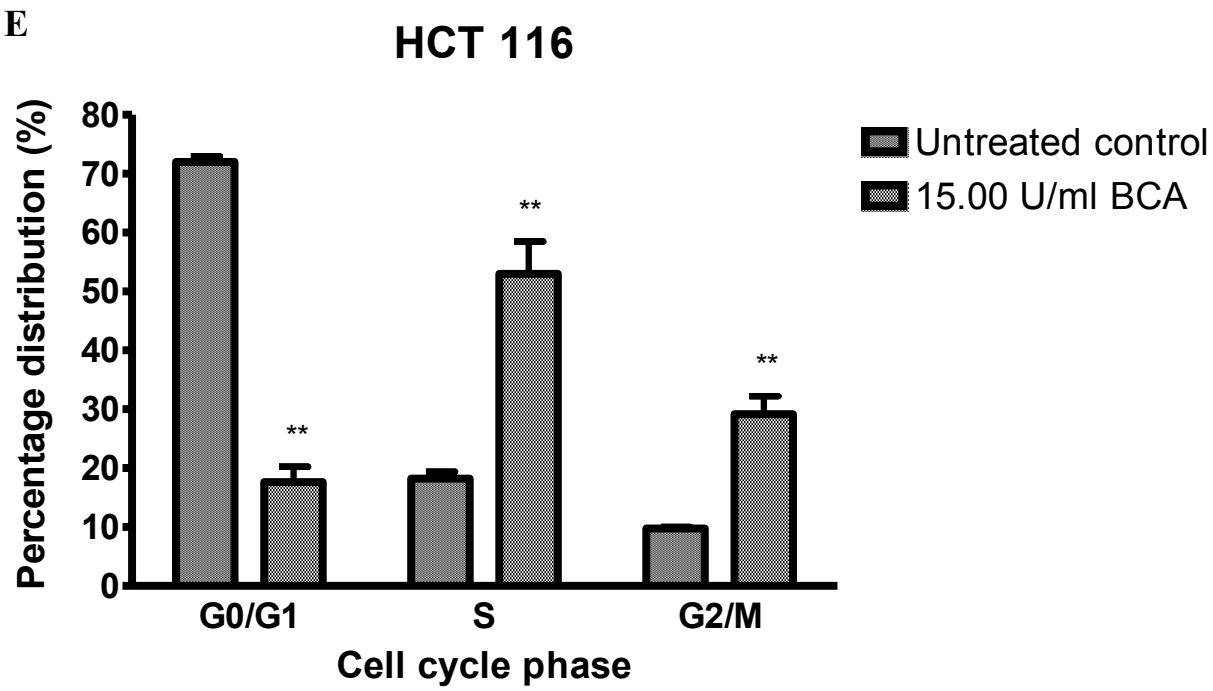

Figure 4. 8. Flow cytometric analysis revealing the cell cycle distribution of different cell lines in response to treatment with BCA. (A) MKN45 was exposed to various concentrations of BCA for 72 h; a significant arrest in the S-phase was recorded even in the presence of the lowest concentration of BCA. Interestingly, similar treatment of HCT-15 (B) induced G2/M-phase arrest in a dose-dependent manner. Data were collected from at least three independent experiments and the values reported as means ± SD. One-way ANOVA revealed a significant S and G2/M phase arrest in MKN45 ($P < 0.0001$) and HCT-15 ($P < 0.001$), respectively. *Post hoc* Dunnett's test: * $p < 0.05$, ** $p < 0.01$. Gastric cancer cell lines, (C) AGS and (D) BGC823, were both arrested in S-phase when exposed to 15 U/ml BCA for 72 h. Moreover, HCT116 colorectal cancer (E) exhibits S and G2/M dual-phase arrest in response to the same treatment. Data are collected from at least three independent experiments and the values reported as means ± SD. Student's *t-test*: $^{*}P < 0.05$ and $^{**}P < 0.01$.

4.5.4. BCA induces caspase-dependent apoptosis in some gastric and colorectal cancer cell lines

The flow cytometric analysis on the panel of cell lines suggested an induction of cell cycle arrest by BCA and an increase in sub-G1 population, indicating a certain sub-population of cells may undergo apopotic cell death. To confirm this observation, cancer cells incubated with BCA were assayed for apoptosis through PI and fluorophore-conjugated annexin V double staining. Cell lines that have been shown to undergo apoptotic cell death were further investigated. By studying the activation of caspase-3 and alteration of mitochondria membrane potential, this might provide further information to understand the pathway leading to apoptosis.

4.5.5. Annexin V-FITC and PI double staining reveals apoptosis

Externalization of phosphatidylserine (PS) from the inner cytosolic leaflet to the outer surface of the plasma membrane is one of the important features of apoptosis. Double staining using PI and annexin V-FITC revealed the above observation and provided a quantitative measurement of cell population that undergoes apoptosis. The cells stained with neither PI nor annexin V-FITC in the Q3 quadrant represents the live cells as the intact plasma membrane excluded the fluorescence probes from entering the cells. Cells stained with annexin V-FITC but not PI, quadrant Q4, represents the cells in the early stage of apoptosis where the membrane remained intact but PS was translocated to the surface of plasma membrane and bound by the fluorophore labeled annexin V-FITC. Cells in the later stage of apoptosis were stained by both PI and annexin V, as the apoptotic cells in the culture environment were not being removed by phagocytosis, gradually losing membrane integrity and becoming permeable to the PI molecule, thus appearing in quadrant Q2. By adding up the events in Q2 and Q4, it provided a quantitative measurement of the apoptotic cell death. MKN45 cells incubated with 15 U/ml BCA for 24, 48 and 72 hours were stained with PI and annexin V-FITC (Figure 4. 9). The dot-plot diagrams showing the progressive increase of the annexin V stained cell (Q2 and Q4) population during the course of incubation represent the progression of apoptosis. The percentage of apoptotic cell death was estimated by adding up the events in the Q4 (PI negative, annexin V-FITC positive) and Q2 quadrants (PI positive, Annexin V-FITC positive), that is the population of cells in the early and late stage of apoptosis, respectively. In the absence of BCA, the apoptosis percentage of MKN45 increased very slightly from 3% to about 5% over 72 h of culture while 15 U/ml BCA did not seem to trigger apoptosis in MKN45 after 24 h of treatment (Figure 4. 10A). However, the

percentage of apoptosis increased gradually to 11.33% in 48 h and further increased to 23.35% after 72 h of incubation. Similar observation was obtained with HCT-15: although percentage of apoptosis in the control increased from 6 to 16 % over 72 h of incubation, a substantial population (~40%) was found to undergo apoptosis in response to the treatment with 50 U/ml BCA in 72 h (Figure 4. 10 B). To further evaluate the dose-response effect on apoptosis, MKN45 and HCT15 were exposed to various concentrations of BCA for 72 h and in general, the percentage of apoptosis increased with escalating dosage. The apoptosis percentages of amount about 26% and 44% were recorded when MKN45 (Figure 4. 10 C) and HCT-15 (Figure 4. 10 D) cells were exposed to the highest dosage of BCA, respectively. To evaluate if the apoptotic death induced by BCA could also occur to the remaining cell lines, similar studies were performed by incubating the cells with 15 U/ml BCA for 72 h. Apoptotic cell death was shown in BGC823 and HCT116, with the extent of apoptosis more dramatic in HCT116 (Figure 4. 10 E). For AGS, no observable difference in apoptosis was seen between the treatment and untreated control, which suggest that BCA induced cell death mechanisms other than apoptosis in this cell line.

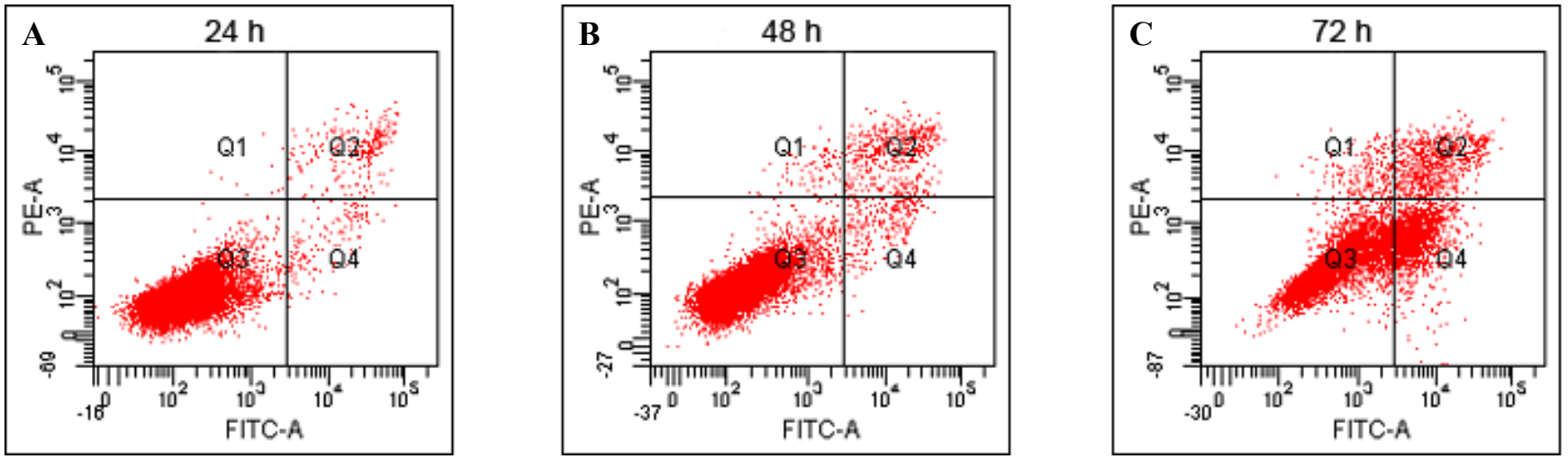

Figure 4. 9. Dot-plot diagram showing the progression of apoptosis in MKN45 during the course of 72 h BCA treatment. MKN45 was double-stained with PI and annexin V-FITC after (A) 24, (B) 48 and (C) 72 h of 15 U/ml BCA incubation.

A

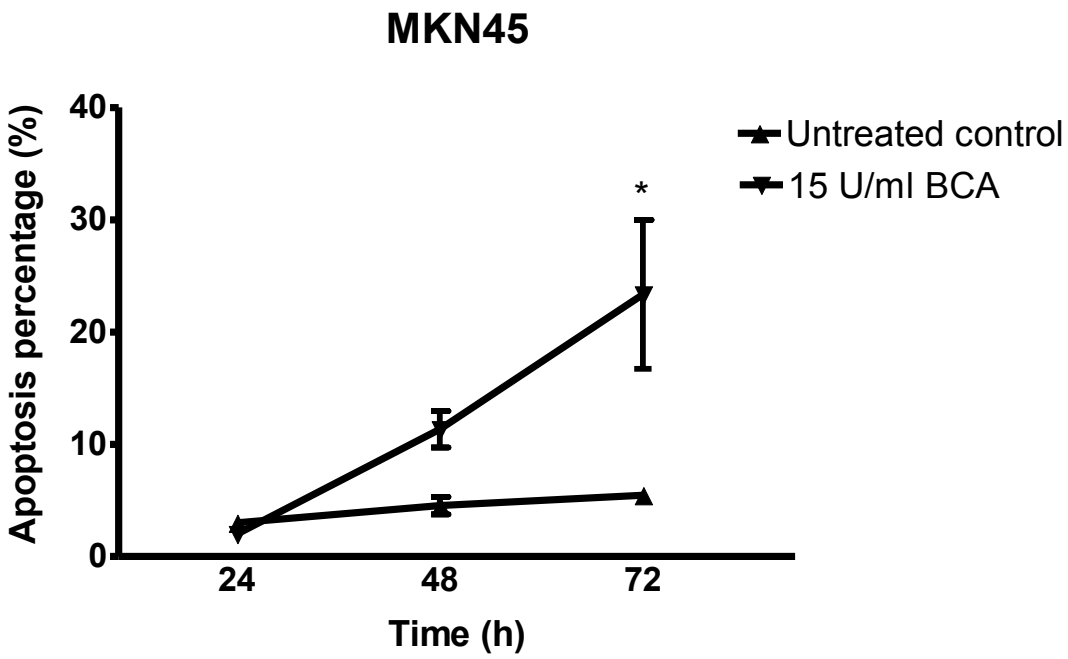
MKN45
Apoptosis percentage (%)
40
30
20
10
0
24
48
72
Time (h)
*
Untreated control
15 U/ml BCA

B

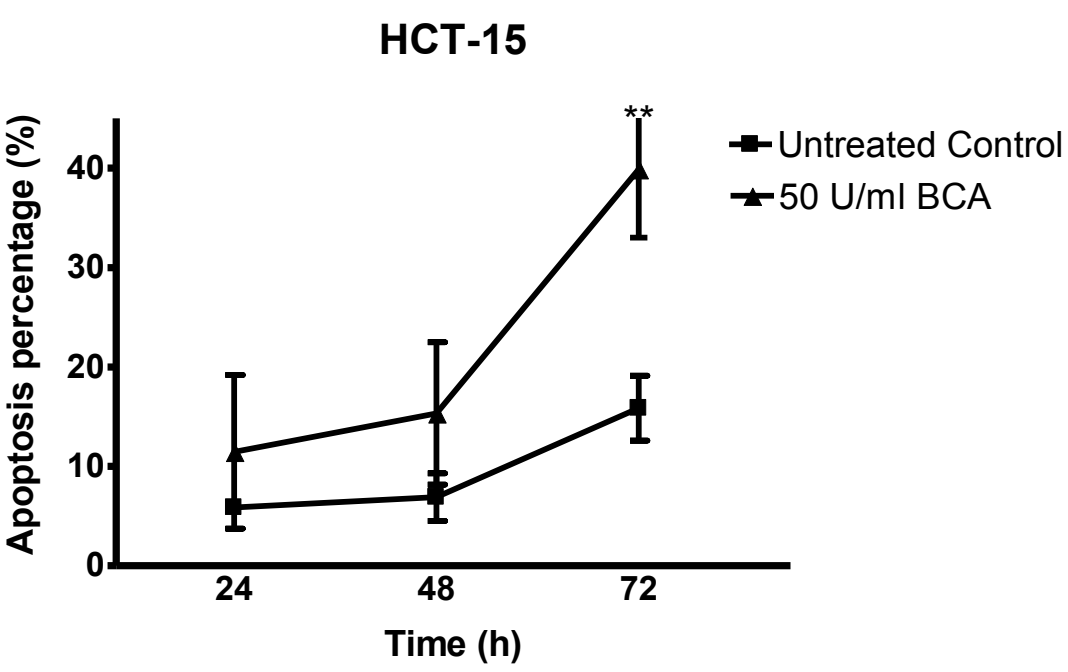
HCT-15
Apoptosis percentage (%)
40
30
20
10
0
24
48
72
Time (h)
**
Untreated Control
50 U/ml BCA

C

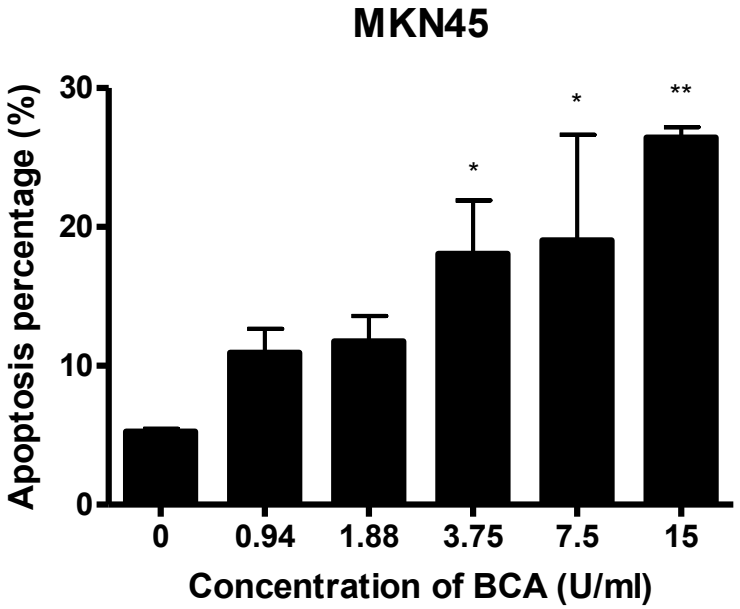
MKN45
Apoptosis percentage (%)
30
20
10
0
*
*
**
0
0.94
1.88
3.75
7.5
15
Concentration of BCA (U/ml)

D

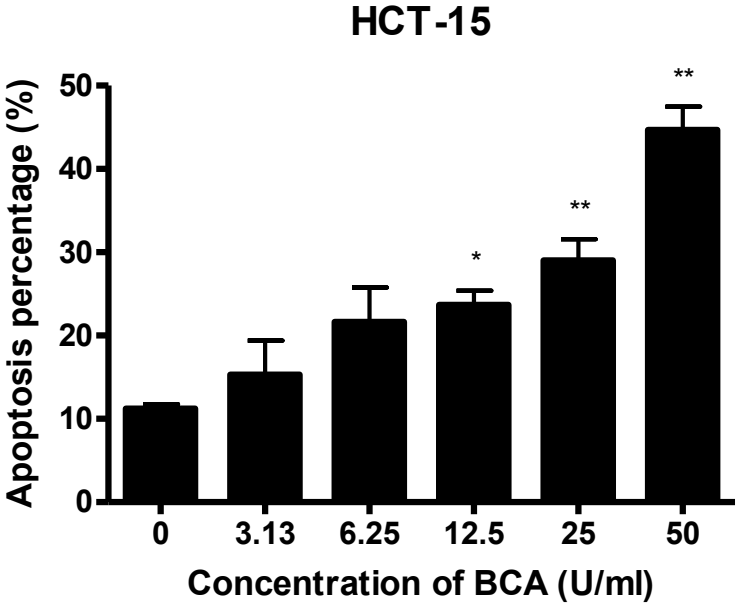
HCT-15
Apoptosis percentage (%)
50
40
30
20
10
0
*
**
**
0
3.13
6.25
12.5
25
50
Concentration of BCA (U/ml)

E

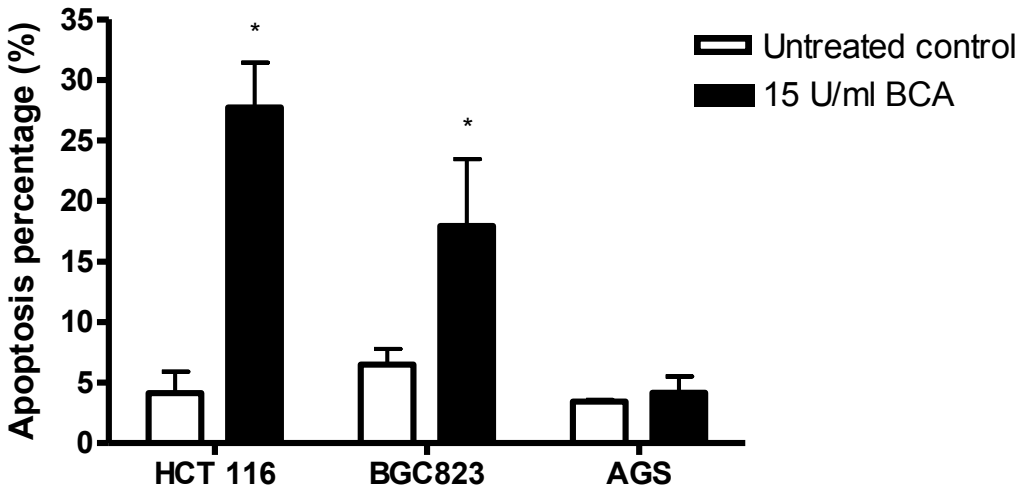

Figure 4. 10. Treatment with BCA induces apoptotic cell death in some of the gastric and colorectal cancer cell lines. MKN45 (A) and HCT-15 (B) were incubated with 15 and 50 U/ml BCA, respectively. The extent of apoptotic induction at 24, 48 and 72 h was assayed by PI and annexin V-FITC double staining. Progression of apoptosis was observed in the presence of BCA while the untreated control showed consistent levels of apoptosis over the period of time. Results were obtained from 3 to 4 independent experiments and data plotted as means ± SD. Student's *t-test*, $^{*}p < 0.05$ and $^{**}p < 0.01$. BCA induced apoptosis in a dose-dependent manner. (C) MKN45 and (D) HCT-15 were incubated for 72 h with 0 - 15 and 0 - 50 U/ml BCA, respectively. In response to the escalating dose of BCA, one-way ANOVA revealed a significant increase of apoptosis in MKN45 ($P < 0.01$) and HCT-15 ($P < 0.0001$). *Post hoc* Dunnett's test: $^{*}p < 0.05$, $^{**}p < 0.01$. Similarly, incubating HCT116, BGC823 and AGS (E) with 15 U/ml BCA for 72 h elicited the apoptotic cell death in HCT116 and BGC823 but not AGS. The results were obtained from more than 3 independent experiments and data plotted represent means ± SD. Student's *t-test*, $^{*}p < 0.05$.

4.5.6. Caspase-3 dependent apoptotic cell death

Caspase-3 activation is one of the most important biochemical hallmarks of apoptosis. Caspase-3 exists in the cell in the form of an inactive pro-enzyme which can be activated by initiator caspases such as caspase-8, 9 or 10. Caspase-3 is also considered as the most important execution caspase, since both the activation of death receptor (extrinsic pathway), such as binding of ligand to tumor necrosis factor (TNF) receptor, and intracellular signals integrated to mitochondria pathway (intrinsic pathway) can lead to the activation of caspase-8 and caspase-9, respectively. These initiation caspases in turn converge to activate the executioner caspase-3. Upon activation, the 32 kDa pro-enzyme will be cleaved into 2 subunits, a 12 kDa and a 17 kDa polypeptide, which form a heterodimer; association of two heterodimers result in the formation of active heterotetramer. Activated caspase-3 exhibits proteolytic activity that cleaves a spectrum of cellular protein substrates specifically after aspartic acid residue and resulting in a cascade of events inducing DNA fragmentation, degradation of cytoskeleton and formation of apoptotic bodies. However, apoptotic cell death through the release of apoptosis inducing factor (AIF) from the mitochondria to the cytosol and translocated to the nucleus will result in DNA fragmentation for which the cell death may be independent of caspase. Therefore, to investigate if BCA-induced apoptotic cell death is caspases-dependent, and to confirm the results of annexin-V and PI double staining, determining caspase-3 activity may consolidate our understanding toward the pro-apoptotic effects of BCA on cancer cells.

Cell lines that have been shown to undergo BCA-induced apoptosis were further evaluated by the activation of caspase-3. HCT-15 was incubated in various

concentrations of BCA for 72 h; the cell lysate was analyzed by Western blotting using the caspase-3 antibody against both zymogen and activated enzyme. The activated caspase-3, as manifested at 12 and 17 kDa, and the zymogen bands increased in intensity with the concentration of BCA. This confirms the involvement of caspase-3 in the BCA-induced apoptotic cell death (Figure 4. 11A). Using FITC-DEVD-FMK, a fluorophore labeled caspase inhibitor that binds irreversibly to active caspase-3, we studied the kinetics of caspased-3 activation in MKN45 over 72 h of 15 U/ml BCA incubation. Cells incubated with BCA were harvested after 24, 48 and 72 h of incubation and stained with the labeled caspase-3 inhibitor (Figure 4. 11B). The level of active caspase-3 is comparable to untreated control in the first 24 hours of BCA incubation, and increased significantly to 11.8 and 24.4% in 48 and 72 h, respectively. Similar results were also obtained in HCT116 and BGC823 when exposed to 15 U/ml BCA for 72 h (Figure 4. 11C): the active caspase-3 fraction increasing to 20% suggests the involvement of caspase-3 in apoptotic cell death.

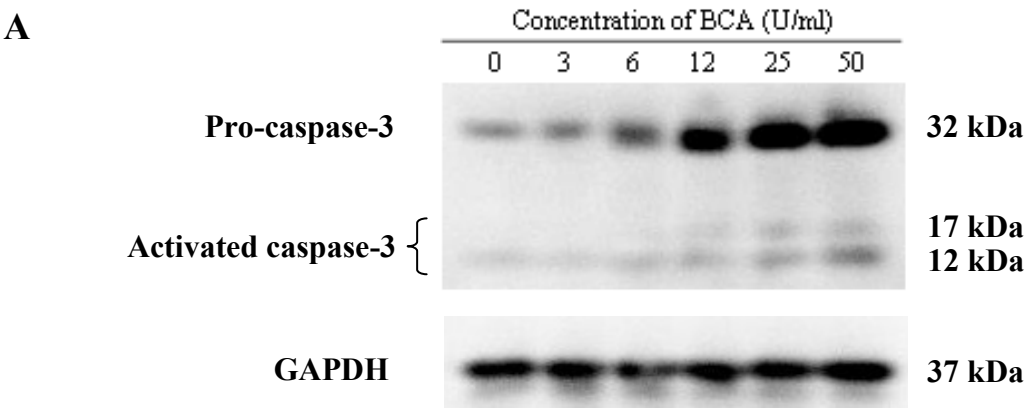
A
Concentration of BCA (U/ml)
0
3
6
12
25
50
Pro-caspase-3
32 kDa
Activated caspase-3
17 kDa
12 kDa
GAPDH
37 kDa

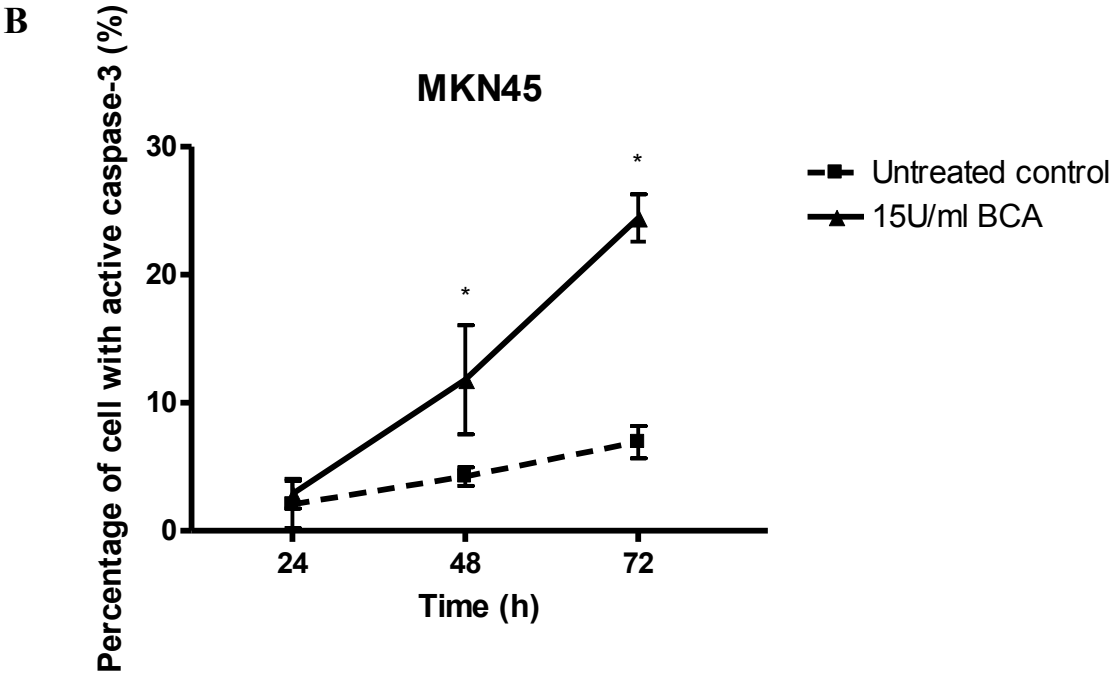
B
MKN45
Percentage of cell with active caspase-3 (%)
30
20
10
0
24
48
72
Time (h)
*
*
Untreated control
15U/ml BCA

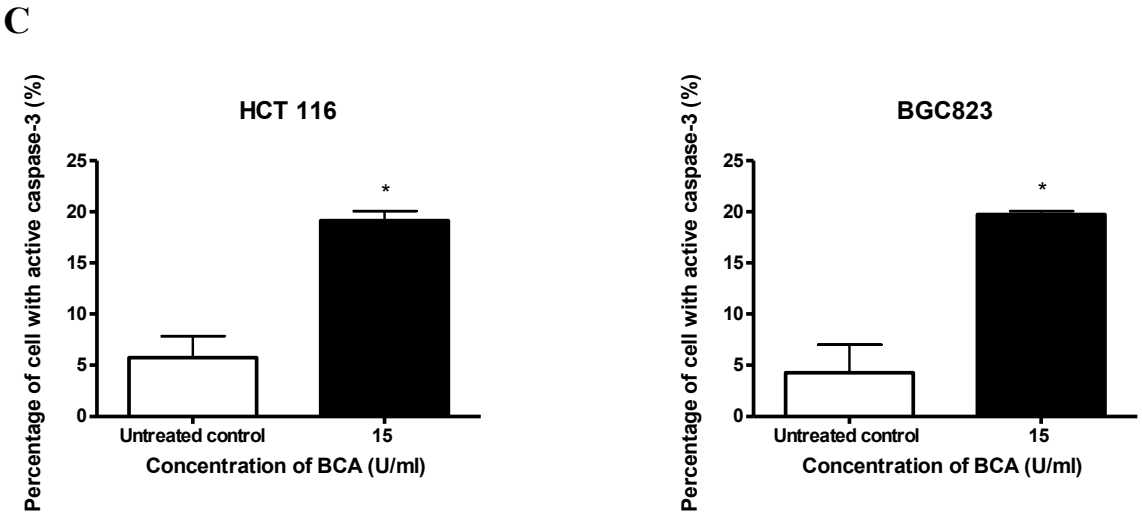
C
HCT 116
Percentage of cell with active caspase-3 (%)
25
20
15
10
5
0
*
Untreated control
15
Concentration of BCA (U/ml)
BGC823
Percentage of cell with active caspase-3 (%)
25
20
15
10
5
0
*
Untreated control
15
Concentration of BCA (U/ml)

Figure 4. 11. Induction of apoptosis by BCA is possibly through the activation of caspase-3. (A) HCT-15 was treated with various doses of BCA for 72 h and the cell lysates were collected for western blot analysis of active caspase-3. Treatment with increasing concentration of BCA leads to the activation of caspase-3 as manifested by the cleavage of 32 kDa inactive pro-enzyme to two subunits of 12 and 17 kDa polypeptides. (B) During the course of 72 h incubation with BCA, staining of active caspase-3 using FITC-DEVD-FMK revealed the activation of caspase-3 in MKN45 over time. The active caspase-3 increased to a significant level as early as 48 h and further increased with the duration of treatment ($p < 0.05$). (C) Activation of caspase-3 in HCT 116 and BGC823 were assayed after incubating these cell lines with 15 U/ml BCA for 72 hours. A significant increase in active caspase-3 suggests that it plays a role in mediating the apoptosis as manifested by PI and annexin V-FITC double staining ($p < 0.05$).

4.5.7. Initiation of apoptosis though mitochondrial outer membrane permeabilization

Apoptotic events upstream of the caspase-3 activation are centered in the mitochondria, where live and death signals from different cellular processes are integrated, and the decision on apoptotic cell death following the intrinsic pathway is mediated through mitochondrial outer membrane permeabilization (MOMP) (Elmore, 2007). The transmembrane potential could be dissipated before, during or after MOMP. By evaluating the transmembrane potential, insight might be pointed into the relationship between mitochondria apoptotic pathway and arginine depletion. The fluorescent cationic dye, JC-1, accumulates at high concentration in the mitochondria of healthy cells with active transmembrane potential, resulting in the formation of J-aggregates which emit red fluorescence. When the mitochondrial potential is impaired, the lipophilic dye leaks out to the cytosol to form J-monomer that gives green fluorescence signals.

In the absence of BCA, majority of the cells were emitting red fluorescence suggesting the formation of J-aggregates in the mitochondria with active transmembrane potential (Figure 4. 12). However, a substantial increase of the cell population with J-monomer strongly suggests the impairment of transmembrane potential after 72 h of treatment with 15 U/ml BCA.

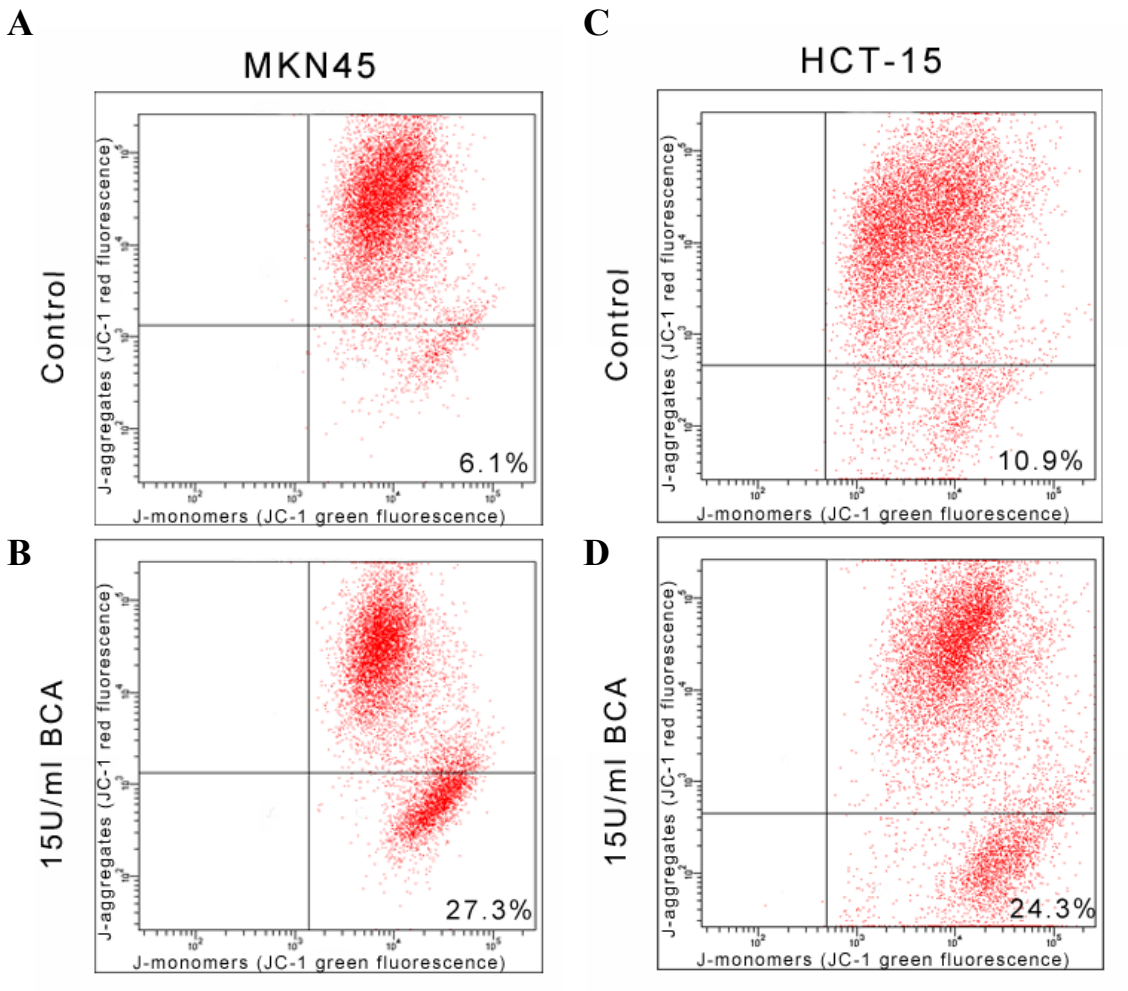

Figure 4. 12. Treatment with BCA induces mitochondrial outer membrane permeabilization. MKN45 and HCT-15 were treated with 15 U/ml BCA for 72 h before JC-1 staining. The majority of the control population emitted red fluorescence, indicating the dye accumulates in mitochondria with active transmembrane potential and results in the formation of J-aggregates that emit red fluorescence in majority of the control population (**A** & **C**). Treatment with BCA impaired the transmembrane potential probably through MOMP. The dye leaked from mitochondria to the cytosol and gave J-monomer that emitted green fluorescence on excitation (**B** & **D**). Similar results were

obtained from 3 independent experiments and representative data are presented for illustration purpose.

4.6. Summary:

The above *in vitro* studies demonstrated that arginine is an important amino acid in supporting the growth of gastric and colorectal cancer cell lines. By culturing the cells in various concentrations of arginine, we found that cell viability was directly proportional to the amount of arginine in the medium. Supplementing the same amount of arginine to the arginine deficient medium can almost completely restore the growth of different cancer cell lines to that comparable to cells cultured in commercially available RPMI medium.

Further studies with BCA and ADI demonstrated the efficacy of these arginine-depleting enzymes in retarding the growth of cancer cells. Treatment with BCA induced growth inhibition in all gastric and colorectal cancer cell lines tested while ADI could only suppress the growth of HCT 116. Profiling of urea cycle enzymes expression revealed the lack of OTC expression while ASS is found consistently expressed in different cancer cell lines. The expression profiles are consistent with the model that ASS+, ASL+ and OTC- cells should be sensitive to treatment with BCA but not ADI. Different levels of ASS expression were found in the panel of cell lines, and of these 5 cell lines, except HCT 116, were resistant to ADI treatment. In addition to the urea cycle enzyme expression, citrulline rescue of BCA-induced growth inhibition further confirms the role of ASS in recycling citrulline to arginine. The exception of HCT 116 which expressed ASS (mRNA and protein) but was inefficiently rescued by citrulline may suggest other mechanisms that influencing the utilization of citrulline and it will be further elaborated in the discussion.

The growth inhibitory effects induced by BCA are at least partly mediated by cell cycle arrest and apoptosis. In response to the treatment with BCA, the gastric cancer cell lines, MKN45, AGS and BGC823 were arrested in the S-phase of cell cycle. Interestingly, similar treatment of colorectal cancer induced G2/M-phase arrest in HCT-15 but S and G2/M dual-phase arrest in HCT 116, suggesting a tumor specific-response to arginine depletion. In addition to cell cycle arrest, BCA also induced apoptotic cell death in 4 out of 5 cell lines. Cell lines, except AGS, undergo apoptotic cell death via the mitochondria (intrinsic) pathway. Mitochondria outer membrane permeabilization leads to the release of apoptotic factors and in turn activates the cascade of caspase molecules including executioner caspase-3 and results in the hallmark of biochemical and morphological changes associated with apoptosis.

5. *In vivo* efficacy and preliminary pharmacological studies

5.1. Precis:

The promising anti-cancer effects demonstrated by BCA on gastric and colorectal cancer cell lines provided solid ground for further evaluation of BCA in preclinical settings. The use of microbial enzymes, such as ADI and asparaginase (Avramis & Tiwari, 2006; L. Feun & Savaraj, 2006; Pieters et al., 2011; Shen & Shen, 2006), for therapeutic purposes has been limited by their short residence time in the circulatory system due to enzymatic degradation, immunogenicity and rapid clearance through urinary filtration. Formulation with PEG extends the circulation half-life of these enzymes by increasing their hydrodynamic volume, shielding the protease cleavage sites and masking the immunogenic epitopes (Asselin et al., 1993; Ensor et al., 2002; Holtsberg et al., 2002; Kontos & Hubbell, 2012; Takaku et al., 1993). Such improvement will lead to an increase in overall exposure to the therapeutics. The effect of PEG conjugation, however, was affected by a number of factors such as the size and structure of PEG used, number of PEG conjugated per molecule, site and chemistry of modification as well as the intrinsic properties of the therapeutic protein. Therefore, the pharmacological properties of these therapeutic proteins need to be elucidated on a case-by-case basis (Caliceti & Veronese, 2003).

In this chapter, the pharmacological properties of BCA would be evaluated in mouse model. In single-dose pharmacokinetics study, the effects of pegylation on the circulation half-life and overall exposure of BCA would be revealed. To study the pharmacodynamics of BCA at molecular level, arginine concentration in the systemic circulation was monitored by amino acid analyzer (AAA). Macroscopically, BCA-

mediated arginine depletion could be manifested as anti-tumor efficacy in the MKN45 gastric tumor xenograft model. Tumor bearing mice receiving different regimens were monitored for a number of parameters including tumor volume, body weight over the course of treatment and final tumor weight, and the percentage tumor growth inhibition was estimated at the end of the experiment. Drug combination study investigating the possible synergistic effects of BCA with a chemotherapeutic currently used for gastric cancer may provide insight into how a more effective treatment strategy could be developed.

5.2. Pharmacokinetics of native and pegylated BCA

Pharmacokinetics is the study of kinetics of drug absorption, distribution and elimination (metabolism and excretion). These pharmacokinetic properties of protein therapeutics are usually affected by the formulation and route of delivery, and would in turn determine the regimen of therapeutic. With the help of pharmacokinetic models, these parameters should be optimized so as to achieve the desired pharmacological responses and at the same time, minimize the toxicity associated with the dosages. In this study, the effects of pegylation on BCA were evaluated using BALB/c mouse model. Understanding of the pharmacokinetics of native and pegylated BCA may provide useful information for the development of regimens for the efficacy study in xenograft bearing BALB/c nude mice. Considering the ease of administration through intraperitoneal (i.p.) route, it is commonly used in animal studies. Assuming that the drug administrated through i.p. could be completely and rapidly partition to the blood circulation, the elimination half-life by non-compartmental analysis could be roughly estimated by measuring the BCA activity in the blood circulation after single dose injection which will in turn provide information to develop the regimen for efficacy study. Since the extra-vascular route of administration was used, the apparent volume of distribution and clearance cannot be calculated unless further study from the intravenous injection of pegylated BCA to the BALB/c mice will be done in the future to which the bioavailability and the mean absorption time from extra-vascular injection could be elucidated. Thus, the errors such as overestimation of elimination half-life due to the delayed in the partition from extra-vascular compartment could be eliminated.

Mice of 4 to 8 weeks old were assigned randomly into two groups and each group consisted of 7 mice. Single dose of 250 Units native or pegylated BCA was administered via i.p. injection. Blood samples were collected from saphenous vein of the thigh before injection (time 0), and 4, 8, 24, and 48 h after injection of native BCA, while the blood samples from the group receiving pegylated BCA were collected at 0, 6, 24, 48, 72, 96, 120 and 144 h. Sera were prepared from the blood samples and the enzymatic activity of BCA was assayed for all collected samples. The mean serum activity-time curves were constructed and shown in Figure 5. 1. When comparing to the blood samples collected 4 h after injection, the native BCA activity dropped rapidly to about 50% at 8 h and fell almost to the baseline level at 24 h, while sustained activity above baseline was observed up to 144 h for pegylated BCA.

Using noncompartmental analysis, a simple and straightforward approach was adopted for the current study to estimate the terminal half-life values of native and pegylated BCA, which are about 6.9 and 87.8 h, respectively. Thus, the half-life was extended by 12.7-fold after pegylation. The AUC of serum BCA activity-time curve was calculated by the trapezoidal rule which measures the overall exposure of BCA. The difference between the two AUC values shows that pegylation increased the overall exposure by 5.4-fold.

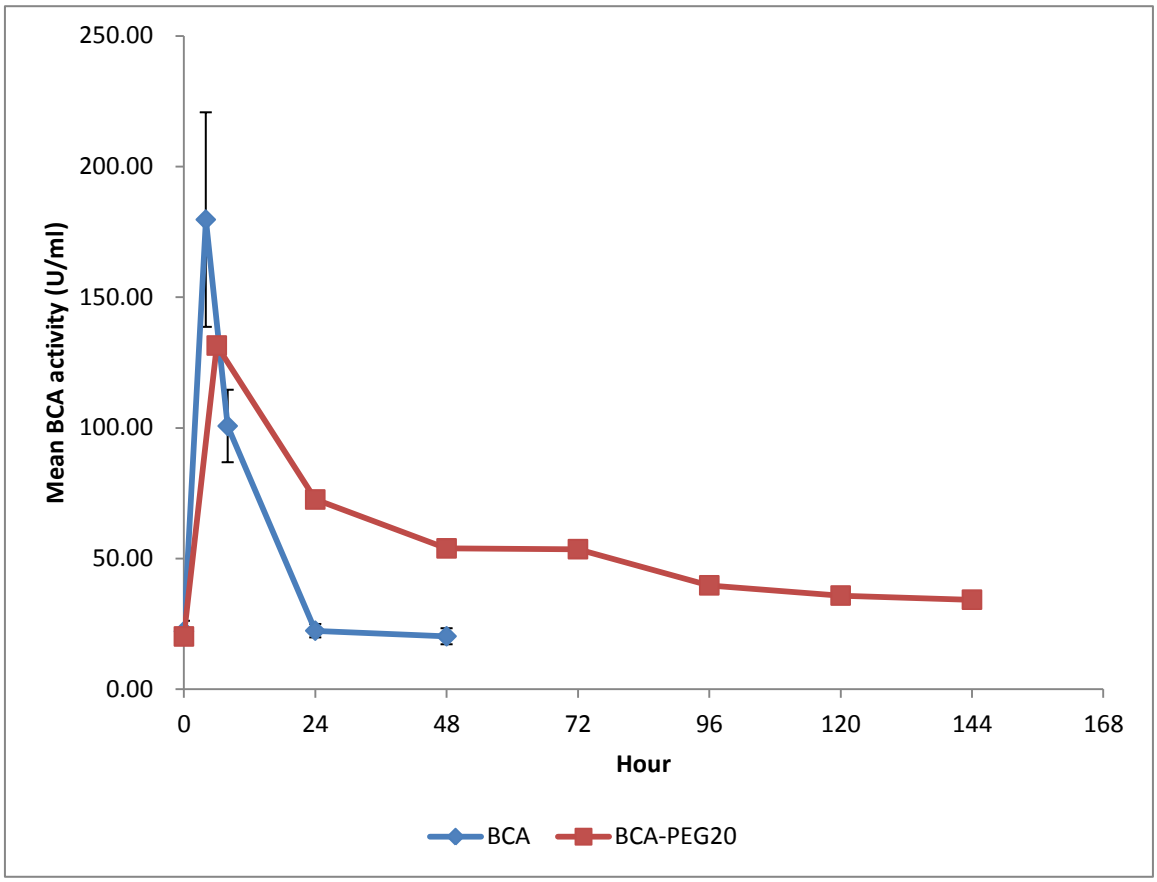

Figure 5. 1. Pharmacokinetic profiles of native and pegylated BCA administered through i.p. injection. The mean serum BCA activity following single dose i.p. injection of 250 Units of native or pegylated BCA was measured as a function of time. Data are means ± SEM, n = 5 and 6 for native and pegylated BCA, respectively.

5.3. Pharmacodynamics of BCA

Pharmacodynamics studies how drugs act on our body after administration. The pharmacological effect of BCA at the molecular level is the breakdown of arginine to ornithine and urea, while arginine depletion is manifested as the efficacy of BCA in retarding the growth of tumor xenografts in nude mice.

The serum samples collected at different time points for the pharmacokinetics studies were also used for the pharmacodynamics analysis. The proteins content in the serum were removed by acid precipitation and arginine levels were measured by chromatographic techniques with an AAA instrument.

For a single-dose i.p. injection of 250 Units of native BCA, the serum arginine levels dropped below the detection limit in 4 h and remained at an undetectable level after 8 h of injection (Figure 5. 2). At 24 h, the serum arginine concentrations rebound to about 80% of the serum level as shown at time zero.

Intraperitoneal injection of 250 Units pegylated BCA lowered the serum arginine level to an undetectable level by 6 h. Complete depletion of arginine lasted for 5 to 6 days. At 168 h, the arginine levels gradually increased to about 36% of plasma arginine concentrations as collected at time 0, and almost complete restoration was observed at 216 h. The extended period of arginine depletion is in coherence with the improved pharmacokinetic properties through pegylation of BCA.

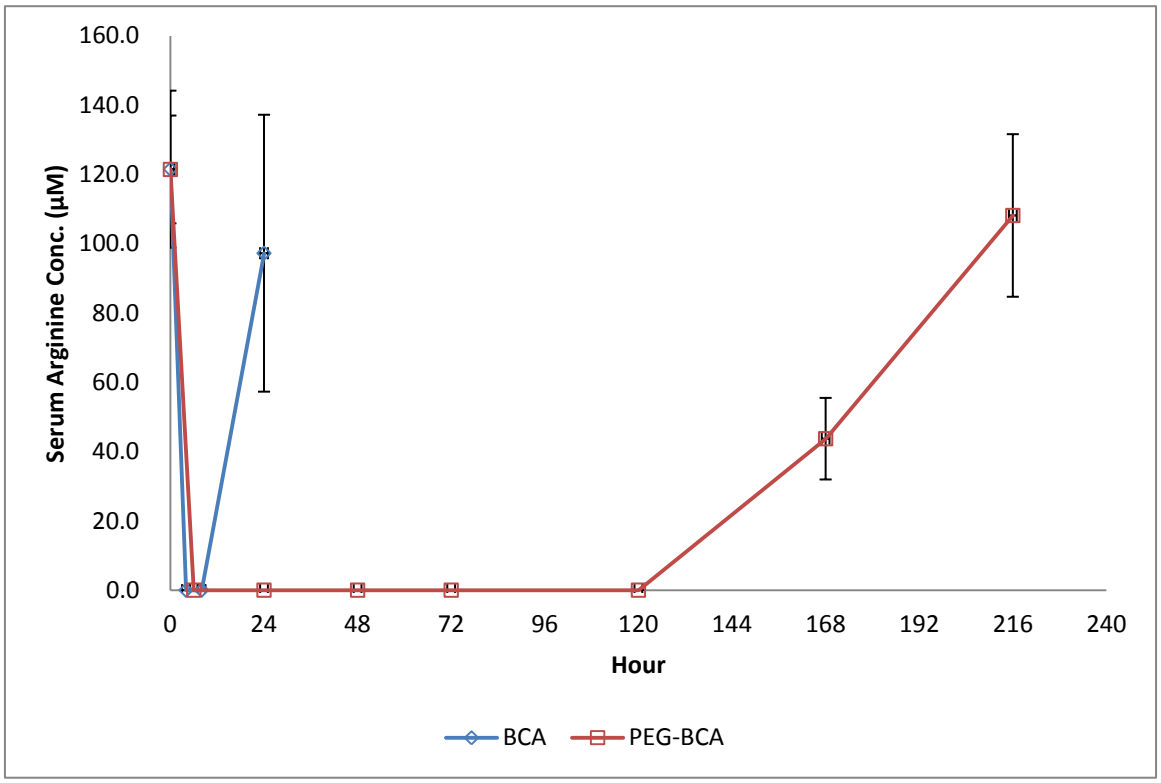

Figure 5. 2. The single-dose pharmacodynamic study of native and pegylated BCA. The blood samples collected for the pharmacokinetic study were assayed for the arginine content using amino acid analyzer (AAA). Data are means ± SEM, n = 4 and 7 for native and pegylated BCA, respectively.

5.4. Growth inhibitory effects of BCA on the MKN45 gastric cancer xenograft model

Having demonstrated the *in vitro* efficacy of BCA on the panel of colorectal and gastric cancer cell lines and the improvement of pharmacokinetic and pharmacodynamic properties of BCA through pegylation, the *in vivo* efficacy of BCA was elucidated with the MKN45 gastric cancer xenograft model. The inhibitory effects of BCA on tumor xenografts were monitored by measuring the tumor volumes over the course of treatment, while the toxicities of different treatments were reflected through monitoring the mice body weights. Final tumor mass values were measured at the end of the experiment, providing validation against the measurement of tumor size by volume.

The MKN45 tumor xenograft was prepared by injecting $1x10^6$ MKN45 cells subcutaneously to the flank of BALB/c nude mice. In order to prepare sufficient number of nude mice for the efficacy study, when the tumors reached 1.5-2.0 cm in diameter, they were excised, cut into tumor fragments and implanted into the flank of nude mice. The growth of newly transplanted tumors was monitored until stable growth was maintained. The mice were randomized and divided into 4 groups and each group consisted of 10 mice with average tumor volume of about 400 mm^3. To study its *in vivo* growth inhibitory effects, 250 Units of pegylated BCA were administered intraperitoneally twice per week to nude mice bearing the tumor xenograft, while the control group received PBS as vehicle control. To compare the efficacy of pegylated BCA to a clinically established chemotherapeutic, fluorouracil (5-FU) was included in this study. The concentration of 10 mg/kg 5-FU was injected into one group of mice once per week, while an additional group of mice received combination therapy of 5-FU and

pegylated BCA, following the same regimen as when they were used singly. Tumor volumes were measured twice per week throughout the treatment period and the fold changes with reference to the initial volume are shown in

Figure 5. 3. The PBS control group exhibited exponential growth while the tumor growth was significantly inhibited in all treatment groups. The relative tumor volume was found to be significantly smaller for the group treated with pegylated BCA, and interestingly, the growth inhibitory effect of pegylated BCA was found to be similar to 5-FU throughout the course of treatment. Moreover, combination of 5-FU and pegylated BCA showed a synergistic effect and gave the highest potency among the 3 treatment groups.

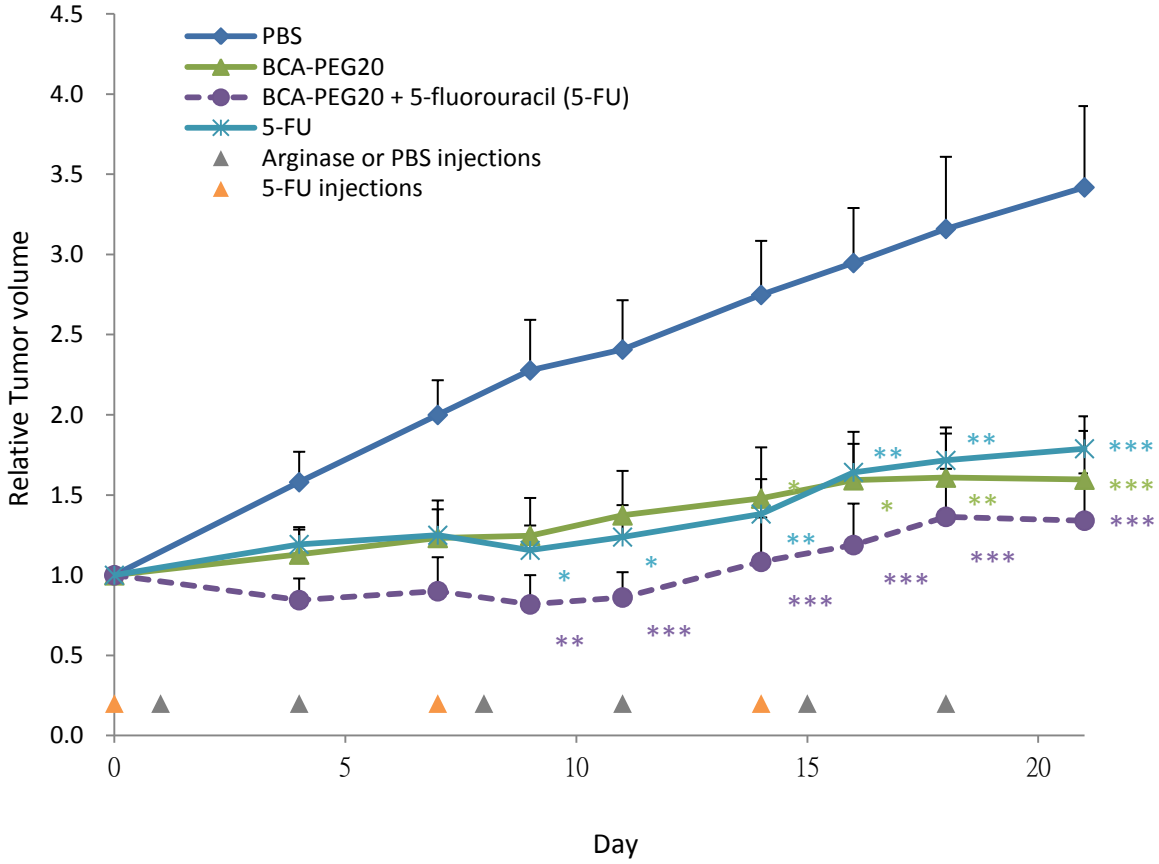

Figure 5. 3. The growth inhibitory effects of different treatments on the MKN45 gastric cancer xenograft model. The mice were randomized into 4 groups and administered with PBS (Control), 250 Units of pegylated BCA (twice per week), 10 mg/kg 5-FU (weekly) or combination of both pegylated BCA and 5-FU through i.p. injection. Tumor volumes were measured twice per week and fold changes compared to Day 0 wre reported. Data are means + SEM, n = 10 per group. Two-way ANOVA with Bonferroni correction, *, $p<0.05$, **, $p<0.01$, ***, $p<0.001$ vs PBS control.

5.5. Final tumor weight

In addition to the tumor volumes calculated from the diameters of solid tumors, final tumor weight provides the most consistent and reproducible reflection of tumor size at experimental end-point (Euhus et al., 1986; Tomayko & Reynolds, 1989). After three weeks of treatment, the mice were sacrificed and the tumors harvested for actual weight measurement. In line with tumor volume results, treatment with pegylated BCA and/or 5-FU significantly reduced the final tumor weight when compared to the PBS control (Figure 5. 4). Treatment with pegylated BCA or 5-FU resulted in 50-60% reduction in tumor weight. Combination therapy exhibited an even more dramatic effect on tumor suppression, where the tumor weight was reduced by 80% in relation to vehicle control, while the tumor weight was about 50% when compared to the mice receiving either therapeutic on its own.

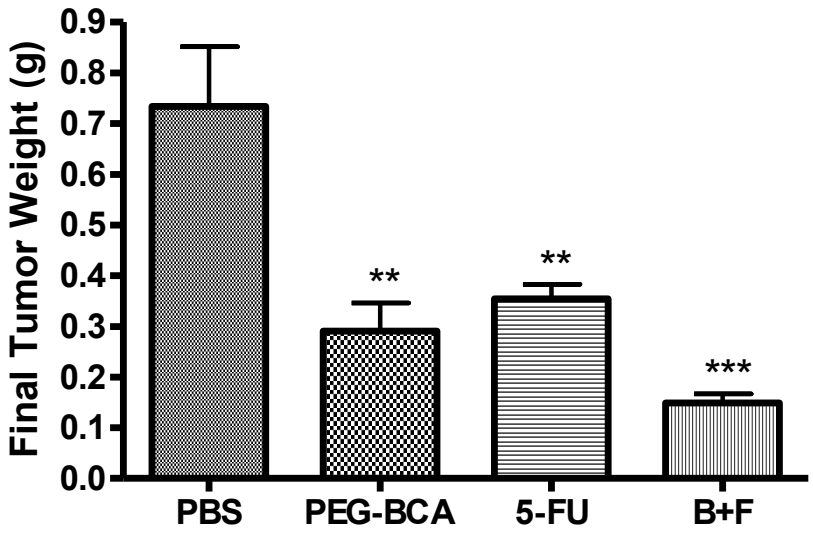

Figure 5. 4. Effects of different drugs on the final tumor weight at the end of the treatment. Data are means + SEM, n = 10. **, $p<0.01$, ***, $p<0.001$ by one-way ANOVA with Tukey post-test. The B+F treatment means combination therapy of PEG-BCA and 5-FU.

5.6. Mice body weight

Treatment-associated toxicity usually manifests as significant weight loss of the nude mice during the course of treatment. Thus, body weight was measured before receiving the first injection at Day 0 and once per week throughout the treatment. The mouse body weights from different treatment groups were plotted relative to Day 0 as shown in Figure 5. 5. Across different treatment groups, the mouse body weights at termination are comparable to those at Day 0, and no significant weight loss was observed in any of the group throughout the experiment.

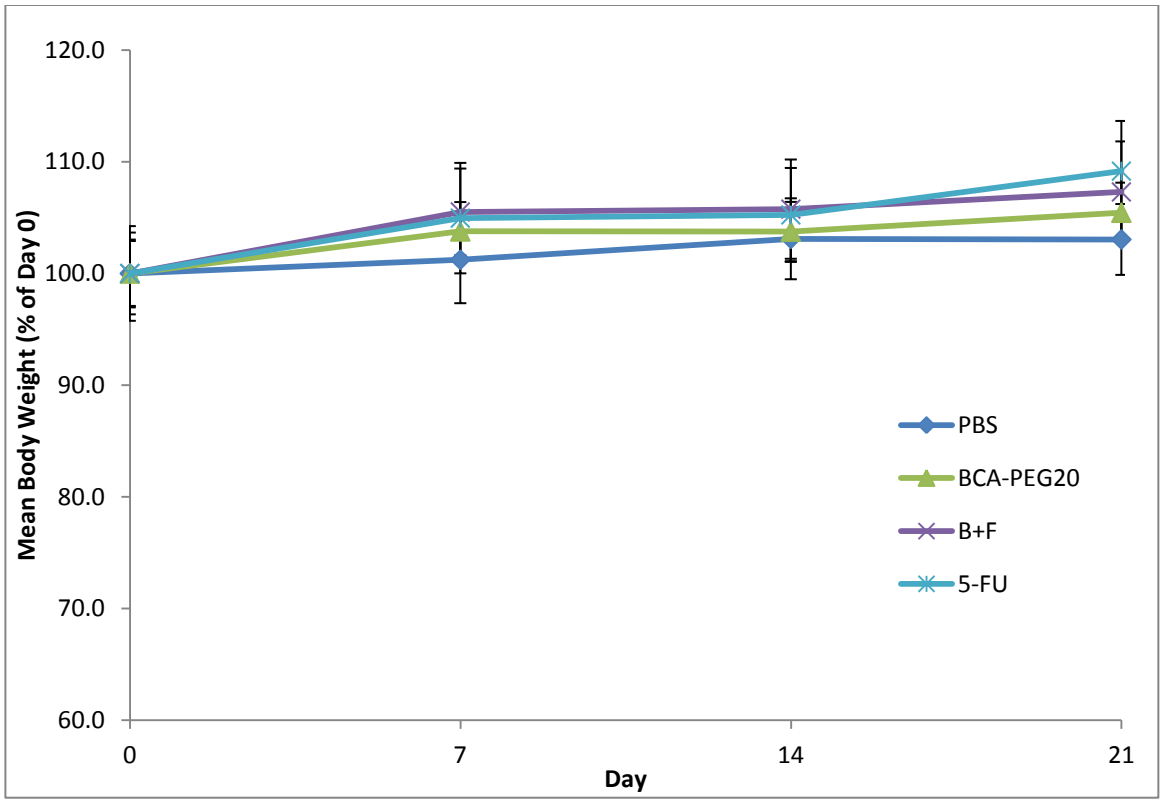

Figure 5. 5. Body weight of tumor-bearing mice throughout the course of treatment. Body weights are within 10% variation and no unacceptable weight loss was observed throughout the treatment. Data are means ± SEM, n = 10 per group.

5.7. Summary

Single-dose pharmacokinetic study of BCA demonstrated that the circulation half-life of native BCA, when administrated intraperitoneally, was extended from 6.9 to 87.8 h after pegylation. The AUC value was increased by 5.4 times as compared to the native BCA.

Single-dose of native BCA reduced the serum arginine to an undetectable level for at least 8 h and rebounded by 24 h post-injection. On the other hand, serum arginine was reduced to an undetectable level for 5 to 6 days when pegylated BCA was administered through i.p. injection.

Our efficacy study showed that pegylated BCA could significantly suppress the tumor growth *in vivo* and its efficacy is comparable to 5-FU in terms of the tumor volume measured during the treatment. Combination of 5-FU and pegylated BCA resulted in synergistic effect. These results are in coherence with the final tumor weight measurements, where treatment with pegylated BCA or 5-FU alone led to 60 and 52% tumor suppression, respectively. Combination therapy further reduced the tumor weight by up to 80% when compared to the control.

The body weight remained steady throughout the course of our different treatments and thus no unacceptable treatment-associated toxicity was observed.

6. Discussion

Success in developing human arginase to treat HCC patient in phase I clinical study extends our interest to further explore the underlying principle of arginine depleting enzymes that lead to the growth inhibitory effects on cancer cells (Yau et al., 2012). Although the anti-cancer effects of arginase has been demonstrated in HCC, melanoma, leukemia, prostate and breast cancer, testing on gastric and colorectal cancer are unprecedented with arginase. Limitations of the multi-pegylated human arginase BCT-100 include the heterogeneous nature of the pegylated arginase, causing the difficulty in detailed characterization and the possibility of batch to batch variation. Therefore, we aimed to develop a more defined therapeutic using the arginase from the extreme thermophile *Bacillus caldovelox.*

Since the isolation of *Bacillus caldovelox* from the hot spring in Yellowstone National Park, only a few studies have been performed on the characterization and understanding of the structure-function relationship of BCA by x-ray crystallography (Bewley et al., 1999; Patchett et al., 1991). Considering the high thermostability of BCA revealed by these studies, production of BCA could be greatly simplified through introducing a heat treatment step to the purification scheme (Bewley et al., 1999; Bewley et al., 1996; Patchett et al., 1991). Besides, based on the high resolution crystal structure of BCA deposited in the PDB (2CEV), a 6xHis-tag was added to the extended C-terminal end of BCA to facilitate the purification. A surface exposed serine residue was mutated to cysteine (S161C) for site-directed mono-pegylation.

In order to produce BCA in sufficient quantity for characterization, *in vitro* and *in vivo* studies, the DNA sequence encoding the engineered BCA was cloned into the pET-3a

vector. The expression of BCA in *E. coli* cells was driven by the T7 promoter under the induction of IPTG. The *E. coli* cells obtained from shake flask culture or fermentation were collected and purification of the recombinant BCA was established based on the publication by Maria *et al* and modifications were made with reference to our rational engineering (Bewley et al., 1999; Bewley et al., 1996). After obtaining the soluble fraction from cell lysate, we found that a heat-treatment step increased the purity of the target protein by 1.6-fold. Instead of ammonium sulfate precipitation, nickel affinity column was used to facilitate the purification after the heat treatment. Small scale shake flask culture produced 0.11 g/L of purified BCA from a 2-step purification while 5-L fermentation doubles the yield to 0.22 g/L and it is comparable to the reported value, 0.2 g/L, for the wild-type BCA (Bewley et al., 1996). The purity of native engineered BCA is improved by about 3-fold after the 2-step purification. The major contaminant having the size of about 27 kDa on the SDS-PAGE is likely to be the proteolysis product of BCA which was formed during the sample preparation for the SDS-PAGE analysis (Patchett et al., 1991).

Further characterization and comparison in between the wild-type and the engineered BCA shows that the modification did not dramatically altered the physical properties of BCA. The pI of the engineered BCA was found to be about 5.9 which is slightly more basic compared to the wild-type BCA (pI 5.2-5.5) and likely attributed to the 6xHis-tag introduced to the C-terminus of BCA. The hexameric structure of engineered BCA or BCA-ABD was similarly determined by gel filtration chromatography for which the oligomeric structure of BCA was not affected by the presence of the 6xHis-tag or ABD. Through revealing the oligomeric structure of BCA, aggregates were identified in both

wild-type and engineered BCA. Although these aggregates present in different amount, the cysteine mutation introduced to the protein surface might not be the cause of aggregation in engineered BCA. Instead, we observed the formation of aggregates increase with the period of storage (unpublished data) and which may explain the reason why prolonged storage of the native BCA will result in diminution of specific activity while pegylation stabilized the BCA and prevented further aggregation. The presence of aggregates in protein therapeutic has been linked to immunogenicity. Formation of aggregates could happen in different stages of protein preparation, ranging from purification through column chromatography to bottling of the final product. Development of binding and neutralizing antibody to human protein therapeutics such as interferon, factor VIII and insulin has been reported (Antonelli & Dianzani, 1999). Antibodies against the protein therapeutics not only rendered the drug ineffective but also led to the devastating results if it cross-reacted with the endogenous protein (Antonelli & Dianzani, 1999). Moreover, Sherman *et al* showed that immunological responses after repeated administration of pegylated uricase/urate oxidase have been observed if trace amount of aggregates is present in the native preparation. In contrast, prior removal of aggregates in the native protein by ion-exchange chromatography reduced the immunogenicity of the pegylated conjugate for which undetectable level of anti-uricase antibody could be measured after repeated injection (Sherman et al., 2008). Thus, our preparation of the native BCA could be further improved by eliminating the aggregates before pegylation.

Development of protein therapeutics originated from bacterial and non-human mammalian sources has been widely used in different pathophysiological conditions such

as cancer, gout and immunodeficiency disease. It is conceivable that the use of non-human protein for therapeutic purposes would lead to the issue of immunogenicity. Therefore, proper formulation of protein therapeutic through pegylation has been shown to reduce renal clearance by increasing the hydrodynamic volume of these proteins to above the size threshold of glomerular filtration, masking the immunogenic epitopes and amino acid residuals that are susceptible to protease cleavage. Conjugation of PEG to surface lysine residues has been the mainstay for therapeutic enzymes such as Adagen, Oncarspar and Krystexxa (Alconcel et al., 2011). Although these drugs has been approved by FDA, the drawback of random pegylation lead to a heterogeneous mixture of pegylated proteins with different numbers and sites of PEG attachment which exists in various amounts and makes the characterization even more complicated. Since pegylation has direct impact on the pharmacological properties of therapeutic proteins, regulatory authorities not only imposed stringent control on the characterization of pegylated proteins but also the consistence of the final product when produced from different batches (F. M. Veronese & Pasut, 2005).

Therefore, a proof of concept study was carried out to develop a more defined arginase therapeutic through site-specific mono-pegylation of BCA. Pegylation of BCA was achieved through the reaction between the thiol group of cysteine residue engineered on the surface of BCA and 20 kDa PEG (ME-200MA) activated with maleimide. Pegylation of BCA was optimized with different molar excess of ME-200MA, pH, temperature and duration of incubation. The extent of pegylation increases with the molar excess of ME-200MA. The most dramatic improvement happened when PEG increased from 1 to 10 equivalents while increasing the amount of PEG to 20 equivalents could slightly improve

the extent of pegylation. Thus, further optimization on the pegylation conditions, through adjusting the pH, temperature and duration of incubation, were maintained at 10 equivalents of PEG so as to minimize the cost of optimization process. However, the above optimization do not result in an observable improvement when compared to the pegylation condition carried out at 4°C, pH 7 and overnight incubation where the stability of maleimide functional group in ME-200MA was found relatively stable in neutral aqueous condition (Hermanson, 2013).

According to the results of SDS-PAGE, the majority of BCA was modified by PEG. The trace amount of the native BCA imply that some of the subunits may not be conjugated with PEG and resulted in less than 6 PEG attached to some of the hexameric BCA. Since one of the purposes of pegylation is to minimize the immunogenicity of foreign protein, the presence of trace amount of unpegylated protein may still rendering the protein therapeutic more immunogenic when compared to complete pegylation of BCA and so limited the use for repeated injections. Although the current pharmacokinetics study was based on single dose injection and efficacy study was done on immunodeficient mice bearing tumor xenograft, improvement on the pegylation of BCA should be considered.

Incomplete pegylation do not seem to happen only in the pegylation of BCA, development of other mono-pegylated therapeutic such as anti-TNF-α single-chain antibodies (scFv) for the treatment of rheumatoid arthritis and Crohn's disease also encountered the similar problem. Conjugation of maleimide activated PEG to the anti-TNF-α single-chain antibodies resulted in a mixture containing both native and pegylated anti-TNF-α scFv. The strategy used by Yang *et al* to obtain the pegylated anti-TNF-α scFv in almost homogeneity was based on a purification step using cation-exchange

chromatography which successfully purifies the pegylated scFv from the mixture containing free PEG and unreacted scFv (Yang et al., 2003). Other strategy based on the understanding of the BCA physical properties could be further explored. Earlier studies elucidating the requirement of manganese to maintain the quaternary structure of BCA showed that over 95% of BCA would be dissociated from the hexameric structure to become monomer when incubated at pH 2.5 for 10 minutes. This property may allow the dissociation of the pegylated BCA into monomeric structure and thus separation of unpegylated BCA by gel filtration column could become possible. Through adjusting the pH value of the fraction containing the monomeric pegylated BCA to pH 9, it allows the reassociation of the BCA monomer to hexameric structure (Lavulo et al., 2001; Patchett et al., 1991). Besides, dissociating oligomeric structure of human arginase to monomer through mutating the surface interacting residues has been shown to retain the wild-type activity (Sabio et al., 2001). Similarly, BCA may be dissociated into monomer, by mutating the conserved amino acid residues, for pegylation where the separation of pegylated BCA from the native and unpegylated BCA could be facilitated by filtration or size exclusion chromatography. Although unpegylated BCA could be likely separated by the above remedies, additional steps of purification would definitely increase the cost of production. Rational screening for other surface exposed residues for PEG conjugation may be also considered in the hope of further improving the pegylation efficiency. Currently, improvement on the pegylation efficiency was achieved only through increasing the molar excess of PEG and 20 equivalents of PEG were used to prepare the pegylated BCA for characterization, *in vitro* and *in vivo* studies because it gave the highest yield among the conditions tested.

Characterization of pegylated BCA through SDS-PAGE visualized the shift of BCA molecular weight from 33 kDa to almost 100 kDa which makes it almost double from the calculated molecular weight, 53 kDa. Such difference is attributed to the hydrophilic properties of the PEG molecule. Ethylene oxide is the basic repeating unit of PEG and each repeating unit can associate with 2-3 water molecules. Hence, the electrophoretic mobility of pegylated BCA on SDS-PAGE was retarded and seemingly larger than the calculated molecular weight (Bailon et al., 2001; Maxfield & Shepherd, 1975; Roberts et al., 2002). More precise estimation of the molecular weight for pegylated BCA was done by using MALDI-ToF mass spectrometry. Pegylated BCA was desalted and mixed with the matrix to allow crystallization. The crystals were irradiated with nitrogen laser and predominantly singly charged ions were generated for time-of-flight mass spectrometry analysis. Unlike the multiple pegylation technology exploited by different therapeutic proteins such as Adagen, Ocarspar and Krystexxa that produced a mixture of protein containing different numbers of PEG and positional isomers, pegylation of BCA via a site-specific cysteine residue resulted in two major species showing 33.4 and 55.0 kDa on the chromatogram which are corresponding to the native and pegylated BCA, respectively. The peak intensities do not refer to relative abundance of these 2 species as the ionization efficiencies of native and pegylated BCA may exhibit differently. Capillary electrophoresis (CE) coupled with UV detector set to 220 nm could be established to determine the ratio of these 2 species when necessary. The pegylated BCA exhibited a broader peak width when compared to the native BCA and such difference is attributed to the polydispersed nature of PEG molecules. In general, the polydispersity indexes range

from 1.01 for low molecular weight PEGs (< 5 kDa) to approximately 1.05 for PEGs up to 30 kDa are the acceptable standard for PEG reagents (Jevsevar et al., 2010).

Through site-specific monopegylation of BCA, it allows easy characterization because a single PEG chain was conjugated to the defined cysteine residue that rationally engineered to BCA and thus positional isomer does not exist after pegylation. More importantly, conjugation of PEG avoiding modification of amino acids near to the active site allows the pegylated BCA to retain comparable activity. In contrast, multiple pegylation is an uncontrolled process for which conjugation usually based on reactive ε-amino group on lysine residues. Random conjugation of PEG to the therapeutic protein could sometimes resulted in reduced biological activity possibility due to steric hindrance imposed by PEG that interfere the binding of the drug molecule to the target receptor or modification of lysine residue in the active site that involved in catalytic reaction. For example, a number of studies trying to prolong the circulation half-life of ADI via pegylation have all resulted in about 50% reduction of the enzyme activity providing that the PEG to ADI ratio had already been optimized (Holtsberg et al., 2002; Takaku et al., 1993; Wang et al., 2006). Increasing the number of equivalents of PEG for ADI conjugation would further reduce the enzyme activity to less than half that of the native enzyme. Regardless the size and chemistry of the linker for pegylation, an inverse relationship between the numbers of PEG conjugated to ADI and the residual activity after pegylation was demonstrated (Holtsberg et al., 2002). A more extreme example from the random pegylation of uricase with straight chain 5000 Da PEG completely abolished its activity and only partial retainment of enzyme activity could be achieved

through addition of excessive amount of uric acid to protect the active site during pegylation (Schiavon et al., 2000).

For the therapeutic ptotein based on receptor interaction, steric hindrance imposed by pegylation may disrupt the interaction between the receptor and drug molecule and thus reducing the efficacy of the protein therapeutic. The development of growth hormone (GH) antagonist was based on the glysine to lysine substitution of the wild-type GH at position 120 (G120K) which can dimerize the cell surface GH receptor but not activating the downstream signaling pathway. Although pegylation of GH-G120K extend the circulation half-life from 30 min to more than 100 h but, at the same time, reduced the binding affinity by 186-fold when compared to the native GH. Fortunately, further optimization, based on molecular modeling, through introducing eight more mutations to the antagonist (B2036) not only could improve the affinity of the antagonist but also minimized the effect of steric hindrance due to the conjugation of PEG via the two lysine residues close to the biding site. When compare to the pegylated GH-G120K, pegylation of B2036 improve the binding affinity by 6.6-fold but still 28-fold lower than the native GH. Hence, extended circulation half-life through pegylation together with high dose of pegylated B2036 is still necessary to compensate for the lost of binding affinity and compete with the ligand for the growth hormone receptor. This may explain why a high dose of daily regimen of pegylated B2036 is required for the treatment of acromegaly (Fishburn, 2008; Kopchick et al., 2002; Muller et al., 2004; R. J. Ross et al., 2001).

Despite a number of approved pegylated protein therapeutics are based on random pegylation, regulatory authorities are imposing more stringent requirement to characterize the pegylated protein such as the abundance of the therapeutic protein with different

numbers of PEG conjugated, identifying positional isomers as well as the possible sites of conjugation (Mero et al., 2009; F. M. Veronese & Pasut, 2005). Since all these differences can contribute to the variation of pharmacological properties, it is of paramount importance to demonstrate the robustness and consistence among different batches of pegylation. In view of this situation, more specific pegylation chemistry with second generation of PEG reagents was exploited for the pegylation of BCA (Roberts et al., 2002). Site-specific conjugation is a rational approach considering the structural and functional information in the hope of maximizing the protein pharmacological activities and so a more efficacious protein therapeutic could be formulated. Moreover, site-specific monopegylation is a robust, defined process and highly reproducible between batches which make the production control far easier than the random pegylation approach (Chapman, 2002; Pfister & Morbidelli, 2014).

Recently, advancement in developing discrete PEG reagents allow coupling of a defined mass of PEG to therapeutic protein which not only simplify the overall characterization process but also provide an even more precise control on the pharmacological properties of protein therapeutics. Although the largest size of discrete PEG available is limited to 2 kDa for straight chain PEG and 8 kDa for branched chain PEG, higher molecular weight PEG with longer chain length may be developed in the foreseeable future (Davis & Crapps, 2011; Povoski et al., 2013). It is noteworthy that the use of discrete PEG may become the standard of practice as a recent IND application approved by FDA required the company to switch from disperse PEG to discrete PEG so as to make sure the reproducibility of the drug production process ("Quanta Biodesign Ltd,").

A pilot scale production of BCA starting from 5L fed-batch fermentation to purification using XK50 column with 196 ml bed volume of metal affinity media successfully purified 1096 mg of BCA. After pegylation, the purification scheme aimed to remove free PEG and reduce the endotoxin levels was established based on understanding from the characterization of pegylated BCA. Prior to the affinity purification of pegylated BCA from the reaction mixture, a filtration step with 50 kDa cutoff membrane allows partial removal of free PEG but pegylated BCA was retained. Since excessive PEG interfere the binding of pegylated BCA to the metal affinity column, pegylated BCA and free PEG could be found simultaneously in the flow through fraction which accounted for about 30% reduction of the yield. Either an additional step to recycle the flow through fraction on the metal affinity column or to further expand the column capacity to improve the recovery should be investigated in the future.

Instead of extending the circulation half-life of therapeutic proteins through increasing the hydrodynamic radius above the renal clearance threshold, such as coupling to PEG or fusing to recombinant PEG mimetics, we also tried to do some preliminary studies to prolong the circulation half life of BCA based on the understanding of FcRn mediated recycling mechanisms (Andersen et al., 2011). Albumin is the most abundant proteins in the blood circulation; it is normally present in plasma at 50 mg/ml and has a circulation half-life of 19 days in human (Peters, 1985). The extended circulation half-life of albumin was found associated with the FcRn receptor in a pH dependent manner where the albumin binds to FcRn at acidic pH in the endosomes of endothelial and hematopoietic cells. The FcRn bound albumin is recycled to the cell surface and dissociated from the receptors at physiological pH (Andersen et al., 2011). Such recycling process rendering

the extended circulation half-life for albumin and it is conceivable that fusion of albumin to therapeutic proteins will also extend the circulation half-life. This strategy has been used to prolong the circulation half-life of interferon, named Albinterferon alfa-2b, which is in the phase III clinical trial for the treatment of chronic hepatitis C virus (Kontermann, 2011). The circulation half-life of Albinterferon alfa-2b is extended to 200 h which allow injection at biweekly interval (Nelson et al., 2010).

In addition to albumin fusion, a technically simpler approach using albumin binding domain (ABD) to associate with albumin for the extension of protein therapeutic half-life has been developed. The ABD is a small moiety make up of 46 amino acids which is originated from protein G of Streptococcus strain G148 and found to have different affinity towards albumin from a wide range of species. For example, ABD is found to have nanomolar affinity to human serum albumin (HSA) (Johansson et al., 2002; Kraulis et al., 1996; P. A. Nygren et al., 1990). Fusion of ABD to different therapeutic proteins could be obtained in high yield in the bacteria expression system while the biological activity and albumin binding affinity could be retained. Affibody, single chain diabody (scDb), CD4 and soluble complement receptor 1 (sCR1) has been fused with various streptococcal protein G derived albumin binding domains and the circulation half-life for some of these proteins has been prolonged to different extent comparable to pegylation (Makrides et al., 1996; P.A.; Nygren et al., 1991; R. Stork et al., 2007; Tolmachev et al., 2007). For example, fusion of scDb-ABD and pegylated scDb exhibit similar circulation half-life of 53.0 h and 47.9 h, respectively; but the biodistribution of scDb-ABD in the tumor is about 2-fold higher when compared to the pegylated scDb (R. Stork et al., 2009). The increased tumor accumulation is due to the smaller hydrodynamic radius of ABD-

scDb and albumin complex (4.8 nm) compared to pegylated scDb (7.9 nm) which makes the complex to have better extravasations and tumor penetration (R. Stork et al., 2009).

Fusion to therapeutic enzyme such as BCA is unprecedented and our preliminary data showed that fusion of ABD to BCA could be successfully expressed in *E. coli* cells with retained albumin binding and enzymatic activity. Through resolving the BCA-ABD and albumin complex on the native PAGE, we demonstrated the specific binding of BCA-ABD to albumin in a proportional manner. The shift of BCA-ABD and albumin complex to higher molecular weight when analyzed on a gel filtration column further confirmed the binding in the native state and at the same time revealing the hexameric structure of BCA-ABD.

Fusion of BCA-ABD leads to the reduction of enzymatic activity by one-third when compared to the parental BCA molecule but addition of various amounts of HSA does not further reduce the activity. Even in the presence of bovine serum albumin, the BCA-ABD maintains cytotoxicity to MKN45 gastric cancer cell line. Similar observations have been reported for the trispecific ABD-scDb fusion protein to retargeting the CD3 expressing T-cell to the carcinoembryonic antigen (CEA) positive cancer cells. The effector cell activation as measured by the IL-2 release assay was reduced by 3-fold and further reduction by a factor of four was observed in the presence of HSA (R. Stork et al., 2007).

In spite of the promising results from biochemical study, the BCA-ABD should be further optimized for the binding affinity and enzyme activity before *in vivo* study. Since current studies only provide qualitative measurement to the binding of BCA-ABD to HSA, a

more precise quantitative measurement using, for example, Biacore, may allow the comparison of the ABD affinity before and after fusion to BCA. Moreover, a high affinity version of ABD, ABD035, with femtomolar affinity to HSA may be engineered to the BCA-ABD fusion protein in the hope of further extension of circulation half-life and lowered the renal clearance through reducing the unbound fraction (Hopp et al., 2010; Jonsson et al., 2008; Orlova et al., 2013). Careful design of the fusion protein through rearrangement of the ABD to either carboxyl- or amino-terminus or adding a linker in different lengths between the ABD and target protein may alleviate the steric hindrance imposed by the ABD domain (Andersen et al., 2011).

Since the report of differential requirement of arginine in human melanoma and HCC cell lines, the development of targeted therapeutic through systemic deprivation using arginine depleting enzyme, such as arginase and ADI, has been revived (Cheng et al., 2007; Ensor et al., 2002; Takaku et al., 1993). Thus far, encouraging results from the *in vitro* and animal studies of ADI with different cancer types, such as leukemia, mesothelioma, neuroblastoma, renal cell carcinoma, stomach, pancreatic, lung and prostate cancer have been reported (Bowles et al., 2008; Gong et al., 2000; Kelly et al., 2011; J. E. Kim et al., 2009; R. H. Kim et al., 2009; Szlosarek et al., 2006; Yoon et al., 2007). Most if not all of the reported cancer types showing preclinical response to ADI are now entered to different stages of clinical trial (https://clinicaltrials.gov/). Even considering the prevalence of ASS+ tumor and the possibility to induce ASS expression in certain cancer types, ADI is still warrant for further investigation in clinical setting toward different tumor types (Dillon et al., 2004; Lam et al., 2009). For arginase, it should be considered as a better candidate for arginine depletion because it converts

arginine to ornithine for which recycling would be hampered even in ASS positive tumor while OTC is not expressed (Lam et al., 2009). Although pegylated recombinant human arginase is now in clinical trial for HCC, only a few reports are available in the literature mentioning the use of arginase for the treatment of human melanoma, leukemia and prostate cancer (Hernandez et al., 2010; Hsueh et al., 2012; Lam et al., 2009; Lam et al., 2010). The ASS expression levels in the gastric and colorectal cancers are relatively higher when compared to other cancer types (Dillon et al., 2004). In this regard, we are trying to extend our investigation to the arginine requirement by gastric and colorectal cancers and its response toward different arginine depleting enzymes for which the mechanisms leading to grow retardation, such as cell cycle arrest and apoptosis, and resistance to the arginine depleting enzyme will be elucidated.

Having understood the auxotrophic requirement of arginine by cancer cells in general, withdrawal or lowering the arginine levels lead to the retarded growth of cancer cells in culture (D. N. Wheatley et al., 2000). This agree with our findings that the growth of 3 gastric and 2 colorectal cancer cell lines in culture is proportional to the amount of arginine added to the AFM supplemented with dialyzed serum. The data support further evaluation of these gastric and colorectal cancer cell lines for *in vitro* study using different arginine depleting enzymes, BCA and ADI. Interestingly, all cell lines responded to BCA and the effect of growth inhibition is proportional to the amount of BCA added to the culture while ADI only inhibits the growth of HCT116 in a dose-dependent manner and leaving the rest of the cell lines having the same growth rate as control. HCT116 is the only cell line that retarded by both ADI and BCA for which ADI was found 4 times more potent than BCA and similar results for SK-MEL-28 has been

reported (Cheng et al., 2007). Generally, when the cell line could be inhibited by both arginine depleting enzymes, ADI always found to be more potent than arginase presumably due to the lower Km value of argine for ADI.

To explain the reason why the cell lines responded differently to BCA and ADI, we try to correlate the products generated by different arginine depleting enzymes, the intracellular expression of urea cycle enzymes through measuring the transcript and protein expression levels and the ability to recycle the end-products, viz citrulline and ornithine, which are also the intermediates of the urea cycle. Arginase breaks down arginine to equimolar concentration of ornithine and urea. Successful recycle of ornithine to arginine not only requires OTC but also ASS and ASL (Cheng et al., 2007; D. N. Wheatley & Campbell, 2003; D. N. Wheatley et al., 2005). Among the 5 cell lines tested in our study, coupled expression of ASS and ASL was found in every tested cell line, but none of them expresses OTC and similar observation has been reported in both HCC and melanoma cell lines. Thus, BCA exhibits a strong growth inhibitory effect on all of the cell lines in culture because of the incapability to regenerate arginine for proliferation. Despite none of the cell lines expressed OTC in this study, previous report demonstrated that transfection of expression plasmid carrying the OTC cDNA to hepatoma and melanoma cell lines can confer resistance to arginase treatment in culture (Cheng et al., 2007; Lam et al., 2010). For ADI, it converts arginine to equimolar concentration of citrulline and ammonia. Cell lines lacking or having low level expression of ASS was suggested to exhibit retarded growth by ADI. In contrast, cell lines expressing ASS can utilize citrulline from the enzymatic reaction to regenerate arginine via the coupled ASS and ASL enzymatic reaction (Bowles et al., 2008; Shen et al., 2003). Transfection of human

cDNA encoding ASS not only reverses the growth inhibitory effect for both HCC and melanoma cell lines in culture but also in animal study while down-regulation of ASS using RNA interference could overcome the issue of ADI resistance (Ensor et al., 2002; Kelly et al., 2011; Syed et al., 2013; F. L. Wu et al., 2011). In general, our findings are in good agreement with this model for which MKN45, BGC823, AGS and HCT-15 expressing ASS are resistant to ADI treatment.

The only exception is HCT-116 which expresses ASS but is sensitive to ADI treatment. We also come across similar reports in the lecture explaining the growth inhibitory effect of ADI toward the cell line exhibiting low ASS activity (R. H. Kim et al., 2009; Shen et al., 2003). However, comparatively lower expression of ASS has been observed in MKN45 and HCT116 while low ASS expression in HCT116 sensitized the cells to ADI treatment but MKN45 cells remain resistant. The inconsistence of HCT116 expressing ASS but inhibited by ADI was further evaluated by incubating various concentrations of citrulline in the presence of BCA. When compared to a melanoma cell line, A375, with known absence of ASS expression, as high as 2 mM citrulline added to the culture medium could not rescue the cells and showing almost identical dose-response curve as the BCA treatment while HCT116 could be minimally rescued by the highest concentration of citrulline. On the contrary, the MKN45 and HCT-15 cells achieved more than 75% recovery with different concentrations of arginine added to the culture. These data, in complementary to the expression analysis of urea cycle enzymes, provide further support to the role of ASS in regenerating arginine via the precursor citrulline (Storr & Burton, 1974; D. N. Wheatley et al., 2005). However, HCT116 cells, expressed ASS and ASL, were poorly rescued by the citrulline added to the culture. It is speculated that the

ASS enzyme may not be catalytically active, possibly due to mutations of the enzyme and this should be verified by DNA sequencing of the gene in the future. In our study, we only tested the capability of different cell lines in the utilization of arginine precursor, citrulline, while ornithine was not included because these cell lines lack the OTC expression. Inefficient utilization of argininosuccinate by cancer cell lines expressing ASS has been reported previously saying that conversion of citrulline to argininosuccinate is a tightly coupled reaction for which ASL would preferably use argininosuccinate directly channeled from ASS instead of from the exogenous supply in culture medium (D. N. Wheatley et al., 2005). Thus, recycling of argininosuccinate in culture is omitted in the current study.

The established correlation between the tumors with ASS expression and resistance to ADI treatment further extends the role of ASS as biomarker in clinical setting, where the ASS expression levels in biopsy samples were measured by immunohistochemistry and real-time PCR (L. G. Feun et al., 2012; Ott et al., 2012). However, the above study demonstrated that even HCT116 cells expressing ASS could become sensitive to the ADI treatment. In view of the above situation, we would suggest to test primary culture of patient biopsy in AFM supplemented with citrulline. Furthermore, in addition to measure the transcript and protein expression levels for the urea cycle enzymes, the enzyme activities of ASS and OTC should be determined and it may provide further evidence to the utilization of arginine precursors. Although the expression of ASS is an established biomarker to predict the tumor response towards ADI treatment, more recent studies further suggested that epigenetic status of ASS also showed an excellent correlation to the ASS mRNA and protein expression levels in some of the cancer types, such as HCC,

glioblastoma, lymphoma, mesothelioma and ovarian cancer (Delage et al., 2012; Nicholson et al., 2009; Syed et al., 2013; Szlosarek et al., 2006; L. Wu et al., 2013). These data may provide further support to clinical researchers dedicated to identify ASS negative patients for ADI treatment. Moreover, some recent studies with ovarian cancer suggested that methylation of ASS predicted poor clinical outcome with carboplatin-based adjuvant chemotherapy while negative ASS methylation status during diagnosis would become positive at relapse. This observation may allow the design of interval treatment plan through monitoring the epigenetic status of the ASS gene. The cells expressing ASS (negative ASS methylation) could be treated by platinum compound at the beginning and once it developed resistance with down-regulated ASS expression (positive ASS methylation), we can switch to the treatment by arginine depleting enzyme (Nicholson et al., 2009).

On the other hand, although introducing ASS as a biomarker for ADI therapy has led to some encouraging results in clinical trial, induction of ASS during the treatment with ADI resulted in the development of resistance and relapse in some of the melanoma patients (L. G. Feun et al., 2012; Shen et al., 2003). *In vitro* studies of ADI treatment with a panel of melanoma cell lines also confirm the induced ASS expression (Manca et al., 2011). The underlying mechanism leading to the induced ASS expression during ADI treatment was found related to the activation of Ras signaling pathway for which the negative transcription factor HIF-1α was down regulated while the positive transcription factor C-Myc was found up regulated. Both of these transcription factors bind to the ASS promoter E-box element but exerting opposing effect to the ASS transcription. In the absence of ADI, HIF-1α bound to the E-box element and silenced the expression of ASS

while addition of ADI to the culture down regulated HIF-1α during ADI treatment (Kuo et al., 2010; Tsai et al., 2009). At the same time, up regulation of c-Myc replaced HIF-1α and transactivate the ASS gene expression. Reversal of such resistance either through regulating the activity of c-Myc and HIF-1α or targeting the activated RAS/AKT/GSK-3β pathway using pan-PI3K inhibitors or AKT inhibitors has been proposed for combination therapy (Tsai et al., 2012).

In view of the limitation that the down regulation of ASS is required to sensitize the cancer cell for ADI treatment, the potential induction of ASS during the course of therapy, the generation of citrulline end-product by ADI and growth retardation in only one of the five cancer cell lines when treated by ADI in our study, we opt to further our study to investigate a more promising arginine depleting enzyme, BCA, for which the underlying mechanisms leading to the growth attenuation of the gastric and colorectal cancer cell lines would be evaluated by both cell cycle analysis and the involvement of programmed cell death.

To evaluate the effect of BCA on the cell cycle distribution of gastric and colorectal cell lines, the cancer cell lines were exposed to various concentrations of BCA for 72 h and the DNA content was revealed by propidium iodide (PI) staining followed by flow cytometric analysis. All gastric cancer cell lines were found to arrest in the S-phase. For the colorectal cancer cell lines tested, HCT-15 was arrested in G2/M phase while HCT116 exhibited dual-phase (S and G2/M) arrest. The data obtained in this study are consistent with the previous report that cancer cell lines having defective control in the restriction point in the G1 phase of cell cycle would become unable to arrest at G1/S transition during arginine depletion. The malignant cells keep cycling into the S phase

and prolonged sojourn in S-phase resulted in rapid demise of cancer cells (Scott et al., 2000; D. N. Wheatley et al., 2000). On the contrary, normal cells can withstand arginine depletion by arresting the cell cycle machinery at G1 phase through the down regulation of cdk4 (Lamb & Wheatley, 2000). Thus, the cells remain viable in arginine free medium for at least 3 weeks and thrive when arginine was replenished into the culture (Philip et al., 2003).

Similar observation of cell cycle arrest induced by human arginase has been reported in HCC and melanoma cell lines. For example, depletion of arginine in HCC cell lines lead to Hep3B arrested at G2/M phase while HepG2 and PLC/PRF/5 were arrested at S-phase (Lam et al., 2009). Strikingly, arrest in different phases of cell cycle has been reported when melanoma cell line, A375, was treated by human arginase and ADI. During the treatment with human arginase, S and G2/M phase arrest was observed in A375 cells whereas ADI only induced G2/M phase arrest. Whether this observable difference was due to the different catalytic end products generated by ADI and human arginase may require further elucidation (Lam et al., 2010). Interestingly, a recent report suggested that human arginase could be a potential treatment for T-ALL leukemia through inducing cell cycle arrest at G0/G1 phase and apoptosis. Although incoherence as it may seem that cancer cells should keep progressing into the S phase, but treatment with malignant T cells arrest in G0/G1 phase and induced apoptosis. In the same report, primary T cells also undergo G0/G1 phase arrest but not inducing apoptosis (Hernandez et al., 2010). These results further support the notion that malignant cells exhibit defective cycle control and proceed to apoptosis instead of entering quiescent even arrested at the G0/G1 phase.

Besides, the transition in cell cycle is controlled by a well conserved family of cyclin-dependent kinases (CDKs). The CDKs become active when they form complexes with different cyclins and mediate cell cycle progression. Thus, future experiment to understand the expression of these cell cycle effectors should not only further confirm our findings from flow cytometric analysis but also lead us to understand the mechanisms signaling the cells to arrest in a particular phase of cell cycle at molecular level.

More importantly, through the cell cycle distribution analysis, it was suggested that arginine deprivation could be exploited to synchronize or "staging" the cancer cell to cell cycle specific cytotoxic agents (D. N. Wheatley, 2004). For example, targeting the S phase arrest in HCC has been achieved through combining the antimetabolite, fluorouracil (5-FU). This antimetabolite exerts its action not only through inhibiting activity of thymidylate synthase and blocking the synthesis of thymidine but also incorporating these metabolites to disrupt DNA synthesis (Longley et al., 2003). In addition, cancer cells with dual phase arrest may considerably have more options for combination therapy using anti-mitotic alkaloid agents, vinblastine or colchicines (Lam et al., 2010; Denys N Wheatley, 2012).

When the gastric and colorectal cancer cell lines exposed to BCA and subjected to cell cycle distribution analysis, notably increases to the sub-G1 fraction has been seen in some of the cell lines which may indicate programmed cell death during the treatment with BCA. Although earlier study suggested that depletion of essential amino acid should slow down protein synthesis and producing similar effect to cycloheximide which should delay apoptosis but arginine depletion lead to rapid demise of cancer cells and thus such

hypothesis remains controversial at that time (Scott et al., 2000; D. N. Wheatley et al., 2000).

Recently, apoptotic cell death following treatment with arginine depleting enzyme has been reported (Delage et al., 2012; Gong et al., 2000; Kelly et al., 2011; Lam et al., 2010). To further evaluate if BCA could induce apoptotic cell death in the gastric and colorectal cancer cell lines, we collected the cells after incubation with BCA for 72 h and stained with annexin V-FITC and PI. Apoptotic cell death has been observed in all cell lines except AGS. HCT116 and BGC823 cells undergo apoptosis after treatment with 15 U/ml BCA for 72 h. For MKN45 and HCT-15 cells, treatment with BCA induced apoptotic cell death in time-dependent and dose-dependent manner. These data agree with the imaging study of HeLa cells when 24 h of arginine free culture did not induce considerable changes on the cellular morphology whereas more extensive morphological changes such as rounding up and disintegrating in culture could be observed after 48 h of incubation (D. N. Wheatley et al., 2000).

Since activation of executioner caspase-3 was considered as the hallmark of programmed cell death, the BCA-induced apoptosis was further evaluated by detecting the active caspase-3 in these cell lines. The activation of caspase-3 in HCT-15 was confirmed by detecting both zymogen and activated subunits of caspase-3 using anti-caspase-3 antibody. These data were found in accord with the dose-dependent apoptotic cell death as measured by annexin V-FITC and PI double staining. Similarly, detection of active caspase-3 using irreversible inhibitor, FITC-DEVE-FMK, also resulted in dose-dependent apoptosis inMKN45 while HCT116 and BGC823 were also found to undergo caspase-dependent cell death after 72 h treatment with BCA. Since the activation of

caspase-3 could be resulted from the cross-talk exist between the intrinsic and extrinsic pathways, we evaluated the changes in the mitochondria outer membrane permeability (MOMP) as it has been regarded as the marker for apoptotic cell death through intrinsic pathway (Elmore, 2007; Hernandez et al., 2010; Salido & Rosado, 2009). The MOMP of MKN45 and HCT-15 cells were measured by JC-1 dye for which it accumulates in mitochondria and forming aggregates in the absence BCA. After 72 h of 15U/ml BCA treatment, the increased MOMP was manifested as the increased the JC-1 monomer indicating the apoptotic cell death was possibly mediated through the intrinsic pathway. Since apoptosis via MOMP usually activated a cascade of events, it would be even more ascertain to conclude the apoptotic cell death via the intrinsic pathway if the activation of initiator caspase-9 instead of caspase-8 could be confirmed in the future (Elmore, 2007).

Moreover, combination therapy targeting different signaling pathways other than the intrinsic apoptotic may offer a more complete eradication of cancer cells. For example, combination of tumor necrosis factor-related apoptosis-inducing ligand (TRAIL) with ADI has been reported to potentiate the cytotoxicity of ADI to melanoma cells in culture. The rationale of choosing TRAIL for combination is based on the observation that ADI induced intrinsic apoptotic cell death and up regulation of death receptors DR4/5 during the treatment. Synergy has been observed through binding of TRAIL to the death receptor, leading to the formation of death-inducing signaling complex (DISC) which in turn activated initiator caspase-8 and mediated the apoptotic cell death via extrinsic pathway (You et al., 2010). In the earlier study, the synergistic effect was possibly due to simultaneous activation of both intrinsic and extrinsic apoptotic pathway by ADI and TRAIL, respectively. Moreover, more recent study published by the same research group

also suggested that the activated caspased-8 do not only initiate the apoptotic cell death via the extrinsic pathway but itself, together with the activated caspase-3, 6, 9 and 10, may also mediate the cleavage of autophagic protein, Beclin-1 and atg-5, and preventing the autophagic process while re-diverting the cell to apoptosis (You et al., 2013).

Besides, the results from annexin V-FITC and PI double staining did not reveal significant apoptotic cell death in AGS cells which may suggest cell death by other mechanisms such as autophagy. Autophagy is considered as a process to protect the cells under adverse conditions such as, during chemotherapy and nutrient starvation (Bhutia et al., 2010; Mizushima & Klionsky, 2007; O'Donovan et al., 2011). Autophagy is regulated by evolutionarily conserved ATG proteins and these proteins control the formational of phagophore which will finally enclose a portion of cytoplasm in a double-membrane structure called autophagosome. Lysosome will fuse with autophagosome and lead to the degradation of the enclosed materials by lysosomal enzymes (Sheen et al., 2011). The catabolic processes allow the regeneration of basic metabolites and thus allow the cells to sustain the unfavorable conditions. It has been reported that treatment with ADI does not induce apoptotic cell death in prostate cancer cell line during the 72 h of incubation and more strikingly, increased caspases activity could be detected after 6 days of treatment with prostate cancer cell line when autophagy could no longer provide arginine and undergo apoptosis (R. H. Kim et al., 2009; Savaraj et al., 2010). It would be very likely that if the BCA treatment could be extended from 3 to 6 days on AGS cell line; we may detect apoptosis at that time. However, extended incubation may introduce uncertainty to the nutrient contents of the medium which may also impose stress to the cells in addition to arginine depletion. Thus, cancer cells lacking apoptotic cell death after 3 days of

treatment with arginine depleting enzymes may be further evaluated by autophagy. This could be easily verified by harvesting the cells after treatment and detect the conversion of LC3-I to LC3-II using western blot (Mizushima et al., 2010). Furthermore, combination therapy with autophagic inhibitor such as chloroquine (CQ) has been shown to abrogate the pro-survival effects of autophagy and accelerating the cells to undergo apoptosis (Kelly et al., 2011; R. H. Kim et al., 2009; Syed et al., 2013). Chloroquine exerts its effects by inhibiting the acidification of lysosome and preventing the fusion and degradation of autophagosome (Maycotte et al., 2012).

With the promising *in vitro* data and the understanding to the mechanisms leading to the apoptotic cell death in gastric and colorectal cancer cell lines. We further our study to investigate pharmacological properties of pegylated BCA as well as *in vivo* anti-tumor efficacy on the gastric cancer xenograft model. Pegylation has been extensively used to extend the circulation half-life of therapeutic proteins. Nowadays, around 10 pegylated therapeutics have been approved by FDA and 9 of them are protein therapeutics. More importantly, there are many pegylated therapeutics in different phases of clinical trial and they are expected to come into market in the near future. Since the launch of the first pegylated enzyme for the treatment of severe combined immunodeficiency in 1990, Adagen®, FDA has been imposing stringent requirement to the characterization and consistence of the pegylated therapeutics. In our study, we dedicated to the formulation of monopegylated BCA with straight chain PEG of 20 kDa which make it easily characterized with minimum batch to batch variation as illustrated in Chapter 3. Since nude mice xenograft model will be used for *in vivo* efficacy, the pharmacological profile of pegylated BCA will be evaluated in normal BALB/c model. Result from signle-dose

pharmacokinetic study through injecting 250 Unit of pegylated BCA per mice suggested that the circulation half-life is extended by 12.7-fold, from 6.9 h to 87.8 h. Compared to arginine depleting enzyme entered into clinical trial, the circulation half-life of recombinant human arginase was extended from 10-15 min to 3 days after modification with random conjugations of 1-6 mPEG-SPA of MW 5000 Da, hrArg-peg$_{5,000mw}$. The result is comparable to our monopeyglated BCA (Cheng et al., 2007; Cheng et al., 2005; Tsui et al., 2009). However, random pegylation of *Mycoplasma hominis* ADI using 20,000 Da PEG extend the circulation half-life from 5 h to 7 days (Pasut et al., 2008).

The prolonged circulation half-life of BCA was manifested as the sustained low levels of arginine in the systemic circulation. Through pegylation of BCA, at least 5 days of undetectable level of arginine could be achieved while almost complete restoration of arginine has been observed in 24 h with native BCA. Pegylated BCA with comparatively longer circulation half-life than hrArg-peg$_{5,000mw}$ is reflected as a more extended period of arginine deprivation in the systemic circulation (Cheng et al., 2007). These results suggested that pegylation of BCA could maintain a sustained low level of arginine in the circulation and also provided insight to set up a twice per week regime for efficacy study during which undetectable level of arginine could probably be maintained in between injections. In addition to the results from single dose pharmacokinetics and pharmacodynamics study, monitoring of blood arginine levels and the BCA activity during the course of twice per week regime should be included so as to provide further support to the observed efficacy in the future.

Future study with PEG molecule in different chain lengths, shapes and conjugation chemistries may further extend the circulation half-life of BCA with retained enzymatic

activity and hopefully prolong the arginine depletion period to lower the injection frequency from twice per week to weekly injection.

The *in vivo* efficacy study of pegylated BCA in MKN45 gastric cancer xenograft model reveals significant inhibition to the tumor growth. Since MKN45 has been induced to arrest in S phase during BCA treatment, we further explored if cell cycle dependent drug, 5-FU, could confer synergistic effects when combined with pegylated BCA. The chemotherapeutic, 5-FU, exhibited similar *in vivo* efficacy to the pegylated BCA when injected singly. Encouragingly, enhanced antitumor effect could be observed when pegylated BCA was used in combination with 5-FU. These results are in coherence with the final tumor weight measured at the sacrification. When compared to the control, treatment with either pegylated BCA or 5-FU could achieve 50-60% of tumor inhibition while combination therapy could inhibit up to 80% of tumor growth. Similarly, treatment of Hep3b tumor xenograft through combination of hrArg-peg$_{5,000mw}$ and 5-FU also resulted in synergistic effect. The hrArg-peg$_{5,000mw}$ *per se* also inhibited the tumor growth. Interestingly, when the same dose (10 mg/kg) of 5-FU was injected to the nude mice bearing Hep3b tumor xenografts, subclinical tumor response has been reported but comparable anti-tumor efficacy by 5-FU and BCA has been observed with the MKN45 tumor xenografts (Cheng et al., 2007). This may reflect the tumor specific response and higher dose of 5-FU may be required to produce the similar response in Hep3B. Besides, further study with HCT-15 tumor xenograft in nude mice model should further consolidate the anti-tumor effect of BCA to colorectal cancer. Considerations on the combination therapy should be further explored starting from the *in vitro* study for which different therapeutics could be use together with BCA to quantitatively determine the

synergistic effect through calculating the combination index. Selected drugs demonstrating synergistic effects with BCA from cell culture study should be further evaluated in the *in vivo* study to which similar approach could be adopted with reduced data points. Thus, a rational approach for combination therapy and drug synergism study could be quantitatively expressed.

The easiest way to monitor the treatment associate toxicity could be done by monitoring the mice body weight throughout the study period. All treatment groups give less than 10% variation relative to the Day 0 control may suggest minimal treatment associated toxicity while the overall health conditions could be further evaluated by measuring such as blood glucose level, liver function and kidney function during the treatment period. These data could be valuable to the establishment of the safety profile of BCA in pre-clinical setting. A recent phase I clinical study of pegylated human arginase in advanced HCC patients also illustrated a low toxicity profile (Yau et al., 2012). Thus, further support the notion that systemic arginine depletion using arginase is a relatively safe approach for cancer treatment.

Throughout this study, a scientifically sound approach to inhibit tumor growth has been further confirmed with more understanding to the mechanisms lead to the growth attenuation including cell cycle arrest and programmed cell death from the *in vitro* study. A proof of concept study through rational design to facilitate cloning, purification, pegylation and characterization of monopegylated BCA has been produced in sufficient quantity for *in vivo* pharmacological and efficacy study. The *in vivo* data not only demonstrated the growth inhibiting effects of pegylateted BCA on the gastric cancer xenograft model but more encouraging results from 5-FU combination therapy. These

results warrant arginase for further research especially to understand the impact of arginine depletion to different signaling pathways leading to promote or against cell death through which combinational therapy with sound scientific knowledge could be introduced. With the development of therapeutics targeting arginine depletion, it is hoped that cancer patients suffering from these incurable disease could be brought under control in a foreseeable future.

References

Alconcel, S. N. S., Baas, A. S., & Maynard, H. D. (2011). FDA-approved poly(ethylene glycol)-protein conjugate drugs. *Polymer Chemistry, 2*, 1442-1448.

Andersen, J. T., Dalhus, B., Cameron, J., Daba, M. B., Plumridge, A., Evans, L., Brennan, S. O., Gunnarsen, K. S., Bjoras, M., Sleep, D., & Sandlie, I. (2012). Structure-based mutagenesis reveals the albumin-binding site of the neonatal Fc receptor. *Nat Commun, 3*, 610.

Andersen, J. T., Pehrson, R., Tolmachev, V., Daba, M. B., Abrahmsen, L., & Ekblad, C. (2011). Extending half-life by indirect targeting of the neonatal Fc receptor (FcRn) using a minimal albumin binding domain. *J Biol Chem, 286*, 5234-5241.

Andersen, J. T., & Sandlie, I. (2009). The versatile MHC class I-related FcRn protects IgG and albumin from degradation: implications for development of new diagnostics and therapeutics. *Drug Metab Pharmacokinet, 24*, 318-332.

Antonelli, G., & Dianzani, F. (1999). Development of antibodies to interferon beta in patients: technical and biological aspects. *Eur Cytokine Netw, 10*, 413-422.

Asselin, B. L., Whitin, J. C., Coppola, D. J., Rupp, I. P., Sallan, S. E., & Cohen, H. J. (1993). Comparative pharmacokinetic studies of three asparaginase preparations. *J Clin Oncol, 11*, 1780-1786.

Avramis, V. I., & Tiwari, P. N. (2006). Asparaginase (native ASNase or pegylated ASNase) in the treatment of acute lymphoblastic leukemia. *Int J Nanomedicine, 1*, 241-254.

Bach, S. J., & Lasnitzki, I. (1947). Some aspects of the role of arginine and arginase in mouse carcinoma 63. *Enzymologia, 12*, 198-205.

Bach, S. J., & Maw, G. A. (1953). Creatine synthesis by tumor-bearing rats. *Biochim Biophys Acta, 11*, 69-78.

Bach, S. J., & Swaine, D. (1965). The Effect of Arginase on the Retardation of Tumour Growth. *Br J Cancer, 19*, 379-386.

Bailon, P., Palleroni, A., Schaffer, C. A., Spence, C. L., Fung, W. J., Porter, J. E., Ehrlich, G. K., Pan, W., Xu, Z. X., Modi, M. W., Farid, A., Berthold, W., & Graves, M. (2001). Rational design of a potent, long-lasting form of interferon: a 40 kDa branched polyethylene glycol-conjugated interferon alpha-2a for the treatment of hepatitis C. *Bioconjug Chem, 12*, 195-202.

Bang, Y. J., Van Cutsem, E., Feyereislova, A., Chung, H. C., Shen, L., Sawaki, A., Lordick, F., Ohtsu, A., Omuro, Y., Satoh, T., Aprile, G., Kulikov, E., Hill, J., Lehle, M., Ruschoff, J., & Kang, Y. K. (2010). Trastuzumab in combination with chemotherapy versus chemotherapy alone for treatment of HER2-positive advanced gastric or gastro-oesophageal junction cancer (ToGA): a phase 3, open-label, randomised controlled trial. *Lancet, 376*, 687-697.

Bardelli, A., & Janne, P. A. (2012). The road to resistance: EGFR mutation and cetuximab. *Nat Med, 18*, 199-200.

Bardelli, A., & Siena, S. (2010). Molecular mechanisms of resistance to cetuximab and panitumumab in colorectal cancer. *J Clin Oncol, 28*, 1254-1261.

Bendele, A., Seely, J., Richey, C., Sennello, G., & Shopp, G. (1998). Short communication: renal tubular vacuolation in animals treated with polyethylene-glycol-conjugated proteins. *Toxicol Sci, 42*, 152-157.

Bertuccio, P., Chatenoud, L., Levi, F., Praud, D., Ferlay, J., Negri, E., Malvezzi, M., & La Vecchia, C. (2009). Recent patterns in gastric cancer: a global overview. *Int J Cancer, 125*, 666-673.

Bewley, M. C., Jeffrey, P. D., Patchett, M. L., Kanyo, Z. F., & Baker, E. N. (1999). Crystal structures of Bacillus caldovelox arginase in complex with substrate and inhibitors reveal new insights into activation, inhibition and catalysis in the arginase superfamily. *Structure, 7*, 435-448.

Bewley, M. C., Lott, J. S., Baker, E. N., & Patchett, M. L. (1996). The cloning, expression and crystallisation of a thermostable arginase. *FEBS Lett, 386*, 215-218.

Bhutia, S. K., Dash, R., Das, S. K., Azab, B., Su, Z. Z., Lee, S. G., Grant, S., Yacoub, A., Dent, P., Curiel, D. T., Sarkar, D., & Fisher, P. B. (2010). Mechanism of autophagy to apoptosis switch triggered in prostate cancer cells by antitumor cytokine melanoma differentiation-associated gene 7/interleukin-24. *Cancer Res, 70*, 3667-3676.

Bowles, T. L., Kim, R., Galante, J., Parsons, C. M., Virudachalam, S., Kung, H. J., & Bold, R. J. (2008). Pancreatic cancer cell lines deficient in argininosuccinate synthetase are sensitive to arginine deprivation by arginine deiminase. *Int J Cancer, 123*, 1950-1955.

Caliceti, P., & Veronese, F. M. (2003). Pharmacokinetic and biodistribution properties of poly(ethylene glycol)-protein conjugates. *Adv Drug Deliv Rev, 55*, 1261-1277.

Caserman, S., Kusterle, M., Kunstelj, M., Milunovic, T., Schiefermeier, M., Jevsevar, S., & Gaberc Porekar, V. (2009). Correlations between in vitro potency of polyethylene

glycol-protein conjugates and their chromatographic behavior. *Analytical Biochemistry, 389*, 27-31.

Center, M. M., Jemal, A., & Ward, E. (2009). International trends in colorectal cancer incidence rates. *Cancer Epidemiol Biomarkers Prev, 18*, 1688-1694.

Chapman, A. P. (2002). PEGylated antibodies and antibody fragments for improved therapy: a review. *Adv Drug Deliv Rev, 54*, 531-545.

Cheng, P. N., Lam, T. L., Lam, W. M., Tsui, S. M., Cheng, A. W., Lo, W. H., & Leung, Y. C. (2007). Pegylated recombinant human arginase (rhArg-peg5,000mw) inhibits the *in vitro* and *in vivo* proliferation of human hepatocellular carcinoma through arginine depletion. *Cancer Res, 67*, 309-317.

Cheng, P. N., Leung, Y. C., Lo, W. H., Tsui, S. M., & Lam, K. C. (2005). Remission of hepatocellular carcinoma with arginine depletion induced by systemic release of endogenous hepatic arginase due to transhepatic arterial embolisation, augmented by high-dose insulin: arginase as a potential drug candidate for hepatocellular carcinoma. *Cancer Lett, 224*, 67-80.

Constantinou, A., Chen, C., & Deonarain, M. P. (2010). Modulating the pharmacokinetics of therapeutic antibodies. *Biotechnol Lett, 32*, 609-622.

Cunningham, D., Humblet, Y., Siena, S., Khayat, D., Bleiberg, H., Santoro, A., Bets, D., Mueser, M., Harstrick, A., Verslype, C., Chau, I., & Van Cutsem, E. (2004). Cetuximab monotherapy and cetuximab plus irinotecan in irinotecan-refractory metastatic colorectal cancer. *N Engl J Med, 351*, 337-345.

Dardé, V., Barderas, M., & Vivanco, F. (2007). Depletion of High-Abundance Proteins in Plasma by Immunoaffinity Substraction for Two-Dimensional Difference Gel Electrophoresis Analysis. In F. Vivanco (Ed.), *Cardiovascular Proteomics* (Vol. 357, pp. 351-364): Humana Press.

Davis, P. D., & Crapps, E. C. (2011). Selective and specific preparation of discrete PEG compounds: Google Patents.

De Roock, W., De Vriendt, V., Normanno, N., Ciardiello, F., & Tejpar, S. (2011). KRAS, BRAF, PIK3CA, and PTEN mutations: implications for targeted therapies in metastatic colorectal cancer. *Lancet Oncol, 12*, 594-603.

Delage, B., Luong, P., Maharaj, L., O'Riain, C., Syed, N., Crook, T., Hatzimichael, E., Papoudou-Bai, A., Mitchell, T. J., Whittaker, S. J., Cerio, R., Gribben, J., Lemoine, N., Bomalaski, J., Li, C. F., Joel, S., Fitzgibbon, J., Chen, L. T., & Szlosarek, P. W. (2012). Promoter methylation of argininosuccinate synthetase-1 sensitises lymphomas to arginine

deiminase treatment, autophagy and caspase-dependent apoptosis. *Cell Death Dis, 3*, e342.

Dillon, B. J., Prieto, V. G., Curley, S. A., Ensor, C. M., Holtsberg, F. W., Bomalaski, J. S., & Clark, M. A. (2004). Incidence and distribution of argininosuccinate synthetase deficiency in human cancers: a method for identifying cancers sensitive to arginine deprivation. *Cancer, 100*, 826-833.

Dinndorf, P. A., Gootenberg, J., Cohen, M. H., Keegan, P., & Pazdur, R. (2007). FDA drug approval summary: pegaspargase (oncaspar) for the first-line treatment of children with acute lymphoblastic leukemia (ALL). *Oncologist, 12*, 991-998.

Durden, D. L., & Distasio, J. A. (1980). Comparison of the immunosuppressive effects of asparaginases from Escherichia coli and Vibrio succinogenes. *Cancer Res, 40*, 1125-1129.

Elmore, S. (2007). Apoptosis: a review of programmed cell death. *Toxicol Pathol, 35*, 495-516.

Ensor, C. M., Holtsberg, F. W., Bomalaski, J. S., & Clark, M. A. (2002). Pegylated arginine deiminase (ADI-SS PEG20,000 mw) inhibits human melanomas and hepatocellular carcinomas *in vitro* and *in vivo*. *Cancer Res, 62*, 5443-5450.

Euhus, D. M., Hudd, C., LaRegina, M. C., & Johnson, F. E. (1986). Tumor measurement in the nude mouse. *J Surg Oncol, 31*, 229-234.

Feun, L., & Savaraj, N. (2006). Pegylated arginine deiminase: a novel anticancer enzyme agent. *Expert Opin Investig Drugs, 15*, 815-822.

Feun, L., You, M., Wu, C. J., Kuo, M. T., Wangpaichitr, M., Spector, S., & Savaraj, N. (2008). Arginine deprivation as a targeted therapy for cancer. *Curr Pharm Des, 14*, 1049-1057.

Feun, L. G., Marini, A., Walker, G., Elgart, G., Moffat, F., Rodgers, S. E., Wu, C. J., You, M., Wangpaichitr, M., Kuo, M. T., Sisson, W., Jungbluth, A. A., Bomalaski, J., & Savaraj, N. (2012). Negative argininosuccinate synthetase expression in melanoma tumours may predict clinical benefit from arginine-depleting therapy with pegylated arginine deiminase. *Br J Cancer*.

Fishburn, C. S. (2008). The pharmacology of PEGylation: balancing PD with PK to generate novel therapeutics. *J Pharm Sci, 97*, 4167-4183.

Forsgren, A., & Sjöquist, J. (1966). "Protein A" from S. Aureus: I. Pseudo-Immune Reaction with Human γ-Globulin. *The Journal of Immunology, 97*, 822-827.

Foser, S., Weyer, K., Huber, W., & Certa, U. (2003). Improved biological and transcriptional activity of monopegylated interferon-alpha-2a isomers. *Pharmacogenomics J, 3*, 312-319.

Frejd, F. Y. (2012). Half-Life Extension by Binding to Albumin through an Albumin Binding Domain *Therapeutic Proteins* (pp. 269-283): Wiley-VCH Verlag GmbH & Co. KGaA.

Frokjaer, S., & Otzen, D. E. (2005). Protein drug stability: a formulation challenge. *Nat Rev Drug Discov, 4*, 298-306.

Ganson, N. J., Kelly, S. J., Scarlett, E., Sundy, J. S., & Hershfield, M. S. (2006). Control of hyperuricemia in subjects with refractory gout, and induction of antibody against poly(ethylene glycol) (PEG), in a phase I trial of subcutaneous PEGylated urate oxidase. *Arthritis Res Ther, 8*, R12.

Gill, P., & Pan, J. (1970). Inhibition of cell division in L5178Y cells by arginine-degrading mycoplasmas: the role of arginine deiminase. *Can J Microbiol, 16*, 415-419.

Gilroy, E. (1930). The influence of arginine upon the growth rate of a transplantable tumour in the mouse. *Biochem J, 24*, 589-595.

Global Cancer Facts & Figures 2nd Edition. (2011). *American Cancer Society.* .

Gong, H., Zolzer, F., von Recklinghausen, G., Havers, W., & Schweigerer, L. (2000). Arginine deiminase inhibits proliferation of human leukemia cells more potently than asparaginase by inducing cell cycle arrest and apoptosis. *Leukemia, 14*, 826-829.

Gong, H., Zolzer, F., von Recklinghausen, G., Rossler, J., Breit, S., Havers, W., Fotsis, T., & Schweigerer, L. (1999). Arginine deiminase inhibits cell proliferation by arresting cell cycle and inducing apoptosis. *Biochem Biophys Res Commun, 261*, 10-14.

Grace, M., Youngster, S., Gitlin, G., Sydor, W., Xie, L., Westreich, L., Jacobs, S., Brassard, D., Bausch, J., & Bordens, R. (2001). Structural and biologic characterization of pegylated recombinant IFN-alpha2b. *J Interferon Cytokine Res, 21*, 1103-1115.

Greeberg, D., & Sassenrath, E. N. (1953). Lack of effect of high potency arginase on tumor growth. *Cancer Res, 13*, 709-715.

Gülich, S., Linhult, M., Nygren, P.-Å., Uhlén, M., & Hober, S. (2000). Stability towards alkaline conditions can be engineered into a protein ligand. *Journal of Biotechnology, 80*, 169-178.

Hanahan, D., & Weinberg, R. A. (2011). Hallmarks of cancer: the next generation. *Cell, 144*, 646-674.

Harris, J. M., & Chess, R. B. (2003). Effect of pegylation on pharmaceuticals. *Nat Rev Drug Discov, 2*, 214-221.

Hermanson, G. T. (2013). Chapter 6 - Heterobifunctional Crosslinkers. In G. T. Hermanson (Ed.), *Bioconjugate Techniques (Third edition)* (pp. 299-339). Boston: Academic Press.

Hernandez, C. P., Morrow, K., Lopez-Barcons, L. A., Zabaleta, J., Sierra, R., Velasco, C., Cole, J., & Rodriguez, P. C. (2010). Pegylated arginase I: a potential therapeutic approach in T-ALL. *Blood, 115*, 5214-5221.

Holley, R. W. (1967). Evidence that a rat liver â€œinhibitorâ€ of the synthesis of DNA in cultured mammalian cells is arginase. *Biochimica et Biophysica Acta (BBA) - Nucleic Acids and Protein Synthesis, 145*, 525-527.

Holtsberg, F. W., Ensor, C. M., Steiner, M. R., Bomalaski, J. S., & Clark, M. A. (2002). Poly(ethylene glycol) (PEG) conjugated arginine deiminase: effects of PEG formulations on its pharmacological properties. *J Control Release, 80*, 259-271.

Hopp, J., Hornig, N., Zettlitz, K. A., Schwarz, A., Fuss, N., Muller, D., & Kontermann, R. E. (2010). The effects of affinity and valency of an albumin-binding domain (ABD) on the half-life of a single-chain diabody-ABD fusion protein. *Protein Eng Des Sel, 23*, 827-834.

Hsueh, E. C., Knebel, S. M., Lo, W. H., Leung, Y. C., Cheng, P. N., & Hsueh, C. T. (2012). Deprivation of arginine by recombinant human arginase in prostate cancer cells. *J Hematol Oncol, 5*, 17.

Hubbell, J. A. (2010). Drug development: Longer-lived proteins. *Nature, 467*, 1051-1052.

Irons, W. G., & Boyd, E. F. (1952). Arginase as an anti-carcinogenic agent in mice and human beings. *Ariz Med, 9*, 39-44.

Jackman, J., & O'Connor, P. M. (2001). Methods for synchronizing cells at specific stages of the cell cycle. *Curr Protoc Cell Biol, Chapter 8*, Unit 8 3.

Jemal, A., Bray, F., Center, M. M., Ferlay, J., Ward, E., & Forman, D. (2011). Global cancer statistics. *CA Cancer J Clin, 61*, 69-90.

Jevsevar, S., Kunstelj, M., & Porekar, V. G. (2010). PEGylation of therapeutic proteins. *Biotechnol J, 5*, 113-128.

Johansson, M. U., Frick, I. M., Nilsson, H., Kraulis, P. J., Hober, S., Jonasson, P., Linhult, M., Nygren, P. A., Uhlen, M., Bjorck, L., Drakenberg, T., Forsen, S., & Wikstrom, M.

(2002). Structure, specificity, and mode of interaction for bacterial albumin-binding modules. *J Biol Chem, 277*, 8114-8120.

Jonsson, A., Dogan, J., Herne, N., Abrahmsen, L., & Nygren, P. A. (2008). Engineering of a femtomolar affinity binding protein to human serum albumin. *Protein Eng Des Sel, 21*, 515-527.

Kelly, M. P., Jungbluth, A. A., Wu, B. W., Bomalaski, J., Old, L. J., & Ritter, G. (2011). Arginine deiminase PEG20 inhibits growth of small cell lung cancers lacking expression of argininosuccinate synthetase. *Br J Cancer, 106*, 324-332.

Kim, J. E., Kim, S. Y., Lee, K. W., & Lee, H. J. (2009). Arginine deiminase originating from Lactococcus lactis ssp. lactis American Type Culture Collection (ATCC) 7962 induces G1-phase cell-cycle arrest and apoptosis in SNU-1 stomach adenocarcinoma cells. *Br J Nutr, 102*, 1469-1476.

Kim, R. H., Coates, J. M., Bowles, T. L., McNerney, G. P., Sutcliffe, J., Jung, J. U., Gandour-Edwards, R., Chuang, F. Y., Bold, R. J., & Kung, H. J. (2009). Arginine deiminase as a novel therapy for prostate cancer induces autophagy and caspase-independent apoptosis. *Cancer Res, 69*, 700-708.

Knop, K., Hoogenboom, R., Fischer, D., & Schubert, U. S. (2010). Poly(ethylene glycol) in Drug Delivery: Pros and Cons as Well as Potential Alternatives. *Angewandte Chemie International Edition, 49*, 6288-6308.

Kontermann, R. E. (2011). Strategies for extended serum half-life of protein therapeutics. *Curr Opin Biotechnol, 22*, 868-876.

Kontos, S., & Hubbell, J. A. (2012). Drug development: longer-lived proteins. *Chem Soc Rev, 41*, 2686-2695.

Kopchick, J. J., Parkinson, C., Stevens, E. C., & Trainer, P. J. (2002). Growth hormone receptor antagonists: discovery, development, and use in patients with acromegaly. *Endocr Rev, 23*, 623-646.

Kraulis, P. J., Jonasson, P., Nygren, P. A., Uhlen, M., Jendeberg, L., Nilsson, B., & Kordel, J. (1996). The serum albumin-binding domain of streptococcal protein G is a three-helical bundle: a heteronuclear NMR study. *FEBS Lett, 378*, 190-194.

Kronvall, G., Simmons, A., Myhre, E. B., & Jonsson, S. (1979). Specific absorption of human serum albumin, immunoglobulin A, and immunoglobulin G with selected strains of group A and G streptococci. *Infect Immun, 25*, 1-10.

Kuo, M. T., Savaraj, N., & Feun, L. G. (2010). Targeted cellular metabolism for cancer chemotherapy with recombinant arginine-degrading enzymes. *Oncotarget, 1*, 246-251.

Kuusela, P. (1978). Fibronectin binds to Staphylococcus aureus. *Nature, 276*, 718-720.

Lam, T. L., Wong, G. K., Chong, H. C., Cheng, P. N., Choi, S. C., Chow, T. L., Kwok, S. Y., Poon, R. T., Wheatley, D. N., Lo, W. H., & Leung, Y. C. (2009). Recombinant human arginase inhibits proliferation of human hepatocellular carcinoma by inducing cell cycle arrest. *Cancer Lett, 277*, 91-100.

Lam, T. L., Wong, G. K., Chow, H. Y., Chong, H. C., Chow, T. L., Kwok, S. Y., Cheng, P. N., Wheatley, D. N., Lo, W. H., & Leung, Y. C. (2010). Recombinant human arginase inhibits the *in vitro* and *in vivo* proliferation of human melanoma by inducing cell cycle arrest and apoptosis. *Pigment Cell Melanoma Res, 24*, 366-376.

Lamb, J., & Wheatley, D. N. (2000). Single amino acid (arginine) deprivation induces G1 arrest associated with inhibition of cdk4 expression in cultured human diploid fibroblasts. *Exp Cell Res, 255*, 238-249.

Lavulo, L. T., Sossong, T. M., Jr., Brigham-Burke, M. R., Doyle, M. L., Cox, J. D., Christianson, D. W., & Ash, D. E. (2001). Subunit-subunit interactions in trimeric arginase. Generation of active monomers by mutation of a single amino acid. *J Biol Chem, 276*, 14242-14248.

Lejon, S., Frick, I. M., Bjorck, L., Wikstrom, M., & Svensson, S. (2004). Crystal structure and biological implications of a bacterial albumin binding module in complex with human serum albumin. *J Biol Chem, 279*, 42924-42928.

Linhult, M., Binz, H. K., Uhlén, M., & Hober, S. (2002). Mutational analysis of the interaction between albumin-binding domain from streptococcal protein G and human serum albumin. *Protein Science, 11*, 206-213.

Longley, D. B., Harkin, D. P., & Johnston, P. G. (2003). 5-fluorouracil: mechanisms of action and clinical strategies. *Nat Rev Cancer, 3*, 330-338.

Lottenberg, R., Broder, C. C., & Boyle, M. D. (1987). Identification of a specific receptor for plasmin on a group A streptococcus. *Infect Immun, 55*, 1914-1918.

Maeda, H., Wu, J., Sawa, T., Matsumura, Y., & Hori, K. (2000). Tumor vascular permeability and the EPR effect in macromolecular therapeutics: a review. *J Control Release, 65*, 271-284.

Magalhaes, P. O., Lopes, A. M., Mazzola, P. G., Rangel-Yagui, C., Penna, T. C., & Pessoa, A., Jr. (2007). Methods of endotoxin removal from biological preparations: a review. *J Pharm Pharm Sci, 10*, 388-404.

Makrides, S. C., Nygren, P. A., Andrews, B., Ford, P. J., Evans, K. S., Hayman, E. G., Adari, H., Uhlen, M., & Toth, C. A. (1996). Extended *in vivo* half-life of human soluble

complement receptor type 1 fused to a serum albumin-binding receptor. *J Pharmacol Exp Ther, 277*, 534-542.

Manca, A., Sini, M. C., Izzo, F., Ascierto, P. A., Tatangelo, F., Botti, G., Gentilcore, G., Capone, M., Mozzillo, N., Rozzo, C., Cossu, A., Tanda, F., & Palmieri, G. (2011). Induction of arginosuccinate synthetase (ASS) expression affects the antiproliferative activity of arginine deiminase (ADI) in melanoma cells. *Oncol Rep, 25*, 1495-1502.

Martin, D., & Lenardo, M. (2001). Morphological, Biochemical, and Flow Cytometric Assays of Apoptosis *Current Protocols in Molecular Biology*: John Wiley & Sons, Inc.

Maxfield, J., & Shepherd, I. W. (1975). Conformation of poly(ethylene oxide) in the solid state, melt and solution measured by Raman scattering. *Polymer, 16*, 505-509.

Maycotte, P., Aryal, S., Cummings, C. T., Thorburn, J., Morgan, M. J., & Thorburn, A. (2012). Chloroquine sensitizes breast cancer cells to chemotherapy independent of autophagy. *Autophagy, 8*, 200-212.

Mero, A., Spolaore, B., Veronese, F. M., & Fontana, A. (2009). Transglutaminase-mediated PEGylation of proteins: direct identification of the sites of protein modification by mass spectrometry using a novel monodisperse PEG. *Bioconjug Chem, 20*, 384-389.

Miyazaki, K., Takaku, H., Umeda, M., Fujita, T., Huang, W. D., Kimura, T., Yamashita, J., & Horio, T. (1990). Potent growth inhibition of human tumor cells in culture by arginine deiminase purified from a culture medium of a Mycoplasma-infected cell line. *Cancer Res, 50*, 4522-4527.

Mizushima, N., & Klionsky, D. J. (2007). Protein turnover via autophagy: implications for metabolism. *Annu Rev Nutr, 27*, 19-40.

Mizushima, N., Yoshimori, T., & Levine, B. (2010). Methods in mammalian autophagy research. *Cell, 140*, 313-326.

Molineux, G. (2004). The design and development of pegfilgrastim (PEG-rmetHuG-CSF, Neulasta). *Curr Pharm Des, 10*, 1235-1244.

Morar, A. S., Schrimsher, J. L., & Chavez, M. D. (2006). PEGylation of Proteins: A Structural Approach. *BioPharm International 19*.

Muller, A. F., Kopchick, J. J., Flyvbjerg, A., & van der Lely, A. J. (2004). Clinical review 166: Growth hormone receptor antagonists. *J Clin Endocrinol Metab, 89*, 1503-1511.

Nelson, D. R., Benhamou, Y., Chuang, W. L., Lawitz, E. J., Rodriguez-Torres, M., Flisiak, R., Rasenack, J. W., Kryczka, W., Lee, C. M., Bain, V. G., Pianko, S., Patel, K.,

Cronin, P. W., Pulkstenis, E., Subramanian, G. M., McHutchison, J. G., & Team, A.-S. (2010). Albinterferon Alfa-2b was not inferior to pegylated interferon-alpha in a randomized trial of patients with chronic hepatitis C virus genotype 2 or 3. *Gastroenterology, 139*, 1267-1276.

Nicholson, L. J., Smith, P. R., Hiller, L., Szlosarek, P. W., Kimberley, C., Sehouli, J., Koensgen, D., Mustea, A., Schmid, P., & Crook, T. (2009). Epigenetic silencing of argininosuccinate synthetase confers resistance to platinum-induced cell death but collateral sensitivity to arginine auxotrophy in ovarian cancer. *Int J Cancer, 125*, 1454-1463.

Nygren, P. A., Eliasson, M., Abrahmsen, L., Uhlen, M., & Palmcrantz, E. (1988). Analysis and use of the serum albumin binding domains of streptococcal protein G. *J Mol Recognit, 1*, 69-74.

Nygren, P. A., Flodby, P., Andersson, R., Wigzell, H., & Uhlén, M. (1991). *In vivo* stabilization of a human recombinant CD4 derivative by fusion to a serum-albumin-binding receptor. *Vaccines, 91*, 363-368.

Nygren, P. A., Ljungquist, C., Tromborg, H., Nustad, K., & Uhlen, M. (1990). Species-dependent binding of serum albumins to the streptococcal receptor protein G. *Eur J Biochem, 193*, 143-148.

O'Donovan, T. R., O'Sullivan, G. C., & McKenna, S. L. (2011). Induction of autophagy by drug-resistant esophageal cancer cells promotes their survival and recovery following treatment with chemotherapeutics. *Autophagy, 7*, 509-524.

Olsson, A., Eliasson, M., Guss, B., Nilsson, B., Hellman, U., Lindberg, M., & Uhlen, M. (1987). Structure and evolution of the repetitive gene encoding streptococcal protein G. *Eur J Biochem, 168*, 319-324.

Orlova, A., Jonsson, A., Rosik, D., Lundqvist, H., Lindborg, M., Abrahmsen, L., Ekblad, C., Frejd, F. Y., & Tolmachev, V. (2013). Site-specific radiometal labeling and improved biodistribution using ABY-027, a novel HER2-targeting affibody molecule-albumin-binding domain fusion protein. *J Nucl Med, 54*, 961-968.

Ott, P. A., Carvajal, R. D., Pandit-Taskar, N., Jungbluth, A. A., Hoffman, E. W., Wu, B. W., Bomalaski, J. S., Venhaus, R., Pan, L., Old, L. J., Pavlick, A. C., & Wolchok, J. D. (2012). Phase I/II study of pegylated arginine deiminase (ADI-PEG 20) in patients with advanced melanoma. *Invest New Drugs*.

Park, I. S., Kang, S. W., Shin, Y. J., Chae, K. Y., Park, M. O., Kim, M. Y., Wheatley, D. N., & Min, B. H. (2003). Arginine deiminase: a potential inhibitor of angiogenesis and tumour growth. *Br J Cancer, 89*, 907-914.

Pasut, G., Sergi, M., & Veronese, F. M. (2008). Anti-cancer PEG-enzymes: 30 years old, but still a current approach. *Adv Drug Deliv Rev, 60*, 69-78.

Patchett, M. L., Daniel, R. M., & Morgan, H. W. (1991). Characterisation of arginase from the extreme thermophile 'Bacillus caldovelox'. *Biochim Biophys Acta, 1077*, 291-298.

Peters, T., Jr. (1985). Serum albumin. *Adv Protein Chem, 37*, 161-245.

Petsch, D., & Anspach, F. B. (2000). Endotoxin removal from protein solutions. *J Biotechnol, 76*, 97-119.

Pfister, D., & Morbidelli, M. (2014). Process for protein PEGylation. *J Control Release, 180*, 134-149.

Philip, R., Campbell, E., & Wheatley, D. N. (2003). Arginine deprivation, growth inhibition and tumour cell death: 2. Enzymatic degradation of arginine in normal and malignant cell cultures. *Br J Cancer, 88*, 613-623.

Pieters, R., Hunger, S. P., Boos, J., Rizzari, C., Silverman, L., Baruchel, A., Goekbuget, N., Schrappe, M., & Pui, C. H. (2011). L-Asparaginase Treatment in Acute Lymphoblastic Leukemia. *Cancer, 117*, 238-249.

Pisal, D. S., Kosloski, M. P., & Balu-Iyer, S. V. (2010). Delivery of therapeutic proteins. *J Pharm Sci, 99*, 2557-2575.

Povoski, S. P., Davis, P. D., Colcher, D., & Martin, E. W., Jr. (2013). Single molecular weight discrete PEG compounds: emerging roles in molecular diagnostics, imaging and therapeutics. *Expert Rev Mol Diagn, 13*, 315-319.

Quanta Biodesign Ltd.). from http://www.quantabiodesign.com/

Roberts, M. J., Bentley, M. D., & Harris, J. M. (2002). Chemistry for peptide and protein PEGylation. *Adv Drug Deliv Rev, 54*, 459-476.

Robinson, L. B., & Wichelhausen, R. H. (1956). Contamination of human cell cultures by pleuropneumonialike organisms. *Science, 124*, 1147-1148.

Ross, C., Clemmesen, K. M., Svenson, M., Sorensen, P. S., Koch-Henriksen, N., Skovgaard, G. L., & Bendtzen, K. (2000). Immunogenicity of interferon-beta in multiple sclerosis patients: influence of preparation, dosage, dose frequency, and route of administration. Danish Multiple Sclerosis Study Group. *Ann Neurol, 48*, 706-712.

Ross, R. J., Leung, K. C., Maamra, M., Bennett, W., Doyle, N., Waters, M. J., & Ho, K. K. (2001). Binding and functional studies with the growth hormone receptor antagonist,

B2036-PEG (pegvisomant), reveal effects of pegylation and evidence that it binds to a receptor dimer. *J Clin Endocrinol Metab, 86*, 1716-1723.

Rozak, D. A., Orban, J., & Bryan, P. N. (2005). G148–GA3: A streptococcal virulence module with atypical thermodynamics of folding optimally binds human serum albumin at physiological temperatures. *Biochimica et Biophysica Acta (BBA) - Proteins and Proteomics, 1753*, 226-233.

Sabio, G., Mora, A., Rangel, M. A., Quesada, A., Marcos, C. F., Alonso, J. C., Soler, G., & Centeno, F. (2001). Glu-256 is a main structural determinant for oligomerisation of human arginase I. *FEBS Lett, 501*, 161-165.

Salido, G. M., & Rosado, J. A. (2009). Apoptosis involvement of oxidative stress and intracellular Ca2+ homeostasis. Netherlands: Netherlands : Springer Science+Business Media B.V., 2009.

Sasada, M., & Terayama, H. (1969). The nature of inhibitors of DNA synthesis in rat-liver hepatoma cells. *Biochim Biophys Acta, 190*, 73-87.

Sasaki, T., Shintani, M., & Kihara, K. (1984). Inhibition of growth of mammalian cell cultures by extracts of arginine-utilizing mycoplasmas. *In Vitro, 20*, 369-375.

Savaraj, N., You, M., Wu, C., Wangpaichitr, M., Kuo, M. T., & Feun, L. G. (2010). Arginine deprivation, autophagy, apoptosis (AAA) for the treatment of melanoma. *Curr Mol Med, 10*, 405-412.

Savoca, K. V., Abuchowski, A., van Es, T., Davis, F. F., & Palczuk, N. C. (1979). Preparation of a non-immunogenic arginase by the covalent attachment of polyethylene glycol. *Biochim Biophys Acta, 578*, 47-53.

Savoca, K. V., Davis, F. F., van Es, T., McCoy, J. R., & Palczuk, N. C. (1984). Cancer therapy with chemically modified enzymes. II. The therapeutic effectiveness of arginase, and arginase modified by the covalent attachment of polyethylene glycol, on the taper liver tumor and the L5178Y murine leukemia. *Cancer Biochem Biophys, 7*, 261-268.

Schiavon, O., Caliceti, P., Ferruti, P., & Veronese, F. M. (2000). Therapeutic proteins: a comparison of chemical and biological properties of uricase conjugated to linear or branched poly(ethylene glycol) and poly(N-acryloylmorpholine). *Farmaco, 55*, 264-269.

Scott, L., Lamb, J., Smith, S., & Wheatley, D. N. (2000). Single amino acid (arginine) deprivation: rapid and selective death of cultured transformed and malignant cells. *Br J Cancer, 83*, 800-810.

Sheen, J. H., Zoncu, R., Kim, D., & Sabatini, D. M. (2011). Defective regulation of autophagy upon leucine deprivation reveals a targetable liability of human melanoma cells *in vitro* and *in vivo*. *Cancer Cell, 19*, 613-628.

Shen, L. J., Lin, W. C., Beloussow, K., & Shen, W. C. (2003). Resistance to the anti-proliferative activity of recombinant arginine deiminase in cell culture correlates with the endogenous enzyme, argininosuccinate synthetase. *Cancer Lett, 191*, 165-170.

Shen, L. J., & Shen, W. C. (2006). Drug evaluation: ADI-PEG-20--a PEGylated arginine deiminase for arginine-auxotrophic cancers. *Curr Opin Mol Ther, 8*, 240-248.

Sherman, M. R., Saifer, M. G., & Perez-Ruiz, F. (2008). PEG-uricase in the management of treatment-resistant gout and hyperuricemia. *Adv Drug Deliv Rev, 60*, 59-68.

Siegel, R., Desantis, C., Virgo, K., Stein, K., Mariotto, A., Smith, T., Cooper, D., Gansler, T., Lerro, C., Fedewa, S., Lin, C., Leach, C., Cannady, R. S., Cho, H., Scoppa, S., Hachey, M., Kirch, R., Jemal, A., & Ward, E. (2012). Cancer treatment and survivorship statistics, 2012. *CA Cancer J Clin, 62*, 220-241.

Simon-Reuss, I. (1953). Arginase, an antimitotic agent in tissue culture. *Biochim Biophys Acta, 11*, 396-402.

Sjolander, A., Nygren, P. A., Stahl, S., Berzins, K., Uhlen, M., Perlmann, P., & Andersson, R. (1997). The serum albumin-binding region of streptococcal protein G: a bacterial fusion partner with carrier-related properties. *J Immunol Methods, 201*, 115-123.

Sorensen, P. S., Ross, C., Clemmesen, K. M., Bendtzen, K., Frederiksen, J. L., Jensen, K., Kristensen, O., Petersen, T., Rasmussen, S., Ravnborg, M., Stenager, E., & Koch-Henriksen, N. (2003). Clinical importance of neutralising antibodies against interferon beta in patients with relapsing-remitting multiple sclerosis. *Lancet, 362*, 1184-1191.

Stork, R., Campigna, E., Robert, B., Muller, D., & Kontermann, R. E. (2009). Biodistribution of a bispecific single-chain diabody and its half-life extended derivatives. *J Biol Chem, 284*, 25612-25619.

Stork, R., Muller, D., & Kontermann, R. E. (2007). A novel tri-functional antibody fusion protein with improved pharmacokinetic properties generated by fusing a bispecific single-chain diabody with an albumin-binding domain from streptococcal protein G. *Protein Eng Des Sel, 20*, 569-576.

Stork, R., Zettlitz, K. A., Müller, D., Rether, M., Hanisch, F.-G., & Kontermann, R. E. (2008). N-Glycosylation as Novel Strategy to Improve Pharmacokinetic Properties of Bispecific Single-chain Diabodies. *Journal of Biological Chemistry, 283*, 7804-7812.

Storr, J. M., & Burton, A. F. (1974). The effects of arginine deficiency on lymphoma cells. *Br J Cancer, 30*, 50-59.

Syed, N., Langer, J., Janczar, K., Singh, P., Lo Nigro, C., Lattanzio, L., Coley, H. M., Hatzimichael, E., Bomalaski, J., Szlosarek, P., Awad, M., O'Neil, K., Roncaroli, F., & Crook, T. (2013). Epigenetic status of argininosuccinate synthetase and argininosuccinate lyase modulates autophagy and cell death in glioblastoma. *Cell Death Dis, 4*, e458.

Szlosarek, P. W., Klabatsa, A., Pallaska, A., Sheaff, M., Smith, P., Crook, T., Grimshaw, M. J., Steele, J. P., Rudd, R. M., Balkwill, F. R., & Fennell, D. A. (2006). *In vivo* loss of expression of argininosuccinate synthetase in malignant pleural mesothelioma is a biomarker for susceptibility to arginine depletion. *Clin Cancer Res, 12*, 7126-7131.

Szymkowski, D. E. (2005). Creating the next generation of protein therapeutics through rational drug design. *Curr Opin Drug Discov Devel, 8*, 590-600.

Takaku, H., Misawa, S., Hayashi, H., & Miyazaki, K. (1993). Chemical modification by polyethylene glycol of the anti-tumor enzyme arginine deiminase from Mycoplasma arginini. *Jpn J Cancer Res, 84*, 1195-1200.

Takaku, H., Takase, M., Abe, S., Hayashi, H., & Miyazaki, K. (1992). In vivo anti-tumor activity of arginine deiminase purified from Mycoplasma arginini. *Int J Cancer, 51*, 244-249.

Tolmachev, V., Orlova, A., Pehrson, R., Galli, J., Baastrup, B., Andersson, K., Sandstrom, M., Rosik, D., Carlsson, J., Lundqvist, H., Wennborg, A., & Nilsson, F. Y. (2007). Radionuclide therapy of HER2-positive microxenografts using a 177Lu-labeled HER2-specific Affibody molecule. *Cancer Res, 67*, 2773-2782.

Tomayko, M. M., & Reynolds, C. P. (1989). Determination of subcutaneous tumor size in athymic (nude) mice. *Cancer Chemother Pharmacol, 24*, 148-154.

Tsai, W. B., Aiba, I., Lee, S. Y., Feun, L., Savaraj, N., & Kuo, M. T. (2009). Resistance to arginine deiminase treatment in melanoma cells is associated with induced argininosuccinate synthetase expression involving c-Myc/HIF-1alpha/Sp4. *Mol Cancer Ther, 8*, 3223-3233.

Tsai, W. B., Aiba, I., Long, Y., Lin, H. K., Feun, L., Savaraj, N., & Kuo, M. T. (2012). Activation of Ras/PI3K/ERK Pathway Induces c-Myc Stabilization to Upregulate Argininosuccinate Synthetase, Leading to Arginine Deiminase Resistance in Melanoma Cells. *Cancer Res, 72*, 2622-2633.

Tsui, S. M., Lam, W. M., Lam, T. L., Chong, H. C., So, P. K., Kwok, S. Y., Arnold, S., Cheng, P. N., Wheatley, D. N., Lo, W. H., & Leung, Y. C. (2009). Pegylated derivatives

of recombinant human arginase (rhArg1) for sustained *in vivo* activity in cancer therapy: preparation, characterization and analysis of their pharmacodynamics *in vivo* and *in vitro* and action upon hepatocellular carcinoma cell (HCC). *Cancer Cell Int, 9*, 9.

Veronese, F. M., Caliceti, P., & Schiavon, O. (1997). Branched and Linear Poly(Ethylene Glycol): Influence of the Polymer Structure on Enzymological, Pharmacokinetic, and Immunological Properties of Protein Conjugates. *Journal of Bioactive and Compatible Polymers, 12*, 196-207.

Veronese, F. M., & Pasut, G. (2005). PEGylation, successful approach to drug delivery. *Drug Discov Today, 10*, 1451-1458.

Wang, M., Basu, A., Palm, T., Hua, J., Youngster, S., Hwang, L., et al. (2006). Engineering an arginine catabolizing bioconjugate: Biochemical and pharmacological characterization of PEGylated derivatives of arginine deiminase from Mycoplasma arthritidis. *Bioconjug Chem, 17*, 1447-1459.

Wheatley, D. N. (2004). Controlling cancer by restricting arginine availability--arginine-catabolizing enzymes as anticancer agents. *Anticancer Drugs, 15*, 825-833.

Wheatley, D. N. (2012). Amino acid deprivation as the primary intervention in cancer therapy: cellular basis of effective combinatorial therapy with arginase as the platform. *Biomedical research, 23*, 149-154.

Wheatley, D. N., & Campbell, E. (2002). Arginine catabolism, liver extracts and cancer. *Pathol Oncol Res, 8*, 18-25.

Wheatley, D. N., & Campbell, E. (2003). Arginine deprivation, growth inhibition and tumour cell death: 3. Deficient utilisation of citrulline by malignant cells. *Br J Cancer, 89*, 573-576.

Wheatley, D. N., Kilfeather, R., Stitt, A., & Campbell, E. (2005). Integrity and stability of the citrulline-arginine pathway in normal and tumour cell lines. *Cancer Lett, 227*, 141-152.

Wheatley, D. N., Scott, L., Lamb, J., & Smith, S. (2000). Single amino acid (arginine) restriction: growth and death of cultured HeLa and human diploid fibroblasts. *Cell Physiol Biochem, 10*, 37-55.

Wiswell, O. B. (1951). Effects of intraperitoneally injected arginase on growth of mammary carcinoma implants in the mouse. *Proc Soc Exp Biol Med, 76*, 588-589.

Wu, F. L., Liang, Y. F., Chang, Y. C., Yo, H. H., Wei, M. F., & Shen, L. J. (2011). RNA interference of argininosuccinate synthetase restores sensitivity to recombinant arginine deiminase (rADI) in resistant cancer cells. *J Biomed Sci, 18*, 25.

Wu, L., Li, L., Meng, S., Qi, R., Mao, Z., & Lin, M. (2013). Expression of argininosuccinate synthetase in patients with hepatocellular carcinoma. *J Gastroenterol Hepatol, 28*, 365-368.

Yang, K., Basu, A., Wang, M., Chintala, R., Hsieh, M. C., Liu, S., Hua, J., Zhang, Z., Zhou, J., Li, M., Phyu, H., Petti, G., Mendez, M., Janjua, H., Peng, P., Longley, C., Borowski, V., Mehlig, M., & Filpula, D. (2003). Tailoring structure-function and pharmacokinetic properties of single-chain Fv proteins by site-specific PEGylation. *Protein Eng, 16*, 761-770.

Yau, T., Cheng, P. N., Chan, P., Chan, W., Chen, L., Yuen, J., Pang, R., Fan, S. T., & Poon, R. T. (2012). A phase 1 dose-escalating study of pegylated recombinant human arginase 1 (Peg-rhArg1) in patients with advanced hepatocellular carcinoma. *Invest New Drugs*.

Yoon, C. Y., Shim, Y. J., Kim, E. H., Lee, J. H., Won, N. H., Kim, J. H., Park, I. S., Yoon, D. K., & Min, B. H. (2007). Renal cell carcinoma does not express argininosuccinate synthetase and is highly sensitive to arginine deprivation via arginine deiminase. *Int J Cancer, 120*, 897-905.

You, M., Savaraj, N., Kuo, M. T., Wangpaichitr, M., Varona-Santos, J., Wu, C., Nguyen, D. M., & Feun, L. (2013). TRAIL induces autophagic protein cleavage through caspase activation in melanoma cell lines under arginine deprivation. *Mol Cell Biochem, 374*, 181-190.

You, M., Savaraj, N., Wangpaichitr, M., Wu, C., Kuo, M. T., Varona-Santos, J., Nguyen, D. M., & Feun, L. (2010). The combination of ADI-PEG20 and TRAIL effectively increases cell death in melanoma cell lines. *Biochem Biophys Res Commun, 394*, 760-766.